Faculty of Science and Engineering

Progress Towards Controlled Re-entry and Recovery of CubeSats

Fergus William Downey

This thesis is presented for the Degree of
Doctor of Philosophy
of
Curtin University

March 2023

Declaration

To the best of my knowledge and belief this thesis contains no material previously published by any other person except where due acknowledgement has been made. This thesis contains no material which has been accepted for the award of any other degree or diploma in any university.

28 March 2023

Abstract

Essential to advancing planetary science is the collection and study of extra-terrestrial samples from all around the Solar System. These samples can either be collected in the form of sample collection and return missions or fall to Earth in the form of meteorites and be tracked and located on the Earth's surface using camera networks. Although the latter is considered more cost-effective and straightforward to implement, large-scale sample return missions offer tremendous value in their ability to choose a target and return a sample in pristine condition. However, sample return missions suffer from a significant setback, being the extremely high cost. Funding is commonly only available to one sample collection mission at a time, leaving many fascinating exploration opportunities missed.

The controlled re-entry and recovery phase is a significant part of the high costs associated with sample collection and return. Requiring advanced navigation and guidance tools, thermal protection systems, and recovery methods to land at precise locations on the Earth, systems for successful sample recovery can be expensive to test and develop. Methods to improve and reduce the cost of developing and testing these systems can make many missed opportunities more economically feasible.

The CubeSat small satellite form factor offers a unique ability to make this improvement. Conceptualised to take advantage of rocket rideshare opportunities and increase access to space by reducing launch costs, the platform is now used for secondary payloads on many discovery class missions, performing low-cost, high-risk, high-reward research. Developing the systems required for controlled

re-entry and recovery of CubeSats can reduce the cost of performing valuable sample collection and return missions, resulting in many more opportunities to explore the Solar System.

Controlled re-entry and recovery systems for CubeSats can also provide other unique opportunities. Similar in design are the entry, descent, and landing systems used for landing on the surface of extra-terrestrial planets and moons. The ability to reduce the development costs of these systems is advantageous and just as valuable to planetary science and the study of the Solar System. Landing on Mars and Titan is part of many mission concepts planned for the near future. Including a CubeSat lander or landers on these missions could provide valuable science for minimal overhead costs.

Additionally, reducing the cost and size of complete controlled re-entry and recovery systems in low Earth orbit can enable new science and industry opportunities. Highlighted as a unique application is the rapid return of biological science conducted in microgravity environments. As the launch of satellites to low Earth orbit becomes more prevalent, the ability to reduce space debris and the number of defunct satellites will become more necessary. De-orbiting defunct or end-of-life satellites that are no longer required is another application for controlled re-entry technologies. Finally, a complete system can offer unique opportunities to study the upper atmosphere and extreme re-entry environment. One of the reasons for the high cost of developing controlled re-entry and recovery technologies is the poor ground test equipment able to simulate the re-entry environment. With a better understanding of this environment, the cost of developing larger systems could be reduced.

This doctoral thesis features the progress made towards performing controlled re-entry and recovery missions using CubeSats. A significant part of this progress was the development of the novel Binar CubeSat Bus platform. The platform design is hardware cost-effective, payload space maximised, and reusable without compromising system capabilities. These design features make the Binar CubeSat Bus the ideal tool for developing and testing CubeSat controlled re-entry and recovery systems. The platform was assembled, integrated, tested, and launched as the first ever Western Australian space mission, Binar-1. The mission was the

first demonstration of the custom-designed systems, providing valuable lessons learned that have improved the platform design and mission lifecycle to its final reusable state. The improved platform will be demonstrated on the upcoming Binar-2, 3, and 4 mission.

The first critical requirement for demonstrating CubeSat controlled re-entry was the development of a CubeSat tracking system. Due to the relative speed of CubeSats in low Earth orbit, standard techniques for observing re-entry are limited. Passive radar systems which supply two line elements to satellite operators are inaccurate at re-entry altitudes, and ground station networks are expensive to set up and maintain. Open-source ground station networks and communication satellite constellations provided an alternative. By merging the two options and simulating them using open-source python libraries, an optimal method for tracking the re-entry of CubeSats was demonstrated. Using commercial and custom hardware solutions, this optimal tracking method has been integrated with the Binar CubeSat Bus and will have its first real-world test on the upcoming Binar-2, 3, and 4 mission.

Now well established and preparing to perform its second mission, Binar-2, 3, and 4, the Binar CubeSat Bus is ready to demonstrate and test technologies for controlled re-entry and recovery of CubeSats. A crucial growth in the capabilities of small satellites, the successful demonstration of controlled re-entry and recovery will provide more frequent opportunities to visit and explore the unknown areas of the Solar System.

"Born too early to explore the Universe, too late to discover the Earth, but lucky enough to enjoy the here and now."

- Anonymous

Acknowledgements

This research was supported by the Australian Government through the Research Training Program (RTP) scholarship, the Western Australian State Government through funding provided to the Binar Space Program, and receives institutional support from Curtin University.

Philip Bland—Thank you for this amazing opportunity to explore a path I never thought possible. Your passion and drive to build and sustain a planetary science ecosystem in Western Australia have been inspirational and motivated me to continue pushing forward even when we haven't had the best of luck. Over the last 4 years, I have been one of the major beneficiaries of your hard work, and for that, I am extremely grateful.

Jonathan Paxman—Thank you for always being able to point myself and the Binar team in the right direction when a challenge gets the better of us. Your guidance and optimism have been crucial in motivating me to finish my PhD. I hope you continue to be part of the Binar Space Program for many years to come.

Ben and Stuart—Thank you for keeping me sane on those hard days and having the ability to sit down and enjoy a beer. I look forward to gazing back at our time as PhD students together and reflecting on all of our amazing achievements.

The Binar team—Thank you for your amazing effort and hard work in building and making the Binar Space Program the enjoyable and exciting place it is today.

My friends—Thank you for putting up with my deep sighs every time I am asked about my PhD. I promise it is done this time!

My parents: Yvette and Shaun—Thank you for taking the leap nearly 20 years ago and relocating the family to Western Australia. Without growing up fascinated under the stars I may never have started this journey.

Correna—Thank you for your patience and kindness on the days when I needed it most. Never again will you have to hear the phrase "After my PhD is finished!" I cannot wait for the year we have ahead of us!

Contents

List of First Author Abstracts and Publications

This thesis includes a number of abstracts and publications that were created as a part of this work.

First Author Conference Publications

Appendix A.1:

This publication was delivered as a conference proceeding following the acceptance of the abstract and presentation.

F. W. Downey, S. Buchan, B. Hartig, D. Busan, J. Cook, P. A. Bland and J. Paxman, "Binar Space Program: Binar-1 Results and Lessons Learned" conference proceeding of the 36th Small Satellite Conference at the Utah State University in Logan, Utah, USA.

First Author Conference Abstracts

Appendix A.2:

This abstract was delivered as a conference presentation following its acceptance.

F. W. Downey, B. Hartig, N. Brough, S. Buchan, M. Cupak, D. Busan, P. A. Bland, J. Paxman and R. Howie, "The Binar Space Program: Developing a reliable and efficient CubeSat Electronics Power System" presented at the 19th Australian Space Research Conference (ASRC 2019) in Adelaide, Australia.

Appendix A.3:

This abstract was delivered as a conference presentation following its acceptance.

F. W. Downey, B. Hartig, S. Buchan, C. Tay, J. Cook, D. Busan, P. A. Bland, J. Paxman and R. Howie, "Binar Space Program: Binar-1 Results and Lessons Learned" presented at the 20th Australian Space Research Conference (ASRC 2022) in Sydney, Australia.

List of Coauthored Abstracts and Publications

Contributions were made to the following coauthored abstracts and publications as a part of this work, but they are not included as part of this thesis.

Coauthored Articles

S. R. G. Buchan, N. D. Brough, F. W. Downey, D. C. Busan, B. A. D. Hartig, R. M. Howie, M. Cupak, P. A. Bland, J. Paxman, "Reliable Software Development For Small Satellite Missions: A Binar-1 Case Study," *Journal of Small Satellites*, under review.

S. R. G. Buchan, F. W. Downey, K. McMullan, B. A. D. Hartig, E. Trifoni, J. Mathew, P. A. Bland, J. Paxman, R. M. Howie, "Experimental Results and Modelling of the Binar-1 CubeSat On-Board Power Management in Thermal Vacuum Conditions," *Robotics and Autonomous Systems*, under review.

Coauthored Conference Publications

S. Buchan, F. Downey, B. Hartig, D. Busan, J. Cook, C. Tay, K. McMullan, T. Ward, R. Howie, P. Bland and J. Paxman, "Binar CubeSat Program: Mission Two Payloads and Operation Plan" presented at the 36th Small Satellite Conference at the Utah State University in Logan, Utah, USA.

Coauthored Conference Abstracts

N. Brough, S. Buchan, F. Downey, B. Hartig, M. Towner, M. Cupak, R. Howie, J. Paxman and P. Bland, "The Binar CubeSat Program: Attitude Control for Small Satellites" presented at the 19th Australian Space Research Conference (ASRC 2019) in Adelaide, Australia.

B. Hartig, P. Bland, J. Paxman, R. Howie, M. Towner, M. Cupak, D. Busan, N. Brough, F. Downey and S. Buchan, "The Binar CubeSat Program: Past, Present and Beyond" presented at the 19th Australian Space Research Conference (ASRC 2019) in Adelaide, Australia.

S. Buchan, P. Bland, J. Paxman, B. Hartig, N. Brough, F. Downey, D. Busan, M. Towner, M. Cupak and R. Howie, "The Binar CubeSat Program: Design and Development of a CubeSat Digital Twin" presented at the 19th Australian Space Research Conference (ASRC 2019) in Adelaide, Australia.

List of Abbreviations Used In This Thesis

ADCS	**A**ttitude **D**etermination and **C**ontrol **S**ystem
BCB	**B**inar **C**ubeSat **B**us
BCC	**B**inar **C**ubeSat **C**ore
BCM	**B**inar **C**ubeSat **M**otherboard
CDR	**C**ritical **D**esign **R**eview
CICs	**C**over-glass **I**ntegrated **C**ells
COTS	**C**ommercial **O**ff **T**he **S**helf
CSIRO	**C**ommonwealth **S**cientific and **I**ndustrial **R**esearch **O**rganisation
DFN	**D**esert **F**ireball **N**etwork
DRAMA	**D**ebris **R**isk **A**ssessment and **M**itigation **A**nalysis
EDL	**E**ntry **D**escent and **L**anding
eMMC	**e**mbedded **M**ulti-**M**edia **C**ard
EPS	**E**lectricl **P**ower **S**ystem
ESA	**E**uropean **S**pace **A**gency
FFC	**F**lat **F**lexible **C**onnector
FRR	**F**light **R**eadiness **R**eview
GEO	**G**eostationary **E**arth **O**rbit
GFO	**G**lobal **F**ireball **O**bservatory
GPI	**G**eneral-**P**urpose **I**nput
GPIO	**G**eneral-**P**urpose **I**nput-**O**utput
GPO	**G**eneral-**P**urpose **O**utput
GPS	**G**lobal **P**ositioning **S**ystem
I2C	**I**nter-**I**ntegrated **C**ircuit
IC	**I**ntegrated **C**ircuit

IMU	**I**nertial **M**easurement **U**nit
ISS	**I**nternational **S**pace **S**tation
JAXA	**J**apan **A**erospace **E**xploration **A**gency
JEM	**J**apanese **E**xperimentation **M**odule
J-SSOD	**J**EM-**S**mall **S**atellite **O**rbital **D**eployer
LED	**L**ight **E**mitting **D**iode
LEO	**L**ow **E**arth **O**rbit
MPPC	**M**aximum **P**eak **P**ower **C**ontroller
NASA	**N**ational **A**eronautics and **S**pace **A**dministration
NEA	**N**ear **E**arth **A**steroids
OCC	**O**ver **C**urrent in **C**harge
OCD	**O**ver **C**urrent in **D**ischarge
OSCAR	**O**rbital **S**pace**C**raft **A**ctive **R**emoval
OVP	**O**ver **V**oltage **P**rotection
PCB	**P**rinted **C**ircuit **B**oard
PDR	**P**reliminary **D**esign **R**eview
P-POD	**P**oly-**P**icosatellite **O**rbital **D**eployer
RAAN	**R**ight **A**scension of the **A**scending **N**ode
RBF	**R**emove **B**efore **F**light
RPC	**R**emote **P**rocedure **C**all
SARA	**S**urvival **A**nd **R**isk **A**nalysis
SBD	**S**hort **B**urst **D**ata
SCP	**S**hort **C**ircuit **P**rotection
SMA	**S**hape **M**emory **A**lloy
SOA	**S**tate **O**f the **A**rt
SpAARC	**Sp**ace **A**utomation **A**I and **R**obotics control **C**omplex
SPI	**S**erial **P**eriferal **I**nterface
SSTC	**S**pace **S**cience and **T**echnology **C**entre
STK	**S**ystems **T**ool **K**it
SWaP	**S**ize **W**eight **a**nd **P**ower
TLE	**T**wo **L**ine **E**lement
TPS	**T**hermal **P**rotection **S**ystem
TRL	**T**echnology **R**eadiness **L**evel
UART	**U**niversal **A**syncronous **R**eceive-**T**ransmit
UHF	**U**ltra **H**igh **F**requency

USB	**U**niveral **S**erial **B**us
UVP	**U**nder **V**oltage **P**rotection
VHF	**V**ery **H**igh **F**requency

List of Figures

List of Tables

Chapter 1

Introduction

This doctoral thesis presents progress towards performing controlled re-entry and recovery missions using CubeSats. Traditionally, controlled spacecraft re-entry and recovery is reserved for astronaut return and high-value sample collection missions. However, with modern-day advances in the miniaturisation of technology, the ability to perform sample collection missions on smaller satellites is a reasonable prospect. Using CubeSats for this application is beneficial as it can reduce cost and increase mission frequency, increasing the quantity and improving the quality of samples available for studying the Solar System.

This doctoral thesis describes the development of a novel CubeSat platform enabling the development of controlled re-entry and recovery systems for CubeSats. This CubeSat platform, now known as the Binar CubeSat Bus (BCB), was initially designed to be low-cost and payload space maximised without compromising the system capabilities. Following the design, the CubeSat was assembled, integrated, and tested at Curtin University before being launched on Commercial Resupply Mission 23 (CRS-23) to the International Space Station (ISS). It was deployed on the 6^{th} of October 2021 as the first-ever Western Australian space mission, Binar-1. The mission provided valuable lessons learned and an opportunity to start the development of controlled re-entry and recovery systems using the platform.

Implementing the lessons learned has improved the reusability of the BCB. A further reduction in hardware costs has resulted from finishing the custom design. Included in the custom design completion was a modular payload system. The unique payload design has enabled the platform to deliver high school, research, and industry payloads and improved reusability. The platform can now remain the same between missions, with only the payload defining the objective of the CubeSat. Due to the countless possible design methods, this reusability is critical for developing and testing controlled re-entry and recovery systems.

The next step in progressing towards controlled re-entry and recovery of CubeSats was the development of an upgrade to the BCB for tracking the re-entry. The system is necessary to demonstrate the performance of controlled re-entry technologies. With a method to validate the control system's ability to correctly guide the CubeSat to enter the atmosphere at an appropriate location, the performance of the technology can be quantified. Being the first step in controlled re-entry and recovery, this is significant, as a successful demonstration of a controlled re-entry technology is required to begin flight testing of the following stages.

The upcoming Binar-2, 3, and 4 mission will be the first demonstration of the re-entry tracking system and design improvements. Reusing the BCB efficiently and more frequently will enable the development and testing of many controlled re-entry and recovery technologies. Through the successful design and implementation of the BCB, progress has been made towards controlled re-entry and recovery using CubeSats.

1.1 What Are CubeSats?

At the start of the new millennium, researchers and space scientists aimed to develop a new and more cost-effective method of performing space missions. Current methods were either highly theoretical or required extreme amounts of funding. The solution to this was the production of a new generation of small satellites called CubeSats [1][2]. By developing a new deployer called the Poly Picosatellite Orbital Deployer (P-POD), rocket launches carrying large spacecraft could now share the ride with smaller satellites, optimising the use of the rocket. By reducing the significant barrier to entry for space activities, universities and research

institutes have started working on missions for space science and exploration. Over the last two decades, usage of the form factor has exploded, not only as an education platform, but now performing valuable space research outside of LEO [2][3][4].

The CubeSat form factor works by launching out of a standardised deployer that can attach to large rockets carrying other payloads. The first deployer developed was the P-POD by California Polytechnic State University [1]. There are now multiple deployers that fit different rockets from different countries. However, all stick to the same form factor size guidelines of the 10x10x10cm units, better known as 1U. The P-POD and many other deployers can launch 3U of CubeSat either as one single 3U CubeSat or as three individual 1U CubeSats. Each CubeSat unit has a mass limit of 1.33kg or 4kg for the 3U launch pod. This containerisation has allowed the CubeSat launch business to sell launch slots on larger rockets at affordable prices. As the adoption of the form factor has grown, so too have the launch size opportunities, with 6U and 12U launch pods for larger CubeSat missions now available [4][5][6].

Before the CubeSat form factor, university spacecraft development was rare due to the expensive launch costs. As the market is now open with many ride-sharing capabilities, start-up businesses have been able to provide universities with the tools they need to take their payloads to space. Commercial Off The Shelf (COTS) CubeSat and small satellite businesses are now competitively able to offer complete CubeSat packages with payload integration. This is a largely University and Small to Medium Enterprise (SME) market which aims to test newly developed space payloads. From the NASA State of the Art Document, there are 17 different suppliers of CubeSat platforms [7]. All these companies compete to provide a viable solution for universities and SMEs. However, these platforms can still be expensive for many new university teams with limited funding. Additionally, once the platform is purchased, customizability is limited, and testing can be challenging with minimal access to the proprietary designs. This results in some universities taking an alternate approach to CubeSat design.

Educational institutes can also develop custom space hardware as an alternative to buying complete CubeSat solutions. This provides a learning platform for

early career engineers in spacecraft design, assembly, integration, and testing and allows the university to benefit by developing a space program. The practice also creates new start-ups, increasing competitiveness in the CubeSat marketplace. A program run by NASA known as the CubeSat Launch Initiative (CSLI) is directly promoting this work [8][9][10]. The initiative has helped many universities get involved in space system design and operation. The program uses the CubeSat form factor to fund and find launches through another program called the Educational Launch of Nanosatellites (ELaNa). ELaNa leverages existing NASA launches and newly developed CubeSat launch ventures that can provide an alternate solution in the future. The program goals have enabled North America to improve its STEM education pipeline by engaging with students and teachers and enabling many new science and space capabilities [8]. A significant contribution from the program to future CubeSat development is the CubeSat 101 handbook which details the work required for developing a CubeSat as a beginner[3]. This document is now helping internationally to start CubeSat programs and further improve the capabilities of universities and space technology development.

1.1.1 Example CubeSat Missions

Missions that have flown in the past are great examples of the capabilities of CubeSats. Initially operating in LEO, CubeSats have now begun to explore interplanetary space and assist in exploring extra-terrestrial bodies. Some of the impressive feats of CubeSats and their achievements towards planetary science are highlighted here, demonstrating the growing power of the form factor and the need for more capabilities, such as controlled re-entry and recovery, to be developed.

The LightSail CubeSats

LightSail 1 and LightSail 2 were two CubeSats launched in 2015 and 2019, respectively. The successful demonstration of LightSail 2 significantly advanced the Planetary Societies' mission to promote solar sail technology and engage the community in space research. The CubeSats carried solar sails with a surface area of $32m^2$ and were the first to demonstrate CubeSat light propulsion. The Planetary Society also used the missions to excite the public about new space capabilities. Bill Nye, a TV show host and CEO of the Planetary Society, and Neil deGrasse Tyson contributed to the outreach targets of the CubeSats [11][12]. The signif-

icance of these CubeSats was the demonstration of a long-distance propulsion system, now being used to explore Near Earth Asteroids (NEAs) (Section 1.1.1).

The MarCO CubeSats

The MarCO CubeSats, MarCO A and MarCO B, were two 6U class CubeSats that flew past Mars as a proof of concept mission for small interplanetary Satellites. They were the first-ever CubeSats to operate in interplanetary space. The CubeSats assisted the InSight Mission by acting as a secondary communication relay during the controlled re-entry phase of the mission. The two CubeSats carried new technologies not seen on CubeSats before, and after being successful, have led to the development of more interplanetary CubeSats [13].

LICIACube

Along for the ride with the recent NASA mission, the Double Asteroid Redirection Test (DART), was the Italian CubeSat LICIACube. The CubeSat was developed to be deployed from the main spacecraft before impact to observe the result from afar and capture additional data. Carrying imager payloads for tracking the Didymos-Dimorphos asteroid system and imaging the DART impact, the CubeSat provided valuable data on the results of the impact [14]. The success of this CubeSat demonstrates the ability to assist larger missions in collecting data and performing planetary research.

The Artemis 1 CubeSats

Along with the recent successful launch of Artemis 1 was the launch of ten secondary CubeSats. The CubeSats aimed to perform valuable space science, which can provide additional information about the Moon and other planetary bodies. NEA Scout is one of the missions that is not targeting the Moon. By being deployed from the upper stage of NASA's Space Launch System (SLS), the mission will be the first to use a solar sail to travel to a NEA. Once there, the deep space CubeSat will image and analyse its target asteroid. The spacecraft will also use a tracking system to lock onto the asteroid and plan its arrival. The demonstration of these two technologies will pioneer the exploration of near-Earth objects using CubeSats [15].

1.2 Why is CubeSat Controlled Re-entry and Recovery Important?

Controlled re-entry and spacecraft recovery have been performed since the dawn of space exploration to return valuable intelligence from spy satellites before advanced communication systems existed and to return the first humans from the Moon [16][17]. Since then, the technology has been improved for other purposes. Humans are still returned through the atmosphere from the International Space Station (ISS). Sample return missions are always being considered and planned to help improve the quality of extra-terrestrial samples used in studying the Solar System.

Although initially stipulated as an education and test platform, CubeSats are now used for valuable space science missions due to the reduced cost. This benefit alone makes the platform attractive for sample return mission applications. Recent sample collection and return missions such as Stardust (comet Wild-2) [18][19], Hayabusa (asteroid Itokowa) [20], Hayabusa 2 (asteroid Ryugu) [21][22], and the ongoing OSIRIS-REx (asteroid Bennu) [23][24] have returned or are returning extra-terrestrial samples for USD$200million [19], USD$100million [20], USD$200million [25] and USD$1billion [26] respectively. Although all these missions have high costs, they continue to be a favoured mission architecture due to their unique and continued benefits to studying the Solar System. Other discovery missions have limited lifetimes and often require compromises regarding payload instrument sensitivity to fit within mass and power envelopes and maximise the science payload lifetime. Sample return missions do not have these constraints. Once the material is returned to Earth, it is available for analysis for decades, with the most sensitive instruments available. Importantly, because it is curated with long-term analysis in mind, new data can be recovered using increasingly advanced techniques, generating new insights into Solar System formation and evolution as technology advances. Apollo samples continue to be analysed >50 years after they were returned and continue to generate new insights into the Moon's geological history. Although Apollo is the most expensive mission in history, the sample return aspect of Apollo meant that it is also the most cost-effective, delivering a better return in terms of science per dollar (based on publications and citations) than any other mission [27][28].

Sample return missions typically have some of the most complex mission architectures compared to other Solar System discovery missions. If it were possible to simplify elements of the mission architecture and lower the mission costs, the potential to create more research prospects would be possible. CubeSats offer increased opportunities in this area due to the reduced size and launch price. However, atmospheric entry behaviour is very different at this volume compared to large spacecraft and thus requires further investigation to understand the process. Although the returned mass would be small, modern analytical techniques only need a small amount of material to be adequate, further reinforcing the concept of CubeSats or other small spacecraft for Solar System sample collection missions. The prime example is the Stardust mission re-entry capsule. Returning only 1-10 micrograms of comet sample, the science value is still being appreciated many years later [29].

With tremendous advantages to be gained, the planetary science research question "Can a CubeSat be used to perform controlled re-entry and recovery from extra-terrestrial samples?" was formed. This question formed the basis of this thesis, separating the answer to the question into many challenges. These challenges were technology and engineering challenges, which when solved, provide a new capability which can pursue the planetary science research question.

Extra-terrestrial sample return to Earth was the initial prompt for this work. However, the same technology could be applied to other planetary atmospheres. Developing a CubeSat with Entry, Descent and Landing (EDL) capabilities creates various other mission possibilities. The ability to deliver sensors and devices to the surface of Mars or Titan using small and inexpensive spacecraft can provide valuable data about the surface properties in a variety of targeted locations. This sort of information could be paramount in determining where to land more complex science instruments on these planetary bodies.

Although the primary motivation for this work was planetary science in the form of sample collection and return missions, there are many secondary applications of controlled re-entry and recovery systems. These applications include:

- Extreme data quantity return,

- Global disaster response,
- Space debris prevention,
- Testing of Thermal Protection Systems (TPS) for larger spacecraft applications, and
- Collecting data on the upper atmosphere and re-entry environment.

Industry and government applications included data return and global disaster response. Many instruments in space collect extreme quantities of data that can take extended periods to transmit to Earth. The capability to safely return the data via controlled re-entry and recovery can prove valuable for missions with short lifetimes. The application of CubeSat controlled re-entry and recovery to global disaster response is a concept that has yet to be explored. A more affordable controlled re-entry and recovery solution with high-accuracy landing abilities could support areas in a time of need.

An additional driver for controlled re-entry is mitigating the buildup of debris and inactive satellites in Earth orbit. A well-known phenomenon is the Kessler effect, which estimates the critical mass in space at which a collision would cascade, causing multiple collisions [30]. If LEO starts to approach this mass and a collision were to happen, space may become inaccessible for many years. As such, the ability to remove nonoperational satellites from orbit is essential. The first stage, controlled re-entry, or the process of removing the satellite from its current orbit around the Earth, has the potential to assist in this area. CubeSats launched into LEO at less than 400km altitude will de-orbit within approximately one to two years. However, as you move further away from Earth, orbits decay slower, and satellites can remain in orbit around the Earth for over 25 years, even after becoming nonoperational [31]. This atmospheric effect of drag is discussed in more detail in Section 1.4. Additionally the technology is beginning to have an even greater demand as recently the Federal Communications Commission reduced the allowable de-orbit time of satellites in LEO from 25 years to 5 years [32] in order to limit the build up of space debris. This means that all LEO CubeSats with

lifetimes predicted to be longer than this will need an exemption, or require a de-orbit systems. This overlap between re-entry and de-orbiting systems can be used to prevent the build-up of space debris in LEO.

The capability to test innovative TPS in re-entry environments is a useful application of controlled re-entry and recovery CubeSats. New technologies for re-entry are often tested in settings that could be a better or more accurate representation of actual re-entry conditions. By developing a CubeSat re-entry platform, the performance of TPS in actual re-entry conditions can be evaluated.

One of the main reasons ground re-entry testing is not an accurate representation of the actual re-entry environment is due to the quality of the data available. Re-entry CubeSats can be used to collect more re-entry environment data improving the understanding of the upper atmosphere in the process. The low cost is another contributing factor to this solution, as multiple re-entry CubeSats can be used to build an extensive data set on the re-entry environment. The same technology can also be applied to other extra-terrestrial bodies. Planets such as Mars could be probed with multiple atmospheric entry CubeSats to collect data on the upper and lower atmosphere of the planet [33][34].

CubeSat re-entry can be used to advance many aspects of space science and industry. It can be used to return or deliver high-value payloads to Earth, enable low-cost lander missions utilising atmospheric entry at Mars, provide a de-orbit system that can remove inactive satellites from Earth, act as a test bed for larger re-entry systems, and be used to improve knowledge on the re-entry environment. This list of applications and potential solutions demonstrates the importance of CubeSat controlled re-entry and recovery technologies. Not only is it essential for planetary science but also for industry and government applications.

1.3 How Can CubeSats Perform Controlled Re-entry and Recovery?

Three main stages are required for controlled re-entry and recovery. The first is the initial de-orbit that starts the descent into the atmosphere. Numerous methods exist for de-orbit. However, most of these methods are used for reducing

space debris and hence lack control systems to target re-entry locations [7]. The second stage is surviving the re-entry environment. CubeSats typically disintegrate upon reaching the atmosphere between 90-120km altitude[30]. However, for re-entry and recovery to be successful, a system needs to be designed to survive the extreme re-entry environment and deceleration experienced. Re-entry systems have been used on larger spacecraft, but few exist for CubeSats. The final stage is recovery. Once surviving the second stage, the now free-falling mass must be slowed and tracked before reaching the ground. The CubeSat can be recovered if all phases are successful, completing the mission.

De-orbiting is a frequently performed task carried out by most spacecraft which are required to return to Earth for reuse or be destroyed by being brought back through the atmosphere. CubeSat de-orbit is a newer concept, as traditionally, most CubeSats orbit low enough to naturally de-orbit and enter Earth's atmosphere in under two years. As the form factor becomes more utilised, more advanced CubeSat missions are heading further away from Earth and hence are required to use de-orbit systems to prevent the build-up of space debris [31]. The primary strategy used for the de-orbit of larger spacecraft is propulsion systems. They are used to create a reverse thrust, slowing the orbital speed and causing a rapid orbital decay to Earth. This same system is one option for CubeSat de-orbit, however, due to the small size, propulsion systems are not always used, and as such, this solution is not always optimal. Other alternatives include solar sails and drag sails. Solar sails can be used as an alternate propulsion mechanism that can slow the orbit of a satellite. The system works by using solar radiation to create thrust. This method is now being employed by some interplanetary CubeSats which are travelling far beyond the Earth-Moon system and require a long duration of thrust to complete their journey [11][12][15]. Drag sails use the minimal atmosphere at higher altitudes to create a slow drag on the spacecraft, reducing orbital speeds. An explanation of how this process works is described in more detail in Section 1.4. This technology is being advanced to help prevent space debris, and most systems deploy the sail to create drag and begin the end-of-life de-orbit process [11][12][33]. Although other de-orbit systems are available, the ones mentioned here can target re-entry locations. This makes their development beneficial to controlled re-entry and recovery missions, as further development of control systems can improve re-entry targeting.

In the past, many large spacecraft, including the Apollo capsule and the Space Shuttle, have performed atmosphere re-entry. Now, the technology is used to recycle rocket thrusters, return extra-terrestrial samples from space, and return astronauts from the ISS. The process involves advanced materials and Thermal Protection Systems (TPSs) to ensure its success. To perform the procedure, many companies and government space agencies have developed simulation software to forward plan and check safety. CubeSat controlled re-entry and recovery has yet to be demonstrated successfully. This is one of the main investigation areas for the complete process. Current ideas include using a TPS to return the complete CubeSat, similar to the Space Shuttle [33][35], while others suggest using a capsule design [36], similar to the Apollo missions. Inspiration will need to be taken from larger spacecraft to successfully survive the atmosphere re-entry stage of the process.

Recovery is the final stage in the complete controlled re-entry and recovery process. Once making it through the atmosphere, a safe landing in a desired location is required. The de-orbit phase predetermines the landing location, planning a re-entry location at the beginning. A landing is performed depending on the mass, shape and contents of the spacecraft being recovered. The potential options are a hard or soft landing, using a stowed parachute or propulsion system to slow the descent once nearing the ground. With many large spacecraft, the latter option is used as a hard landing will not suit the precious payloads carried. This can be seen on the spacecraft that return astronauts and extra-terrestrial samples, which all use a stowed parachute to slow the final descent of the spacecraft from its terminal velocity. This can be applied to the final designs of CubeSat recovery systems, as the stowed parachutes' area of effect scales with the size and mass of the spacecraft attempting to land.

Once the CubeSat is safely landed, it must be located and recovered. As such, a system must be on board to transmit location information. To achieve this, the CubeSat recovery system needs to contain a power system, communications system, attitude determination system, onboard processing system, landing system such as a parachute, and the recovered payload. Larger spacecraft integrate these systems into the re-entry vehicle, which determines and decides autonomously what the re-entry spacecraft should do to reach its target location.

Larger spacecraft returning astronauts integrate life support systems within the re-entry spacecraft, making up their payload system. The similarity between core spacecraft systems and re-entry vehicle systems needs to be considered during design. Adopting the systems from the main CubeSat in the re-entry vehicle is ideal. However, isolating the vehicle, except for a power connection, may improve redundancy. Testing the recovery CubeSat core systems is essential to a successful recovery and can be tested with sub-orbital launches, verifying the functionality of the systems.

Completing the three stages of re-entry is a challenge for CubeSats but has the potential to enable the CubeSat form factor to perform more advanced missions in the future. An already well-developed technology for larger spacecraft, controlled re-entry and recovery for CubeSats needs to be explored and demonstrated from LEO. As identified in this section, to perform controlled re-entry and recovery, many options are available for each of the three phases. As such, the focus of this thesis was to remove the initial challenges of investigating these options without limiting the range of possibilities.

1.4 Re-entry Aerodynamics

To understand the re-entry environment and the challenges associated with satellite re-entry and recovery, aerodynamics in different flow regimes need to be understood. The flow regime refers to the medium at which an object is moving through, determining how the gas surrounding an object reacts as the object passes through. As objects descend through the atmosphere the flow regime changes. To determine the flow regime, the Knudsen number is used. This is defined as the relationship connecting the mean free path between successive collisions of air molecules and the flow field characteristic length. This is shown in Equation 1.1.

$$Kn = \frac{MFP}{L_C} \tag{1.1}$$

Where MFP is the mean free path between successive collisions, and L_C is the flow field characteristic length. The MFP can be calculated using Equation 1.2.

$$MFP = \frac{1}{\sqrt{2}\pi\sigma_d^2 n_d} \tag{1.2}$$

Where σ_d is the effective diameter of the gas particles, and n_d is the number density which is calculated as the ratio between the air density and molecule mass. For the Earth, all of these parameters are considered a constant, except for the air density. As such, as a satellite descends though the Earths atmosphere, the Knudsen number decreases.

The Knudsen number distinguishes three flow regimes which are applicable to spacecraft re-entry. These correspond to the following [37]:

- Free molecular regime: $Kn > 10$
- Transition regime: $0.01 < KN < 10$
- Continuum regime: $Kn < 0.01$

During the re-entry process all three flow regimes are experienced. The greater Knudsen number is present at altitudes above the Karman line (100km altitude) and begins to move into the Transition regime before reaching the continuum flow regime experienced at the Earth's surface. As such the understanding of aerodynamics in all flow regimes and their applications is essential to the development of CubeSat controlled re-entry and recovery systems.

In all flow regimes and the stages of satellite re-entry, the main forces influencing the satellite are the forces of gravity, lift, and drag. Although other planetary bodies (such as the Sun and Moon), solar radiation pressure, and albedo all contribute minor forces, these are often neglected when developing controlled re-entry and recovery models. Although considered in orbital analysis and prediction models, when orbits of satellites reach lower altitudes, the forces of gravity, drag, and lift become more influential. This simplification also assists in the modelling process due to the complexity of modelling lift and drag. If the minor forces are included in simulations of re-entry, less computational effort can be used to

calculate the major forces.

When compared to the forces of lift and drag, the force of gravity acting on a satellite is the least complex. These forces have been mapped and modelled across the globe, usually only requiring a geodetic location input to determine the acting gravitational force. Many tools available tools can provide this information computationally efficient when compared to the forces of lift and drag. Such models include SGP4, WGS84, and EGM2008. SGP4 was used throughout Chapter 4 of this thesis as it contains simplified models for the drag force and atmospheric density.

The remaining aerodynamic forces that are critical in all flow regimes are the forces of drag and lift. These aerodynamic forces are calculated using the simplified equation 1.3 [38].

$$F = \frac{1}{2}\rho|v|^2 A(C_D i + C_L j) \tag{1.3}$$

Where i and j are the unit vectors corresponding to perpendicular and parallel to the velocity vector v respectively, ρ is the atmospheric density, and A is the surface area of the object perpendicular to the velocity vector.

This equation becomes the critical challenge when modelling CubeSat re-entry due to the high complexity of calculating the aerodynamic coefficients and atmospheric density. Factors that influence the aerodynamic coefficients include shape, attitude, atmosphere temperature and composition, satellite temperature and composition, and any other underlying gas surface interactions [38]. The latter of which forms one of the greatest unknowns, with many different models having been developed to improve modelling accuracy. This manifests to become a multi-factor challenge which is extremely computationally expensive to perform, especially in the free molecular flow regime where little information can be collected outside of satellite re-entry experiments.

Depending on the attitude and shape of the system, often the lift coefficient is

also excluded. Early research from Cook demonstrated that for many satellites with uncontrolled spinning motions, the lift force would have little to no impact. However, for larger flat satellites with controlled attitude, the lift would be significant [39]. Later studies have suggested that this was correct [40] with flat or blunt shaped objects being ideal to slow down re-entering satellites and reduce thermal loading. New research also suggests that controlled spins generating the Magnus effect can also cause significant lift on some re-entering satellites [41]. This is useful research as it can be used to focus computational effort into calculating the drag coefficient.

There are some models which provide methods for calculating the ballistic coefficients of satellites in all flow regimes. These can be used to simulate the re-entry process of CubeSats. However, many assumptions are used in the calculations to increase the computational efficiency. These assumptions become critical when developing a CubeSat controlled re-entry and recovery system. As the theory is extensive and was not applied directly in this thesis, further theory has not been provided. Suggestions for further reading to assist future development of CubeSat controlled re-entry and recovery systems can be found here [37][42][43][44][45][46][47].

The density of the flow medium also adds to the computational requirements of modelling-controlled re-entry and recovery. The air density can vary depending on the solar radiation cycle, and atmospheric winds and weather patterns. Some models which can be used to simulate atmospheric density, and are often inputs to the models cited above, include the COSPAR International Reference Atmosphere (CIRA-2012), MOWA Climatological Mode (DTM2013) [48], and the Jacchia-Roberts Atmospheric Density Model.

1.5 Existing CubeSat Controlled Re-entry and Recovery Technologies

Exploring the existing work done for controlled re-entry and recovery of CubeSats provided insight into the applications of the technology and challenges faced during development. The list includes the following re-entry projects and programs:

- The CAPE Project,
- The QARMAN QubeSat,
- The ADEPT device,
- The JAXA EGG device,
- The D3 device, and
- The Exo-break.

1.5.1 CAPE Project

CubeSat Atmospheric Probe for Education (CAPE) was a CubeSat program developed by the Institute of Space Systems (IRS) at the University of Stuttgart in Germany to create a new test bed for their Atmospheric Entry Module (AEM) called MIkro-RückkehrKApsel 2 / Micro Re-entry Capsule 2 (MIRKA2) [49]. The program aimed to develop useful payloads before integrating them into the final CAPE Service and De-orbit Module (SDM) CubeSat planned for the deployment from the ISS [49]. The SDM planned to de-orbit using an in-house developed Pulsed Plasma Thruster (PPT) [50] so that MIRKA2 could be released from an altitude of 125km [49]. A mission scenario example is provided by Starlinger et al. in Figure 1.1. The CAPE program has performed a series of precursor missions that are helping to validate the SDM and AEM modules. These precursor missions include MIRKA2-RX (REXUS), MIRKA2-HyEnD (Hybrid Engine Development) and MIRKA2-ICV (Iridium Communications Verification).

MIRKA2 is a CubeSat-sized re-entry vehicle designed to validate the behaviour of the Resin-Impregnated Carbon Ablator (RICA) TPS being developed at the University of Stuttgart [51]. Due to its behaviour, it uses the same shape as NASA's Re-Entry Breakup Recorder (REBR). Designed by the University of Stuttgart in Germany, its goal was to teach aerospace students about re-entry system design while developing a test platform for larger re-entry technology [49][51]. The capsule contains major space components such as an Inertial Measurement Unit

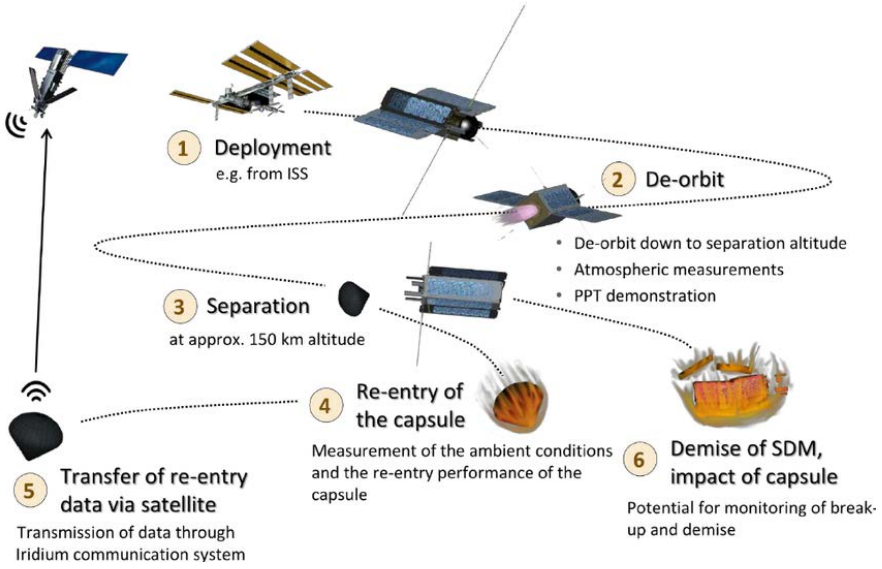

Figure 1.1: The CAPE mission scenario, showing the release of the AEM from the SDM. The AEM, also known as MIRKA2, is a CubeSat-sized re-entry capsule [49].

(IMU), batteries, and Global Positioning System (GPS), as well as multiple thermocouples, two dynamic pressure sensors and a radiometer. The capsule also had room for a secondary payload, although this has limited options available due to the shape of the free space [51].

Communications from the AEM was listed as a challenge of the re-entry mission, needing to transmit data before the collision with the Earth. It is a well-known phenomenon that during re-entry, the plasma shield created due to the rapid heating of the atmosphere restricts radio communications. As such, the MIRKA2 module used an Iridium 9603 data modem, the smallest Iridium transceiver available [51]. It was calculated that there was a 60-second window of communication for the AEM once it completed its blackout stage. Along with this short communication window, the transmitter will only be able to transmit at 35B/s [51]. This low data rate meant that the capsule needed to select the data it sends so that it may be located once hitting the ground. It is also specified that it is unlikely that the capsule will be able to transmit once landed due to its orientation [51].

Further detailing the work on MIRKA2, the IRS used an in-house simulation tool called REENT to simulate the re-entry trajectory [52]. These modelling tools can help optimise a re-entry body's shape and give the designer feedback on where to place critical sensors. This led to crucial changes early in the design of MIRKA2,

where more sensors needed to be added to verify the design. A focus on validating the RICA ablation material was done using these simulation tools to determine the best way to collect performance data. The sensor planned to validate the material was an ARAD sensor, TRL 6 sensors designed by NASA [52].

The MIRKA2-RX (REXUS) mission was a suborbital mission designed to test the onboard electronics of the re-entry capsule [36]. A dummy heat shield was used, as in comparison to the actual mission, very minimal heating would occur. The experiment was also designed to further assist the CAPE mission by testing the LOTUS (Low Orbit Technical Unit Separator), which will be used to deploy the CubeSat-sized re-entry pods from larger spacecraft [36]. The SDM will use a LOTUS to release and activate the AEM, so the RESUX mission was ideal for testing both systems. LOTUS uses a deactivation rod which the AEM slides onto to deactivate the power systems of the capsule. This rod qualifies the CubeSat for launch as it deactivates all power systems. LOTUS opens using spring systems and a burn wire to eject the AEM [36]. Unfortunately, during the REXUS test mission, the AEM did not activate appropriately until impacted with the ground. No testing data could be gathered from the mission [49].

Along with MIRKA2-RX, the CAPE program has also performed other verification tests. MIRKA2-HyEnD was another rocket launch test used to improve on the mistakes of the REXUS mission. However, problems still occurred with some of the units as the communication system failed before launch [49]. This contributed to the re-entry capsule modifications leading up to another suborbital test. MIRKA2-ICV was a high-altitude balloon test conducted in Cape Town in 2017. This was planned as another final test of the AEM, which had not been functioning correctly in previous tests. From the IRS website blog, it appears the AEM failed to power on once again, not providing enough data to verify the re-entry pod for the CAPE CubeSat.

The AEM still needs to complete a full re-entry test, and no CubeSat missions are planned. Information on the Nanosats Database [53] suggests that all CAPE missions have been cancelled. This indicates that the program was either not able to maintain funding or the results of its missions were made private. No information is available on the university website or social media.

1.5.2 QARMAN

QARMAN (QubeSat for Aerothermodynamic Research and Measurements on AblatioN) is an integrated 3U CubeSat designed by the Von Karman Institute in Belgium. The CubeSat (or "QubeSat") carries a variety of payloads that can characterise the CubeSats environment as it re-enters the Earth's atmosphere. Of the included payloads, there were thermocouples, pressure sensors, photodiodes, and spectrometers [54]. All the payloads were required to operate in the extreme re-entry environment and, as such, were qualified through an intense testing and qualification process before being integrated for launch. Isa Eray Akyol notes the iterations and changes made to some of the payloads post-testing [54]. Performing testing under various conditions, the qualification process was very detailed to ensure the survival of payloads during re-entry [33][54]. Extra care needed to be taken when designing re-entry system payloads to ensure the survival in the re-entry environment [54][55].

QARMAN was made to record the re-entry environment conditions on a cost-effective platform and demonstrate a test bed for re-entry materials and payloads. The CubeSat uses a new TPS made of P50 cork capable of protecting the CubeSat while gathering re-entry data [54]. The CubeSat was deployed from the ISS in February 2020, beginning its journey back to Earth. The planned mission profile was presented by Masutti et al. and can be seen in Figure 1.2 [33]. Before deployment from the ISS, the CubeSat was subject to extreme testing, including a plasma wind tunnel test. The mission description stated that once the CubeSat reaches its descent altitude, it will provide a wealth of knowledge to the research community regarding the environment of re-entering CubeSat-sized objects. Unfortunately, the Von Karman Institute has reported that the CubeSat did not de-orbit fast enough due to a reduction in solar activity at the time of launch. This resulted less atmospheric drag and caused the CubeSat to enter an unplanned extended illumination period which is predicted to have overheated the CubeSat and caused the power system to fail [35].

1.5.3 ADEPT

Adaptive Deployable Entry and Placement Technology (ADEPT) is an atmospheric entry device that has been under development at NASA since 2011

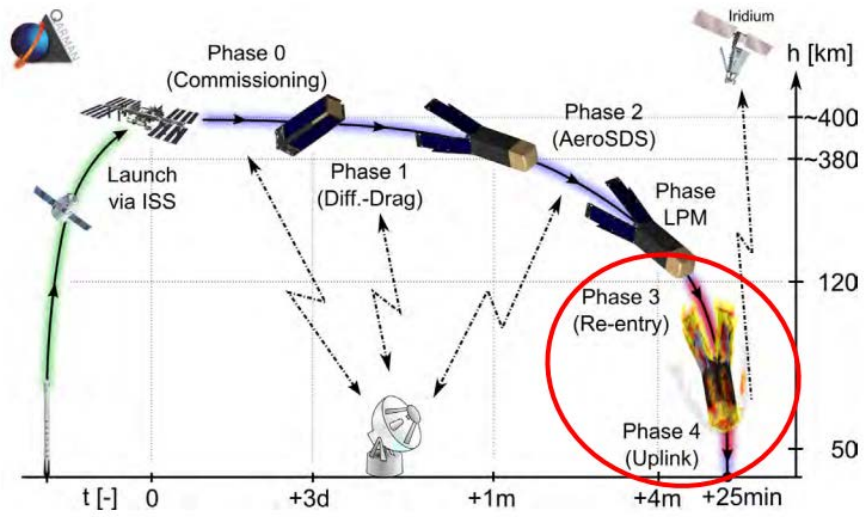

Figure 1.2: The planned QARMAN mission profile [33]. Unfortunately, the CubeSat did not re-enter Earth's atmosphere when expected and failed as a result of extended exposure to the Sun.

[56][57]. The design of ADEPT makes it suitable for a variety of mission sizes. However, the Nano-ADEPT is the design suited to the CubeSat form factor or mission classes of 5-15 kilograms [56]. This fits within the 3-12U CubeSat form factor. The design is intended to be up-scaled and is theorised to be capable of providing shielding to large re-entry vehicles in the future. The intended application for the technology is for entry onto terrestrial planets such as Venus, and Mars [58]. ADEPT uses multiple layers of a 3D woven carbon fabric that provides thermal protection and structure to the design. The shield is held in place by eight ribs that expand out using a spring system on the 3U variant and an electronic system on the 12U variant. The ribs are angled at 70 degrees to create a blunt shape typical to re-entry systems. The end nose cap holds the whole structure together and is covered in an ablative TPS. As a NASA project, ADEPT has been developed under a technology maturation strategy with four key pillars to ready the system for a launch. These pillars included:

- Deployment prototypes
- Subsonic Aeroloads Wind Tunnel
- System Level Arc Jet (SPRITE-C)

- Sounding Rocket Flight Test

Completing these pillars validates ADEPT for a CubeSat launch. Recent progressions in the program have led to the development of control flaps for the design. These will assist in controlling the landing location of ADEPT and are being developed to advance the technology further. Reference has been made to the possibility of using the Exo-break (Section 1.5.6) as a de-orbit technology to speed up testing [56].

The deployment prototypes for ADEPT used 3D printed structures, and a spring and lock mechanism to hold the ribs in place [56]. The design process is suitable in the early stages to test the deployment concept at a low cost. The designs helped to determine the fabric tension and size requirements for full-scale structures, as well as provide feedback on how to model the re-entry of the prototype design.

Subsonic Aeroloads Wind Tunnel testing took place at NASA Ames Research Centre in Moffett Field, California. The tunnel is a 7x10 foot, Mach 0.3, subsonic, atmospheric, closed-circuit single return tunnel. The test aimed to see the deflection of the fabric at different pre-tensions and angles of attack [59]. Knowledge of how much the material deflects is crucial for modelling the shape change in the shield at higher speeds. The test also helped to determine the best pre-tensions for the protection to minimise the amount of deflection in the mesh. The results showed some signs of fabric relaxation in the manufacturing process that needed to be improved for full-scale testing. Another concept tested by the wind tunnel experiment is that of directionality. It was shown that by varying the rib angle slightly, the angle of attack of ADEPT would change effectively, creating lift if used during re-entry, a similar effect to moving the centre of mass [59].

Small Probe Re-entry Investigation for TPS Engineering (SPRITE) is a newly developed test procedure for verifying the aerothermal functionality of re-entry devices. The SPRITE test was performed at NASA Ames arc jet facility [56][58]. SPRITE-C is the SPRITE test name for ADEPT, where a new structure having only an angle of attack of 55 degrees was used to verify the material performance. Seventy degrees could not be used as it would have a too large diameter for the flow diffuser of the arc jet [56]. The test first aimed to analyse the robustness

of the carbon fabric under two separate heat pulses from the arc jet, simulating aerocapture and re-entry heating. The other test included punching a 6mm hole through the fabric and assessing its integrity. Both tests showed that the TPS can function effectively under these conditions and that there was no compromise to the TPS [56][58].

The Sounding Rocket Flight Test (SR-1) was a suborbital performance test of the re-entry structure (Figure 1.3). The sounding rocket reached speeds of Mach 3 and provided a deployment and stability test of ADEPT [60][61]. The performance indicators were deployment in an entry configuration and supersonic aerodynamic stability without active control for ADEPT. The test resulted in full deployment and all vital signs being active, which achieved the first goal of the re-entry test. The second requirement of stability was fulfilled. ADEPT only exceeded its stability threshold of 20 degrees at approximately Mach 0.4 [60]. However, the test showed that the spin rate increased through the supersonic deceleration. This was not accounted for and was investigated post-experiment. The next step in developing this technology includes a re-entry and landing component for a complete controlled re-entry and recovery mission.

1.5.4 EGG

The Japanese Aerospace Exploration Agency (JAXA) has developed a Cube-Sat de-orbit system called re-Entry satellite with Gossamer aeroshell and GPS/iridium (EGG). The design uses an inflatable shell torus and membrane, which, once inflated, creates drag to increase the de-orbit speed and act as heat shielding during re-entry (Figure 1.4). It is predicted that from a standard ISS launch, the EGG will de-orbit in 12 days on average compared to 580 days if not deployed [62]. The first test flight of the EGG device also carried a modified faraday cup for attitude sensing. The sensor measured the rate of flow of ions in the upper atmosphere, enabling the operators to determine the directionality of the satellite as it came through the atmosphere. This was able to be used as an additional attitude determination system [62].

The EGG satellite was launched and tested in May of 2017, designed to de-orbit without propulsion and to survive up to an orbit height of 100km. The satellite provided data on the temperature profile of the inflatable aeroshell and supporting

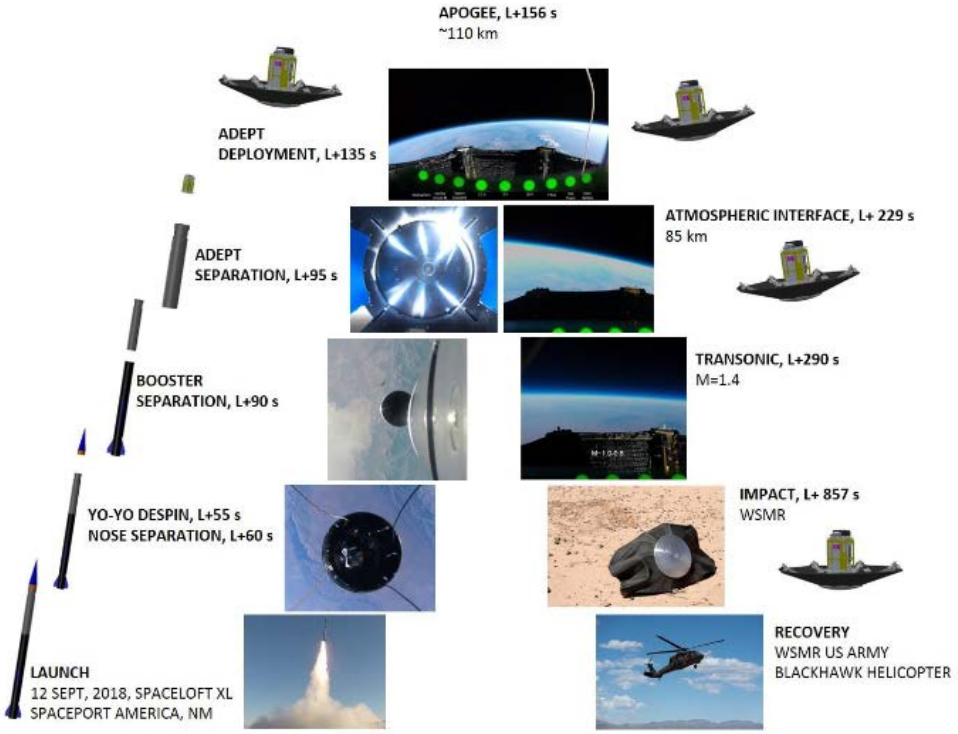

Figure 1.3: The ADEPT sounding rocket flight test profile [60].

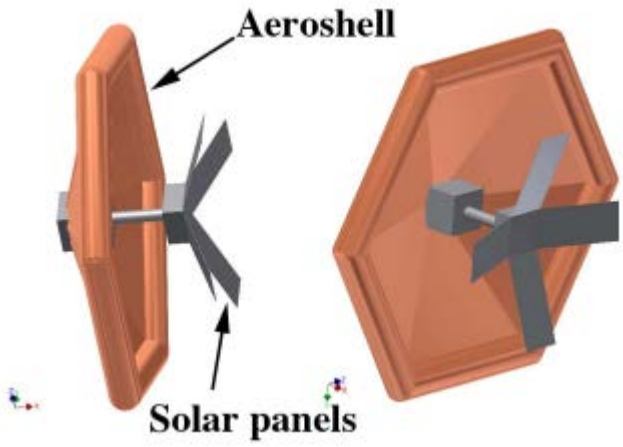

Figure 1.4: CAD Designs of the EGG CubeSat once the aeroshell has been deployed [62].

torus. This information was used to progress the technology to larger applications outside the CubeSat form factor [63]. The technology is being planned for use in other Earth re-entry applications and has recently been applied on the secondary Artemis 1 CubeSat, OMOTENASHI [63].

OMOTENASHI was a secondary payload on Artemis 1 launched by NASA as one of 10 CubeSat missions to the Moon [64]. The technology was applied as an inflatable crash shield to protect the CubeSat during a planned landing on the Moon. Although not the intended application of the technology, it shows how the inflatable drag device can be multi-purposed for numerous stages of the controlled re-entry and recovery process.

The inflatable design of EGG has been implemented before as part of the Membrane Aeroshell for Atmospheric-entry Capsule (MAAC). This Japanese-led work has also led to the development of larger re-entry systems called Titans. Following the results obtained from the EGG launch in 2017, work has been done to investigate how changing parameters affect the functionality of inflatable re-entry bodies. Investigations into the changing of aeroshell angle, torus material, and the effects of deformation on the membrane during re-entry have been performed [63][65][66][67]. All of these investigations will enable JAXA to develop a more extensive re-entry system for Earth's atmosphere. In its current state, however, the technology is not prepared to return valuable payloads to Earth. It can only assist in de-orbiting spacecraft faster, reducing space debris.

1.5.5 Drag De-orbit Device

The Drag De-orbit Device (D3) (Figure 1.5) is a boom-style drag modulator that relies on the trace atmosphere in LEO to de-orbit small spacecraft. Although D3 is not a complete re-entry system, what makes D3 stand out over other CubeSat de-orbit systems is its ability to extend and retract, making it controllable. This idea allows it to control a CubeSat re-entry as the point of entering the atmosphere can be targeted by varying the length of the booms. The system also aims to use its booms to passively control its attitude [68][69]. The concept has been developed by The University of Florida ADAMUS lab with funding from NASA and the Florida Space Research Initiative.

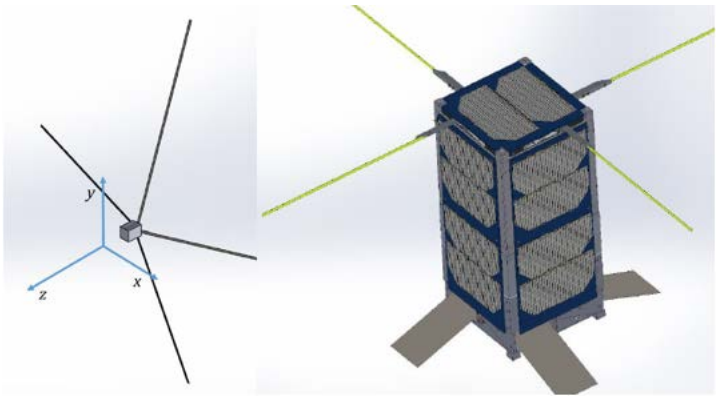

Figure 1.5: The D3 fully deployed (left) and partially stowed (right) CAD are pictured above. The design uses four deployable and retractable booms to control the re-entry rate, and attitude of the CubeSat [70].

The technology uses four booms that can extend and retract at 20 degrees to the normal face of each side of the CubeSat they are mounted to. Using four motors to drive each boom, the booms maintain rigidity by being folded, similar to a tape measure. The bending in the centre of the boom gives structural strength to each member while having a minimal effect on the ability of the boom to extend and retract. Each boom is 3.7m long and 4cm wide, a size chosen for its capability to de-orbit a 12U 15kg CubeSat from 700km altitude within 25 years [68][69]. The first demonstration mission will test the boom deployment systems using a CubeSat made from TRL 9 COTS subsystems. The mission aims to verify the D3 simulations and functionality in LEO [71][70]. The maiden test flight was delayed to the second half of 2022, and results still need to be published.

1.5.6 Exo-Break

Exo-break is a de-orbit technology developed and tested on the Technology Educational Satellite (TechEdSat) platforms. These CubeSats have been developed since 2012 as a collaboration between San Jose State University, Sweden's AAC Microtec, and NASA AMES Research centre. The initial goal was to improve student understanding of space systems, but more research objectives were included as this progressed. TechEdSat-3 was the first launch and test of the Exo-break in 2013 [72]. The original system only implemented a single deployed drag sail that caused the 3U CubeSat to de-orbit faster from the ISS than if it had no sail. This initial test has led to many more tests of the Exo-break with various configurations and other technology to include targeting capabilities [72].

Figure 1.6: The Exo-break technology as pictured after deployment from the ISS on TechEdSat 10. This version of the Exo-break was able to be controlled to manipulate the re-entry location [73]

Multiple tests of the Exo-break have been conducted through TechEdSat missions and SOAREX suborbital flights. TechEdSat-5 first tested the idea of changing the angle of attack of the Exo-Break using a winch to adjust the tension on the supporting cords affecting the surface area of the sail [74]. This test conducted in 2017 was first verified on the SOAREX-8 and 9 suborbital flights, which demonstrated the functionality of the systems in LEO, ensuring that the test could be recorded precisely [72]. Other TechEdSat launches post TechEdSat-5 include TechEdSat-6, which was launched in late 2017 and tested a finer accuracy de-orbit modulation system, TechEdSat-8 furthered the re-entry system by testing an automated re-entry targeting system to prepare for a controlled re-entry, and TechEdSat-10 (Figure 1.6) which was launched in early 2020, included a Thermal Protection System, to thoroughly test and observe the capability of Exo-break to return a payload from the ISS[75].

1.6 Pathway Towards Controlled Re-entry and Recovery

Following the investigation into existing controlled re-entry and recovery systems, a pathway towards controlled re-entry and recovery was developed. The pathway identifies a set of key challenges, that if solved can lead to the development of a capability able to perform the planetary science research objectives that require low cost controlled re-entry and recovery systems. The developed pathway

included four main challenges that needed to be solved. These four challenges were:

- The development of a reusable, capable, and cost-effective CubeSat platform for developing the required systems to meet the remaining challenges,

- The development of a system capable of tracking and verifying controlled re-entry and recovery technologies,

- The development of a controlled re-entry technology or technologies capable of targeting an atmospheric re-entry location, and

- The development of a landing and recovery system capable of surviving atmospheric re-entry and landing within a target landing zone.

If these challenges can be solved, then the combined effort of the technologies developed will be able to perform planetary research missions capable of targeting the long-term science objectives.

The first challenge, the development of a reusable, capable, and cost-effective CubeSat platform, was determined after an investigation into the available Commercial of The Shelf (COTS) CubeSat systems. The available CubeSat technology was identified as lacking for performing a complete CubeSat controlled re-entry and recovery mission. As such, a completely custom CubeSat platform needed to be developed if the controlled re-entry and recovery system was ever to be developed. This platform needed to be hardware cost-effective, reusable, contain ample payload space and have all the general system capabilities of a CubeSat. By meeting these goals, the CubeSat would be highly suited to frequent testing and development of the remaining technology challenges identified in this pathway.

The second challenge, the development of a re-entry tracking system, was identified when the testing methods of the existing systems became understood. One of the advantages of developing a highly cost-effective platform is the ability to

collect real data and perform physical re-entry tests rather than relying on purely theoretical analysis. The existing capabilities all relied on large budgets and single mission objectives without a programmatic focus to development. This meant that the missions all had a heavy theoretical basis were single mission success was critical. If the first challenge can be met successfully, then the reduced platform cost can be used to the full advantage to meet the third and fourth challenges. However, to observe the performance of the systems developed, a tracking system was required to demonstrate the other systems performance. This formed this challenge as if it can be solved, then the remaining challenges can be solved without requiring high levels of theoretical development as the reduced cost can absorb the risk of the developed system failing.

The third challenge, the development of a controlled re-entry technology, forms one of the more obvious technology challenges that needs to be solved to meet the planetary science objectives. If the previous two challenges can be solved, then both the cost effective and reusable platform merged with the re-entry tracking system can be used to develop a controlled re-entry system or systems. The system development process will need to investigate a variety of methods for controlled re-entry, including the methods previously identified in this chapter as well as any new ideas that emerge in the time before development is completed. Controlled re-entry will require some modelling and understanding of the re-entry physics. However, modelling accuracy can be reduced to test technologies in the real environment thanks to the completion of the previous two challenges. If this challenge can be solved, then the next challenge can be safely worked towards.

The final challenge, the development of a landing and recovery system, is the other more obvious development challenge. Once the other three challenges on the pathway have been solved, the final landing and recovery technology can be developed. Once a controlled re-entry and recovery system has been developed, the landing and recovery system can be safely tested through physical demonstrations rather than requiring complex modelling to develop the final objective. This can be highly beneficial, as due to the re-entry tracking system, live demonstration data can be collected to improve the technology during development rather than relying on assumption based theoretical simulations. If this final challenge can be overcome, then the planetary science objectives can begin to be met. Using

the landing and recovery capability, sample return and planetary investigation missions can be developed and executed to provide valuable planetary science knowledge.

The investigation into existing controlled re-entry and recovery systems assisted in creating a pathway towards controlled re-entry and recovery of CubeSats. Due to the complexity of the challenges identified only the first two challenges were investigated in this thesis. The first, being the development of a reusable and cost-effective platform, and the second being the development of a re-entry tracking system.

1.7 Overview of This Thesis

The contents of this thesis and the contributions of this doctorate are separated into four body chapters. Each chapter represents a significant step in developing the novel Binar CubeSat Bus, a platform capable of developing and testing controlled re-entry and recovery technologies. A conclusion and future work chapter is also included to provide guidance for future research projects and to summarise the contributions of this thesis.

1.7.1 Chapter 2

The first requirement for performing controlled re-entry and recovery missions using CubeSats was the need for a CubeSat platform. This chapter includes an overview of the custom design, assembly, integration, and testing approaches used for the Binar-1 CubeSat. A comparison is made to the designs of COTS CubeSats, highlighting the advantages of the Binar-1 custom design and how the resulting design met its target objectives.

1.7.2 Chapter 3

Deployed from the ISS on the 6^{th} of October 2021, Binar-1 was the first CubeSat mission built and delivered by Western Australia. This chapter includes a summary of the Binar-1 mission, its operations, mission results, and lessons learned. The implementations of these lessons learned were included in Chapter 5.

1.7.3 Chapter 4

To improve the capabilities of the BCB to be able to demonstrate controlled re-entry technologies, a method to track and observe the CubeSat re-entry location was required. The standard approach for tracking CubeSats is not accurate enough for this application, so an alternate solution was developed. This chapter details the design of a system that can track CubeSats just before they enter the atmosphere. To verify the solution's suitability, simulations were performed, highlighting the predicted availability and accuracy of the system in determining the final atmospheric re-entry location.

1.7.4 Chapter 5

The preliminary Binar-1 BCB only partially met the initial platform objectives due to the work efforts focusing on critical parts of the design. Learning from the Binar-1 mission, the critical design parts were improved, and the remaining objectives were implemented. This chapter includes the design and mission lifecycle improvements to the BCB for the Binar-2, 3, and 4 mission. The advances enable the final BCB to be a platform for carrying controlled re-entry and recovery technologies in the near future.

1.7.5 Chapter 6

This chapter summarises the thesis results and highlights the contributions made to the field. A future works section also identifies potential research and engineering projects which can begin controlled re-entry and recovery mission design and improve the CubeSat re-entry tracking system.

1.7.6 Other Contributions

This doctoral thesis includes the contributions that progress towards developing, testing, and performing controlled re-entry and recovery missions. However, three areas of work that formed a major contribution outside the scope of the thesis are not discussed elsewhere.

Many hours of work have gone into completing the paperwork necessary for delivering Binar-1 and beginning the process for Binar-2, 3, and 4. This was essential

engineering and project management work required for performing space missions and has been a tremendous learning experience for all team members involved. Passing this experience on and training new staff is now part of the process leading into Binar-2, 3, and 4. This work included:

- Developing system description documentation for launch providers and external parties,
- Liaising with the launch provider and supplying additional documentation to meet launch requirements,
- Creating design schematics and drawings to assist fabricators and manufacturers,
- Editing and maintaining safety review paperwork templates, and
- Completing engineering review presentations and documentations.

Essential for developing a space ecosystem in Western Australia, time spent writing articles, conducting interviews, and presenting at forums has been critical. This contribution has been important for inspiring younger engineers and sharing the Binar Space Program's achievements and future ambitions.

Building the workplace environment of the Binar Space Program as an inclusive and enjoyable environment for all involved has taken considerable effort. Ensuring the program can survive and sustain itself is essential for meeting the long-term objectives of this thesis. This team effort has assisted the Binar Space Program in growing from just three PhD students to a constantly growing team, all enthusiastic about the program's goals, in just under four years.

References

[1] J. Puig-Suari, C. Turner, and W. Ahlgren, "Development of the standard CubeSat deployer and a CubeSat class PicoSatellite," in *2001 IEEE Aerospace Conference Proceedings (Cat. No.01TH8542)*, vol. 1, Mar. 2001, 1/347–1/353 vol.1. DOI: 10.1109/AERO.2001.931726.

[2] H. Heidt, J. Puig-Suari, A. Moore, S. Nakasuka, and R. Twiggs, "CubeSat: A New Generation of Picosatellite for Education and Industry Low-Cost Space Experimentation," *Small Satellite Conference*, Aug. 2000. [Online]. Available: https://digitalcommons.usu.edu/smallsat/2000/All2000/32.

[3] "CubeSat 101: Basic Concepts and Processes for First-Time CubeSat Developers," en, *NASA CubeSat Launch Initiative*, p. 96, Oct. 2017. [Online]. Available: https://www.nasa.gov/sites/default/files/atoms/files/nasa_csli_cubesat_101_508.pdf.

[4] H. Polat, J. Virgili-Llop, and M. Romano, "Survey, Statistical Analysis and Classification of Launched CubeSat Missions with Emphasis on the Attitude Control Method," *Journal of Small Satellites*, vol. 5, pp. 513–530, Jan. 2016.

[5] M. Swartwout, "The first one hundred CubeSats: A statistical look," *Journal of Small Satellites*, vol. 2, pp. 213–233, Jan. 2014.

[6] A. Poghosyan and A. Golkar, "CubeSat evolution: Analyzing CubeSat capabilities for conducting science missions," en, *Progress in Aerospace Sciences*, vol. 88, pp. 59–83, Jan. 2017, ISSN: 0376-0421. DOI: 10.1016/j.paerosci.2016.11.002. [Online]. Available: http://www.sciencedirect.com/science/article/pii/S0376042116300951.

[7] "State-of-the-Art of Small Spacecraft Technology," English, Oct. 2021. [Online]. Available: http://www.nasa.gov/smallsat-institute/sst-soa.

[8] J. Crusan and C. Galica, "NASA's CubeSat Launch Initiative: Enabling broad access to space," en, *Acta Astronautica*, vol. 157, pp. 51–60, Apr. 2019, ISSN: 0094-5765. DOI: 10.1016/j.actaastro.2018.08.048. [Online]. Available: http://www.sciencedirect.com/science/article/pii/S0094576517303107.

[9] S. Higginbotham, *CubeSat Launch Initiative*, Library Catalog: NASA NTRS, Jan. 2016. [Online]. Available: https://ntrs.nasa.gov/search.jsp?R=20160002253.

[10] G. L. Skrobot, *Project ELaNa and NASA's CubeSat Initiative*, Library Catalog: NASA NTRS, Aug. 2010. [Online]. Available: https://ntrs.nasa.gov/search.jsp?R=20110001319.

[11] B. Betts, B. Nye, J. Vaughn, *et al.*, "LightSail 1 Mission Results and Public Outreach Strategies," en, *Fourth International Symposium on Solar Sailing*, p. 5, 2017.

[12] D. A. Spencer, B. Betts, J. M. Bellardo, A. Diaz, B. Plante, and J. R. Mansell, "The LightSail 2 solar sailing technology demonstration," en, *Advances in Space Research*, Jun. 2020, ISSN: 0273-1177. DOI: 10.1016/j.asr.2020.06.029. [Online]. Available: http://www.sciencedirect.com/science/article/pii/S027311772030449X.

[13] A. Klesh, B. Clement, C. Colley, *et al.*, "MarCO: Early Operations of the First CubeSats to Mars," *Small Satellite Conference*, Aug. 2018. [Online]. Available: https://digitalcommons.usu.edu/smallsat/2018/all2018/474.

[14] E. Dotto, V. Della Corte, M. Amoroso, *et al.*, "LICIACube - The Light Italian Cubesat for Imaging of Asteroids In support of the NASA DART mission towards asteroid (65803) Didymos," en, *Planetary and Space Science*, vol. 199, p. 105 185, May 2021, ISSN: 0032-0633. DOI: 10.1016/j.pss.2021.105185. [Online]. Available: https://www.sciencedirect.com/science/article/pii/S0032063321000246.

[15] T. R. Lockett, J. Castillo-Rogez, L. Johnson, *et al.*, "Near-Earth Asteroid Scout Flight Mission," *IEEE Aerospace and Electronic Systems Magazine*, vol. 35, no. 3, pp. 20–29, Mar. 2020, Conference Name: IEEE Aerospace and Electronic Systems Magazine, ISSN: 1557-959X. DOI: 10.1109/MAES.2019.2958729.

[16] *CORONA: The First Recovery of Film from Space — Central Intelligence Agency*, 2012. [Online]. Available: https://www.cia.gov/news-information/featured-story-archive/2012-featured-story-archive/corona-the-first-recovery-of-film-from-space.html (visited on 07/31/2020).

[17] *CORONA: Declassified — Central Intelligence Agency*, 2015. [Online]. Available: https://www.cia.gov/news-information/featured-story-archive/2015-featured-story-archive/corona-declassified.html (visited on 07/31/2020).

[18] D. E. Brownlee, P. Tsou, J. D. Anderson, *et al.*, "Stardust: Comet and interstellar dust sample return mission," en, *Journal of Geophysical Research: Planets*, vol. 108, no. E10, 2003, ISSN: 2156-2202. DOI: 10.1029/2003JE002087. [Online]. Available: https://agupubs.onlinelibrary.wiley.com/doi/abs/10.1029/2003JE002087%4010.1002/%28ISSN%292169-9100.STARDUST1.

[19] P. Tsou, "Stardust encounters comet 81P/Wild 2," en, *Journal of Geophysical Research*, vol. 109, no. E12, E12S01, 2004, ISSN: 0148-0227. DOI: 10.1029/2004JE002317. [Online]. Available: http://doi.wiley.com/10.1029/2004JE002317.

[20] H. Yano, T. Kubota, H. Miyamoto, *et al.*, "Touchdown of the Hayabusa Spacecraft at the Muses Sea on Itokawa," *Science*, vol. 312, no. 5778, pp. 1350–1353, Jun. 2006, Publisher: American Association for the Advancement of Science. DOI: 10.1126/science.1126164. [Online]. Available: https://www.science.org/doi/10.1126/science.1126164.

[21] T. Yada, M. Abe, T. Okada, *et al.*, "Preliminary analysis of the Hayabusa2 samples returned from C-type asteroid Ryugu," en, *Nature Astronomy*, vol. 6, no. 2, pp. 214–220, Feb. 2022, Number: 2 Publisher: Nature Publishing Group, ISSN: 2397-3366. DOI: 10.1038/s41550-021-01550-6. [Online]. Available: https://www.nature.com/articles/s41550-021-01550-6.

[22] Y. Tsuda, M. Yoshikawa, M. Abe, H. Minamino, and S. Nakazawa, "System design of the Hayabusa 2—Asteroid sample return mission to 1999 JU3," en, *Acta Astronautica*, vol. 91, pp. 356–362, Oct. 2013, ISSN: 0094-5765. DOI: 10.1016/j.actaastro.2013.06.028. [Online]. Available: https://www.sciencedirect.com/science/article/pii/S009457651300218X.

[23] D. S. Lauretta, S. S. Balram-Knutson, E. Beshore, *et al.*, "OSIRIS-REx: Sample Return from Asteroid (101955) Bennu," en, *Space Science Reviews*, vol. 212, no. 1, pp. 925–984, Oct. 2017, ISSN: 1572-9672. DOI: 10.1007/s

11214-017-0405-1. [Online]. Available: https://doi.org/10.1007/s11214-017-0405-1.

[24] C. W. Hergenrother, C. K. Maleszewski, M. C. Nolan, *et al.*, "The operational environment and rotational acceleration of asteroid (101955) Bennu from OSIRIS-REx observations," en, *Nature Communications*, vol. 10, no. 1, p. 1291, Mar. 2019, Number: 1 Publisher: Nature Publishing Group, ISSN: 2041-1723. DOI: 10.1038/s41467-019-09213-x. [Online]. Available: https://www.nature.com/articles/s41467-019-09213-x.

[25] *NASA - NSSDCA - Hayabusa2 - Details*. [Online]. Available: https://nssdc.gsfc.nasa.gov/nmc/spacecraft/display.action?id=2014-076A (visited on 12/21/2022).

[26] *Cost of OSIRIS-REx*, en. [Online]. Available: https://www.planetary.org/space-policy/cost-of-osiris-rex (visited on 12/21/2022).

[27] I. Crawford, "The scientific legacy of Apollo," en, *Astronomy and Geophysics*, vol. 53, no. 6, pp. 6.24–6.28, Dec. 2012, ISSN: 1366-8781. DOI: 10.1111/j.1468-4004.2012.53624.x. [Online]. Available: https://ui.adsabs.harvard.edu/abs/2012A&G....53f..24C/abstract.

[28] *NASA: Apollo 50th Anniversary*. [Online]. Available: https://www.nasa.gov/specials/apollo50th/index.html (visited on 01/05/2023).

[29] D. S. Burnett, "NASA Returns Rocks from a Comet," *Science*, vol. 314, no. 5806, pp. 1709–1710, Dec. 2006, Publisher: American Association for the Advancement of Science. DOI: 10.1126/science.1137084. [Online]. Available: https://www.science.org/doi/10.1126/science.1137084.

[30] D. Kessler, N. Johnson, J.-C. Liou, and M. Matney, "The Kessler Syndrome: Implications to Future Space operations," *Advances in the Astronautical Sciences*, vol. 137, Jan. 2010.

[31] L. Qiao, C. Rizos, and A. G. Dempster, "Analysis and Comparison of CubeSat Lifetime," in *Proceedings of the 12th Australian Space Research Conference*, 2013, pp. 249–260.

[32] "FCC adopts new '5-year rule' for deorbiting satellites." (Sep. 29, 2022), [Online]. Available: https://www.fcc.gov/document/fcc-adopts-new-5-year-rule-deorbiting-satellites (visited on 08/03/2023).

[33] D. Masutti, E. Trifoni, E. Umit, *et al.*, *QARMAN re-entry CubeSat : Preliminary Results of SCIROCCO Plasma Wind Tunnel Testing*, en, Jun. 2018. [Online]. Available: https://www.colorado.edu/event/ippw2018/sites/default/files/attached-files/30_-_qarman_ippw_2018_v1.pdf.

[34] E. Gill, P. Sundaramoorthy, J. Bouwmeester, B. Zandbergen, and R. Reinhard, "Formation flying within a constellation of nano-satellites: The QB50 mission," en, *Acta Astronautica*, 6th International Workshop on Satellite Constellation and Formation Flying, vol. 82, no. 1, pp. 110–117, Jan. 2013, ISSN: 0094-5765. DOI: 10.1016/j.actaastro.2012.04.029. [Online]. Available: http://www.sciencedirect.com/science/article/pii/S0094576512001440 (visited on 07/30/2020).

[35] *QARMAN - QubeSat for Aerothermodynamic Research and Measurements on AblatioN*. [Online]. Available: https://www.vki.ac.be/index.php/qarman-home (visited on 12/16/2022).

[36] S. Wizemann, M. Ehresmann, A. Pagan, *et al.*, "MICRO-REENTRY-CAPSULE-2(MIRKA2) REXUS," Dec. 2015. [Online]. Available: https://www.researchgate.net/publication/305806796_MICRO-REENTRY-CAPSULE-2MIRKA2_REXUS#fullTextFileContent.

[37] S. F. Rafano Carná and R. Bevilacqua, "High fidelity model for the atmospheric re-entry of CubeSats equipped with the drag de-orbit device," *Acta Astronautica*, vol. 156, pp. 134–156, Mar. 1, 2019, ISSN: 0094-5765. DOI: 10.1016/j.actaastro.2018.05.049. [Online]. Available: https://www.sciencedirect.com/science/article/pii/S009457651731336X (visited on 08/17/2023).

[38] T. Liang, K. Nie, Q. Li, and J. Zhang, "Advanced analytical model for orbital aerodynamic prediction in LEO," *Advances in Space Research*, vol. 71, no. 1, pp. 507–524, Jan. 1, 2023, ISSN: 0273-1177. DOI: 10.1016/j.asr.2022.09.005. [Online]. Available: https://www.sciencedirect.com/science/article/pii/S027311772200847X (visited on 08/17/2023).

[39] G. E. Cook, "The effect of aerodynamic lift on satellite orbits," *Planetary and Space Science*, vol. 12, no. 11, pp. 1009–1020, Nov. 1, 1964, ISSN: 0032-0633. DOI: 10.1016/0032-0633(64)90077-7. [Online]. Available: https:

//www.sciencedirect.com/science/article/pii/0032063364900777 (visited on 08/18/2023).

[40] J. Ashenberg, "On the effects of time-varying aerodynamical coefficients on satellite orbits," *Acta Astronautica*, vol. 38, no. 2, pp. 75–86, Jan. 1, 1996, ISSN: 0094-5765. DOI: 10.1016/0094-5765(96)00002-1. [Online]. Available: https://www.sciencedirect.com/science/article/pii/0094576596000021 (visited on 08/18/2023).

[41] S. Ramjatan, N. Fitz-Coy, and A. Yew, "Magnus effect on a spinning satellite in low earth orbit," in *AIAA/AAS Astrodynamics Specialist Conference*, ser. AIAA SPACE Forum, American Institute of Aeronautics and Astronautics, Sep. 9, 2016. DOI: 10.2514/6.2016-5257. [Online]. Available: https://arc.aiaa.org/doi/10.2514/6.2016-5257 (visited on 08/18/2023).

[42] J. O. Murcia Piñeros, W. A. dos Santos, and A. F.B.A. Prado, "Analysis of the orbit lifetime of CubeSats in low earth orbits including periodic variation in drag due to attitude motion," *Advances in Space Research*, vol. 67, no. 2, pp. 902–918, Jan. 15, 2021, ISSN: 0273-1177. DOI: 10.1016/j.asr.2020.10.024. [Online]. Available: https://www.sciencedirect.com/science/article/pii/S0273117720307523 (visited on 08/17/2023).

[43] R. G. Wilmoth, R. A. Mitcheltree, and J. N. Moss, "Low-density aerodynamics of the stardust sample return capsule," *Journal of Spacecraft and Rockets*, vol. 36, no. 3, pp. 436–441, May 1999, Publisher: American Institute of Aeronautics and Astronautics, ISSN: 0022-4650. DOI: 10.2514/2.3464. [Online]. Available: https://arc.aiaa.org/doi/10.2514/2.3464 (visited on 08/18/2023).

[44] G. E. Cook, "Satellite drag coefficients," *Planetary and Space Science*, vol. 13, no. 10, pp. 929–946, Oct. 1, 1965, ISSN: 0032-0633. DOI: 10.1016/0032-0633(65)90150-9. [Online]. Available: https://www.sciencedirect.com/science/article/pii/0032063365901509 (visited on 08/18/2023).

[45] K. Moe and M. M. Moe, "Gas–surface interactions and satellite drag coefficients," *Planetary and Space Science*, vol. 53, no. 8, pp. 793–801, Jul. 1, 2005, ISSN: 0032-0633. DOI: 10.1016/j.pss.2005.03.005. [Online].

Available: https://www.sciencedirect.com/science/article/pii/S0032063305000486 (visited on 08/18/2023).

[46] D. Mostaza Prieto, B. P. Graziano, and P. C. E. Roberts, "Spacecraft drag modelling," *Progress in Aerospace Sciences*, vol. 64, pp. 56–65, Jan. 1, 2014, ISSN: 0376-0421. DOI: 10.1016/j.paerosci.2013.09.001. [Online]. Available: https://www.sciencedirect.com/science/article/pii/S0376042113000754 (visited on 08/18/2023).

[47] S. Livadiotti, N. H. Crisp, P. C. E. Roberts, *et al.*, "A review of gas-surface interaction models for orbital aerodynamics applications," *Progress in Aerospace Sciences*, vol. 119, p. 100 675, Nov. 1, 2020, ISSN: 0376-0421. DOI: 10.1016/j.paerosci.2020.100675. [Online]. Available: https://www.sciencedirect.com/science/article/pii/S0376042120300877 (visited on 08/18/2023).

[48] D. R. Jackson, S. Bruinsma, S. Negrin, *et al.*, "The space weather atmosphere models and indices (SWAMI) project: Overview and first results," *Journal of Space Weather and Space Climate*, vol. 10, p. 18, 2020, Publisher: EDP Sciences, ISSN: 2115-7251. DOI: 10.1051/swsc/2020019. [Online]. Available: https://www.swsc-journal.org/articles/swsc/abs/2020/01/swsc190071/swsc190071.html (visited on 08/18/2023).

[49] V. Starlinger, A. Behnke, J.-P. Baumann, *et al.*, "Increasing the Success of CAPE using Precursor Missions," Apr. 2017. [Online]. Available: https://www.researchgate.net/publication/316788037_Increasing_the_Success_of_CAPE_using_Precursor_Missions.

[50] A. Pagan, M. Fugmann, and G. Herdrich, "A System Approach towards a Miniaturized Pulsed Plasma Thruster for a CubeSat-Type Deorbit Module," Sep. 2014. [Online]. Available: https://www.researchgate.net/publication/280084980_A_System_Approach_towards_a_Miniaturized_Pulsed_Plasma_Thruster_for_a_CubeSat-Type_Deorbit_Module.

[51] M. Ehresmann, A. Behnke, J.-P. Baumann, *et al.*, "CubeSat-sized Re-entry Capsule MIRKA2," Apr. 2015. [Online]. Available: https://www.researchgate.net/publication/305807017_CubeSat-sized_Re-entry_Capsule_MIRKA2.

[52] G. Herdrich, J.-P. Baumann, P. Geissler, *et al.*, "MIRKA2: SMALL RE-ENTRY DEMONSTRATOR FOR ADVANCED MINIATURIZED SENSORS," Oct. 2012. [Online]. Available: https://www.researchgate.net/publication/351786281_MIRKA2_SMALL_RE-ENTRY_DEMONSTRATOR_FOR_ADVANCED_MINIATURIZED_SENSORS.

[53] E. Kulu, *Nanosats Database*, en. [Online]. Available: https://www.nanosats.eu/index.html (visited on 12/19/2022).

[54] I. Akyol, "Design of Data Acquisition Subsystem of QARMAN Payloads and Validation in Plasma Facilities-Hardware," Ph.D. dissertation, Aug. 2013. DOI: 10.13140/2.1.1098.1125.

[55] M. Aksulu, "Design of Data Acquisition System of QARMAN Subsystems and Validation in Plasma Facilities – Software," Ph.D. dissertation, Sep. 2013.

[56] B. Smith, A. Cassell, C. Kruger, E. Venkatapathy, C. Kazemba, and K. Simonis, "Nano-ADEPT: An entry system for secondary payloads," in *2015 IEEE Aerospace Conference*, ISSN: 1095-323X, Mar. 2015, pp. 1–11. DOI: 10.1109/AERO.2015.7119095.

[57] A. Cassell, *ADEPT for Interplanetary Small Satellite Missions*, Library Catalog: NASA NTRS, Apr. 2019. [Online]. Available: https://ntrs.nasa.gov/search.jsp?R=20190004912.

[58] A. Cassell, B. Smith, P. Wercinski, *et al.*, "ADEPT, A Mechanically Deployable Re-Entry Vehicle System, Enabling Interplanetary CubeSat and Small Satellite Missions," in *Small Satellite Conference*, Aug. 2018. [Online]. Available: https://digitalcommons.usu.edu/smallsat/2018/all2018/265.

[59] B. Smith, B. Yount, C. Kruger, *et al.*, "Nano-ADEPT aeroloads wind tunnel test," in *2016 IEEE Aerospace Conference*, Mar. 2016, pp. 1–20. DOI: 10.1109/AERO.2016.7500719.

[60] A. Cassell, *ADEPT Sounding Rocket One (SR-1) Flight Test*, Library Catalog: NASA NTRS, Sep. 2019. [Online]. Available: https://ntrs.nasa.gov/search.jsp?R=20190031937.

[61] P. Wercinski, B. Smith, B. Yount, *et al.*, "ADEPT sounding rocket one (SR-1) flight experiment overview," in *2017 IEEE Aerospace Conference*, Mar. 2017, pp. 1–7. DOI: 10.1109/AERO.2017.7943889.

[62] Y. Watanabe, K. Suzuki, O. Imamura, and K. Yamada, "Attitude Estimation of Nano-satellite with Deployable Aeroshell during Orbital Decay," en, *TRANSACTIONS OF THE JAPAN SOCIETY FOR AERONAUTICAL AND SPACE SCIENCES, AEROSPACE TECHNOLOGY JAPAN*, vol. 14, no. ists30, Pf_1–Pf_5, 2016, ISSN: 1884-0485. DOI: 10.2322/tastj.14.Pf_1. [Online]. Available: https://www.jstage.jst.go.jp/article/tastj/14/ists30/14_Pf_1/_article.

[63] Y. Takahashi and K. Yamada, "Aerodynamic heating of inflatable aeroshell in orbital reentry," en, *Acta Astronautica*, vol. 152, pp. 437–448, Nov. 2018, ISSN: 0094-5765. DOI: 10.1016/j.actaastro.2018.08.003. [Online]. Available: http://www.sciencedirect.com/science/article/pii/S0094576518306891.

[64] T. Hashimoto, T. Yamada, M. Otsuki, *et al.*, "Nano Semihard Moon Lander: OMOTENASHI," *IEEE Aerospace and Electronic Systems Magazine*, vol. 34, no. 9, pp. 20–30, Sep. 2019, Conference Name: IEEE Aerospace and Electronic Systems Magazine, ISSN: 1557-959X. DOI: 10.1109/MAES.2019.2923311.

[65] Y. Takahashi, T. Koike, N. Oshima, and K. Yamada, "Aerothermodynamic analysis for deformed membrane of inflatable aeroshell in orbital reentry mission," en, *Aerospace Science and Technology*, vol. 92, pp. 858–868, Sep. 2019, ISSN: 1270-9638. DOI: 10.1016/j.ast.2019.06.047. [Online]. Available: http://www.sciencedirect.com/science/article/pii/S1270963819311137.

[66] Y. Zhao, H. Liu, Z. Liu, and C. Yan, "Numerical study of the cone angle effects on transition and convection heat transfer for hypersonic inflatable aerodynamic decelerator aeroshell," en, *International Communications in Heat and Mass Transfer*, vol. 110, pp. 104–406, Jan. 2020, ISSN: 0735-1933. DOI: 10.1016/j.icheatmasstransfer.2019.104406. [Online]. Available: http://www.sciencedirect.com/science/article/pii/S0735193319302726.

[67] K. Matsumaru, M. Tanaka, O. Imamura, and K. Yamada, "Thermal-durability Evaluation of Inflatable Structure for a Deployable Aeroshell Using ICP Heater," en, *TRANSACTIONS OF THE JAPAN SOCIETY FOR AERONAUTICAL AND SPACE SCIENCES, AEROSPACE TECHNOL-*

OGY JAPAN, vol. 16, no. 6, pp. 520–527, 2018, ISSN: 1884-0485. DOI: 10.2322/tastj.16.520. [Online]. Available: https://www.jstage.jst.go.jp/article/tastj/16/6/16_520/_article.

[68] D. Guglielmo, S. Omar, R. Bevilacqua, *et al.*, "Drag Deorbit Device: A New Standard Reentry Actuator for CubeSats," *Journal of Spacecraft and Rockets*, vol. 56, no. 1, pp. 129–145, 2019, ISSN: 0022-4650. DOI: 10.2514/1.A34218. [Online]. Available: https://doi.org/10.2514/1.A34218.

[69] T. Martin, S. Omar, and R. Bevilacqua, "Controlled Spacecraft Re-Entry of a Drag De-Orbit Device (D3)," en, *UF Journal of Undergraduate Research*, vol. 21, no. 1, Dec. 2019, Number: 1, ISSN: 2638-0668. DOI: 10.32473/ufjur.v21i1.108233. [Online]. Available: https://journals.flvc.org/UFJUR/article/view/108233.

[70] S. Omar, D. Guglielmo, G. Mauro, T. Martin, and R. Bevilacqua, "CubeSat Mission to Demonstrate Aerodynamically Controlled Re-Entry using the Drag De-Orbit Device (D3)," *Small Satellite Conference*, Aug. 2018. [Online]. Available: https://digitalcommons.usu.edu/smallsat/2018/all2018/335.

[71] S. R. Omar and R. Bevilacqua, "Hardware and GNC solutions for controlled spacecraft re-entry using aerodynamic drag," en, *Acta Astronautica*, vol. 159, pp. 49–64, Jun. 2019, ISSN: 0094-5765. DOI: 10.1016/j.actaastro.2019.03.051. [Online]. Available: http://www.sciencedirect.com/science/article/pii/S0094576519300359.

[72] M. Murbach, R. Alena, and A. Luna, "The TechEdSat/PhoneSat Missions for Small Payload Quick Return," *Small Satellite Conference*, Aug. 2016. [Online]. Available: https://digitalcommons.usu.edu/smallsat/2016/S7Comm/6.

[73] F. Tavares, *TechEdSat-10 Deploys from the Space Station*, und, Text, Aug. 2020. [Online]. Available: http://www.nasa.gov/image-feature/ames/techedsat-10-deploys (visited on 12/19/2022).

[74] M. S. P. Murbach, *Modeling the Exo-Brake and the Development of Strategies for De-Orbit Drag Modulation*, Library Catalog: NASA NTRS, Jun. 2016. [Online]. Available: https://ntrs.nasa.gov/search.jsp?R=20160008903.

[75] M. S. P. Murbach, *Modulated Exo-Brake Flight Testing - Modeling and Test Results - Successes with Exo-Brake Development and Targeting for Future Sample Return Capability: TES-6,7,8 Flight Experiments*, Library Catalog: NASA NTRS, Jun. 2019. [Online]. Available: https://ntrs.nasa.gov/search.jsp?R=20190028931.

Chapter 2

Design, Assembly, Integration, and Testing of the Binar-1 CubeSat

Small satellites have become the preferred method for performing entry-level space missions in the new millennium [76]. The ability to reduce mass and maintain capability has become the focal point for reducing launch costs and increasing access to space. As the use of small satellites increases, the need to develop miniaturised technologies capable of meeting the same objectives as larger spacecraft has become necessary. The primary motivation for this work is to improve controlled re-entry and recovery methods for small satellites. As an essential part of expensive planetary research missions, improving controlled re-entry and recovery methods for small satellites can provide more opportunities for sample collection and return and Entry, Descent, and Landing (EDL) on the surface of extra-terrestrial planets and moons. The ability to apply the benefits of small satellites and reduce the cost of these missions can significantly boost planetary research and the understanding of the Solar System.

To develop the necessary technology, first, a platform must be selected. Before the 2000s, the options were limited, with space research being expensive. In the new millennium, however, this has changed with the further development of microelectronics and the foundation of the small satellite form factor, the CubeSat [76]. They are now used in nearly every university class space mission for per-

forming valuable research and providing educational opportunities. The idea of the CubeSat was formed from the concept of rocket ride share and standardisation to reduce launch costs. The compact 10 x 10 x 10 cm units or U that make up CubeSat structures have made it easy to standardise deployment pods that can be mounted on rockets purposed for other larger space missions [2]. Being the popular choice for many small satellite developers, the CubeSat was selected as the platform for technology development. This contributed to the central research topic of progressing towards controlled re-entry and recovery of CubeSats.

After choosing CubeSats as the platform for space research, a design decision needed to be made. Opting to use Commercial Off the Shelf (COTS) CubeSat subsystems or custom design them from scratch was a significant consideration. COTS offers convenience and may reduce development time. However, using the large PC104 headers and single board subsystems results in CubeSats being larger than necessary. Additionally, COTS subsystems with space heritage are expensive for new teams with minimal funding. The dependence on COTS subsystems can be costly for groups wishing to implement a program of repeat missions rather than a one-off science experiment. A combination of these primary challenges meant a COTS CubeSat design was unsuitable when considering the number of missions that would be required for demonstrating all phases of controlled re-entry and recovery.

Discovering this early in the design process, the decision was made to custom design the CubeSat with objectives focused on reducing hardware costs and maximising payload space while not removing system capabilities. These objectives targeted implementing a repeatable mission program for space research rather than a singular science experiment. The result of this work formed the Binar Space Program, a CubeSat launch program focused on developing and launching its CubeSat platform for enabling planetary research, space education, and technology demonstration. Binar is the word for “Fireball” or “Meteor” in the Noongar (Aboriginal Australian peoples of southwestern Australia) language, acknowledging the fate of all CubeSats launched into Low Earth Orbit (LEO), and the history of Western Australia.

This chapter describes how the custom design, assembly, integration, and test-

ing of the Binar-1 CubeSat progresses towards testing controlled re-entry and recovery technologies for CubeSats. The chapter first details the existing design processes that are standard practice for university CubeSat missions highlighting the strengths and weaknesses and explaining the motivation for the initial Binar-1 custom design decision. Next, the methodology for meeting the design objectives is presented in two sections. First, the custom-designed Binar systems, and interfaces with other systems, are documented. This section provides a detailed overview of the design methodologies used when considering hardware cost reduction and payload space maximisation at a minimal trade-off to system capability. Second, the assembly, integration, and testing processes are documented to show the ability of the CubeSat to meet launch requirements and be delivered for launch. The final section of the chapter provides the results and a discussion on the design of the Binar-1 CubeSat. This section explains how the design objectives were met and how the platform compares to COTS subsystem alternatives, justifying the initial motivation.

2.1 Motivation for a Custom Design

According to the Nanosats Database, as of the 1st of August 2022, there have been 1897 CubeSats launched from a variety of global industry, military, and university groups [53]. The design approaches differ between applications. For industry and defence CubeSats, complete CubeSat solutions or busses are typically purchased alongside integration services delivering the payload to space for its commercial or defence objective. This process is expensive, and without significant financial backing, universities are typically not able to afford this. The company leading in this development is Tyvak, supplying over 215 CubeSats to industry and government contractors [77]. Many universities instead opt for a custom design approach that involves purchasing individual COTS subsystems. COTS often refers to consumer electronics in other technology areas. For CubeSats, it can also refer to entire satellite subsystems. These subsystems are typically integrated using the PC104 standard headers and can be used to complete the mission objective when merged with a payload. This approach is generally cheaper than purchasing the complete CubeSat assembly and integration solution and can reduce mission risk and development time. Although when investigating the use of these COTS CubeSat subsystems in CubeSat designs, it was discovered that these benefits were only sometimes achieved.

First-time university CubeSat developers have mentioned challenges when integrating COTS subsystems. The common approach used by first-time teams was to separate each subsystem and assign a group of students to research and purchase a COTS solution. This was often found to result in a different supplier being used for each subsystem, ultimately leading to integration challenges. A recent review of the integration process of three different PC104-based COTS CubeSat subsystems detailed these integration challenges. Cho et al. mention the integration of these subsystems being limited by the communication between multiple microcontrollers located on each subsystem [78]. These microcontrollers all used different variations of the same communication protocol leading to many integration challenges.

Another common challenge was associated with the limited customisation of COTS systems. Once purchased, if mission requirements changed, the subsystems could not be altered to reflect the changes. The developers of the ALBus CubeSat have mentioned charging difficulties with a COTS battery before launch. Due to a requirement change, the battery was unintentionally damaged leading to a delay in the mission schedule [79].

Similarly, the ITASAT and INCA mission developers have mentioned the need to work closely with COTS vendors to ensure the quality of purchases and delivery of appropriate documentation. This adds to the mission workload and integration schedule if new student teams need to become more familiar with the process [80][81]. IDEASSat mentions in its lessons learned the need to collect and vet COTS subsystem test reports [82]. If COTS subsystems are not correctly designed and tested for all possible launch opportunities, changing launch providers or requirements can result in the subsystems not being usable.

Using the PC104 standard headers for integrating COTS subsystems is not space-optimised for use with CubeSats. Initially proposed by the early CubeSat developers in the 2000s as a simple solution to building CubeSats, COTS suppliers still use the headers today. This challenge is not integration critical. However, the connectors are enormous compared to newer compact solutions used in modern-day electronics such as smartphones. The headers occupy >10% of the COTS subsystems PBCs, which could be used for more electronics to improve capabil-

ity. Other university CubeSat teams have commented on the use of the PC104 headers. Both the OreSat and STU-2 CubeSat mission developers describe the PC104 headers as being outdated and inefficient for newer CubeSats leading to a custom design approach [83][84].

The alternative to using COTS subsystems for CubeSat design is to perform a custom design. Although this methodology is more time intensive, it does offer the benefit of providing added educational experience to students in electronics and hardware design. Alongside this, an environment for innovation can be created, leading to new and novel design ideas for CubeSats that can further improve the capabilities of CubeSats. The integration and usage of the PC104 header challenges can also be prevented when using this design approach. Although the development cost may be increased for the first design iteration, the cost can be reduced on subsequent launches if the designed platform is reused. The MiTEE-1 and ABEX mission dvelopers comment on the unique opportunity students received when working on the CubeSats [85][86], recognising the benefits of a custom design.

Having reviewed the two different CubeSat design approaches, a custom design approach was chosen due to the existing engineering and technology development experience within the founding team of doctoral students and the university's Desert Fireball Network [87] closely linked to the team. Using this experience, the risks of extended development time and technology integration challenges could be mitigated. Additionally, with the intent to sustain a long-term program of space launches required for developing controlled re-entry and recovery technologies for CubeSats, the reduced hardware cost and customizability of a custom design were seen to be beneficial. As such, the decision to perform a custom design was able to better meet the long-term launch requirements.

How to Read the Following Two Sections

Due to the complexity of designing, integrating, and testing a CubeSat, the work performed in designing Binar-1 was not completed by an individual but rather by a small team of PhD students and engineers. The process lasted nearly two and a half years of full-time effort, constituting a large portion of the work completed as part of this PhD. To provide context to the complete design, subsections are

included that were not the sole contribution of the author. To identify which work was performed by the author, percentage contributions are included in the heading of each section.

2.2 Design of Binar-1

The custom design of Binar-1 began after the benefits were identified. The primary objectives of the design were:

- Reduce hardware cost,
- Maximise payload space, and
- Maintain system capabilities

To meet these objectives, one of the main outputs was the Binar CubeSat Core (BCC). It is a fully integrated Electrical Power System (EPS), Attitude Determination and Control System (ADCS) and flight computer system that has been tested together throughout its development lifetime. Also, custom designed to meet the design objectives was the Binar structure and Binar software framework. The communications system was the only system not included in the custom design. This was excluded so that the focus of the first mission could be put into the BCCs design, intending to have a custom communications system on the next mission. The payload consisted of two COTS cameras, one for star tracking and the other for Earth imagery.

The complete design of Binar-1 is explained by being separated into its critical subsystems. The BCC contains the EPS, ADCS and flight computer system (Also known as the On-board Data Handling System). These three systems were designed, integrated, and tested together in parallel. Next, the COTS Ultra High Frequency (UHF) transceiver and payload were combined with the bus through the payload and communications adapter board. The transceiver connected directly to the adapter board using the PC104 standard headers, while the payload was connected to the board using a Flat Flexible Connector (FFC). These three main parts of the CubeSat stack were all housed in the custom designed struc-

ture and enclosed by the base plate, four 1U solar panels and the COTS UHF antenna. The final part of the complete Binar-1 design is the software. It was also designed by the Binar Space Program as part of another doctoral project. An exploded view of the design is presented in Figure 2.1 along with the designs power and control system block diagrams in Figure 2.2.

The last prominent feature of the Binar-1 design was that an engineering model could be built for on-the-ground testing due to its low cost. University-level missions often do not report using an engineering model due to the high cost of duplicating COTS subsystems. Typically all funding is used for the flight model instead. The engineering model was built as close to identical as possible. The only difference was the COTS UHF transceiver. To reduce the engineering model cost, a lower-power version was purchased instead. Before the flight model assembly, the engineering model was used to test the BCC and its integration with the other systems. The engineering model was an essential part of operations. Any unexpected operation states could be tested on the engineering model before attempting to communicate with the flight model in orbit.

2.2.1 Design Requirements

External to the three primary design objectives of the custom Binar CubeSat were a set of design requirements. These requirements needed to be met for successful qualification for launch and to meet the mission objectives. A summary of these requirements is provided to add additional context to some of the design decisions for Binar-1. As this was the first Binar mission, the design requirements were not formally set as with more advanced space missions and were altered through out the design process as the Binar team gained a better understanding of the satellite design process. The design requirements were:

- The CubeSat shall have a mass less than 1.33kg as specified by the CubeSat handbook.

- The CubeSat shall operate in LEO with similar conditions to the ISS were it will be deployed from.

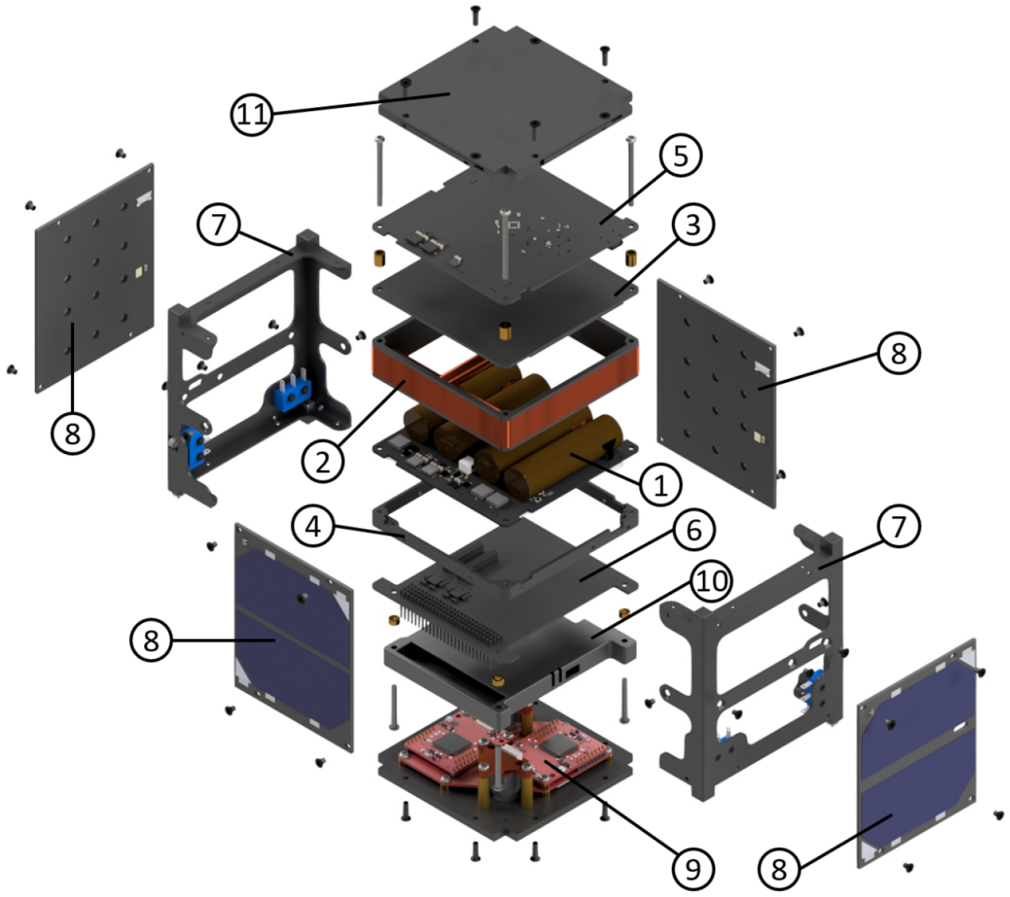

Figure 2.1: Exploded diagram of Binar-1 and its essential systems. 1 is the main custom designed Binar CubeSat Motherboard (BCM) Printed Circuit Board (PCB) which contains the EPS, ADCS, and flight computer system electronics. When merged with 2, 3, and 4, the combined Binar CubeSat Core (BCC) is complete. 5 was intended to be flown as a secondary BCM with limited functionality. However, it was deactivated before launch due to time constraints. 7 are the two rail halves constraining the CubeSat to its required dimensions. 6 and 9 are the payload adapter board and payload base, respectively. The adapter board connects to the COTS transceiver (10), which is connected to the COTS antenna (11). Finally, the solar panels (8) are mounted to the other four faces of the CubeSat.

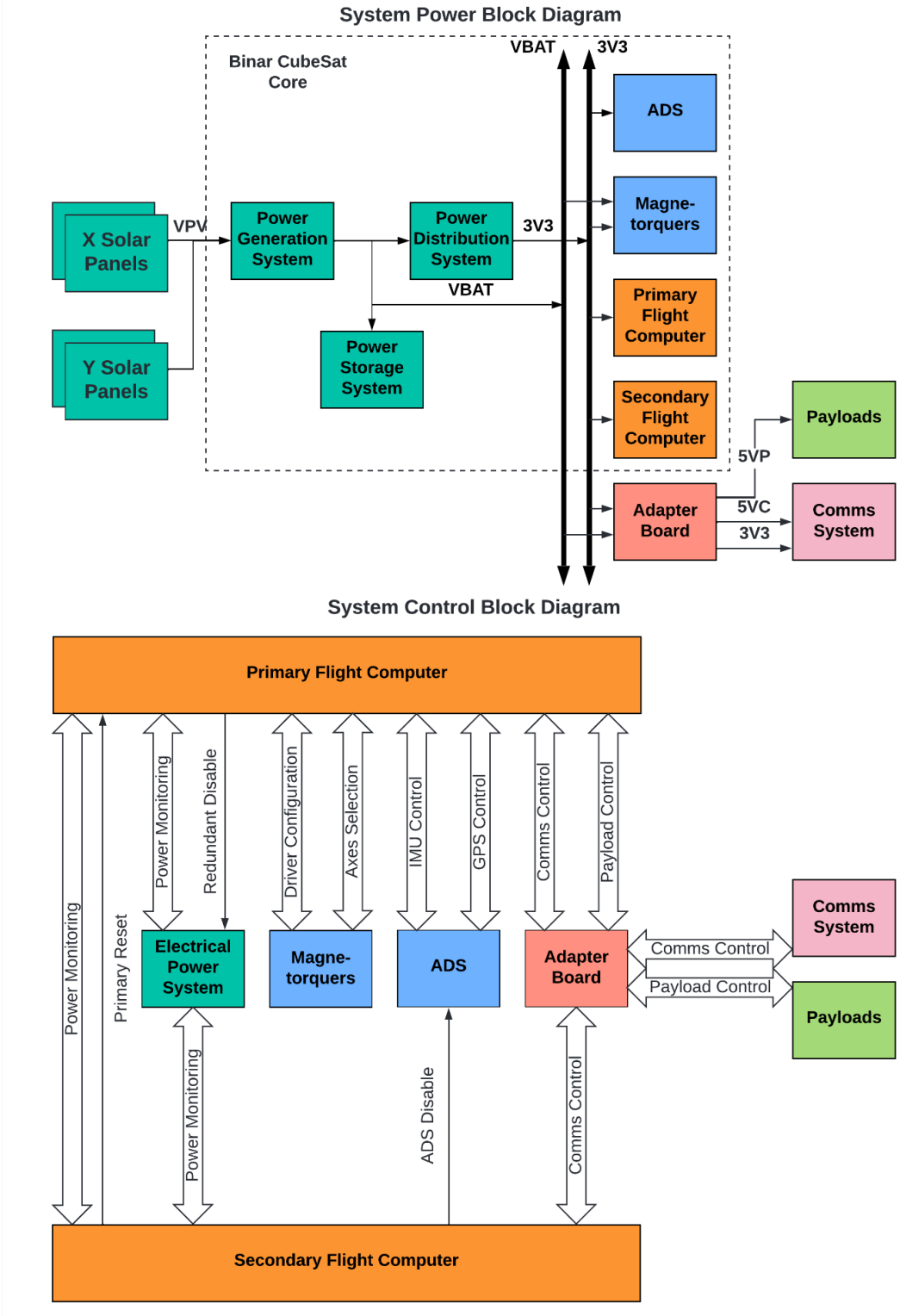

Figure 2.2: The simplified Binar-1 CubeSat system block diagrams. The diagrams were separated into power and signal connections for clarity. Some noteworthy features include the distribution systems on the BCC and the adapter board, and the shared control features of the primary and secondary flight computers.

- The CubeSat shall be operational for as long as necessary to test all of its onboard commands. This is estimated to be a duration of up to two weeks depending on the number of ground station passes.

- The CubeSat EPS shall operate with a power surplus at the beginning of orbit life. Subsystem components will be selected and matched to the power generation system to ensure this power surplus.

- The CubeSat EPS shall have a power storage subsystem cable of operating the CubeSat when solar power is not available.

- The CubeSat communication system shall not depend on the ADCS for a stable connection. i.e. the CubeSat antenna shall be omni-directional.

- The CubeSat communications system shall have a reliable link for remote operations and telemetry downlink.

- The CubeSat ADCS shall be able to slow the CubeSat rotation after deployment to 2 rpm for thermal regulation.

Of these design requirements, the EPS requirement can be considered atypical when compared to other CubeSat missions. The requirement existed in this way due to the trial and error approach to design of Binar-1. This design approach meant that strict power requirements were difficult to manage and constantly changing as different components were used in the trial and error approach. It was found to be more time effective to implement a blanket requirement rather than constantly be managing a specific power generation, storage, and distribution requirements every time components changed.

Additionally, compared to other CubeSat missions, an ADCS design requirement can be considered missing. For the Binar-1 mission no direct pointing was required to use any of the other systems on board. The communications system included an omni-directional antenna providing it with sufficient gain (3dB) in all directions to be received by the ground station, and the payload camera was

only required to capture an image of the stars or Earth meaning direct pointing algorithms were not required.

External to the design requirements were a set of safety requirements that needed to be met for launch to and deployment from the ISS. For the Binar-1 mission, an outsourcing company that manages CubeSat deployments from the ISS Japanese Kibo module was selected for integrating and delivering the Binar-1 CubeSat to space. Operating with a Japanese company, the Japanese Aerospace Exploration Agency (JAXA) launch requirements as specified in the JEM Payload Accommodation Handbook [88] needed to be met. These detailed requirements were important for many of the Binar-1 design decisions ensuring that the CubeSat was able to safely transfer through the ISS without any risk to the astronauts on board.

2.2.2 Binar CubeSat Core (50%)

The BCC contained three of the main spacecraft subsystems in the custom design. At the beginning of the design process, these subsystems began development as part of two undergraduate research projects. After development at a subsystem level, the students were offered the opportunity to start a PhD and decided to integrate the subsystems onto a single Printed Circuit Board (PCB). This became known as the BCC. This feature became crucial to the design as it enabled the CubeSat form factor to shrink from a 2U to a 1U while still meeting the design objectives. The resulting CubeSat, Binar-1, was the first technology demonstrator mission from the Binar Space Program targeted at demonstrating the BCCs functionality. The core design is detailed in this section, including the efforts to meet the design objectives.

Electrical Power System (100%)

The EPS generates, stores, and distributes power, allowing all other subsystems on the CubeSat to operate. Without the EPS, the CubeSat would have no functionality. This system was designed to meet the power requirements of the other systems while attempting to maximise the power available to the payload and not compromise on system capabilities.

The primary considerations for designing a CubeSat EPS include reliability, efficiency, and end-of-life capabilities. These considerations were all made for the design of the BCC and Binar-1. Using modern-day electronics, multiple Integrated Circuits (ICs) were tried and tested to meet the design applications. The system was verified using the rest of the BCC while demonstrating the ADCS and flight computer system. Through doing this, any challenges with the EPS were identified and removed before the launch of Binar-1. Multiple temperature, current, and voltage measurement points were placed across the BCC to demonstrate the technology and provide system telemetry. These measurement points are logged to the flight computer system during operations to show the CubeSat performance.

The design of the EPS was separated into three main subsystems before integration on the BCC. These were the following:

- Power generation subsystem,
- Power storage subsystem, and
- Power distribution subsystem.

Once all the subsystems were successfully developed and tested, they were integrated onto the BCC with the ADCS and flight computer system. Design of the subsystems aimed to meet the three main design objectives. This meant that all the systems were made to be cost-effective and as compact as possible without limiting capability.

Power Generation Subsystem

The power generation subsystem consists of two Maximum Power Point Controllers (MPPCs) and four 1U solar panels. The system works by having a solar panel on both the positive and negative X and Y axes of the CubeSat. On each of these axes, solar panels can only be illuminated one at a time, meaning an MPPC was able to be shared. The solar panel design included two triple junction 3G30C solar cells from AzurSpace connected in series. The solar panels on

each face connected to an MPPC circuit which operated the solar panels at the maximum power point voltage while also stepping up the voltage to charge the BCC batteries included in the power storage subsystem.

The solar panel design process investigated many different methods of assembly. The final design and assembly procedure were based on suggestions from Sandburg et al. and Dahir et al. [89][90]. This process used pre-cover-glassed, bypass diode integrated, and tabbed Cover-glass Integrated Cells (CICs), a PCB structure, and Kapton tape to improve the assembly. An alternate cell adhesion method was tested using an iterative design process and available testing facilities. The previous suggestion used silver epoxy for making the electrical connections [89]. However, flux-free solder paste was shown to provide a simpler alternative. Temperature sensors and the GPS antenna were also included on the solar panels to observe the CubeSat surface temperature during the mission and determine the CubeSat position. The final design and assembly procedure was able to produce and test all four solar panels in two days. The front and back of a completed solar panel are presented in Figure 2.3.

The two matching MPPC circuits were designed to meet the design objectives and be modular for various CubeSat sizes. MPPCs were used over other solar panel power harvesting techniques due to the improved efficiency provided with a limited trade-off to PCB space usage. The circuit uses the LTC3130 buck-boost converter IC with added MPPC functionality. Using a feedback resistor circuit, the IC can provide a set input and output voltage. The IC was chosen for being cost-effective, small, and scalable. Due to the unique design being able to select the input and output voltage using a feedback resister circuit, the IC could be scaled and used with larger 3U panels if required. The circuit also included ideal diodes for preventing the batteries from reverse discharging. The final set-up improved the circuit efficiency and compacted the design, providing the BCC with the capability to supply enough power to the rest of the BCC and its payloads for operation, without compromising the available payload space. The Altium schematic is presented in Figure 2.4. Testing of the design during development showed that the circuit was 89.6% efficient when stepping up from the 1U solar panel peak power voltage to the battery nominal voltage. Combining this efficiency with the 2rpm ADCS design requirement, the CubeSat power budget

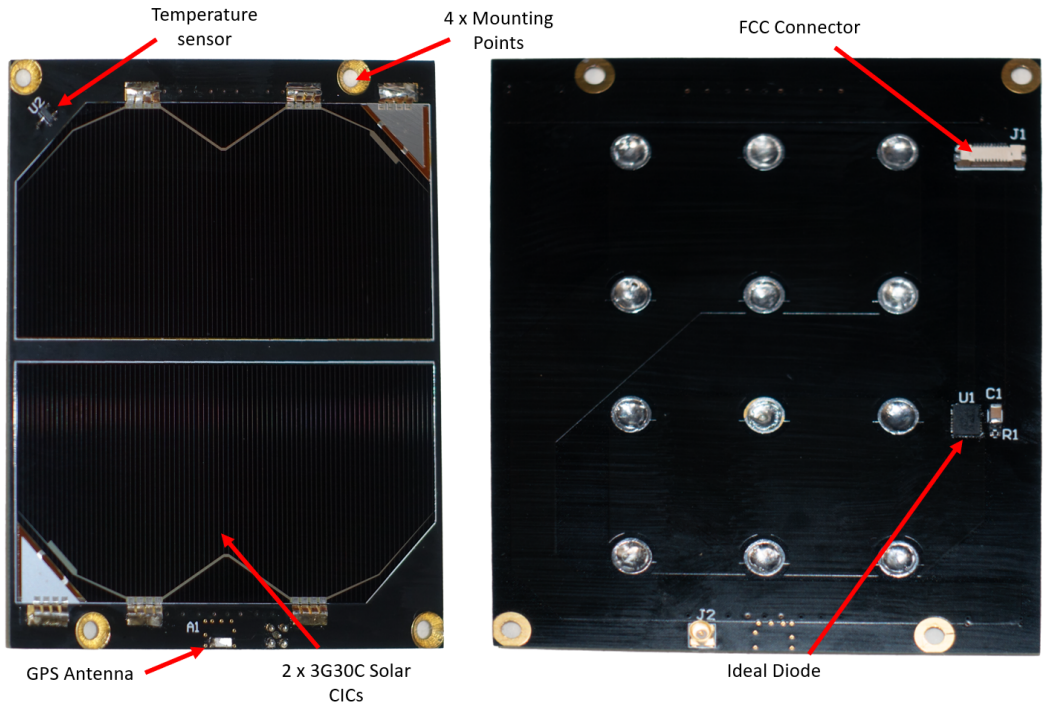

Figure 2.3: The front and back of a completely assembled solar panel used on the Binar-1 mission. On the front of the panels were two 3G30C solar CICs, a temperature sensor, and a GPS antenna. On the back, the ideal blocking diode and FFC connector were mounted. The solar panels are fastened to the surface using four countersunk M3 machine screws.

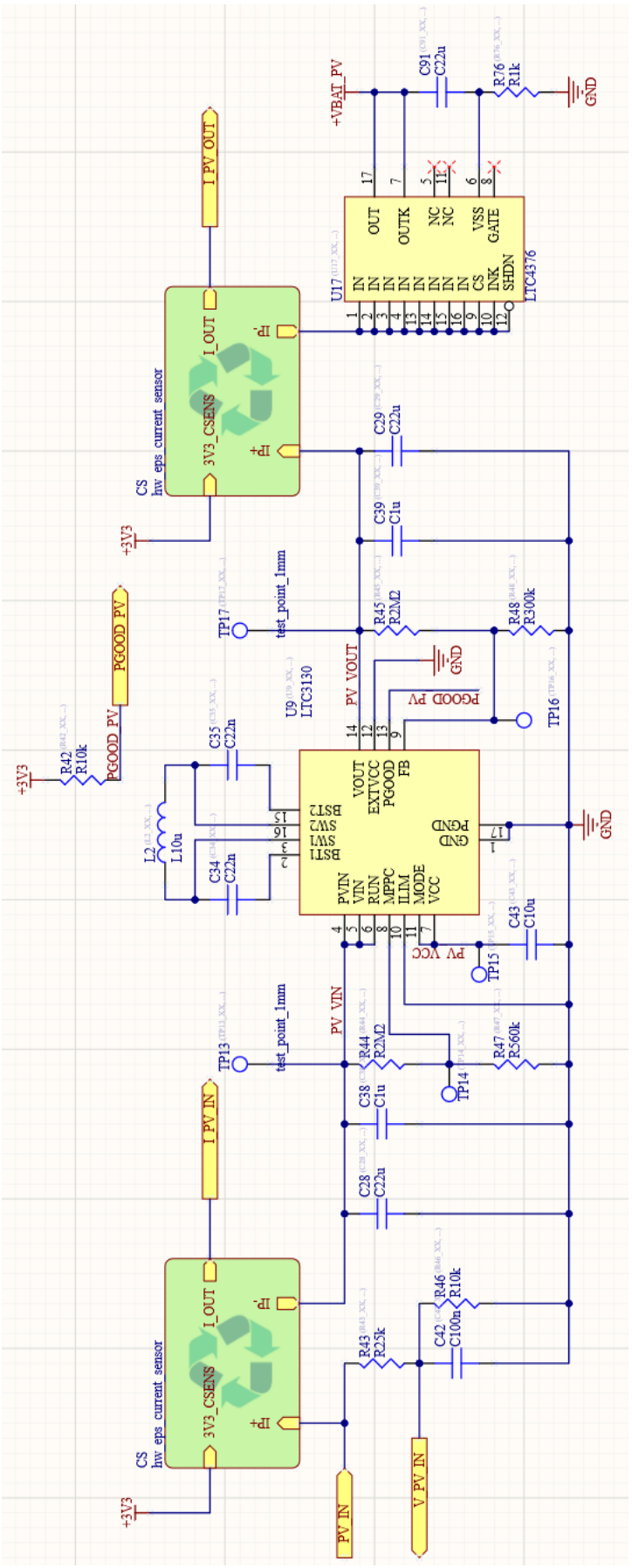

Figure 2.4: The Binar-1 MPPC Altium schematic. The design uses the LTC3130 buck-boost converter IC which has inbuilt MPPC capabilities and is scalable to different solar panel sizes.

demonstrated that the power system could generate an average of 1.6Whr per orbit. This was enough for a power surplus during the operation of Binar-1, meeting the design requirement.

Power Storage Subsystem

The power storage subsystem was a critical design element of the BCC EPS. When the CubeSat enters its orbital eclipse, it depends on the storage system to provide power. Given the planned ISS deployment, it was expected that the CubeSat would need to operate in eclipse for approximately 35 to 40 minutes. As such, the design of the power storage subsystem was required to keep the remaining Binar-1 systems functioning during this period. The system was also critical for operating the CubeSat immediately after deployment and for recovery if an error occurred in orbit. The power storage system needed to be large and efficient to not deplete during the journey from delivery to deployment from the ISS. Additionally, if the battery is large enough to operate the CubeSat for an extended period after a system malfunction, the CubeSat may be instructed to limit its activity and remain operational for an extended period of time.

To achieve this, high-power density 18650 lithium-ion battery cells were used. Typically used in modern CubeSats due to their high-power density and strong packaging [91], they have been optimised through extended usage in the electric vehicle industry. At the time of conception, the recent CubeSat missions, MarCO A and MarCO B (Section 1.1.1) were the first CubeSats to leave Earth orbit and make their way to Mars [13]. On board were the standard form factor lithium-ion 18650 battery cells, which were charged up and used for high-power communications [92]. Due to this flight heritage, these battery cells were chosen to be used in the BCC. After selecting to use this form factor of battery cell, the brand of cell and configuration was determined. At the time of design, the best available cell was the INR18650-35E manufactured by Samsung (Figure 2.5). Four were then arranged in a 2S2P layout to make the complete battery. This configuration was optimised for the other power subsystems, minimising the number of converters required, thus meeting all the primary design objectives.

Two significant challenges were associated with using lithium-based battery cells. The first was the operation temperature. The datasheet for the INR18650-35E

Figure 2.5: The Samsung INR18650-35E lithium-ion battery cell. Each cell has an approximate capacity of 3250mAhr and a nominal voltage of 3.7V. When combined into the final 2S2P battery pack, the BCC has a total power storage of 48.1Whr.

cells specified operating temperature limits of 0 to 60°C. This was a design concern compared to the remainder of the Binar-1 components, which could operate down to -20°C. As such, two heater systems were included in the design. These circuits used a simple analog temperature switch IC and a resistive flexible PCB heater to heat the batteries when the switch IC temperature dropped below 5°C. This heater design heated the battery cells and allowed them to operate during the eclipse if cold temperatures were experienced.

The other major challenge with using lithium-based battery cells was the volatility. When managed incorrectly, lithium-ion cells can ignite and cause harm during assembly, integration, and testing or handling on the ISS. As fire is a critical risk on the ISS, a safety system was included in the power storage subsystem to mitigate this risk. The Japan Aerospace Exploration Agency (JAXA), the deployment authority for Binar-1, specified the requirements for this safety system [88] as mentioned in Section 2.2.1.

The safety system design was performed considering the requirements of JAXA and the CubeSat design objectives. The combined solution needed to consider the five main risks of battery ignition while not compromising the payload space and increasing cost. The five risks of battery ignition were:

- Battery rupture or puncture,
- Battery ageing,
- Battery over-charge,
- Battery over-discharge, and
- Battery short circuit.

Minimising the risk of battery puncture was considered during the structure design. All sharp edges around the batteries were removed to prevent this from occurring. The ability of the structure to meet this safety requirement was ver-

ified through vibration testing (Section 2.3.3) after assembly and integration. The following risk of battery ageing was mitigated before the assembly process through the battery qualification testing (Section 2.3.2) process. This process included complete discharge and charge cycles of the batteries, comparing the performance pre and post vacuum and vibration tests to ensure the batteries were not experiencing early onset decay.

The remaining risks were mitigated using three inhibits for each risk. To achieve this, the design included a battery protection circuit, double insulation, and four deployment switches which disconnect the batteries from the remainder of the CubeSat when stowed in the Japan Experimental Module (JEM)-Small Satellite Orbital Deployer (J-SSOD). The implementation of these inhibits are presented in Figure 2.6. When implementing the inhibits in the design, the design objectives were considered. The protection circuit ICs used were the cost-effective 3x3mm, BQ29800. The small size of this IC meant that the design objectives could be met as the space occupied on the BCC was minimal. The protection circuit Altium schematics are presented in Figure 2.7, 2.8, and 2.9. Hierarchical design principles were used as the protection circuit was repeated for each battery cell. The inhibit switches and double insulation were implemented external to the BCC on the switch wires and Binar structure. The inhibit switch location and functionality are detailed further in Section 2.3.3.

Power Distribution Subsystem

The power distribution subsystem was the simplest of the three subsystems. Common CubeSat power distribution designs choose between a centralised or distributed architecture [93]. To meet the design objectives, a hybrid distribution architecture was used to compromise maximised payload space and system capabilities. The hybrid architecture design was centralised for all systems on the BCC and distributed for all systems external to the BCC. This meant that only one distribution system was present on the BCC, with two being present externally for the remaining systems. Figure 2.10 demonstrates the Binar-1 setup where the centralised distribution subsystem can be seen on the BCC while the distributed distribution subsystems are found near the payloads. The communication system was treated as a payload on Binar-1, intended to be integrated with the BCC on future missions and not be a COTS solution.

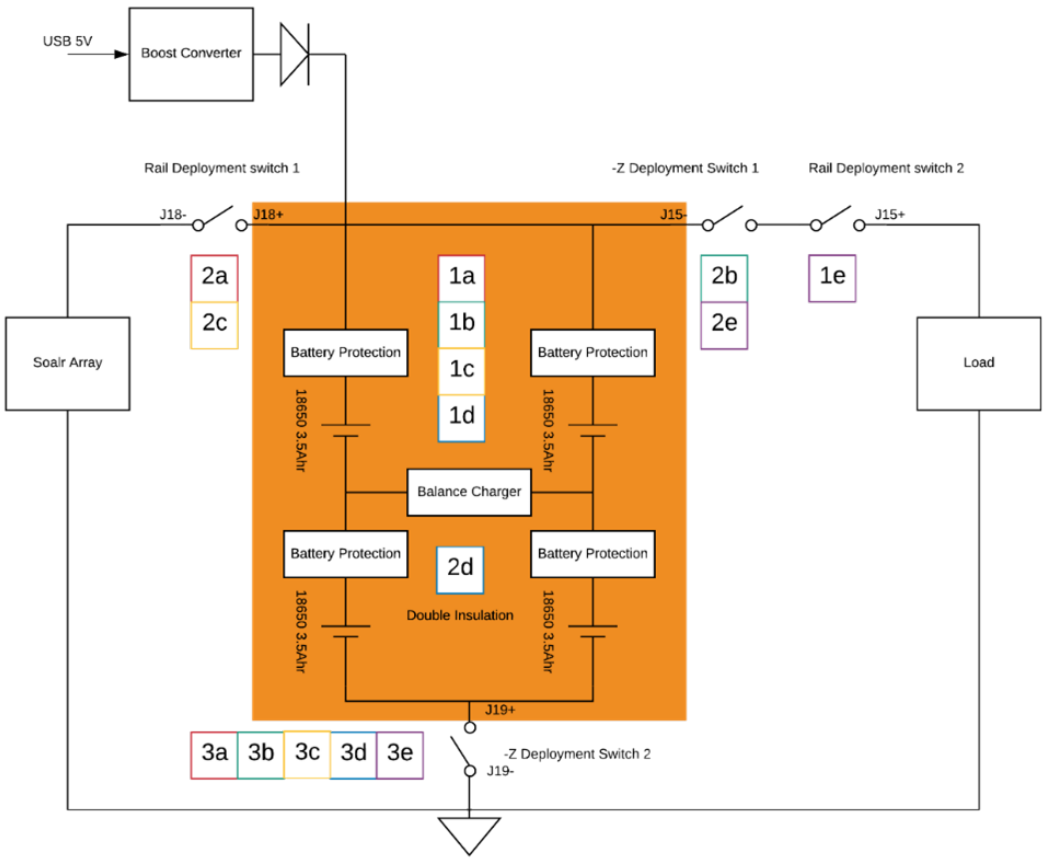

	Inhibit 1	Inhibit 2	Inhibit 3
Over-Charge [a]	Protection IC	Rail SW 1	-Z SW2
Over-Discharge Load Side [b]	Protection IC	-Z SW1	-Z SW2
Over-Discharge Solar Side [c]	Protection IC	Rail SW 1	-Z SW2
External Short [d]	Protection IC	Double Insulation	-Z SW2
Inadvertent Antenna Deployment [e]	Rail SW 2	-Z SW1	-Z SW2

Figure 2.6: The Binar-1 battery safety circuit diagram. The boxes indicate the inhibits. The corresponding risk mitigated for each box is detailed in the accompanying table

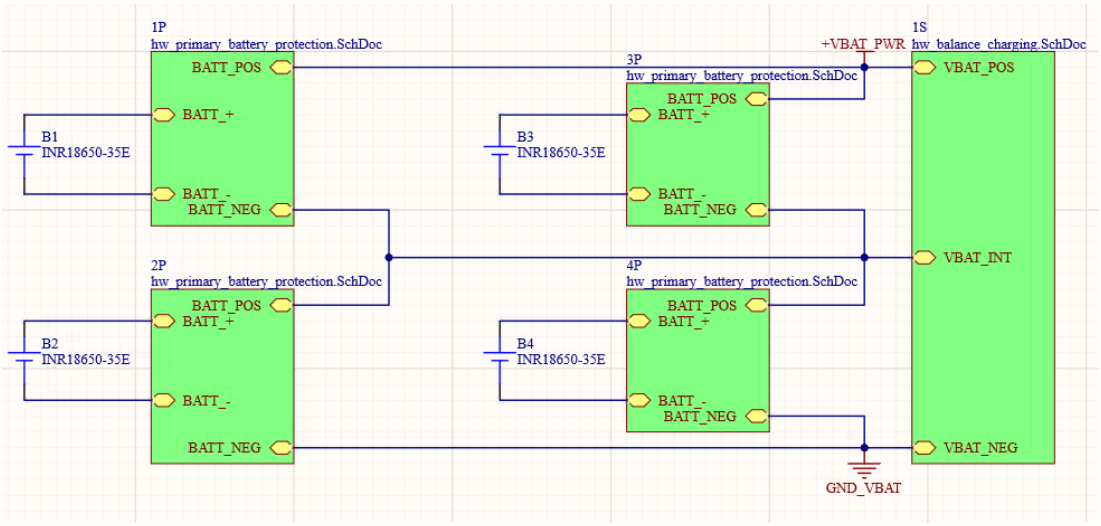

Figure 2.7: The top-level schematic for the battery protection circuitry.

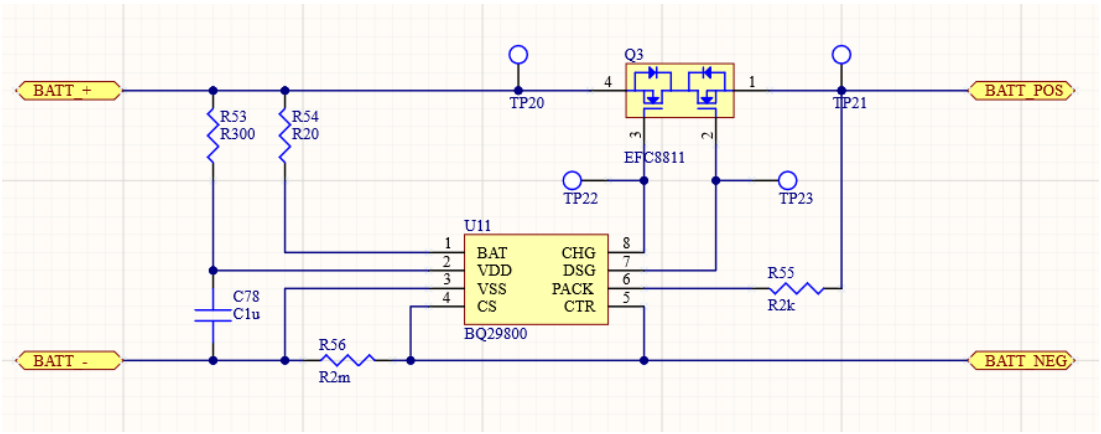

Figure 2.8: Detailed schematic of the primary battery protection block. The BQ29800 was able to provide protection and inhibit many of the risks of cell ignition. These protection features included OCD, OCC, OVP, UVP, and SCP.

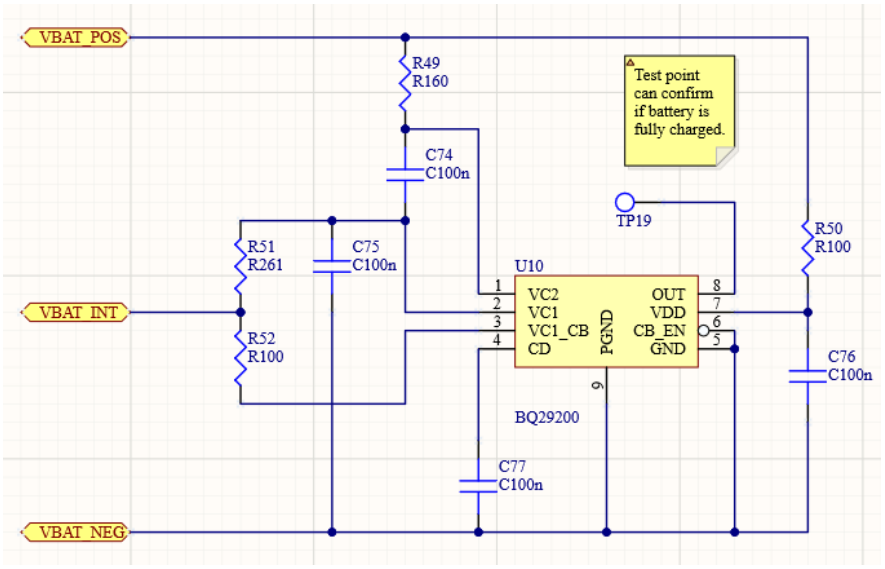

Figure 2.9: Although not required by JAXA for safety, a battery balance charger was included in the design. This circuit aims to improve the lifetime of the battery by preventing the cells from having miss matched voltages after high current discharges.

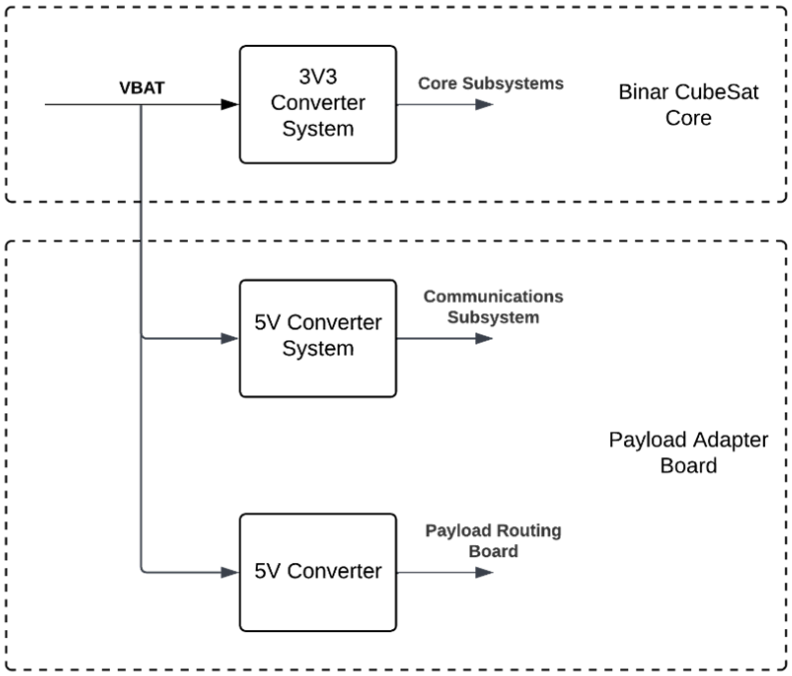

Figure 2.10: Block diagram of the hybrid distribution architecture used on the Binar-1 mission. The distribution subsystem was separated to maximise payload space while not compromising system capability.

The centralised and distributed sections of the power distribution subsystem used a micro power module from Linear systems. The adaptive LTM4622 has its output voltage configured by a single resister, making it simple to change when necessary. During the development of the BCC, many different implementations of this IC were tested until a suitable solution was found. As all the other systems on the BCC relied on a single converter, a hot redundant converter was included to remove this single point of failure. The result used two LTM4622, feeding into a power multiplexer smart IC, which would select from the two regulator IC outputs. One would be preferred over the other if both were operating correctly. However, if one regulator IC were to malfunction, the multiplexer IC would use the functioning IC to supply power. This dual redundancy increases the subsystem reliability and maximised the BCCs system capability. The Altium schematic of the redundancy design for Binar-1 is presented in Figure 2.11.

All other distributed distribution subsystems were found on the payload and communication adapter board. Both the payloads and the communication system required 5V to operate. Following the payload distributed architecture, a separate 5V distribution system was implemented for both the payload and communication system. With the previous regulator IC already being tested, it was reused to power these systems, only needing to change a single resistor to supply 5V. Due to its mission criticality, the communication transceiver from EnduroSat was designed with redundancy. However, instead of a multiplexer IC, both converters were controlled by separate General-Purpose Output (GPO) pins on the flight computer.

Attitude Determination and Control System (0%)

The CubeSat ADCS design was also integrated into the BCC. Separating this system into two components made designing and organising the BCC simpler. The attitude determination system used a 9-axis Inertial Measurement Unit (IMU) containing an accelerometer, gyroscope, and magnetometer. A GPS receiver was also included in the design. These two devices were used to determine the position and spin rate of the CubeSat, as well as the current magnetic field at its location. This information was then used to inform the attitude control system on how to operate and when to schedule mission tasks such as running the camera

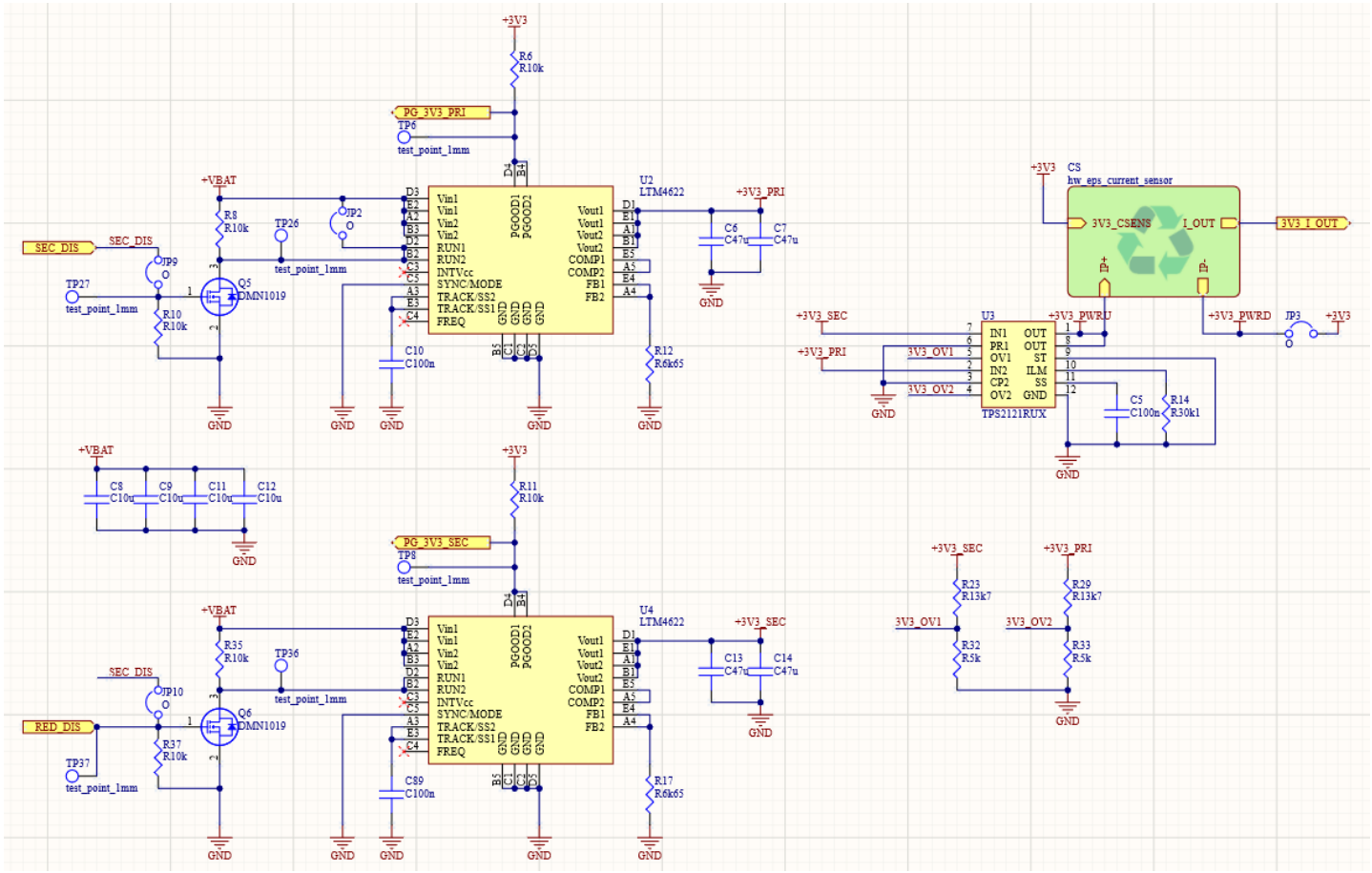

Figure 2.11: Altium Schematic of the centralised BCC power distribution system. Two LTM4622 feed into a TPS2121 power multiplexer which selects between the two power channels providing redundancy.

payloads. The attitude control system used magnetorquers to point the CubeSat by torquing against the Earth's magnetic field. The spin rate could either decrease or increase by changing this magnetic field as the CubeSat rotates. The primary flight computer controlled the complete system, and commands for attitude control were either scheduled from the ground or predetermined on the flight computer to achieve a desired CubeSat attitude. On the Binar-1 mission, the only predetermined attitude control operation was a de-tumble control algorithm.

Attitude Determination Subsystem

The design of the attitude determination subsystem consisted of a selection of sensors that could be used to determine the CubeSat attitude. The first attitude determination sensor included in the design was an integrated 9-axis IMU which contains three different 3-axis sensors. The first of these sensors was an accelerometer that could measure the various forces acting on the CubeSat. The only force expected was the forces created by the magnetorquers. The IMU did not align with the centre of mass, so any torques the magnetorquers created were able to be measured by the accelerometer. The second sensor in the combined IMU was the gyroscope. Measuring the rotational velocity of the CubeSat, this was the primary feedback sensor for the attitude control system. Finally, the IMU contains a magnetometer that can measure the magnetic field of the Earth and magnetorquers. The 9-axis IMU was all combined in a singular IC called the LSM9DS1 supplied by STMicroelectronics. As all this functionality could be compressed into a small and low-cost IC, the determination system could meet the design objectives.

The BCC also contains a GPS for precise timing and location information. This capability was included as many science missions require a GPS receiver or generic GNSS receiver, including testing controlled re-entry and recovery technologies. The GPS used on Binar-1 was supplied by Skytraq and is called the Venus838. Similar to the IMU IC, its small size and low cost meant that the design objectives were met during the attitude determination subsystem design.

Attitude Control Subsystem

A three-axis magnetorquer performed attitude control on the CubeSat mounted to the BCC. Once mounted, each axis magentorquer was controlled by a sep-

arate H-bridge driver. This allowed the CubeSat to effectively create a 3-axis magnet capable of changing the CubeSat orientation when torqued against the Earth's magnetic field. This process is the primary actuation method on Binar-1, as no propulsion system or reaction wheels were featured in the design. Each electromagnet or magnetorquer had a variable electrical current driven through them using a separate H-bridge driver IC which was able to reverse the electrical current direction and modulate the duty cycle, effectively changing the magnetic field direction and strength in each axis. The H-bridge used on Binar-1 was the MC33HB2001FK. It was chosen based on a trade off between input voltage, output current, and package size when compared to other commercially available options.

To integrate the magnetorquer windings with the BCC without compromising on payload space, the BCCs structure had to be specially designed. The design included two long ferrite core magnetorquers that fit within the battery cells. The remaining axis was a large vacuum core magnetorquer wound around the outside of the BCC. This vacuum core magnetorquer had a slightly weaker magnetic field due to the orientation and centre interference. Due to the nature of CubeSat internal components being square, the orientation of the vacuum core magentorquer was made to be square in order to better utilise the available space. A more optimal magnetorquer would be round. Additionally, as the remaining BCC electronics are located in the centre of the magnetorquers, there would be some low amounts interference with the magnetic field created. However, this design challenge was not critical for operation, as the long ferrite core magnetorquers were calculated to be more significant when pointing nadir and zenith payloads. Figure 2.12 highlights the position of the integrated magnetorquers in the BCC.

The flight computer system was programmed to control the attitude control system autonomously after deployment and when commanded from the ground. The autonomous algorithm designed was a B-dot algorithm for de-tumbling the CubeSat after deployment [94]. The algorithm was programmed to activate as soon as Binar-1 had completed deploying its antennas and would operate for approximately 1 hour. The process was included as autonomous to de-tumble the CubeSat from any spin created by the release of the antennas. If the spin rate was too large, the CubeSat might have never been able to communicate with

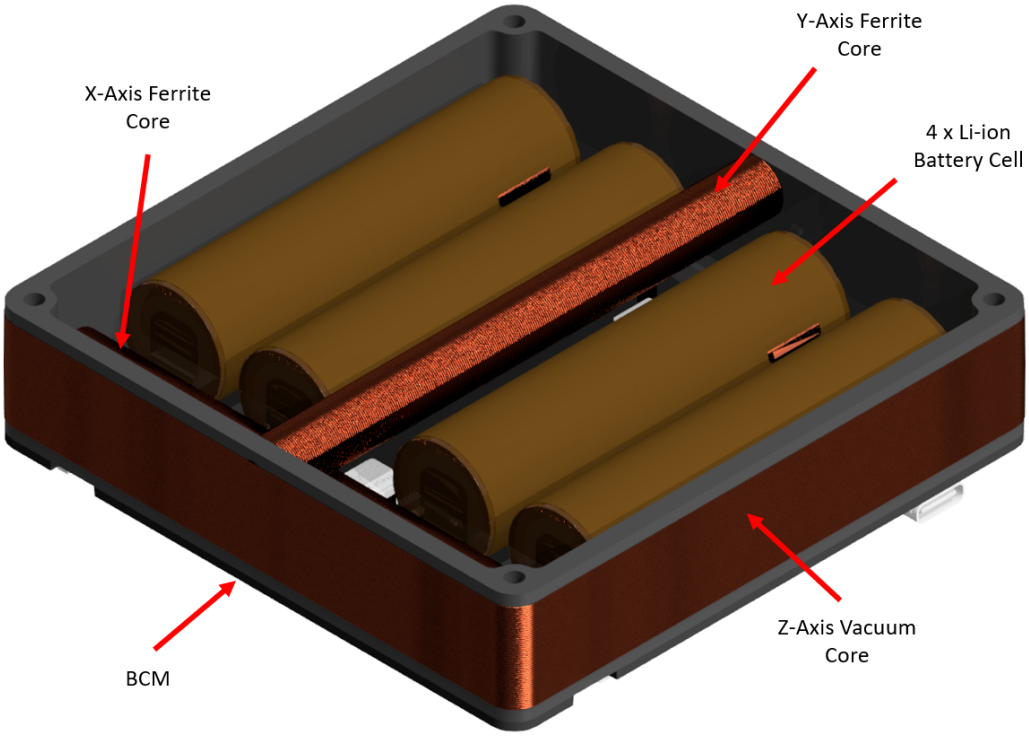

Figure 2.12: The magnetorquers on the BCC were integrated with the large battery to maximise the space efficiency of the BCC. The X and Y axes were long ferrite core magnetorquers, while the Z axis was a vacuum core magnetorquer that surrounded the core.

the ground. The algorithm had a stop condition of 1 degree per second. This rotation rate is suitable for the operation of the communications system at the beginning of the Binar-1 mission and also provides thermal regulation through the CubeSat, preventing one side from overheating.

Flight Computer System (50%)

The flight computer system design was composed of two microcontrollers and an external embedded Multi-Media Card (eMMC) IC, which was used to store telemetry and payload data. The first microcontroller operated as the primary flight computer on the BCC. The second microcontroller was included in the design as a backup flight computer capable of providing essential communications and telemetry if the primary flight computer failed. The external eMMC was added to the BCC to store payload and telemetry data until requested from the ground. Once requested, the data could be sent through the primary flight computer to the communications system, where it could be transmitted to the ground. Only the primary flight computer was able to connect to the eMMC. The systems design was focused on maximising system capability as its functionality was necessary for monitoring and controlling all other systems including future payloads. With the reduced cost and size of modern-day microcontrollers, the selection of the microcontrollers was only based on capability and usability, meaning to develop a platform using the selected microcontroller a large learning curve was not required.

The primary flight computer was a STM32H757XIH6 microcontroller designed by STMicroelectronics. Selected for its high capability and the familiarity of STMicroelectronic devices to the Binar team. The microcontroller operates at 80MHz, has two cores, and 2MB of flash. The IC also features a switch mode power supply, which can be configured to consume reduced power in critical applications such as onboard a CubeSat. The other features of the primary flight computer are three separate 12 channel Analogue to Digital Converters (ADC), Inter-Integrated Circuit (I2C), Universal Asynchronous Receive-Transmit (UART), and Serial Peripheral Interface (SPI) channels, as well as numerous General-Purpose Input-Output (GPIO) pins. All these features were used to interface the primary flight computer with the other BCC systems, including the EPS and ADCS, as well as the payload and communications adapter board that

connected the BCC to these systems. The selection of this flight computer was able to meet the system capability design objective for these reasons.

The secondary flight computer was a STM32L4R9ZIJ6 microcontroller also designed by STMicroelectronics. The smaller, less capable computer was used as a backup due to its low power consumption during operation. The computer was added to the BCC to make recovery attempts if the primary flight computer malfunctioned or salvage basic telemetry if it failed. Connecting to the primary flight computer through a serial UART connection, the secondary flight computer received continuous acknowledgements from the primary flight computer. If the primary flight computer stopped acknowledging, then the secondary flight computer would take over control similar to a watchdog timer. The secondary flight computer could not operate any of the BCCs other systems. However, it could still collect basic system information such as the battery voltage and temperature and deactivate sensors such as the IMU and GPS. The main feature of the secondary flight computer was its connection to the communications system. If the primary flight computer had stopped working, the secondary flight computer would be able to communicate with the ground through this connection.

The other main feature of the flight computer system was the eMMC. eMMC is a type of memory storage that can store information outside of the 2MB of flash on the primary flight computer. As the 2MB of flash was primarily used by software on Binar-1, the eMMC needed to be used to store historical telemetry logs and payload images. The memory storage device is connected to the primary flight computer using the eMMC connection available on the microcontroller. This memory type was selected due to its high radiation tolerance and extensive flight heritage [95].

Other additions to the design of the flight computer included a Universal Serial Bus (USB) connection and two de-bug points for each flight computer. The USB port was used to supply power when the CubeSat was assembled, and the BCC was inaccessible. It was also used to program both computers while the de-bug ports were inaccessible. The de-bug ports were the primary connection for programming and designing the Binar-1 software. Using the Serial Wire Device (SWD) de-bug link, the flight computer software could be stepped through line

by line during development. This was essential for verifying and improving the flight software.

The design of the logic between the secondary and primary flight computers was an important design feature. When considering how the computers should operate together, many issues arose from the computers sharing functionality. As such, some logic gate ICs had to be used to separate the GPO of the computers and allow both to have control over select GPO functionality. This was mainly apparent with some of the attitude determination peripherals. An example is the control of the IMU-enable line. Both flight computers controlled the switch for the IMU, connected through a NOR gate which enabled the IMU when an active low was asserted. Figure 2.13 shows the connections and how the logic gate operated, allowing the secondary flight computer to use the peripheral only when the primary flight computer was not asserting any signals to the NOR gate.

Integration (50%)

Integrating three of the CubeSat systems onto a single PCB was one of the main features of the design that maximised the payload space. On the integrated BCC PCB, also known as the BCM, was the CubeSat EPS, ADCS and flight computer system. Compared to the investigated COTS approach, this saved nearly two circuit boards of space. The integration process was made more accessible by the power of Altium Designer [96]. Altium is an industry-standard tool used for Electronics Design and Assembly worldwide. The software was essential to the design of the integrated PCB and for combining it with the rest of the systems on Binar-1. Using the program, the single 8-layer PCB was designed and tested over two years, resulting in the version 4.2 BCM flown on Binar-1. Throughout the revision process, many small lessons were learned in the electronics and PCB design process. The first version that was able to operate as expected was version 3. This was then used to inform design changes for version 4 which only required minor layout changes to achieve version 4.2 used on Binar-1. The eight layer PCB has 6 layers dedicated to signals, and 2 plane layers, 1 for ground and 1 for power.

When designing the PCB, the layout of the three systems needed to be considered.

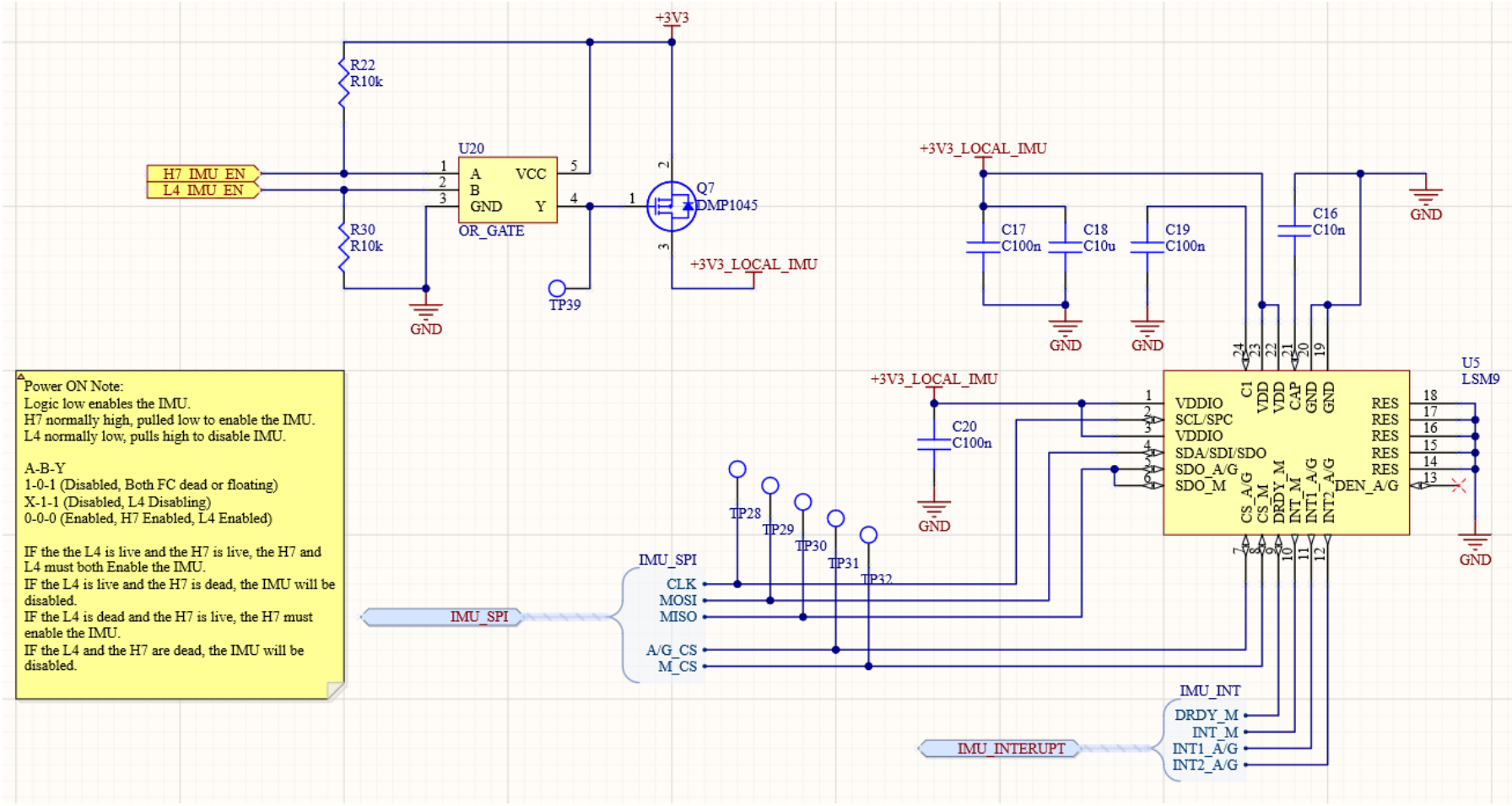

Figure 2.13: Altium implementation of the IMU logic control gate. The implementation gives full control to each flight computer depending on the application.

The EPS was routed on the PCB edge as it needed to connect to the solar panels on each face of the CubeSat. The design used FFC connectors with a shallow profile and small bend radius to connect with the solar panels. These connection points found on the BCCs edge were then routed to the MPPC circuits, which delivered power to the batteries. The distribution system would step down the voltage from the batteries to a usable level for the ADCS and flight computer system located at the BCCs centre. The PCB was routed in the centre to connect the flight computer to all parts of the ADCS system, and monitoring points of the EPS found on the PCB's edges. Figure 2.14 provides a simplified graphic presenting how the BCC was laid out, enabling the systems to be integrated and maximise payload space without compromising the capabilities of the system. The final Binar-1 BCC can be seen in Figure 2.15.

2.2.3 Integrating the Communication System (80%)

A COTS communications system was integrated with the BCC for the Binar-1 mission. The communications system chosen was based on an undergraduate research project conducted alongside the projects that led to the BCCs initial development. The provider was a Bulgarian company called EnduroSat, which supplied two UHF communications systems. One was used for the Binar-1 flight model, and the other for the engineering model. The second system purchased for the engineering model was a low-power variant. This version was purchased as it was cheaper and emitted lower power radio waves when testing. The antenna and the transceiver were modified to make the integration more accessible, meet the maximise payload space design objective, and meet the JAXA safety requirements mentioned in Section 2.2.1. These modifications included modifying the transceiver standoffs and changing the burn wire configuration of the antenna.

An adapter board was designed to integrate the communication and payload systems with the BCC. The adapter board interfaced with the BCC through two 40-pin connectors, providing power and connectivity. The adapter board housed the distributed power systems mentioned in Section 2.2.2 and all the connectors for interfacing with the antenna deployment system, the transceiver, and the payloads. The antenna deployment system was interfaced with the adapter board using the same connector as the COTS antenna. This was the same as the transceiver, which used the large PC104 headers. The payloads were interfaced

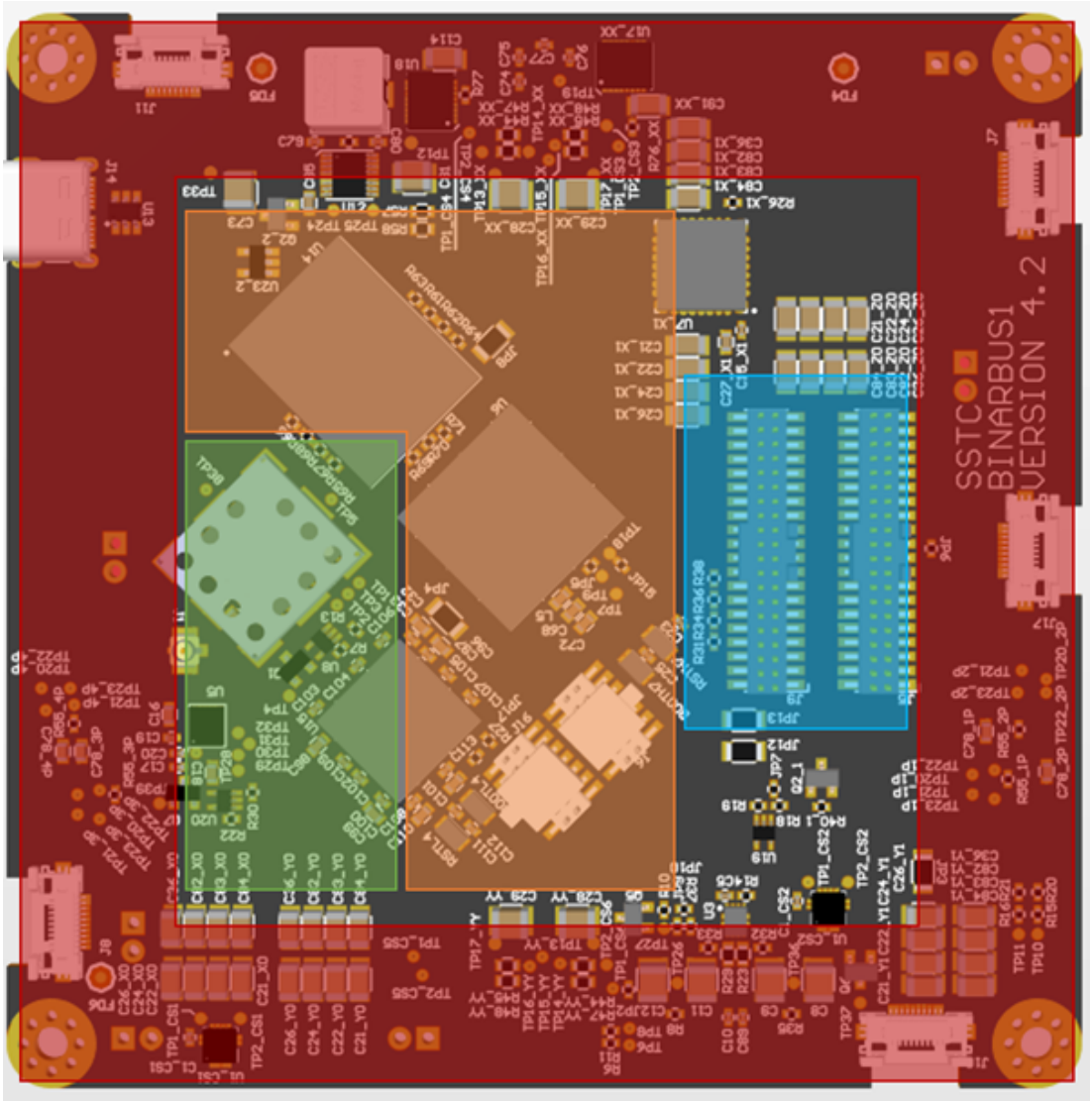

Figure 2.14: Layout of the integrated BCC. The power systems were mainly distributed around the edges along with the magnetorquers (red). The flight computer system (orange) and the remainder of the ADCS (green) were placed in the centre. The Payload connectors (Blue) were placed next to the flight computer.

Figure 2.15: The main novel output of the Binar Space Program, the BCC. The external features include the structure and integrated Z-axis magnetorquer. The Binar EPS, ADCS, and flight computer system are inside the core. Testing the functionality of the custom designs was one of the primary objectives of Binar-1.

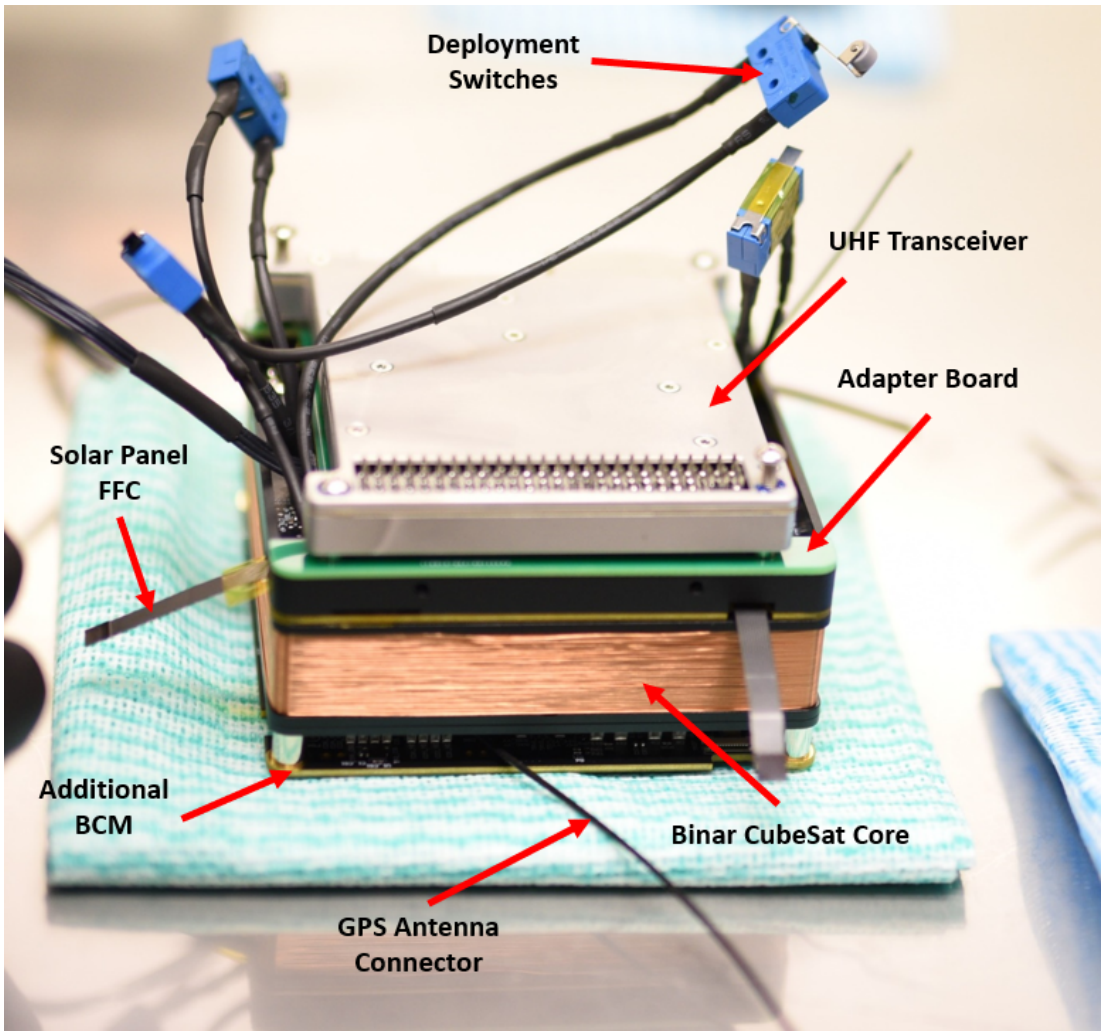

Figure 2.16: The Binar-1 CubeSat stack, including the BCC, additional BCM, RBF bracket, payload and communications adapter board, and EnduroSat type 2 UHF transceiver. The solar panel and UHF fasteners can also be seen. These were connected and tested when finalising the assembly of the BCC.

using a single FFC, the same as the solar panels. Figure 2.16 presents a labelled diagram of the complete Binar-1 stack, including the payload and communications adapter board and transceiver fastened to the PC104 side of the Remove Before Flight (RBF) bracket. This was the final assembly step before the stack was mounted in the structure.

UHF Antenna

Structurally integrating the COTS UHF antenna was simple as it only required four mounting points located at the zenith of the CubeSat. Challenges with the rest of the integration occurred when the team learned about the launch

requirements for ISS-deployed CubeSats. These challenges resulted in the antenna needing to be modified. At first, the supplier's assistance was requested. However, due to COVID-19 and the months-long schedule required for the changes, the team decided to modify the antennas and re-engineer the deployment system to help meet the launch requirements.

There were two launch requirements that the COTS antenna could not meet initially. The first was that the antennas needed to complete a deployment test. Although the test could be conducted, the antennas were required to be reset after the test. The supplier was contacted for information on how to perform this. However, they kept the procedure private due to Intellectual Property (IP) concerns. The alternative was to ship the antenna back to the supplier to be reset. However, the time it would take for the antenna to be shipped and returned would have considerably extended the mission schedule. The second challenge was that if the antenna doors were to deploy on accident after launch, the force exerted on the inside of the launch pod (the J-SSOD) would be too great and cause a blockage or non-direct deployment. As such, the requirements specified that a double deployment safety system needed to be designed and implemented to ensure that if one deployment mechanism failed, there would be a reduced risk of a blockage. As the COTS antenna only had one deployment mechanism, a second needed to be added to meet the launch requirement.

To make the necessary amendments and meet the two launch requirements, the team first had to add another deployment mechanism and reset the antennas at Curtin University using a new method. The approach to adding an extra deployment mechanism was to add a second burn wire to the system. This was challenging, as finding a burn wire that was strong enough to meet the launch requirements and melt using the COTS antenna system required more work. The burn resistors were swapped to a lower resistance to overcome this challenge, increasing the temperature and melting the new burn wire material. This resulted in the burn resistors for each antenna element being swapped out to a 10 Ohm resistor from a 20 Ohm resistor, effectively doubling the power input to the burn wire system. The swap was successful in deploying the antennas and burning the selected wire. However, the increased power through the PCB meant that the copper traces and resistors could only take the load for a few repeat tests. As

such, the deployment system could only be tested twice.

During the testing of the deployment system, the antenna needed to be connected to the adapter board so that the deployment command could be sent from the primary flight computer. During the process, the interface with the COTS system was challenging to navigate, and troubleshooting was necessary to get the antennas to deploy successfully. First, a 5-second delay was added between powering on the antenna and sending the deploy command. If a 5-second delay was not implemented, the antenna microcontroller would freeze and not be recoverable until power cycled. Second, the burn resistors for each antenna deployment mechanism needed to be activated simultaneously for a successful deployment. If both were not activated simultaneously, the resistors did not get hot enough.

UHF Transceiver

EnduroSat also supplied the COTS UHF transceiver. The transceiver was selected in the same research project as the antenna selection, suggesting that the systems work well together and are relatively small compared to other systems. Although this system was planned to be custom-made on the next Binar CubeSat, the selection of the EnduroSat transceiver met the design objectives due to its small size. The transceiver purchased for the flight model could transmit at 2W. When paired with the antenna, was adequate for communications from Binar-1 meeting the design requirement. The transceiver only had one minor hardware modification to be integrated with the BCC. However, the operating system on the transceiver required additional work to integrate with the BCC software.

The only modification was the removal of the overly bulky headers which were replaced with lower profile PC104 connectors, saving up to 5mm in the full CubeSat stack. This size reduction was essential for Binar-1 to make room for deployment switches and to maximise payload space.

Due to the software limits, operating the COTS transceiver and integrating it with the BCC was challenging. The software requirements for mission operations only needed a primary pass-through mode so that the flight computer system could send the communications system data, which would then be immediately transmitted. Although this was a functionality on the COTS transceiver, the op-

eration mode (pipe mode) had a time out of 255 seconds and made the transceiver use more power when active. This complicated the mission design because if this timeout was reached, communications could be lost if the mode was not activated again. The other challenge was system security. Any default commands sent to the transceiver did not have encryption, meaning that if someone knew these commands, they could alter the functionality of the COTS transceiver and jeopardise the CubeSat operations. Due to the COTS transceiver's black-box software, these challenges could not be removed and had to be bypassed. As such, the team had to enable pipe mode regularly to ensure the mode would never be disabled and prevent the transceiver operation mode from being tampered with.

2.2.4 Binar Structure (80%)

The Binar structure design is explained by being separated into the main stack structure and the CubeSat body structure. The structural design of the stack included the integration of the BCC with the payload and communication adapter board and UHF transceiver. The stack structure consists of three main parts: the Remove Before Flight (RBF) bracket, magnetorquer mount, and top cap. The rest of the structural design that made up the Binar-1 CubeSat body was the rail halves, antenna, and payload base plate.

When designing the structural components, sustainable design and design for manufacturing principles were used to meet the design objectives. The structure material was aerospace-grade aluminium 7075 with a hard anodised finish on exterior surfaces. The hard anodisation was necessary for the contact surface with the launch deployer's inside (the J-SSOD). The material is also strong, meaning parts could be thinner, maximising payload space, and commonly used in CubeSat designs.

Sustainable design principles specify reducing the number unique parts required for assembly. This can reduce lead times and design complexity as machining processes can be reused and parts cannot be mismatched. An example of this is the rail half design which match on both sides. Some features on the rail halves, such as the USB cut-out, were not needed on both halves, but were included to limit the number of unique parts and reduce design complexity. Additionally, when designing for manufacturing, simplifying the design can help to reduce part

costs. For space applications, additive manufacturing techniques such as 3D printing were not found to be a suitable option. Subtractive manufacturing was preferred, meaning a milling process was used for all components. The result reduced the manufacturing time and the cost of the structural elements, meeting the design objective.

The BCC was required to mount hardware components such as the magnetorquers and battery cells. The magnetorquer mount was designed to support all the magnetorquer axes in a single frame that could easily be assembled with the main PCB. After all the magnetorquers were wound and integrated with the magnetorquer mount, the magnetorquer ends were soldered directly to terminals on the PCB. The magnetorquer mount was then fastened to the PCB using four M3 bolts and the top cap, which provided additional support to the batteries. The four bolts threaded into the RBF bracket, which had its RBF pin removed to meet the JAXA ISS launch requirements. Around the outside of the bracket were ten M3 bolt connection points used to secure the stack to the rail halves. On the other side of the RBF bracket were four off-set M3 mounting points aligned with the PC104 standard mounting points. These points integrated the UHF transceiver and adapter board with the BCC. Figure 2.17 shows how the BCCs structural design was combined with the UHF transceiver. The complete design was easy to assemble and verified to be thermally and structurally stable through thermal vacuum and vibration testing.

The remaining Binar-1 CubeSat structure used two rail halves to support the integrated stack, with the antenna and the payload base plate constraining the top and bottom. The rail halves used the ten M3 holes on the RBF bracket to connect to the stack. This provided sufficient structural integrity and was verified through vibration testing. The base plate was used to mount the two COTS camera payloads and the payload routing board. After being mounted to the plate, it was connected to the base of the rail halves. The top of the CubeSat was held together using the aluminium plate found inside the COTS UHF antenna. This secured the top of the CubeSat, completing the structural design. Figure 2.18 shows how the integrated stack connects with the rail halves, antenna, and base plate to make the complete CubeSat frame. A picture of the rail half structure being integrated with the CubeSat stack is also presented in

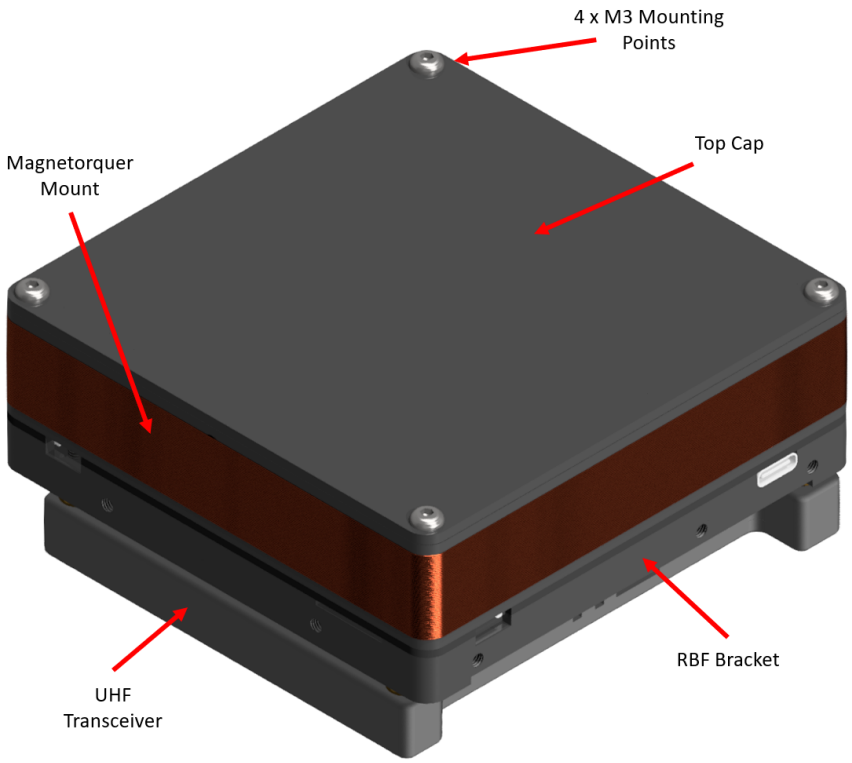

Figure 2.17: Structural design for the main Binar-1 stack. The RBF bracket was used to adapt from the four mounting points on the BCC to the four mounting points used by the PC104 standard headers, while the top cap and magnetorquer mount provided structural stability to the batteries and magnetorquers part of the BCC.

Figure 2.19. With the frame designed, the last structural consideration was the solar panels. These were mounted to the rail halves using four M3 screws in each corner of the CubeSat frame. In addition to the FR4 PCB frames, aluminium plates were included behind the panels to provide additional structural support.

2.2.5 Binar Software Framework (0%)

Binar-1 and the BCC software was designed in parallel with the hardware. This side-by-side development was necessary for the iterative design and verification of Binar-1 as the BCC, communications system, and payloads could only be tested using the software. Written in C and C++ due to extensive space heritage, the Binar Software Framework is an essential feature of the BCC and will be continually upgraded on future Binar missions.

Binar-1 software was designed using strict design principles to prevent bugs and reduce the possibility of software loops. Using a layering format, the flight com-

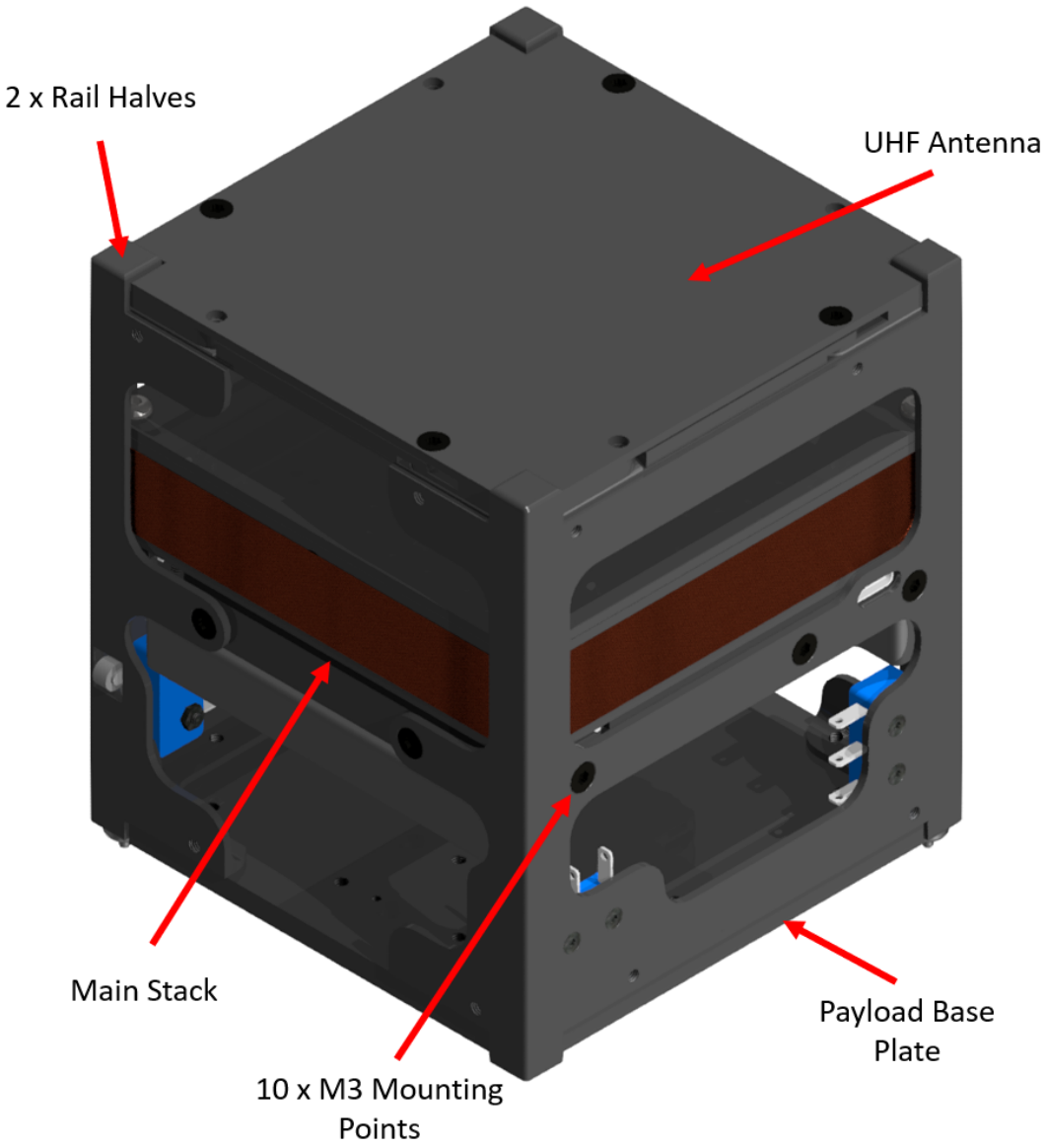

Figure 2.18: The combined Binar-1 structure with the solar panels and payloads removed. The two rail halves matched on each side. This reduced manufacturing costs as the part required less setup time. The physical form can be seen in Figure 2.19.

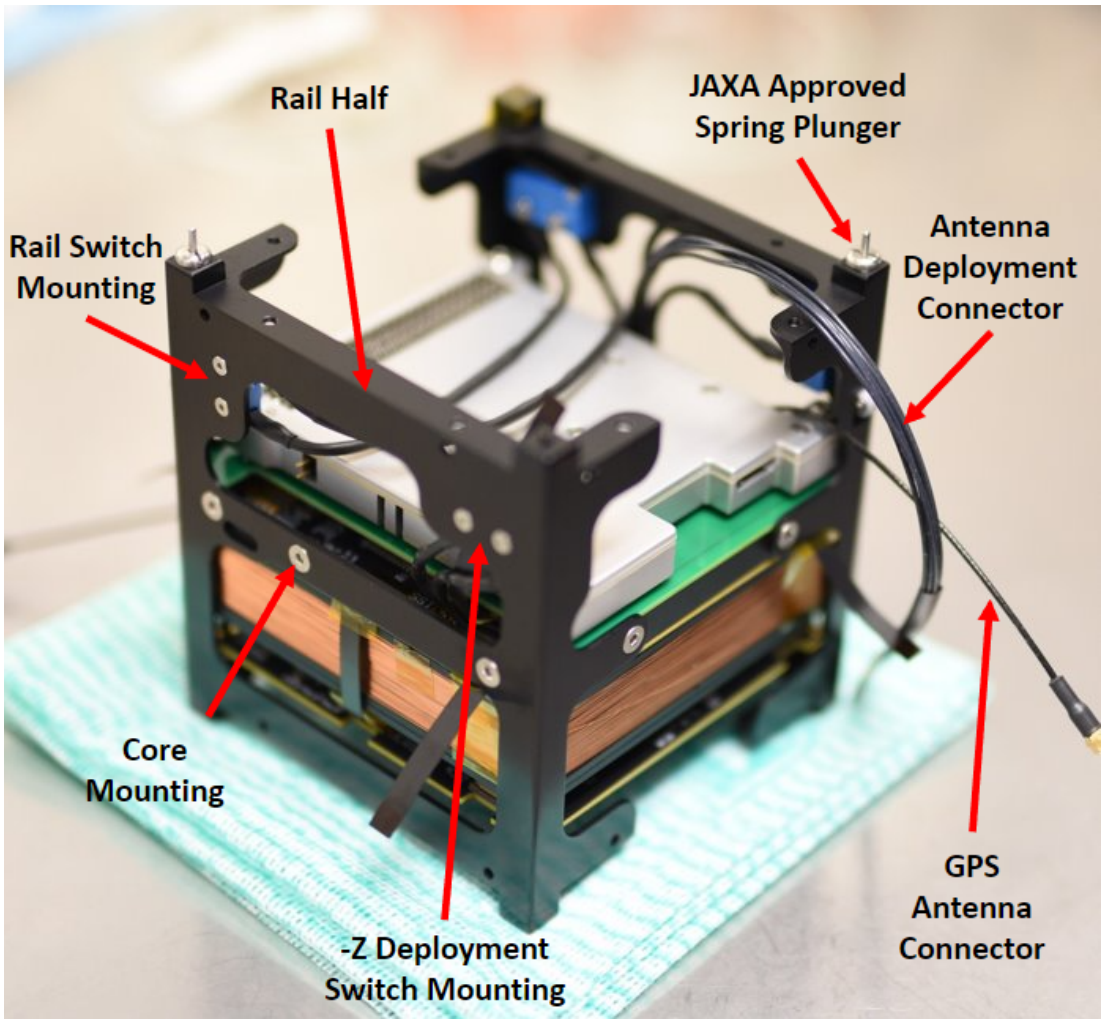

Figure 2.19: The Binar-1 main structure. Once the stack is assembled, the rail halves are connected to each side to form the 1U CubeSat shape. The deployment switches, antenna, payloads, and solar panels are attached to the rail halves to complete the CubeSat.

puter hardware abstraction layer interfaces with the hardware driver layer that interfaces with the application code. This layering process prevents cyclic dependencies. The flight computer hardware abstraction layer enables the use of the flight computer peripherals such as GPIOs, UART and SPI. These are then used by the hardware drivers, which implement the peripherals and define the functions that these peripherals can do. Next, the application code can use these functions autonomously or when scheduled.

The design of the operating software used three main operation modes: the start-up and bootloader mode, safe mode, and application mode. The different operation modes were saved to two memory partition binaries which were then separated to make four binaries stored in 500kB each of the 2MB of flash. This duplication process ensured that the flight computer would always have a working Image to reboot back into when attempting to perform a firmware update.

In the start-up and bootloader operation mode, the CubeSat performs its start-up routines, including the antenna deployment sequence, necessary system checks, firmware update checks and boot bank selection. The antenna deployment sequence was performed on the first boot of the CubeSat after it was deployed from the ISS. The sequence required a 30-minute delay where the CubeSat could not transmit or deploy its antennas. Once the timer finished, the antennas could deploy, and the necessary system checks were performed. These checks observed the battery health, application code, and antenna deployment status. If any checks were unsuccessful, the bootloader would jump to safe mode. If all the checks passed, the bootloader finally checked to see if it needed to perform a firmware update before jumping into the application code. Firmware updates are performed in the bootloader. The bootloader would boot into the selected application code space if a firmware update was not scheduled.

Safe mode operations were a limited version of the CubeSat application code. Some CubeSat commands were removed in safe mode, limiting the operator to requesting telemetry, performing firmware updates, changing boot registers, and clearing status registers. If the safe mode was activated, its operation was intended only to help the CubeSat recharge, recover from corrupt application code, and perform system reboots. Safe mode was stored in the bootloader binaries as

it was intended to be extensively tested and never updated, acting as a secure safe boot for the mission.

Application mode is where autonomous and scheduled application tasks were performed. The primary operation threads were the beacon thread and the Remote Procedure Call (RPC) thread. The beacon thread was run all the time and transmitted a beacon every 22 seconds to help identify the location of the CubeSat. This beacon contained information about the operator of the CubeSat (Binar Space Program) and some system telemetry such as voltages, currents, and temperatures. The RPC thread was always active, waiting for incoming commands from the communication system serial line. Once a command was received, the RPC thread created a new thread to perform the scheduled task.

2.2.6 Integrating the Payloads (80%)

Two cameras with different purposes were integrated with the BCC for the Binar-1 mission. One was for capturing images of the stars, and the other was for images of the Earth. Both cameras integrated with the BCC through the adapter board and an FFC connector that connected to the payload routing board. Not only were the cameras flown on Binar-1 for the possibility of capturing images, but the cameras were also integrated to test the BCCs design and its ability to operate payloads.

Based on a COTS camera sensor called the OpenMV [97], the star tracker camera can take low-resolution pictures of the stars. The camera was operated in Grayscale mode taking 640x480 images as fast as 75 FPS. The main goal of the camera was to return grey-scale images that can be used to see either stars or the Earth in its images. The system interfaced with the BCC through the payload routing board to the payload and communications adapter board before finally making its way to the primary flight computer. Here, images taken can be processed and stored in the eMMC until requested from the ground. The main interface was the power which can be controlled via a GPO from the flight computer, and SPI, which was used to return the images to the flight computer. Once the camera was powered on, it would boot and take a photo. The image was immediately sent to the flight computer, which would store the image in the eMMC. After the flight computer had received and stored the image, it would

disable the power system, powering down the camera. Figure 2.20 shows how the star tracker camera interfaces with the BCC through the routing and adapter boards.

The higher resolution camera was based on a COTS camera that interfaces with a Raspberry Pi Zero (RP0) soldered directly to the payload routing board. The connections through the payload routing board followed the same path as the star tracker camera, connecting to the BCC finally through a UART connection. Unlike the star tracker camera, a sequence of commands was used for operation once powered on. This process configured the camera and prepared it for taking an image. After this, it captured and stored the image on the RP0 for processing. The RP0 processing broke the image into a set of lower-resolution image tiles sent back to the BCC. This was necessary as a whole image could not be sent to the ground due to its file size. As well as the RP0 being able to process the images into frames, it could compress the images into thumbnails. These thumbnails could be used to ensure that the camera was pointing in the correct direction saving on downlink time. Figure 2.20 shows how the higher resolution camera interfaces with the BCC.

2.3 Assembly, Integration, and Testing of Binar-1

This section contains the details of the assembly, integration, and testing performed to meet the launch requirements and verify the design of Binar-1 against its requirements. The subsections are ordered to match the order in which each process was completed. The section has been included to document how the designed CubeSat was able to be successfully launched.

Following the CubeSat design, assembly, integration, and testing were performed. First, the engineering model CubeSat was assembled and integrated as a trial run for the flight model. The engineering model was also taken to the National Space Test Facility (NSTF) in Canberra for an additional verification test in the WOMBAT XL vacuum chamber. The flight model was assembled, integrated, and tested at Curtin University, where it was successfully qualified for launch.

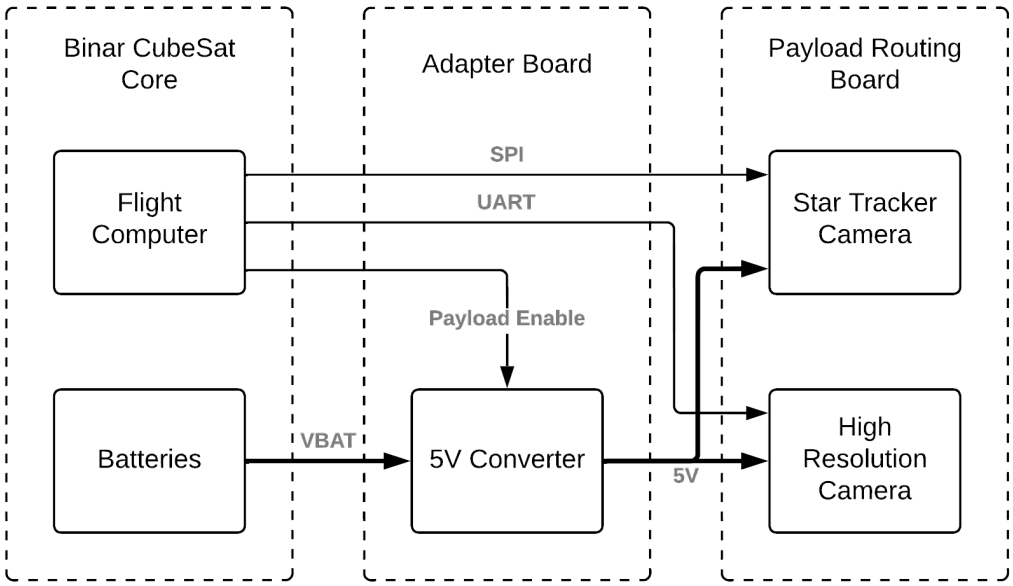

Figure 2.20: Payload interface pathways for Binar-1. The power distribution system for the payloads and communication system was located on the payload and communications adapter board. The payload routing board was only used to provide structural support and deliver electrical connections.

2.3.1 Thermal Vacuum Testing (20%)

Thermal vacuum testing was essential to verify that Binar-1 could operate within its temperature limits. Preliminary testing of the Binar-1 engineering model was performed at Curtin University using a small thermal vacuum chamber. By retrofitting the chamber with a custom thermal management system, the team could perform preliminary testing of the antenna deployment system and battery heaters. The thermal management system included a gravity-fed liquid nitrogen shroud and an electric heater. By pouring liquid nitrogen into the shroud external to the vacuum chamber, the surface temperature of the shroud inside the vacuum chamber to was able to reach <-100°. Once reaching this temperature, a 30-minute cold dwell would begin to test the CubeSats functionality at low temperatures. Following the dwell, the electric heater would enable, increasing the surface temperature to >+100°, where a 30-minute hot dwell would begin testing the functionality at high temperatures. This swing was enough to test the battery heaters, deploy the antennas in a cold state, and observe the CubeSat at its expected minimum (-40°) and maximum (+60°) temperatures. However,

the accuracy of the setup was difficult to verify, so an external thermal vacuum chamber test setup was investigated.

The engineering model was taken to the NSTF in Canberra to verify the results. Operated by the Australian National University (ANU), the WOMBAT XL vacuum chamber was used for five days. The larger chamber has been used to test many Australian CubeSats in the past and was a suitable candidate to verify the performance of the modified chamber at Curtin University. The test featured six cold and hot dwells, stressing the engineering model thermal management system. Unlike the modified chamber at Curtin University, the liquid nitrogen cooling system in the WOMBAT XL is pump fed, allowing for better temperature precision and faster cooling and heating. The six cycles provided acceptable results and verified the modified thermal vacuum chamber at Curtin University as a suitable test method for the flight model.

2.3.2 Battery Qualification Testing (100%)

To qualify for launch, the safety review process needed to be passed. This review process was completed by JAXA and SpaceBD which verified the Binar design met the safety requirements mentioned in Section 2.2.1. The first and longest part of the safety review process was the battery qualification testing. As mentioned previously in Section 2.2.2, one of the possible risks of lithium-ion battery ignition is battery cell ageing. To mitigate this risk, battery cell batch qualification is performed to detect early life failures and guarantee that the battery cells have not aged. The total number of cells in the batch qualification testing was five times the number required for the flight, meaning that 20 cells were tested. From the results, eight cells with the closest matching chemistries were selected and used as flight and flight backup cells. The process was completed through a set of tests, including vibration testing and vacuum testing, where the batteries were qualification tested before and after each test. This means that three tests were performed, one before the vacuum test, one between the vacuum and vibration test, and one after the vibration test.

The qualification test included a visual inspection check, mass measurement, Open Circuit Voltage (OCV) check, and a complete charge and discharge cycle of the battery. After performing these measurements for each of the three tests,

the change between each was required to be within a specified margin to show that the vacuum and vibration test had not damaged the batteries. After the qualification process, the batteries were attached to the BCC during assembly. Before and after the assembly, the complete battery pack was also qualification tested. This was done by performing the test on the entire CubeSat before and after the final CubeSat vibration test. This process further verified the cells and combined battery to ensure that the assembly process and final vibration test had caused no damage to the battery pack. For Binar-1, this testing was highly time-consuming and occupied a large part of the schedule during the assembly process.

2.3.3 Binar-1 Flight Model Assembly (50%)

Following the completion of the battery qualification testing and the successful qualification of the engineering model, the assembly of the Binar-1 flight model began. The most important part of the assembly process was meeting the requirements of the safety review process. Part of this review was an assembly procedure document containing details on the assembly, integration, and testing steps. Throughout the assembly procedure, battery safety function tests were performed, including the battery safety circuit test and the inhibit function test. The antenna deployment test was performed at the end of the assembly procedure. The antennas were then reset, and the vibration test was performed along with a pre and post battery qualification test. Finally, before Binar-1 was shipped, checkout testing included a sharp edge test, fit check test, and an interface verification record.

Battery Safety Testing

Battery safety testing was necessary to validate the battery safety systems. All causes of battery failure seen in Section 2.2.2 were prevented using three inhibits. On Binar-1, these inhibits were the battery safety circuits, double insulation on live terminals, and deployment switches. Figure 2.6 shows how each inhibit was integrated into the design to prevent the batteries from entering a potentially volatile state. The other condition considered for safety was the inadvertent deployment of the antennas. If the antennas were deployed inside the deployment pod, there was a risk that the CubeSat could get stuck. As such, the inhibits also mitigated this risk.

The battery safety circuit test was the first test performed after the battery switch wires were connected to the BCC. From here, the battery was over-charge, over-discharge and short-circuit tested to verify that the protection circuit functioned correctly. The overcharge test was performed using an external programmable power supply which continually discharged the battery until cut off, recording the battery voltage and current as it charged. This was the same for the over-discharge test, where the batteries were continually discharged until cut off. For the short circuit test, the programmable load was used again. The load gradually raised the load current until the battery protection circuit cut off.

After the switches were connected to the switch wires, a check of the double insulation applied was performed. This test used a multimeter to measure between the live point and the insulation layer verifying the insulation layer was appropriate. Additionally, photos were taken to provide a visual inspection verification method. Checking all the BCCs live points was a lengthy process that required good documentation to ensure every point was tested.

Finally, the safety deployment switch stroke length and functionality were tested. On Binar-1, the four safety switches mentioned in Section 2.2.2 required testing. The two negative z-axis switches and the two rail side switches can be seen in Figure 2.21. The BCC and UHF transceiver were first integrated into the stack to test the switching stroke. Then the rail halves were attached. After this, the switches were mounted to the rails. With the switches on the rails, a ruler and microphone were held next to each switch to measure the stroke length and sound of the switch engaging. Each switch was tested separately with a new recording, verifying the correct stroke depths of each switch. To test the functionality, the flight computer bootloader was used. Connecting the USB to the BCC and monitoring the serial connection verified the switch functionality. The flight computer bootloader is run every time the CubeSat was power cycled. By pressing each switch, the serial connection disconnected, which showed that the flight computer was losing power from the battery.

Deployment Testing

After the battery safety testing, the payload base and antenna were attached to the CubeSat. At this point in the assembly, the deployment and RF (Radio

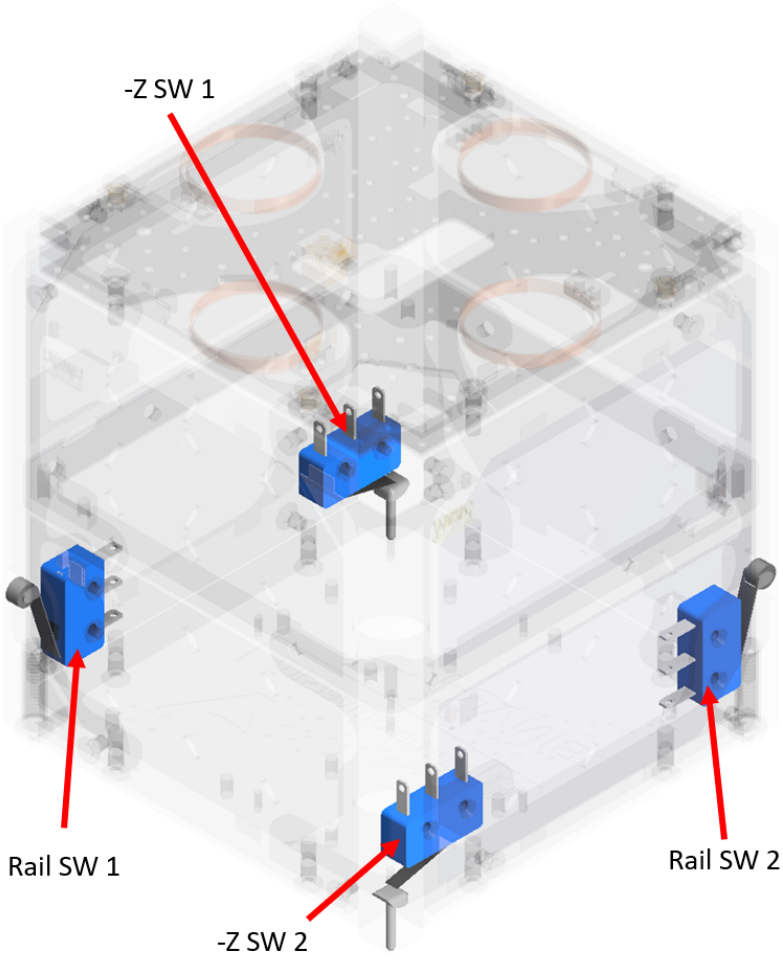

Figure 2.21: Location of deployment switches on the Binar-1 CubeSat. Four switches were necessary to meet the launch safety requirements.

Frequency) test was performed. This verified the switch inhibit functionality further, the first boot 30-minute timer, and the radio operation frequency. Before the antenna was deployed, a batch of flight model deployment wire was tested. The test included a wire strength and stretch test. This verified that the antenna deployment wire was suitable for its application and removed any initial stretch under load, which may have partially deployed the antennas.

Wire strength testing was a full loading test to show that the wire could hold twice as much force than necessary. The maximum loading test was performed by applying weights to a length of wire and verifying that the wire could maintain the required amount of force applied by the antenna doors. The test was enough to demonstrate the burn wires load bearing ability. The stretch test involved a similar test setup. The real force of the antenna deployment mechanism was held on the wire for 48 hours. Over this time, the wire was required to not change in length by more than 1%. Once the wire had been verified for the flight model, it was tied and used to reset the antenna doors.

The antenna deployment and RF test was now able to be completed. The test verified that the bootloader operated correctly and that the three inhibits seen in Figure 2.6 were functioning correctly and restarting the timer. To start the test, all switches were released. After 10-minute intervals, each inhibit switch was pressed. Next, the full 30 minutes were waited until the antennas autonomously deployed. After deployment, the communication system was recorded beaconing using a software-defined radio and waterfall plot to show that the operating frequency was correct. Once the beacon was recorded, basic commands were tested on the satellite including the ping, check voltage, check current, and check temperature commands. Complete log collection and firmware update commands were only tested on the engineering CubeSat due to the extended testing times. After completing these tests, the rest of Binar-1 was assembled and prepared for vibration testing.

Vibration Testing

Before the vibration test, a battery qualification test was performed to verify that the batteries were functioning correctly after the assembly. Once this had been completed, the vibration test was performed. The test involved 3-axis of

Table 2.1: The random vibration profile for Binar-1. The profile combines all possible JAXA launch vehicles, so if there was a last-minute change in the vehicle, the CubeSat could still qualify for launch.

Freq. [Hz]	PSD [G2/Hz]
20	0.03
80	0.04
500	0.04
2000	0.01
Overall	6.811 Grms
Duration	1 min/axis
Direction	3 axes each

random vibration testing at the expected launch conditions. The launch random vibration profile can be seen in Table 2.1. Before each axis was tested, a modal survey was completed to record the natural frequency. After the vibration test, a modal survey was conducted again to ensure that the random vibration test did not change the natural frequency of the CubeSat.

After the random vibration test, a visual inspection test was conducted. This test observed the external screws supporting the CubeSat top, bottom, and side faces. Each screw was marked before the test with a tick mark identifying the initial screw position. The test passed when none of these tick marks had changed. Also, the camera glass lenses and solar cell cover glass needed to be inspected to ensure no cracking or deformation was caused by the random vibration test. After the vibration test, the final battery qualification test was completed, verifying that the performance of the batteries was not affected after being subject to the launch vibration environment.

Final Checkout Testing and Delivery

Before the CubeSat could be shipped, some final safety tests needed to be completed. These included the sharp edge inspection test, fit check test, and interface verification record. After these tests were conducted, the CubeSat was packaged and delivered to JAXA, where it was integrated with the J-SSOD and the JAXA ISS module, completing the design, assembly, integration, and testing of Binar-1.

The sharp edge inspection test was a simple test to notify JAXA personnel integrating the CubeSat of any potentially sharp edges. The test was performed by running a gloved fingertip along the edges of the CubeSat, looking for any cuts in the glove after each pass. No sharp edges were found on Binar-1, as this was accounted for in the structure design. The fit check test was performed to verify that the CubeSat could fit into the J-SSOD once it arrived in Japan. The test was successful for Binar-1, and all switches were observed to click once the CubeSat was fully inserted. Finally, an interface verification record was completed. This final test was a record of the exact weight and dimensions of Binar-1. It was performed as an additional inspection to ensure that Binar-1 could fit inside the J-SSOD.

With the final tests completed, the fully assembled Binar-1 (Figure 2.22) was successfully qualified to launch to the ISS through the safety review process. The design to delivery of the CubeSat was a combined 2-and-a-half-year process contributed to by four full-time PhD students and two staff engineers. The result provided more than just a platform for performing space research. Connecting the university and program with multiple industry partners and space agencies around the world, the Binar Space Program has matured into an emerging CubeSat development group that aims to deliver world-class space research to LEO and beyond.

2.4 Results and Discussion

The design of the Binar CubeSat Bus for Binar-1 was performed with the three primary objectives of reducing hardware costs, maximising payload space, and maintaining system capabilities. To show the effectiveness of the design in meeting these objectives, a comparison to complete COTS systems was made. Although some of the COTS systems are not fully available to the public, there is still enough information to make an effective comparison to the Binar-1 design, demonstrating how it met its design objectives.

2.4.1 Hardware Cost Comparison

One of the primary design objectives of Binar-1 was to reduce the total hardware cost of the combined bus. By achieving this, the team could affordably reuse

the platform to sustain a continued mission program at the University. One of the primary reasons for this objective was to design a platform capable of testing controlled re-entry and recovery systems. Hardware cost was chosen as the focus over other costs in this comparison as the cost to assemble, integrate, test, and operate a CubeSat platform is similar regardless of the design methodology. COTS solutions offer reduced system design time but are still subject to the same verification and validation processes necessary to perform a successful mission. Included in the hardware cost for the CubeSat is every component, excluding the

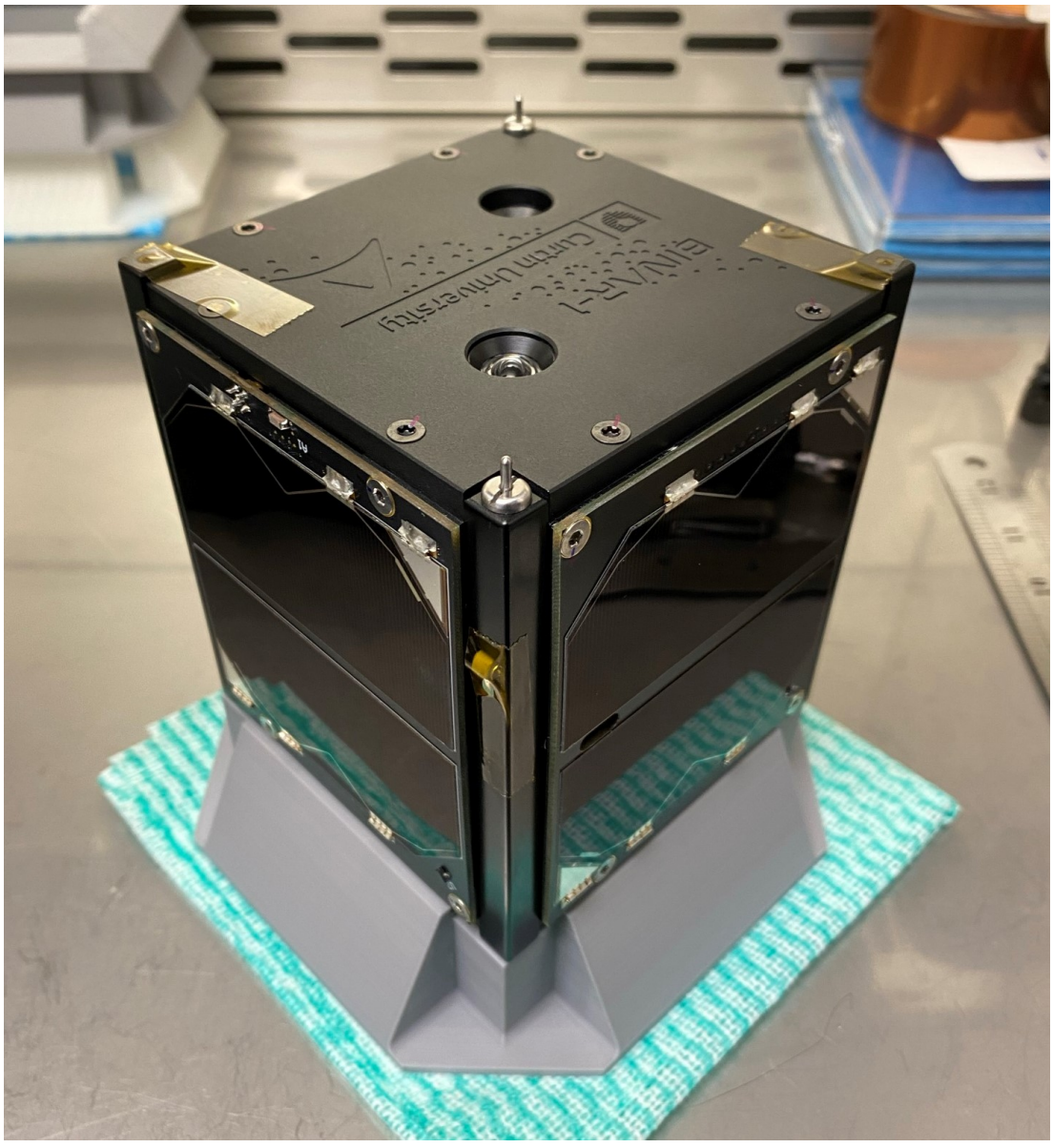

Figure 2.22: The completed Binar-1 ready to be packed and shipped to Japan for integration. Unfortunately, due to the COVID-19 pandemic, the team could not take the case themselves, meaning the CubeSat had to be shipped via mail.

payload cameras, as this is variable for each mission.

The total hardware cost of Binar-1 is presented in Table 2.2. The final price was AUD$17,500, with nearly 60% of that cost being contributed to the COTS UHF system.

To evaluate the success of the design methodology in achieving the reduced cost objective, a survey of COTS suppliers was performed to compare. Due to growing competition in the industry and the complexity of many CubeSat design requirements, the public availability of comparison prices was incomplete. The only solution that included a price was the complete EnduroSat 1U solution which had a total cost of US$37,200 or AUD$48,360. Other solutions were available for comparison of payload space and system capability.

Given the near three times reduction in hardware cost, the reduced cost objective was considered achieved. However, other costs such as labour, prototyping, and testing equipment costs should be considered. In regards to a trade off between purchasing COTS hardware and custom designing hardware, the labour and testing equipment costs would have been the same. For the Binar-1 mission, the launch timeline critical path was constrained by the licensing required for delivery and launch by an Australian party. This means that the employment duration would have been the same and the CubeSat would not have been delivered faster even if a COTS CubeSat was used. This is similar for testing equipment as regardless of the hardware approach, both would have needed to be tested to meet the design requirements.

When considering the prototyping cost, an analysis was performed. For Binar-1, many prototypes were ordered and tested to evaluate component selection and perform system testing. These prototypes added additional costs which are not included in the summary provided in Table 2.2. For the Binar-1 mission two CubeSats where built which had an approximate total hardware cost of of AUD$35,000. If the COTS alternative of EnduroSat had been purchased, this would have cost approximately AUD$96,600. With a saving of AUD$61,600 this can be considered the opportunity cost of prototyping during the design phase of Binar-1. The prototyping cost was recorded to be approximately AUD$150,000,

Table 2.2: Hardware cost breakdown of Binar-1 including all its major components. Some consumables, such as tape and solder, were not included because the costs were negligible compared to the total.

Component	Supplier	Unit Cost	% Of Unit	Cost (AUD)
BCM	MacroFab	8,083.44	0.10	808.34
Batteries	Samsung	32.00	20.00	640.00
Battery Heaters	PCBWAY	191.33	0.25	47.83
Mag Mount	3D Systems	538.50	0.33	161.70
Top Cap	3D Systems	654.00	0.33	218.00
RBF Bracket	3D Systems	485.10	0.33	161.70
Bolts	McMaster-Carr	14.23	0.16	2.28
Transceiver	EnduroSat	5,639.02	1.00	5,639.02
Adapter Board	PCBWAY	275.00	0.20	55.00
Components	Various	35.37	1.00	35.37
Bolts	McMaster-Carr	20.38	0.08	1.63
Switches	Marquardt	7.67	4.00	30.68
Bolts	McMaster-Carr	13.81	0.32	4.42
Rail Halves	3D Systems	1,971.00	0.17	328.50
Bolts	McMaster-Carr	51.14	0.10	5.11
Antenna	EnduroSat	4,834.06	1.00	4,834.06
Bolts	McMaster-Carr	30.09	0.08	2.41
Solar Panels	PCBWAY	945.00	0.27	252.00
Solar Cells	AzurSpace	21,509.78	0.16	3,441.56
Solar Panel Backing	3D Systems	1,510.60	0.33	503.53
Components	Various	17.44	4.00	69.76
Bolts	McMaster-Carr	51.14	0.16	8.18
FFC	PCBWAY	123.90	0.10	12.39
Payload Plate	3D Systems	910.50	0.33	303.50
			Total	$17,567.0

Table 2.3: COTS companies with publicly available 1U platforms and the listed payload space available. Although Binar-1 was not the largest, the other platform capabilities do not match. This is covered in the following section.

Supplier	EnduroSat	AAC Clyde	ISISpace	Near Space Launch	Binar-1
Payload Space (U)	0.53	0.3	0.4	0.588	0.5

which means that 6 CubeSats would need to be built and launched to see the real benefit of the reduced design cost.

2.4.2 Payload Space Comparison

Maximising the payload space design objective was necessary for increasing the amount of science payloads that could be carried by the platform. Included in this motive was the need to maximise the space that a controlled re-entry and recovery system could use. Secondary to this objective was the requirement for the BCC to be reusable between 1U to 3U CubeSat sizes. If the payload space necessary to contain a complete controlled re-entry and recovery system is larger than what is available on a 1U, then the payload space can be increased by only lengthening the structure. Additionally, other science and research objectives are expected at the university as the space industry in Australia grows. By maximising the total available payload space, these research objectives will also be able to be included on future missions.

The total available payload space on Binar-1 was 0.5U. To evaluate the performance of the design to meet the maximised payload space objective, a comparison was made to the payload space available in 1U COTS designs. Table 2.3 presents a list of the companies that were found to have 1U platforms publicly available. The table shows that the payload space available in Binar-1 was not as ample as some of the COTS solutions. However, this is only holds true assuming that the capabilities and reliability of the platforms are the same. As such, the evaluation of this design objective needed to be evaluated in parallel with the capability design requirement.

2.4.3 System Capability Comparison

The capabilities of Binar-1 were maximised to increase the number of research opportunities the platform can perform. This can be seen when observing the design constraints of the main subsystems. The EPS was designed to fit within the BCC, which, when integrated with the ADCS, does not affect the capabilities or payload space. Although the ADCS only used a magnetorquer for control, the determination systems included a GPS, and 9-axis IMU. The added determination methods increase the science capabilities of the platform for future missions. The flight computer system included a dual flight computer system for backup and recovery, as well as ample external storage that can support large data requirements on future missions. To evaluate the capabilities of the CubeSat, a comparison to the capabilities of COTS designs found during the payload space review was performed. Table 2.4 presents a capabilities summary for comparison with Binar-1.

The results show that Binar-1 had some added capabilities compared to the COTS solutions. The other COTS capabilities included sun sensors, reaction wheels, star trackers, and an additional MPPC. Sun sensors were not included on Binar-1 as it was determined that they would not be required to meet the ADCS design requirements. The solution provided by AAC Clyde Space included reaction wheels and a star tracker. The system was an integrated reaction wheel, star tracker, and magnetorquer solution that compromised on payload space, making it the smallest of the solutions found. This is a similar reason why the team chose not to include reaction wheels, as the payload space trade-off for improved pointing accuracy was not required. The number of MPPCs available on Binar-1 was limited to two because this is all that was needed for the platform. In the future, additional MPPC can be added to the BCM if required, meaning the capability can still be added.

The payload space versus capability compromise was one of the significant design challenges overcome to meet the design objectives. As a result of the considerable effort put into the design, comparing the custom design to COTS shows that the compromise has been made effectively for Binar's intended applications and design requirements. The Binar-1 design has matching and additional capabilities

Table 2.4: Capabilities of COTS solutions including the EPS, ADCS, communication system, and flight computer system. Compared to Binar-1, an evaluation of the design requirement can be performed.

Supplier	EnduroSat	AAC Clyde Space	ISISpace	Near Space Launch	Binar-1
Price	USD$37,200	Unknown	Unknown	Unknown	AUD$17,500
Payload Space (U)	0.53	0.3	0.4	0.588	0.5
Comms System	Yes	Yes	Yes	Partial	Yes
Gyroscope	Yes	Yes	Unknown	Yes	Yes
Magnetometer	No	Yes	Unknown	No	Yes
Magnetorquers	Yes	Yes	Unknown	No	Yes
GPS	No	No	Unknown	No	Yes
Sun Sensor	Yes	No	Unknown	No	No
Solar Panels	Yes	Yes	Yes	Yes	Yes
Flight Computer	Yes	Yes	Yes	Yes	Yes
Reaction Wheels	No	Yes	No	No	No
Star Tracker	No	Yes	No	No	No
Capacity (Whr)	20.4	20	28.8	15.8	48.1
3V3 & 5V	Yes	Yes	Yes	Yes	Yes
VBAT (V)	3.7	7.4	7.4	7.4	7.4
Number of MPPC	3	3	3	3	2

while still having a large payload space. Due to the added capability, the payload space is not greater than some of the COTS solutions. However, with further design improvement and the integration of a custom communication system, the available payload space can be optimised further, making it near to or greater than the other available systems. This added capability will provide more opportunities for low cost space science including controlled re-entry and recovery missions.

2.5 Concluding Remarks

Through a comparison to COTS CubeSats, the design of the Binar-1 CubeSat has been shown to reduce hardware costs and maximise payload space without removing any essential system capabilities. The objectives set at the beginning of the design process, have assisted in creating a suitable platform for demonstrating parts of controlled re-entry and recovery for CubeSats. Using this platform, the phases can be demonstrated separately, and then merged when the technology has been successfully demonstrated. Following the delivery of Binar-1, the CubeSat platform became known as the Binar CubeSat Bus (BCB). This platform has become the trademark CubeSat for space in Western Australia and has been further developed for the upcoming Binar-2, 3, and 4 mission. Details on the design improvements are documented in Chapter 5.2.

References

[2] H. Heidt, J. Puig-Suari, A. Moore, S. Nakasuka, and R. Twiggs, "CubeSat: A New Generation of Picosatellite for Education and Industry Low-Cost Space Experimentation," *Small Satellite Conference*, Aug. 2000. [Online]. Available: https://digitalcommons.usu.edu/smallsat/2000/All2000/32.

[13] A. Klesh, B. Clement, C. Colley, *et al.*, "MarCO: Early Operations of the First CubeSats to Mars," *Small Satellite Conference*, Aug. 2018. [Online]. Available: https://digitalcommons.usu.edu/smallsat/2018/all2018/474.

[53] E. Kulu, *Nanosats Database*, en. [Online]. Available: https://www.nanosats.eu/index.html (visited on 12/19/2022).

[76] M. N. Sweeting, "Modern Small Satellites-Changing the Economics of Space," *Proceedings of the IEEE*, vol. 106, no. 3, pp. 343–361, Mar. 2018, ISSN: 1558-2256. DOI: 10.1109/JPROC.2018.2806218.

[77] *Launch Services | Tyvak International*. [Online]. Available: https://www.tyvak.eu/launch-services/ (visited on 12/21/2022).

[78] M. Cho, T. Yamauchi, M. Sejera, Y. Ohtani, S. Kim, and H. Masui, "CubeSat Electrical Interface Standardization for Faster Delivery and More Mission Success," *Small Satellite Conference*, Aug. 2020. [Online]. Available: https://digitalcommons.usu.edu/smallsat/2020/all2020/3.

[79] D. Sadhukhan, A. Guzik, O. Benafan, *et al.*, "Advanced eLectrical Bus (ALBus) CubeSat: From Build to Flight," *Small Satellite Conference*, Aug. 2020. [Online]. Available: https://digitalcommons.usu.edu/smallsat/2020/all2020/9.

[80] K. Rankin, I. McNeil, I. Rankin, and S. Stochaj, "How Not to Build a CubeSat – Lessons Learned from Developing and Launching NMSU's First CubeSat," *Small Satellite Conference*, Aug. 2019. [Online]. Available: https://digitalcommons.usu.edu/smallsat/2019/all2019/54.

[81] L. Sato, L. Costa, J. Fulindi, *et al.*, "The ITASAT – The Lessons Learned from the Mission Concept to the Operation," *Small Satellite Conference*, Aug. 2019. [Online]. Available: https://digitalcommons.usu.edu/smallsat/2019/all2019/51.

[82] Y.-C. Chiu, L. C. Chang, C.-K. Chao, *et al.*, "Lessons Learned from IDEASSat: Design, Testing, on Orbit Operations, and Anomaly Analysis of a First University CubeSat Intended for Ionospheric Science," en, *Aerospace*, vol. 9, no. 2, p. 110, Feb. 2022, ISSN: 2226-4310. DOI: 10.3390/aerospace9020110. [Online]. Available: https://www.mdpi.com/2226-4310/9/2/110 (visited on 12/21/2022).

[83] S. Wu, W. Chen, and C. Chao, "The STU-2 CubeSat Mission and In-Orbit Test Results," *Small Satellite Conference*, Aug. 2016. [Online]. Available: https://digitalcommons.usu.edu/smallsat/2016/TS3YearInReview/8.

[84] A. Greenberg, D. Lay, G. Lebrasseur, *et al.*, "OreSat: A Student Team-Based Approach to an Inexpensive, Open, and Modular (1-3U) CubeSat Bus," *Small Satellite Conference*, Aug. 2021. [Online]. Available: https://digitalcommons.usu.edu/smallsat/2021/all2021/236.

[85] G. Li, L. Spence, M. Miller, *et al.*, "Lessons Learned from the Development and Flight of the First Miniature Tethered Electrodynamics Experiment (MiTEE-1)," *Small Satellite Conference*, Aug. 2021. [Online]. Available: https://digitalcommons.usu.edu/smallsat/2021/all2021/249.

[86] J. Fuchs, M. Halvorson, and V. Lopez, "An Overview of the Alabama Burst Energetics eXplorer (ABEX) Mission," *Small Satellite Conference*, Aug. 2021. [Online]. Available: https://digitalcommons.usu.edu/smallsat/2021/all2021/239.

[87] P. A. Bland, P. Spurný, A. R. Bevan, *et al.*, "The Australian Desert Fireball Network: A new era for planetary science," *Australian Journal of Earth Sciences*, vol. 59, no. 2, pp. 177–187, Mar. 2012, ISSN: 0812-0099. DOI: 10.1080/08120099.2011.595428. [Online]. Available: https://doi.org/10.1080/08120099.2011.595428.

[88] *JEM Payload Accomodation Handbook - Vol. 8 - Small Satellite Deployment Interface Control Document - Rev. D*, Jul. 2020. [Online]. Available: https://iss.jaxa.jp/kibouser/library/item/jx-espc_8d_en.pdf (visited on 12/21/2022).

[89] A. Sandberg and T. Smith, "Streamlining CubeSat Solar Panel Fabrication Processes," *Small Satellite Conference*, Aug. 2016. [Online]. Available: https://digitalcommons.usu.edu/smallsat/2016/TS8StudentComp/2.

[90] A. Dahir, A. Sandberg, and J. Mason, "Advancement, Testing and Validation of an Innovative SmallSat Solar Panel Fabrication Process," *Small Satellite Conference*, Aug. 2017. [Online]. Available: https://digitalcommons.usu.edu/smallsat/2017/all2017/27.

[91] V. Knap, L. K. Vestergaard, and D.-I. Stroe, "A Review of Battery Technology in CubeSats and Small Satellite Solutions," en, *Energies*, vol. 13, no. 16, p. 4097, Jan. 2020, ISSN: 1996-1073. DOI: 10.3390/en13164097. [Online]. Available: https://www.mdpi.com/1996-1073/13/16/4097.

[92] F. C. Krause, J. A. Loveland, M. C. Smart, E. J. Brandon, and R. V. Bugga, "Implementation of commercial Li-ion cells on the MarCO deep space CubeSats," en, *Journal of Power Sources*, vol. 449, p. 227 544, Feb. 2020, ISSN: 0378-7753. DOI: 10.1016/j.jpowsour.2019.227544. [Online]. Available: https://www.sciencedirect.com/science/article/pii/S037877531931537X (visited on 12/21/2022).

[93] A. Edpuganti, V. Khadkikar, M. S. E. Moursi, H. Zeineldin, N. Al-Sayari, and K. Al Hosani, "A Comprehensive Review on CubeSat Electrical Power System Architectures," *IEEE Transactions on Power Electronics*, vol. 37, no. 3, pp. 3161–3177, Mar. 2022, ISSN: 1941-0107. DOI: 10.1109/TPEL.2021.3110002.

[94] R. M. Sharma, R. Kawari, S. Bhandari, S. Panta, R. C. Prajapati, and N. B. Adhikari, "Simulation of CubeSat Detumbling Using B-Dot Controller," en, in *Proceedings of International Conference on Sustainable Expert Systems*, S. Shakya, V. E. Balas, W. Haoxiang, and Z. Baig, Eds., ser. Lecture Notes in Networks and Systems, Singapore: Springer, 2021, pp. 541–553, ISBN: 978-981-334-355-9. DOI: 10.1007/978-981-33-4355-9_40.

[95] M. D'Alessio, C. Poivey, D. Walter, *et al.*, "NAND flash memory in-flight data from PROBA-II spacecraft," in *2013 14th European Conference on Radiation and Its Effects on Components and Systems (RADECS)*, Sep. 2013, pp. 1–6. DOI: 10.1109/RADECS.2013.6937432.

[96] *PCB Design Software & Tools | Altium*, en. [Online]. Available: https://www.altium.com/ (visited on 12/22/2022).

[97] *Small - Affordable - Expandable.* [Online]. Available: https://openmv.io/ (visited on 12/23/2022).

Chapter 3

Results and Lessons Learned from the Binar-1 CubeSat Mission

The first Western Australian space capability, Binar-1, was deployed from the ISS on the 6^{th} of October 2021. The mission aimed to demonstrate the custom-designed Binar systems, which were developed to improve access to space and progress towards long-term research objectives based at Curtin University. These long term research objectives that will be developed using the Binar platform aim to progress the university towards planetary class CubeSat missions performing valuable research in the study of the Solar System. The current research objectives are advanced CubeSat attitude determination and control techniques for precise interplanetary guidance, onboard intelligence for operation in communication-denied environments, and controlled re-entry and recovery systems for extra-terrestrial sample return and surface landings.

Initially, the primary objectives of the Binar-1 mission were to demonstrate the functionality of the newly designed CubeSat systems described in Chapter 2 and learn about the end-to-end space mission lifecycle process. However, with the satellite being the first ever built in Western Australia, another primary objective was added to create awareness about the importance of space research in Western Australia. To maintain a space program rather than perform a single space mission, this additional mission objective was essential to ensure the

community understood the importance of a Western Australian space initiative. This mission objective was achieved through an extensive promotional campaign promoting the launch and its historical significance in Western Australia. The campaign included interviews, newspaper articles, and an event in Perth's Yagan square which live streamed the launch and provide an opportunity for members of the public to be involved. Although not directly relating to the thesis topic, meeting this objective enables the continued development of controlled re-entry and recovery systems as it assists the university in securing funding for future missions.

This chapter summarises the Binar-1 mission and the lessons learned by completing the mission. First, an overview of Binar-1 core subsystems are described, focusing on the elements that relate to the remainder of the chapter. A detailed description of the complete design has been included in Chapter 2. Second, the challenges experienced during assembly and integration, the ground segment, and the operation modes are summarised for context to the mission operations. Third, a summary of the mission operations is provided, detailing the recovery performed and communications received over the first month after deployment. Fourth, the results and lessons learned are explained, these lessons are important for preparing for the next CubeSat mission. Finally, a discussion is provided to highlight how Binar-1 performed compared to other first CubeSat missions performed by universities and the proposed design and mission lifecycle changes that will assist the Binar Space Program in successfully delivering its next mission, Binar-2, 3, and 4.

3.1 The Binar-1 Mission

Binar-1 was the maiden technology demonstrator mission of the Binar Space Program. The primary mission objectives were:

- To demonstrate the functionality of the custom CubeSat systems developed by the Binar Space Program,

- To understand and build capacity in the space mission lifecycle process, and

- To increase awareness about the importance of space research and industry in Western Australia.

Assembly, integration, and testing of the CubeSat were completed in May 2021, when it was delivered to Japan to be integrated for launch on the Commercial Resupply Mission 23 (CRS-23). The integration process was finalised by the launch services company SpaceBD which assisted the team in liaising with the Japanese Aerospace Exploration Agency (JAXA). Launched on a SpaceX Falcon 9 rocket on the 29th of August 2021, Binar-1 made its way to the International Space Station (ISS), where it was deployed into orbit on the 6th of October 2021 by the Japanese astronaut Soichi Noguchi through the Kibo module.

The custom CubeSat systems demonstrated on Binar-1 include the BCC, Binar Structure, and Binar Software Framework. The design and makeup of these systems are summarised for context in Section 3.2. A more detailed explanation of the design is presented in Chapter 2. Various sensors were placed around the CubeSat to monitor the functionality of the design. The flight computer used these sensors to transmit operations data to the ground through the communications system. To meet the technology demonstration objective, the ability to receive and analyse this data formed the basis of the mission success criteria.

The mission success criteria had three stages that could be considered a success for the Binar-1 mission. The minimum success criteria was to receive a beacon or message from the Binar-1 CubeSat. The optimal mission success criteria was to receive telemetry from Binar-1 containing performance data. The stretch mission success criteria for Binar-1 was to operate and collect an image from both payload cameras.

3.2 The Binar-1 CubeSat

The design of Binar-1 can be described by breaking down the CubeSat into its main components and subsystems. This section includes a brief description of the subsystems that are relevant to the remainder of the Chapter. The structure and payload subsystem are the only subsystems that have been excluded. A more detailed description of the included and excluded subsystems is provided in

Chapter 2. Only the simplified descriptions here are necessary to understand the Binar-1 mission operations.

3.2.1 Binar CubeSat Core

The BCC was custom designed by the Binar Space Program with the support of Curtin University from 2018 to 2020. The preliminary design set objectives for the CubeSat to be as integrated as possible to maximise payload space. As such, the team decided early in the development process to combine three major spacecraft systems into a single integrated core. By successfully demonstrating the BCC, the technology can enable the Binar Space Program to house larger payloads on future Binar missions by reusing the design. The BCC contains the EPS, ADCS, and flight computer systems. A summary of the capabilities of the BCC is presented in Table 3.1. Consisting of a single PCB called the Binar CubeSat Motherboard (BCM), the magnetorquers and battery cells are able to be integrated and mounted to the PCB together, minimising the space occupied by the systems. The advanced Computer-Aided Design (CAD) software Altium [96] was used to compress the design onto a single PCB.

Using this integration method, integration challenges between the three systems were limited and optimal positioning of electronic components was possible. Once combined, the integrated BCC occupied 0.35U of the Binar-1 hardware stack leaving 0.65U available for the communications system, payloads, and harnessing. For Binar-1, once these remaining systems were integrated, the remaining space was used to test an additional BCM without the magnetorquers and batteries. This second BCM was a further demonstration of the functionality of the BCC. However, it was disconnected before delivery due to the delays experienced during assembly. Its inclusion is only mentioned as the hardware still flew on the Binar-1 mission and it can be seen on all design figures even though it was inactive during flight. A more detailed explanation of the design of the BCC is provided in Section 2.2.2.

3.2.2 Communication System

Initially intended to be included as part of the BCC, a COTS communication system was used instead. This decision was made due to the limited capacity of

Table 3.1: A summary of the systems and capabilities of the BCC. The integrated core was able to reduce hardware costs, maximise payload space, and maintain system capabilities compared to alternative COTS CubeSat solutions.

EPS	
Battery Capacity	48W
Battery Voltage	7.4V
3V3 and 5V	Yes
MPPC	2
ADCS	
Magnetorquers	3
Gyroscope	Yes
Magnetometer	Yes
GPS	Yes
Flight Computer System	
Flight Computers	2 (Primary and Secondary)
External Memory	4GB

the design team to develop a custom communications system alongside the other systems. As a result, the 2-Watt EnduroSat type 2 Ultra High Frequency (UHF) transceiver and matching crossed-dipole circularly polarised antenna were procured to meet the communications requirements. Additionally, a 1-Watt variant and matching antenna was purchased for the engineering model. It was planned to include a custom communications system in the following mission, completing the in-house design.

As the COTS transceiver used the PC104 standard headers for integration, an adapter board was required to interface with the BCC. The resulting payload and communications adapter board design connected to the base of the BCC and interfaced with the antenna deployment system, transceiver, and payload routing board. A more detailed explanation of the COTS communication system and payload and communication adapter board design is provided in Section 2.2.3.

3.2.3 Binar Software Framework

The Binar Software Framework was developed to be safe, reliable, and portable between CubeSat revisions. A review of space mission mishaps over the past two

decades influenced this by highlighting the common software areas that contribute to mission failure. As such, the Binar Software Framework development addressed these areas and attempted to prevent the same mishaps from occurring. The results of these efforts provided the Binar Space Program with a robust software framework for Binar-1 and future Binar missions.

The software on board the CubeSat had multiple partitions, namely a bootloader and two application binaries. Dual application binaries increased the reliability of the software. If one binary became corrupt, the other would provide a safe boot for the CubeSat. The shift between application binaries used non-volatile memory flags. If these flags were set incorrectly at boot, the bootloader would know that the current binary did not exit correctly and may be corrupt, resulting in the bootloader booting into the other application binary. These flags also recorded other CubeSat errors associated with the EPS and COTS antenna. Like the corrupt binary check, the bootloader would also know if the EPS was functioning incorrectly or if the antenna had not deployed, booting into safe mode instead of an application binary. More detail on the design of the Binar Software Framework is provided in Section 2.2.5.

3.3 Assembly, Integration, and Testing Challenges

The assembly, integration, and testing of Binar-1 was performed over three months following the engineering model's assembly, integration, and testing and completion of the phase 0/1/2 safety review. The engineering model was built before the flight model to practice and improve the procedures. The safety review process was broken into phases 0/1/2 and phase 3. Each stage was necessary to meet launch requirements specified by the Japanese Experimental Module (JEM) Payload Accommodation Handbook, Volume 8, revision D[88].

Following the assembly and integration of the engineering model, additional qualification testing was performed. The Binar-1 engineering model was transported to the National Space Test Facility at the Australian National University in Canberra. Here, the WOMBAT XL vacuum chamber was used to perform thermal vacuum testing, simulating the expected temperature extremes for the planned Binar-1 orbit. For the Binar-1 flight model, a vacuum chamber at Curtin Univer-

sity was modified to include heating and cooling capabilities. This was intended to be used for the acceptance testing of Binar-1.

After completing the vacuum testing of the engineering model, the phase 0/1/2 safety review could begin. Unfortunately, during the design, the JEM Payload Accommodation Handbook [88] underwent a revision from C to D. This changed some of the launch acceptance requirements prompting late design changes. One of these late design changes was the antenna burn wires. Another was the force exerted by the rail switches on the inside of the deployment pod. Previously there was no limit to the force the switches could apply if the switch used a roller lever. This changed in the revision to a force lower than what the Binar switches delivered, meaning the CubeSat was required to secure a requirement waiver for launch, delaying the completion of phase 0/1/2 and the beginning of the flight model assembly, reducing the available testing time.

Following this delay, more challenges occurred during the flight model's assembly and integration. The first challenge was associated with integrating the flight model UHF transceiver. The team did not notice a fine print in the datasheet that mentioned a difference in the interfacing methods for the 1-Watt engineering model transceiver and the 2-Watt flight model transceiver. The result meant that a modification to the payload and communications adapter board was required to convert the interface from UART to I2C serial communications. The amendment required a new PCB to be ordered and assembled, resulting in a significant delay. The next challenge was associated with the UHF antenna.

As a result of the payload accommodation handbook revision change, deployable surfaces with forces greater than 1N required a double hold-down release mechanism. As the antenna was procured before this shift in the requirement, the deployment system needed to be improved to include a double hold-down release mechanism. The first solution included shipping the antenna to the supplier. This would have resulted in a month-long delay. To avoid this delay, the team chose to modify the antenna instead. As such, the team learnt to tie and test the hold-down release mechanism, adjusting the existing antenna. The resulting change was functional. However, it could only be tested a limited number of times due to the delays resulting from the switch waiver, adapter board modification,

and learning how to tie a new hold-down release mechanism.

As a result of the delays, the testing schedule of Binar-1 was shortened to meet the delivery deadline. Following the integration completion, the team could perform basic functionality and safety review testing required for the phase 3 safety review. This included testing all of the telecommands and responses using the included Universal Serial Bus (USB) connection, battery safety testing, vibration testing and interface verification testing. Tests that were not performed included the thermal vacuum test and further testing of the modified deployment system, as it was optional for completion of the safety review and qualification for launch.

3.4 Ground Segment

The Binar Space Program built a ground station and supporting software for the Binar-1 mission. The ground station was designed using custom and COTS components and is located at the Curtin University Bentley campus in Western Australia. One of the main components of the ground station is the tracking software used to track Low Earth Orbit (LEO) satellites. The Binar Space Program designed this software in collaboration with an industry partner Fugro SpAARC (Space Automation AI and Robotics control Complex). The software was used to track Binar-1 and perform operations. The complete design of the Binar ground station will be used on all future Binar missions and enable university students and amateur radio enthusiasts to gain satellite operations experience. Figure 3.1 is a photo of the Binar ground station in operation at the beginning of a Binar pass over Western Australia.

3.5 Operation Modes

Flight operations of Binar-1 included three main operation modes. The first was the bootloader, responsible for checking the CubeSat critical systems, performing the deployment sequence, and booting the spacecraft into either of the other two modes. The second mode was Safe mode which was used to recover the CubeSat if a problem was identified through the onboard checks. In this operation mode, Binar-1 used less power and had reduced functionality. However, was still able to communicate with the ground and be reprogrammed to attempt a recovery. The ADCS was disabled in this operation mode as the omni-directional antenna de-

Figure 3.1: The Binar Ground Station antenna pictured above Curtin University in Perth, Western Australia. The complete system will be used in all Binar LEO missions for the foreseeable future and will play an essential role in satellite operations and communications at the university.

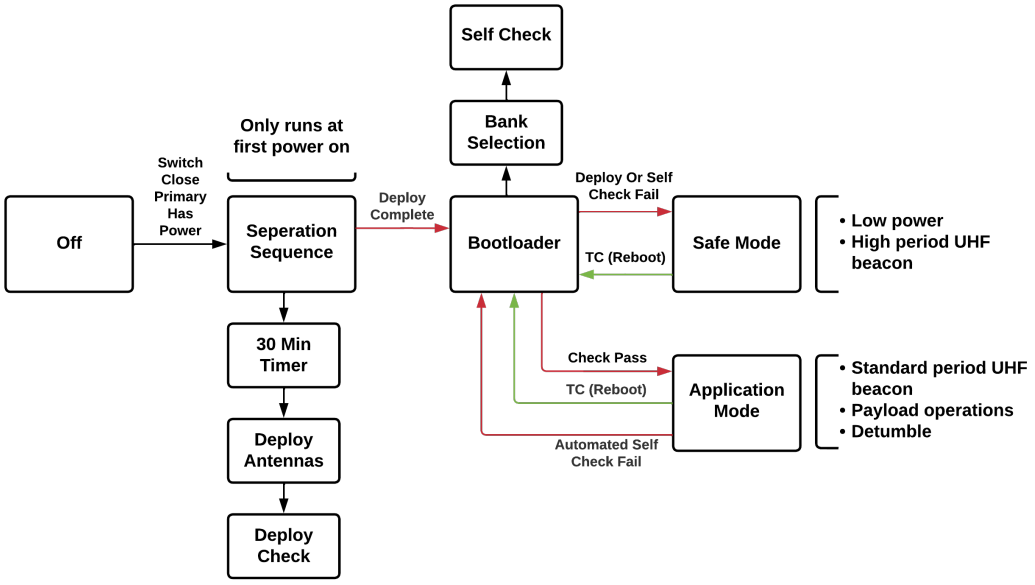

Figure 3.2: Binar-1 operation flow chart. The bootloader and safe mode were contained in the same binary to enable application mode binary updates without modifying the simplified safe mode binary.

sign allowed for communications with the CubeSat without precise pointing. By disabling the ADCS a greater power surplus was available compromising only on the CubeSat spinning at a faster rate. This could have prevented longer communications such as software updates. However, this would have not compromised short transmissions used for determining the safe mode entry cause. If a software update was required the ADCS was able to be operated while in safe mode but only from external commands. When the system checks pass, the bootloader boots the CubeSat into an application mode binary. The third operation mode, application mode, enables all on-orbit tasks for the CubeSat, including operating the payloads, beaconing to the ground, and operating the ADCS. The Binar-1 operation flow chart is presented in Figure 3.2. Built using the Binar Software Framework, the bootloader and application mode binaries were tested constantly throughout the design process, providing Binar-1 with the functionality needed to complete the mission objectives.

3.6 Mission Operations

After completing the assembly, integration, and testing of Binar-1, it was delivered for integration on the 8th of May 2021. After delivery, it was integrated with

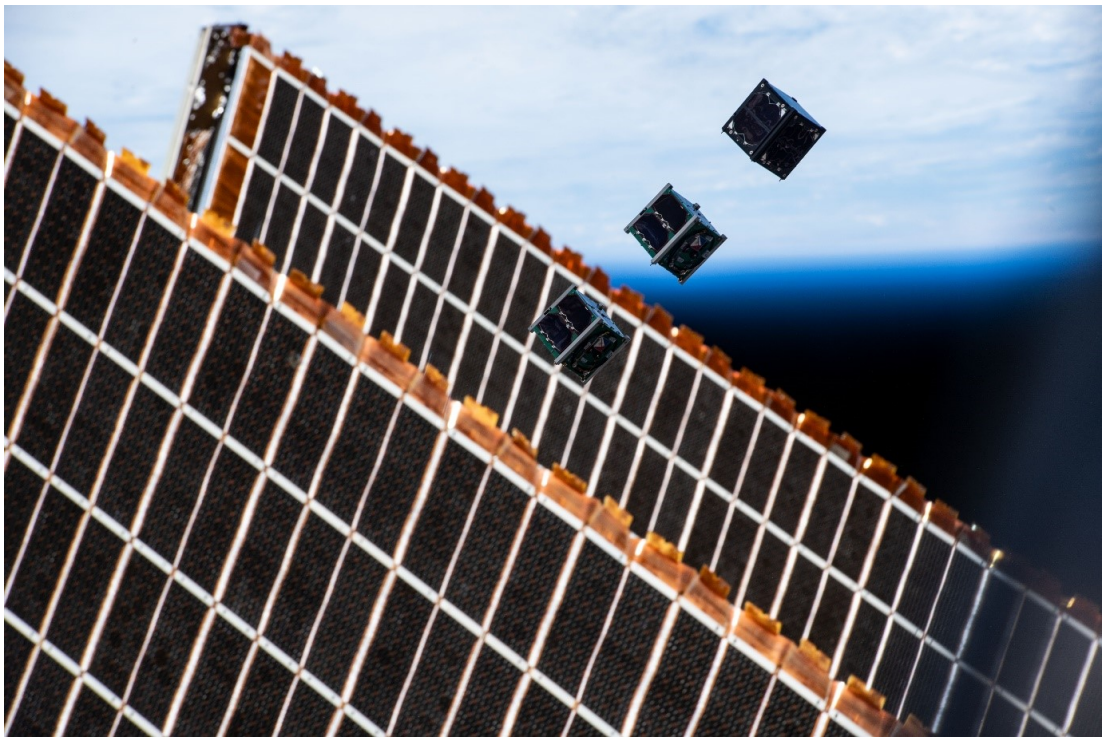

Figure 3.3: Binar-1 (top right), Maya 3 and Maya 4 just after being deployed from the ISS.

the CRS-23 Falcon 9 rocket and launched on the 29th of August 2021 before it was deployed into orbit on the 6th of October 2021 at 17:20 (AWST) along with Maya 3 and Maya 4 (Figure 3.3). After deployment, Binar-1 waited 30 minutes before attempting to deploy its antennas and begin beaconing. The first pass over the Curtin University ground station was expected to occur five and a half hours later at approximately 23:00 (AWST). However, no beacons were heard. This prompted the team to begin transmitting commands on the following passes to attempt to communicate with Binar-1 and test its functionality. Additionally, the SatNOGS [98] service was heavily utilised and monitored to try to observe beacons. SatNOGS is an open source network of ground stations that are used by CubeSat missions to locate and track CubeSats after launch and deployment. After three days of no success, the team began a failure analysis to attempt a recovery.

3.6.1 Failure Analysis

The first possible failure mode identified was a dead on arrival CubeSat or a flat battery. A common failure of first CubeSat missions is that the battery is depleted due to an unexpected power drain between delivery and deployment. If

this had occurred to Binar-1, the CubeSat may never have been recoverable, as such it was overlooked as other failure modes may have occurred that were able to be recovered from.

The second possible failure identified by stepping through the software on Binar-1 was a software error where some system flags were being set in volatile memory instead of non-volatile memory. This error would mean that if the flight computer systems were power cycled, the flag would be reset and not logged correctly. This error was a possible failure cause, as the operation of the redundant 3.3V power distribution system relied on these flags. As the flags reset between power cycles, the result may have caused an indefinite power cycling event where the redundant 3.3V system would be powered off every time the flight computer boots. As this had never been experienced in testing, and recovery would not be possible from this condition, the team moved on with its analysis.

The modified antenna hold-down release mechanism was identified as the next possible failure. The antenna included four separate deployment systems for each of the four antenna elements. As determined by testing performed with the engineering model, if only one of the four antenna elements was deployed, then the beacons could be heard given the correct CubeSat attitude. If none of the antennas had deployed, then recovery would not be possible, so the analysis moved on to a subsequent possible failure, which was discovered in safe mode.

The bootloader would have moved into safe mode if only one, two, or three antenna elements were deployed. This possibility was considered next as it matched the previous failure cause and could have occurred due to the modified hold-down release mechanisms. When testing the functionality of safe mode during the shortened testing schedule, the 30-minute deployment delay and 10-minute deployment attempt timer were removed to reduce testing time. The result meant that after powering on the CubeSat, the flight computer system enabled and configured the communication system, then jumped straight to safe mode to test its functionality. During the actual flight, the delays meant that the configuration performed at start-up would have timed out, resulting in the communications system returning to its default state, needing reconfiguration. Due to the removed timers in testing, the software did not include a command to reconfigure the communi-

cations system when entering safe mode. The result meant that if the satellite only deployed some of its antennas, it would have entered safe mode and not been able to beacon or receive messages due to the incorrect configuration of the communication system. Figure 3.4 presents a simplified bootloader operations flow chart. The flow chart shows how if the antennas were only partially deployed and the battery was over half charged, the bootloader would have moved straight into safe mode. The CubeSat was assumed to be at greater than 50% battery capacity after deployment in the first instance. One of the design features of the communications system was its ability to be configured from ground transmissions. As such, the team began testing with the engineering model to return the CubeSat to its correct configuration to receive beacons if the antennas had only partially deployed. After numerous passes and attempts to configure the communications system, still, no beacons were received on the ground.

As these attempts were unsuccessful, the team decided to determine what the subsequent possible failure could have been. This was identified as the serial communications converter, which was added to the payload and communications adapter board when modified due to the challenges of integrating the COTS transceiver. As the converter was assembled by hand and not correctly vacuum tested, the failure analysis identified this converter as the next possible failure point. If the converter had failed, communications would not be possible with the flight computer. However, if the primary flight computer and EPS were still powering the communications system, the transceiver would still be configurable from the ground.

Following this discovery, the team tested with the engineering model to attempt to configure the transceiver in a secondary beacon mode. This secondary beacon mode only beaconed a secondary string pre-configured to include Binar information and could not provide system telemetry. After successfully enabling the beacon on the engineering model, the same command was attempted to be sent to Binar-1. The first beacon from Binar-1 was received at 5:21 pm (AWST) on the 21st of October 2021, nearly 15 days after deployment from the ISS. The beacon was heard by the Curtin University ground station and a SatNOGS ground station in Perth, as presented in Figure 3.5.

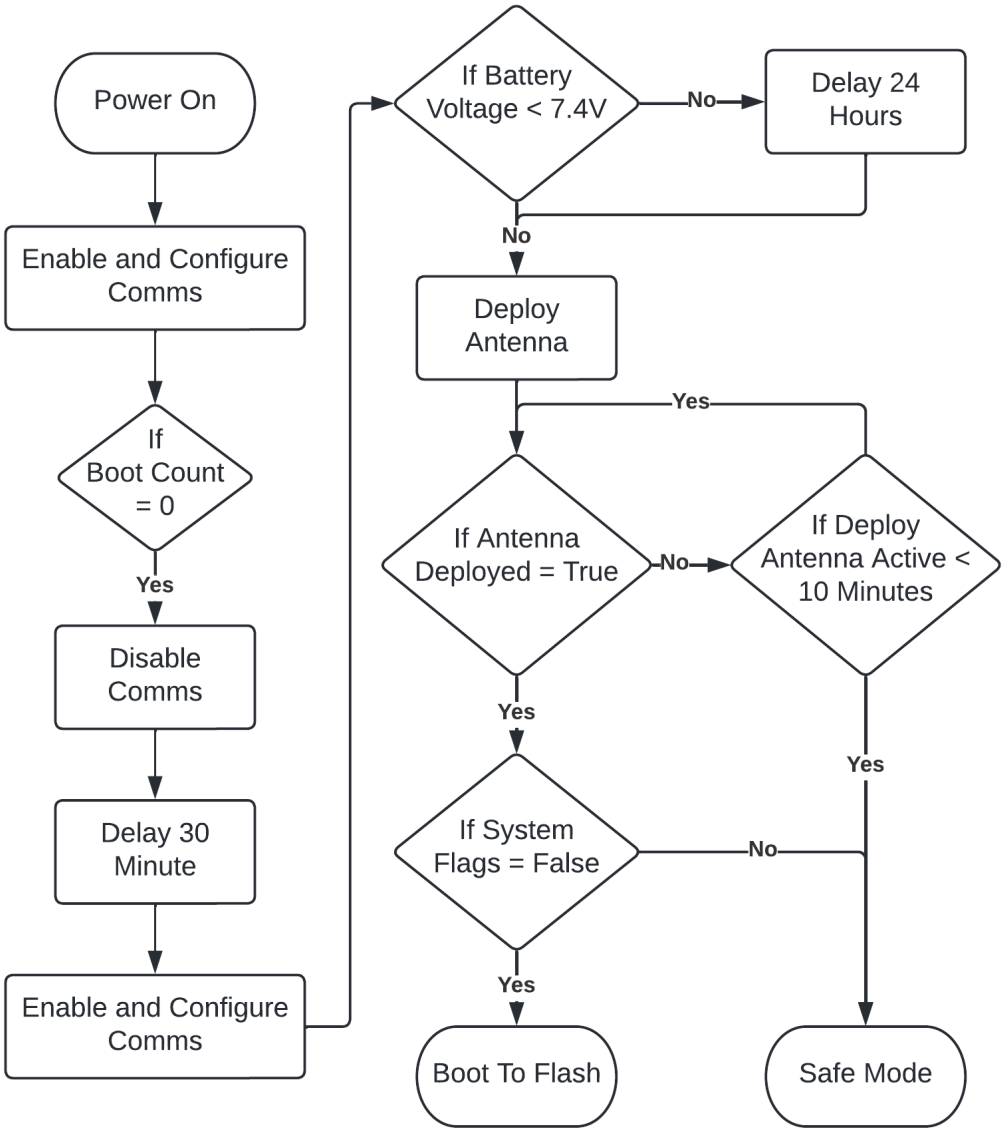

Figure 3.4: A simplified Binar-1 bootloader flowchart. During basic functionality testing, the 30-minute and 10-minute timers were removed to speed up the process. As a result, the implementation of safe mode did not configure the transceiver correctly.

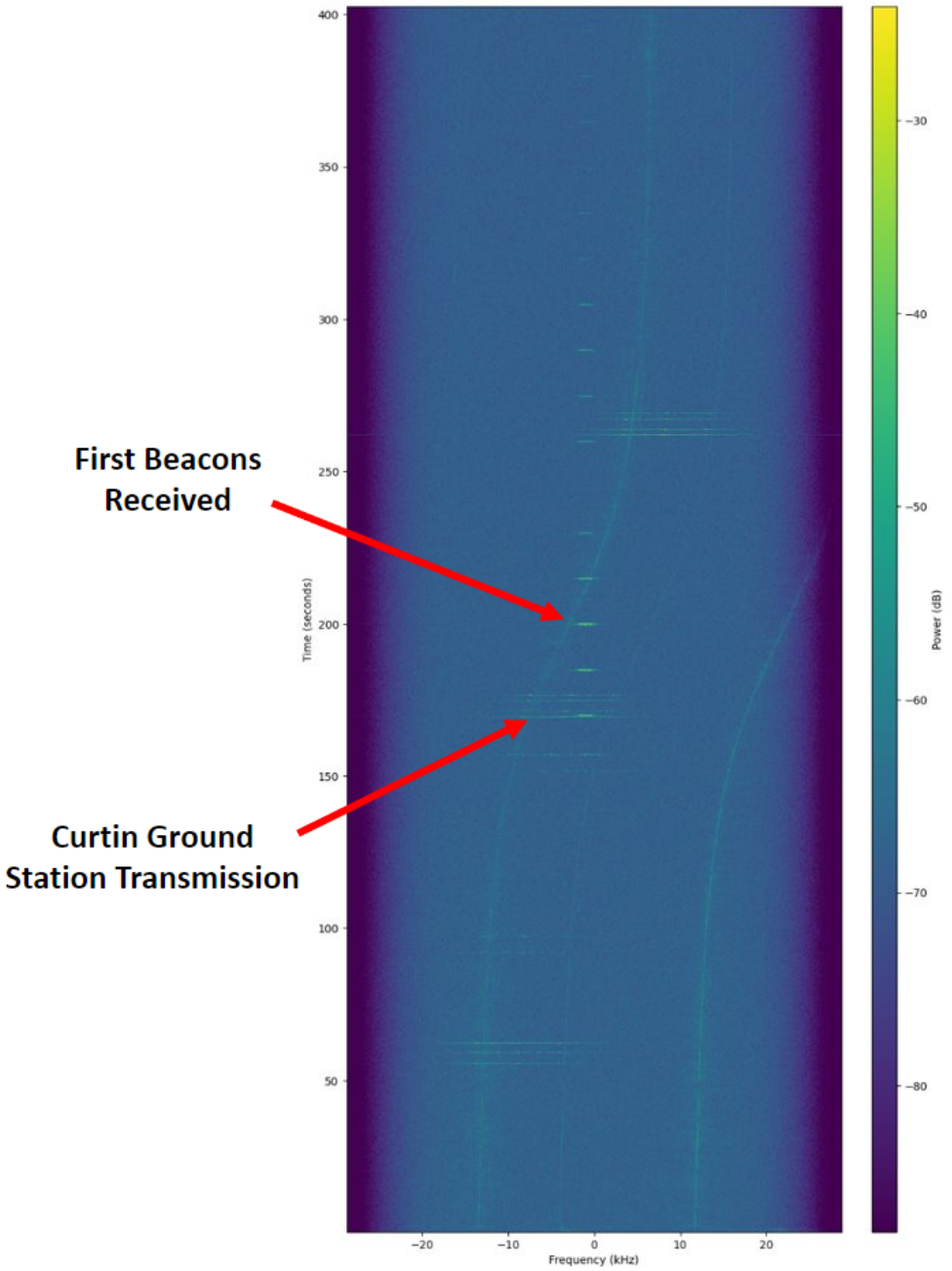

Figure 3.5: SatNOGS beacons being heard over Perth, Western Australia.

3.6.2 Partial Recovery

After the secondary beacon was enabled, it continued to beacon for 11 days until it was suspected that the CubeSat ran out of power. When first attempting to enable the secondary beacon, the command enabled the beacon with a short period and in a high-power usage transmission mode. The intent was to disable the beacon mode on the next pass almost 24 hours later. However, the CubeSat had already drained its batteries by this point. For the remaining ten days, the CubeSat powered on and entered the lower than 50% battery 24-hour loop seen in Figure 3.4, where the secondary beacon mode was activating and transmitting. A command was able to be sent to increase the period and reduce the power usage, returning the CubeSat to a positive power balance. However, the CubeSat could not fully recharge over the 24 hours and was power cycling when attempting to deploy its antennas. The last beacon from Binar-1 was heard at approximately 7:03 am (AWST) on the 2nd of November 2021.

3.7 Results and Discussion

3.7.1 Results

From the received transmissions, Binar-1 was able to provide some results for the technology demonstration objective meeting its minimum success criteria. Although no telemetry was received with quantifiable data for validation, the activation of the beacon and powering of the transceiver demonstrates that the EPS and flight computer system were operational. The CubeSat running out of power due to the short beacon period is in line with the power budget estimates of the team, suggesting that all the solar panels were operational. The ability of the transceiver to transmit the secondary beacons indicates that the flight computer was performing as expected. This is inferred as the flight computer was required to be powered on and in specific operation states for the transceiver to be powered on. Although the suspected hardware failure resulted in the inability to collect technology demonstration data, the inference from the secondary beacons has been considered a partial success by the Binar Space Program.

The other primary objectives of end-to-end space mission lifecycle training and creating awareness of the importance of space in Western Australia were suc-

cessful. Through completing the Binar-1 design, assembly, integration, testing, delivery, and operation processes, the Binar Space Program has learnt many valuable lessons. This education and training will provide the founding and leading members of the Binar Space Program with the ability to repeat and improve the mission lifecycle process, increasing the chance of mission success on following missions. The Binar Space Program created awareness of the importance of space research in Western Australia through the extensive outreach programs run in the lead-up to launch and deployment. Through public demonstrations and launch livestreams, the team gathered significant interest, building a social media and research community following in the state. The following is now being used to share Binar Space Program achievements and interesting facts, growing the understanding of the importance of space in Western Australia. This following will continue to grow when future missions are launched and deployed. Although the technology demonstration objective was only partially accomplished, achieving the other mission objectives has built confidence within the Binar Space Program as it begins work towards its next mission, Binar-2, 3, and 4.

3.7.2 Lessons Learned

Among the many lessons learned during the mission lifecycle process of Binar-1 were five main lessons. These were:

- Lock down high-level requirements early,
- Test as you fly,
- Plan for delays,
- Plan for operations, and
- Remove assumptions where possible.

During the early stages of the development of Binar-1, one of the main challenges was locking down high-level requirements to prevent scope creep and unplanned design inclusions. Many redesigns resulted from constant pressure to include new

features and payloads and the need for clear mission objectives. These redesigns were time costly and increased the mission delivery time. Once the final mission objectives were locked down and realised, the design focused on the technology and the ability to demonstrate its functionality.

The test as you fly lesson was realised by combining many smaller lessons learnt during the testing process. Included in this realisation was the need to use matching hardware for your engineering model, use the communications system in the loop when testing flight functionality, and test mission-critical systems as soon as possible. Matching hardware for the engineering model may have prevented the hardware failure on Binar-1. Through using a lower-powered transceiver with different functionality, a modification was required to the flight model payload and communications adapter board to work with the higher-powered flight transceiver. If two matching systems were purchased, all functionality testing performed during the design or on the engineering model would have resulted in the modification being implemented earlier, preventing the testing schedule delays. If the communications system had been used instead of the USB port while testing all telecommands, the software error in safe mode might have been discovered. Some essential software functions were not tested, as the USB port was used instead. Although this is not the suspected failure cause of Binar-1, testing using the complete system must be implemented on future Binar missions. Finally, testing critical systems such as the deployment circuit needs to be completed as soon as possible. Although the launch requirements were shifted during the design, the need to deploy and learn how to reset the antennas could have been performed much sooner, allowing more time to improve and test the method correctly.

Planning for delays was a lesson learned from the delays experienced during assembly and integration. These delays limited testing time, causing some tests not to be performed to meet the mission deadline. Learning from this, the need for a delay plan to know what tests are necessary, what can be skipped, and the risk that includes ahead of time can prepare for unexpected delays without compromising mission success. In preparation for testing the CubeSat, proper planning was not performed to ensure the CubeSat functionality was acceptable. Had an adequate plan been in place, the software and hardware errors may have

been identified before the testing of the engineering model.

Similar to the plan for delays lesson, detailed planning for operations may have enabled the recovery of the CubeSat to be performed earlier, potentially before the serial converter failed. Before the deployment of Binar-1, the team needed to realise the detail in which the operation should be performed. However, the mission objectives of Binar-1 could be completed just by receiving beacons, the plan for collecting and managing these beacons needed to be more suitable. With proper planning for configuring the transceiver or enabling the secondary beacon before launch, the team may have been able to recover the CubeSat earlier. This may have also prevented the battery power cycling and potentially allowed the CubeSat to fully charge before trying to deploy its antennas again. The team will be able to respond to any operating conditions with correct planning and better operations preparation.

The final lesson learned was to remove assumptions where possible. Due to the small team designing and delivering Binar-1, many assumptions needed to be made without proper verification. Although this reduced the design time after the high-level mission objectives were realised, challenges were faced during the engineering model assembly, integration, and testing. This included difficulties interfacing the COTS antenna, soldering the deployment switch wires, and fastening the deployment switches to the rail halves. Had these assumptions been appropriately verified, the assembly, integration, and testing of the engineering model may have been easier and taken less time, resulting in more time to solve the flight model assembly challenges and perform more detailed testing.

A commonality between all of these lessons learned is the need for sound and robust project management throughout the mission lifecycle. To implement these lessons learned in the Binar mission lifecycle process significant changes were required to ensure the process for the next Binar missions can avoid repeating mistakes. Separating the lessons learned into five focus lessons has enabled the development of a project management structure which can be reused for all future Binar missions.

3.7.3 Discussion

Although the mission technology demonstration objective was only partially successful, the Binar Space Program has grown confident in its design methodology choices. From recent reviews of university CubeSat success and failures, Michael Swartwout [99] provides information on the success rate of independent universities where the Binar Space Program is categorised. With a failure rate of greater than 60%, the ability of Binar-1 to have partial mission success is significant. The team attributes this success to the realisation of needing to understand the systems being flown and performing a custom design process. Although many lessons have been learned and improvements need to be made, establishing a program is possible. Also noted in the data is the improvement universities see in success rates when performing future missions. Implementing the lessons learned is vital to increase the chance of success.

Analysing previous missions that have flown since the conception of Binar-1, the lessons learned were not exclusive to the Binar Space Program. A lesson learned from Montana State University, a prolific independent CubeSat developer, mentions the need to limit scope creep by locking down high-level requirements early [100]. The MiTEE-1 mission development team also noted that due to student graduation, a lack of documentation, and scope creep, mission objectives changed throughout the design affecting the testing procedures and operations plan [85]. The INCA and Aalto-1 mission teams also learned the need to test as you fly. Both mention the need to test COTS subsystems during the design iteration stage, just as with custom-designed systems [80][101]. Although this is a limited set of examples, analysing the success, failures, and lessons learned from previous CubeSat missions suggests that the Binar Space Program is on the correct path to success by addressing these challenges.

Having learnt these lessons, the Binar Space Program needs to implement changes in its mission lifecycle process and hardware and software design to improve its chances of performing successful missions in the future. As the team grows, better systems to manage change and documentation are required to ensure the learnings from Binar-1 are shared with new team members. By completing the custom design and implementing lessons learned, successful missions will be possible as

the skills and understanding of the team are improved. Maintaining the mindset of a program, not a mission, will be necessary for achieving long-term planetary research goals. This is important as the Binar team is on its way to delivering its next mission, Binar-2, 3, and 4.

3.8 Concluding Remarks

The results of the Binar-1 mission have demonstrated the capabilities of the Binar CubeSat Bus (BCB) in its operating environment. This successful demonstration of the Binar-1 mission has achieved some technical goals which have progressed towards performing controlled re-entry and recovery of a CubeSat. The lessons learned from the mission have further improved the platform to where it now includes a re-entry tracking system. Binar-1 was the first test of the CubeSat platform described in Chapter 2, and its success has established the Binar Space Program to sustain itself for the foreseeable future. The lessons learned throughout the process are essential as the team works towards delivering the next mission, Binar-2, 3, and 4. The implementation of these lessons and the improvements made to the design are described in Chapter 5.2.

References

[80] K. Rankin, I. McNeil, I. Rankin, and S. Stochaj, "How Not to Build a CubeSat – Lessons Learned from Developing and Launching NMSU's First CubeSat," *Small Satellite Conference*, Aug. 2019. [Online]. Available: https://digitalcommons.usu.edu/smallsat/2019/all2019/54.

[85] G. Li, L. Spence, M. Miller, *et al.*, "Lessons Learned from the Development and Flight of the First Miniature Tethered Electrodynamics Experiment (MiTEE-1)," *Small Satellite Conference*, Aug. 2021. [Online]. Available: https://digitalcommons.usu.edu/smallsat/2021/all2021/249.

[88] *JEM Payload Accomodation Handbook - Vol. 8 - Small Satellite Deployment Interface Control Document - Rev. D*, Jul. 2020. [Online]. Available: https://iss.jaxa.jp/kibouser/library/item/jx-espc_8d_en.pdf (visited on 12/21/2022).

[96] *PCB Design Software & Tools | Altium*, en. [Online]. Available: https://www.altium.com/ (visited on 12/22/2022).

[98] D. J. White, I. Giannelos, A. Zissimatos, E. Kosmas, and D. Papadeas, "SatNOGS: Satellite Networked Open Ground Station," en, Oct. 2015. [Online]. Available: https://scholar.valpo.edu/cgi/viewcontent.cgi?article=1039&context=engineering_fac_pub.

[99] M. Swartwout, "Reliving 24 Years in the next 12 Minutes: A Statistical and Personal History of University-Class Satellites," *Small Satellite Conference*, Aug. 2018. [Online]. Available: https://digitalcommons.usu.edu/smallsat/2018/all2018/465.

[100] L. Berthoud, M. Swartwout, J. Cutler, D. Klumpar, J. Larsen, and J. Nielsen, "University CubeSat Project Management for Success," *Small Satellite Conference*, Aug. 2019. [Online]. Available: https://digitalcommons.usu.edu/smallsat/2019/all2019/63.

[101] M. R. Mughal, J. Praks, R. Vainio, *et al.*, "Aalto-1, multi-payload CubeSat: In-orbit results and lessons learned," en, *Acta Astronautica*, vol. 187, pp. 557–568, Oct. 2021, ISSN: 0094-5765. DOI: 10.1016/j.actaastro.2020.11.044. [Online]. Available: https://www.sciencedirect.com/science/article/pii/S0094576520307190.

Chapter 4

Design of a Tracking System for Controlled Re-entry and Recovery of CubeSats

The primary planetary science objective of this work is to develop a low cost capability for performing controlled re-entry and recovery. If the cost can be significantly reduced, then the opportunities to perform sample collection and return missions and land on the surfaces of extra terrestrial planets will increase. To realise this cost reduction, CubeSats were identified as the favourable satellite platform demonstrating already significant capabilities at performing valuable science. However, for CubeSats to be able to perform controlled re-entry and recovery, a series of engineering challenges need to be solved before the complete capability can be developed. Following the development of a low cost CubeSat platform, the next challenge can be developed. This challenge was a method for tracking a CubeSat performing controlled re-entry and recovery. If this challenge can be solved then the next stages of a controlled re-entry and recovery capability can be developed and tested easily, due to the data provided by the re-entry tracking system.

A challenge for controlled re-entry and recovery of CubeSats is the ability to

target the re-entry location. The first entry point into the atmosphere is critical for a successful recovery. As such, investigating different methods for controlling the re-entry process and targeting the point at which its CubeSats hit the atmosphere is essential. However, one of the initial challenges with designing these systems is verifying a successfully controlled re-entry when the CubeSat burns up at the target location. Although the objective is to complete controlled re-entry and recover the payload or complete CubeSat, demonstrating successful targeting without recovery methods is be essential for safety purposes. Satellite tracking services provide two Line Element (TLE) information. However, these need to be more accurate for recording the re-entry location, with location accuracy drifting considerably following the initial measurement [102][103]. Similarly, the communications system on the Binar CubeSat Bus (BCB) needs to be able to communicate more frequently to observe the re-entry location reliably.

To be able to begin developing controlled re-entry and recovery technologies for CubeSats, a solution to this challenge was proposed. A re-entry tracking system could be developed by combining the functionality of communication satellite constellations and ground station networks. The system objective is to communicate CubeSat telemetry in the final stages of orbit before burning up in the Earth's atmosphere while not limiting the payload space available on the Binar CubeSat Bus (BCB). This will enable the BCB to record its final re-entry location and demonstrate controlled re-entry technology payloads on future applications on the platform.

This chapter presents the service selection and design of a CubeSat re-entry tracking system planned to observe the re-entry locations of the next Binar CubeSats, Binar-2, 3, and 4. Successful demonstration will enable the design and demonstration of controlled re-entry systems on future Binar missions. First, a communication service review is presented, detailing the selection of suitable services for tracking the re-entry of a Binar CubeSat. Second, the operation design is explained, including how the system can transmit its final re-entry location using the selected services. Third, the methodology and results of simulations performed to predict the accuracy of the system are presented. Finally, the implications of the selection process are discussed, including limitations that need to be accounted for, and other data collection that may be required post-mission to improve the

re-entry location accuracy.

4.1 Communication Service Review

A re-entry tracking system was developed to verify the performance of controlled re-entry and recovery systems. A combination of global communication services with high availability and minimal communication gaps was viewed as the best solution for the system. This chapter aims to investigate and combine the most applicable global communication services for a 1U CubeSat which would house the future controlled re-entry systems. Two services with global capabilities were investigated. The first was ground station networks, and the second was communication satellite constellations. To determine the most appropriate services for the system, all services were compared to a set of criteria that measure the system's usability within a 1U CubeSat platform. These criteria were:

- Flight heritage (at least one successful mission),
- System usage cost (less than AUD$10,000 for the mission), and
- Size, Weight, and Power (SWaP) requirements (fits 1U, less than 10% total mass, less than 20W peak).

4.1.1 Selection Criteria

Flight Heritage

The flight heritage of the communication services was the first criterion evaluated. Performed primarily to reduce risk, the flight heritage analysis also informed the system design by determining if the service could operate on and be licensed for a CubeSat in LEO. Using flight heritage components is highly valued in spacecraft system design for these reasons. The main variables considered during the flight heritage investigation of communication satellite constellations included the total number of missions flown, the number of successful missions flown, the size of the CubeSats, and the launch date. CubeSat databases such as Nanosats [53] and a reputable amateur page, Gunter's Space Page [104], were used to collect flight heritage data for communication satellite constellations. For the flight heritage of

ground stations and there usage with CubeSats, the Technology Readiness Level (TRL) of the network was used as a reference. Communication services with at least one successful mission were then evaluated against the following two criteria for the final selection. The flight heritage of the onboard communications system working with the ground station network was excluded from the review as only the Binar UHF system will be used with the ground stations.

System Usage Costs

One of the significant advantages of CubeSats is the reduced cost through all stages of the mission lifecycle, including operation. For this reason, it is required that the system operation costs remain within budget to avoid going against the ethos of the CubeSat platform. This was discovered to be more applicable to ground station networks used primarily by the space industry for providing a reliable connection and system security. For the communication satellite constellations, the service costs take the form of a one-off connection fee and monthly data subscription like household internet services and phone plans. The only variable considered when evaluating the system usage cost was the affordability of the service to the Binar Space Program. The affordability was determined by measuring the initial set-up and data rate costs. If usage of the system was less than AUD$10,000 for the system operation, it was deemed usable. This limit was set as a benchmark cost for testing controlled re-entry technologies following a discussion with the director of the program.

Size, Weight, and Power

Although the BCB has optimised the payload space available in a 1U, a controlled re-entry system is expected to occupy the entire payload space. Therefore, the re-entry tracking systems SWaP requirements must be minimised so that it doesn't impinge on the fully controlled re-entry or Entry, Descent, and Landing (EDL) system. The SWaP criteria were already met for ground station networks as the Binar platform contains an Ultra High Frequency (UHF) communication system that can be used to transmit the re-entry beacons. For the communication satellite constellations, the variables for the SWaP requirements criteria were the dimensions, weight, continuous power, and maximum power of the smallest modem with flight heritage. For the dimensions and weight requirements, this included the transceiver and antenna. Constellation networks which used smaller

modems and antenna were more preferable. The modem could meet the criteria if these requirements were appropriate for the Binar platform. The service was considered usable and included in the system if this and the cost criteria were met.

4.1.2 Ground Station Networks

The ground station networks reviewed could be split into two categories, commercial networks and open-source networks. A consideration made in this selection process was that the ground station network only needed to receive information from the satellite. As such, it was optional that the ground station network could provide telecommand and satellite control services. Although the BCB now contains a UHF transceiver and S-band transmitter, only ground station networks that can receive UHF communications were considered. This was done as the S-band transmitter is supplied by an industry partner as a technology demonstrator and may not be used on controlled re-entry and recovery missions in the future.

Commercial Ground Station Networks

There is an extensive list of commercial ground station networks with global communication capabilities. With nearly all the services able to track, receive, and transmit to spacecraft, the companies are typically the go-to for operations of high-risk space missions. Of the more established networks, such as Swedish Space Corporation [105] and KSAT [106], the cost was the limiting criterion for use with the Binar re-entry tracking system. An extensive list of the other available companies and their network TRL is well documented in the NASA State of Art (SOA) document for small satellites. The document also provides details on emerging network providers [7].

When evaluating the usability of commercial ground station network services for the re-entry tracking system, the flight heritage criterion was met due to the established and continued operation of the services for many existing missions. For the cost criteria, the commercial solution needed to be more affordable to meet the Binar Space Program's budget. Some of the mentioned commercial networks were approached by the Binar Space Program, and none offered a cost-effective solution that could meet the cost criteria limit. Commercial ground

station networks were not included in the Binar re-entry tracking system because this criterion could not be met.

Open-Source Ground Station Networks

Open-source ground station networks are a new global space collaboration and infrastructure feature. SatNOGS (Satellite Networked Open Ground Station) was the only global solution in this category. First proposed in 2014 as part of the NASA Space Apps Challenge, the project was awarded funds to create the Libre Space Foundation [98][107]. Now managed by this foundation, the SatNOGS project is divided into four main sub-projects that enable makers and amateur radio enthusiasts worldwide to build and add their ground station to the network. As of Q1 2022, the network had over 250 stations performing at least one observation per day of satellite telemetry [108].

Used in the Binar-1 mission, the SatNOGS project captured most of the data received. This makes it highly advantageous to the re-entry tracking system as it already has flight heritage within the Binar Space Program and is free to use. As the service meets all three criteria, it was planned to be included in the final system making it the only ground station network included.

4.1.3 Communication Satellite Constellations

Multiple communication satellite constellations can be used for global communications on the ground, some of which have been proven to work in space. The constellations evaluated in the review included Iridium, Globalstar, Inmarsat, and Orbcomm. Although others were considered, they were not included in the review as they did have any publicly available flight heritage. A proprietary Commercial Off the Shelf (COTS) modem is necessary to use these networks. For each network, the smallest modem with flight heritage was evaluated. These modems were the Iridium 9603, the Globalstar STX3, the Inmarsat ADDVALUE IDRS, and the Orbcomm OG2. A consideration for future assessments of communication satellite constellations is the growing Internet of Things (IoT) market which typically uses these satellite constellations [109]. As these services grow to full maturity, there is a high possibility that the global availability of these services will become appropriate for re-entry tracking. Thus, these constellations should be considered in the future once reaching full maturity.

Iridium

Iridium operates using 66 satellites split into 6 orbital planes of 11. All planes have an inclination of 86.4°, making Iridium the only service in this list with complete global ground coverage. This unique feature of the Iridium constellation is of minimal benefit to re-entry tracking as all landings will be targeted at easily accessible locations and not over the Earth's poles. Another uniqueness of the Iridium system is its method of relaying messages to the end user. Iridium can make interplanar and intraplanar communications with neighbouring Iridium satellites, unlike other communication satellite constellations in this list. Thus, once a member of the satellite constellation receives a message from an Iridium modem, the message is shared between satellites until a satellite with line-of-sight to a ground station can transfer the message to the ground. This onboard processing capability means that all the infrastructure required for a connection is not dependent on a ground station connection, making the service suitable for the global nature of its orbit. A summary of the constellation and its communication methods is visible in Table 4.1.

The smallest available modem for using the network is the Iridium 9603 (Figure 4.1). The modem is a Short Burst Data (SBD) modem that communicates small data packets over the Iridium network to an end user. This modem is the most practical solution for re-entry tracking as it is the smallest and has flight heritage on multiple CubeSat missions.

Table 4.1: Iridium satellite constellation orbital parameters and communication bands.

Variable	Value
Number of satellites	66 (9 spares)
Inclination	86.4°
Altitude	780km (LEO)
Intraplanar separation	32.7°
Interplanar separation	16.4°
RAAN separation	31.6°
Frequency	L-band (1610 - 1626.5 MHz)
Channel bandwidth	±37.5kHz
Antenna cone angle	61.2°

To evaluate the flight heritage criteria of Iridium, a review of CubeSats that have flown an Iridium modem was performed. The study concluded that the flight heritage was appropriate as it had been successfully demonstrated on multiple missions. One of the significant concerns within publications on the use of the service was the effect of doppler shift [111]. Another notable feature of the Iridium constellation was the half-globe plane coverage. As such, the performance of spacecraft in LEO with an Iridium modem will vary based on its orbital plane alignment with the constellation. Time to connect and latency of the messages was shown not to be a concern in missions that did not require immediate two-way communications [112]. This matches the requirements of the re-entry tracking system, as the time for the message to be received is not consequential. Only the transmissions being received by the constellation is essential. The list of satellite missions reviewed is displayed in Table 4.2.

Of interest in this list is the TechEdSat missions, which are developing and testing the Exo-brake (Section 1.5.6) system for controlled re-entry and recovery. Although results have yet to be presented on a successful recovery, presenta-

Figure 4.1: The Iridium 9603 modem [110].

Table 4.2: Previous uses of the Iridium satellite constellations for communications on CubeSats. Sixteen reported successes and three reported failures were investigated. The list is only part of all the CubeSats reported using the Iridium constellation. It only contains CubeSats which reported results.

Name	Size	Launch Date	Performance
TechEdSat-2	1U	21/04/2013	Successful [113]
TechEdSat-3	3U	3/08/2013	Successful [113]
Lamdasat	1U	13/07/2014	Unsuccessful [114]
TechEdSat-4	3U	4/03/2015	Successful [113]
EGG	3U	9/12/2016	Successful [115]
TechEdSat-5	3.5U	9/12/2016	Successful [72]
TechEdSat-6	3U	12/11/2017	Successful [72]
TechEdSat-8	6U	5/12/2018	Successful [72]
EntrySat	3U	17/04/2019	Successful [116]
Mini-Carb	6U	5/12/2019	Successful [112]
TechEdSat-10	6U	13/07/2020	Successful [73][117]
CACTUS-1	3U	17/01/2021	Unsuccessful [118]
TechEdSat-7	2U	17/01/2021	Successful [117]
FEES	0.3U	22/03/2021	Successful [119]
Veery Hatchling	1U	22/03/2021	Successful [120]
ARICA	1U	9/11/2021	Unsuccessful [121]
FEES2	0.3U	21/12/2021	Successful [119]
TechEdSat-13	3U	13/01/2022	Successful [122]
S4-Crossover	6U	03/15/2022	Successful [123]

Table 4.3: SWaP of the Iridium 9603 modem.

Size	31.5mm x 29.6mm x 8.1mm
Weight	11.4g
Transmit power (peak)	6.5W

tions on the design of the satellite show extensive use of the Iridium system, sometimes flying up to three Iridium modems per CubeSat for communications [73][74][75][117][122].

In reviewing the flight heritage of Iridium modems, published mission results on the flight performance were examined. One of the recent publications on the MiniCarb CubeSat provided details on the successful usage of Iridium in LEO. A connection distance limit of 2000km and range rate limit of 7km/s is recommended for connection constraints in simulations from the flight results. The mission also demonstrated that the modem could operate in duplex mode, making it attractive as a backup communication system [112].

The Iridium operating costs were suitable for the Binar Space Program. The highest monthly data rate service offered was 50000 bytes for AUD$79.20. The service also includes a 1-time connection fee of AUD$50.00 per modem and a cost of AUD$0.022 per 10 bytes over the initial data cap. This was deemed affordable for the Binar Space Program as the initial set-up costs were small, and the data rate could be modified to keep the system within budget.

The 9603 modem was able to meet all the SWaP criteria as it can conform to the 1U CubeSat form factor, is less than 133g and does not exceed the peak power limit of the Binar CubeSat Core. A summary of the SWaP of the modem is visible in Table 4.3. As the Iridium constellation and 9603 modem met all the preliminary selection criteria, it was included in the system.

Globalstar

The Globalstar communication satellite constellation operates using 24 satellites in 8 planes with an inclination of 52°. Differing from the Iridium constellation, the Globalstar system requires a connection to a ground station or Globalstar Gateway to receive the messages transmitted by a modem successfully. This limitation to the system restricts the operation of the constellation to over land near a Gateway. A summary of the Globalstar constellation and its communication methods is presented in Table 4.4.

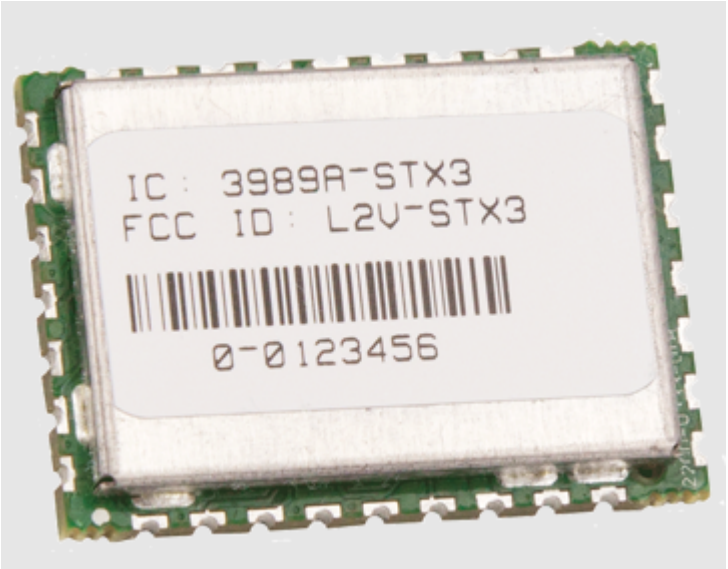

Figure 4.2: The Globalstar STX3 simplex modem [124].

The smallest modem available for use with the Globalstar constellation is the Globalstar STX3 (Figure 4.2). Compared to its Iridium counterpart, it is smaller but only capable of simplex transmissions. This is not a concern for the re-entry tracking system. However, it does not offer the additional benefit of being a backup communication system in other mission phases.

A review of the flight heritage of Globalstar modems on LEO CubeSats found that the constellation was suitable. It also determined that doppler shift is not a concern when using the Globalstar service due to the larger channel bandwidth

Table 4.4: Globalstar satellite constellation orbital parameters and communication bands.

Variable	Parameter
Number of satellites	24 (1 spare)
Inclination	52°
Altitude	1414km (LEO)
Intraplanar separation	120°
Interplanar separation	60°
RAAN separation	45°
Frequency	L-band
Channel bandwidth	1MHz
Elevation angle	10°

[125]. A commonality of the CubeSats reviewed was the use of the EyeStar radio provided by Near Space Launch (NSL). This radio integrates a Globalstar STX3, which it uses as a transmit-only communication system [126]. The radio has flown with a 100% success rate on over 175 missions [123]. Not all 175 missions are included in the review due to the limited publicly available mission results on proprietary industry and defence missions. Recently the EyeStar radio has been upgraded to use the Iridium service stating that the agreement is mutual between all stakeholders [123]. The first of the missions to use the new EyeStar radio with the Iridium modem included was the S4-Crossover mission presented in the Iridium review (Table 4.2). A summary of the study is visible in Table 4.5.

For the cost criteria, the modem was cheaper than the duplex Iridium modem. The monthly price for 1000 messages (maximum 144 bytes per message) was AUD$38.50, with a one-time setup fee of AUD$35.00 and an additional cost of AUD$0.088 per message over 1000. Cheaper than the Iridium service, it was affordable and could remain within budget. Finally, the SWaP requirements are detailed in Table 4.6 and are smaller and more power efficient than the Iridium modem. As all three criteria were met, the service was considered usable in the Binar re-entry tracking system.

Inmarsat

Inmarsat and Thuraya were the only Geostationary Earth Orbit (GEO) satellite constellations investigated. However, no CubeSat missions have been reported using the Thuraya constellation, so it is not included in this chapter. Inmarsat offers communications services in more than one band. Due to the lower power requirements, the L-band system is the only service of interest to the re-entry tracking system. The L-band Inmarsat service has five GEO satellites that can provide connectivity up to latitudes of 70° . Unlike the other two constellations already discussed, Inmarsat doesn't have as many successful missions, likely due to the modems it offers not being easily re-purposed for space like the Iridium 9603 and Globalstar STX3. Of the missions that have flown using the Inmarsat constellation, only one has reported successful communication with an availability of 99%. The modem developed for this mission is now provided by its own company and is called the ADDVALUE IDRS (Figure 4.3). A summary of the

Table 4.5: Recent uses of the Globalstar satellite constellation for communications on CubeSats. Seventeen reported successes and three reported failures were investigated. The list contains only some of the CubeSats reported using the Globalstar constellation. It only includes CubeSat missions that have reported results.

Name	Size	Launch Date	Performance
TNS-0	4.8kg	28/02/2002	Successful [127]
TSAT	2U	18/04/2014	Successful [126][128]
GEARRS-1	3U	13/07/2014	Successful [126]
GEARRS-2	3U	20/05/2015	Successful [126]
SHARC Biarri-Point	5U	18/04/2017	Successful [126]
TNS 0-2	4.8kg	14/06/2017	Successful [127]
MakerSat-0	1U	18/11/2017	Successful [129]
HSAT-1	6U	29/11/2018	Successful [130][131]
TechEdSat-8	6U	5/12/2018	Successful [72]
UNITE	3U	5/12/2018	Successful [132]
SASSI2	3U	17/04/2019	Unsuccessful [133]
ThinSat-1X	ThinSat	17/04/2019	Successful [134][135]
AzTechSat-1	1U	5/12/2019	Successful [136]
MakerSat-1	1U	5/12/2019	Successful [137]
VPM	6U	5/12/2019	Successful [138]
NEUTRON-1	3U	3/10/2020	Unsuccessful [139]
PTD-1	6U	24/01/2021	Successful [140]
ThinSat-2X	ThinSat	20/02/2021	Successful [141]
ARICA	1U	9/11/2021	Unsuccessful [121]
GEARRS-3	3U	13/01/2022	Successful [141]

Table 4.6: SWaP of the Globalstar STX3.

Size	28.7mm x 20.57mm x 4.13mm
Weight	3.97g
Transmit power (peak)	1.5675W

missions that communicated with Inmarsat is visualised in Table 4.7.

The review indicates that the Inmarsat service has potential even with minimal flight heritage. Upon further investigation of the SWaP of the ADDVALUE IDRS, it was clear that the service was not usable in the re-entry tracking system. As its dimensions exceeded the 1U CubeSat form factor and the mass was larger than 133g, the modem was considered unusable. The service cost was private and was never investigated due to the unmet SWaP criteria. The summary of the SWaP requirements of the IDRS is presented in Table 4.8.

Orbcomm

The Orbcomm constellation operates in LEO, similar to Globalstar and Iridium. The constellation consists of 36 satellites in 4 orbital planes, and unlike Globalstar and Iridium, it functions using the Very High Frequency (VHF) band. This is already problematic for CubeSats due to the larger antenna needed for VHF

Figure 4.3: The ADDVALE IDR Inmarsat modem [142].

Table 4.7: Inmarsat CubeSat missions. Kaidun-1 is yet to share any results of using the Inmarsat service.

Name	Size	Launch Date	Performance
VELOX-II	6U	16/12/2015	Successful [142]
Kaidun 1	2U	9/01/2017	No Information

Table 4.8: SWaP parameters of the ADDVALUE IDRS.

Size	125mm x 96mm x 70mm
Weight	1000g
Transmit power (peak)	16.44W

Table 4.9: Orbcomm OG2 SWaP parameters.

Size	40mm x 70mm x 10.5mm
Weight	20g
Transmit power (peak)	10W

communication. There is no flight heritage of the Orbcomm service in LEO. One of its modems was flown on TechEdSat-1 but had to be deactivated due to licensing challenges meaning it was never tested in LEO [144][112]. Even though the flight heritage of the service is not present, the modem options were still investigated to see if they could be used for the first time in space. In Table 4.9, it was determined that the smallest available modem, the Orbcomm OG2 (Figure 4.4), would be suitable for the re-entry tracking system. However, one of the limitations was the previously mentioned antenna size. Although still meeting the size criteria, as the combined modem and antenna was significantly larger than the already selected Iridium and Globalstar modems, the Orbcomm modem was not included in the re-entry tracking system.

Figure 4.4: The Orbcomm OG2 modem [143].

4.1.4 Review Summary

A summary of the communication service review based on the three criteria is provided in Table 4.10. The three communication solutions that were considered usable in the re-entry tracking system were SatNOGS, Iridium, and Globalstar. All three of the services have flight heritage. The UHF communications system included in the BCB was based on a flight heritage design and uses components with flight success. The Iridium 9603 and the Globalstar STX3 have been flown on successful missions. The combined cost of using the services did not exceed the total system operation budget for setup, meaning that the operation time can be calculated for using the three services. The SWaP criteria were also met as the modems were all able to fit into the 1U payload space without taking up considerable room, weighed a combined total of less than 133g, and did not exceed the peak power delivery capabilities of the Binar power system.

4.2 Tracking System Operations

How and when the re-entry tracking system will operate was determined after selecting the appropriate services. The initial concept was to have a separate operation mode in the CubeSat software that will enable once dropping below a critical altitude before re-entry. At this altitude, the CubeSat will begin beaconing on all the selected communication services at 10-second intervals. To successfully receive the beacons, the antenna of the Globalstar and Iridium modems will need to be pointed to the satellite zenith (to be received by the constellations), and the UHF antenna will need to be directed towards the nadir (to be received by the SatNOGS network). The beacon will contain Global Positioning System (GPS) information and basic telemetry, including temperatures, voltages, and currents. The average power consumption and cost of using the combined communication services were calculated in order to determine the altitude to begin operation. The initial cost criteria limit of AUD$10,000 is spread across three satellites for the calculations. This is due to the current mission plan to fly three Binar CubeSats on the next mission. This information was then used to select the appropriate activation altitude that would not drain the batteries too fast or exceed the budget.

Following the calculations for cost and power usage, the maximum operation

Table 4.10: Selection summary for the preliminary criteria. The selected services were SatNOGS, Iridium, and Globalstar.

System	Flight Heritage	Cost	Size	Weight	Power	Frequency	Antenna Size
Commercial ground stations	Yes	High	n/a	n/a	Medium	UHF	n/a
SatNOGS	Yes	Free	n/a	n/a	Medium	UHF	n/a
Iridium	Yes	Low	Small	Small	Medium	L-Band	Small
Globalstar	Yes	Low	Small	Small	Medium	L-band	Small
Orbcomm	No	Low	Small	Small	Medium	VHF	Large
Inmarsat	Yes	High	Large	Large	Large	L-band	Large

Table 4.11: Cost of using communication satellite constellations for re-entry tracking. The Iridium service was more expensive than Globalstar for the same amount of data.

Iridium (1.5 days)

Total Bytes	Initial Cost (AUD/50,000 bytes)	Over Cap Cost (AUD/10 bytes)	Over Cap Total Cost (AUD)	Total Cost (AUD)
1,036,800	79.20	0.022	2,170.96	2,250.16

Globalstar (1.5 day)

Total Messages	Message Cap Cost (AUD)	Over Cap Cost (AUD/Message)	Over Cap Total Cost (AUD)	Total Cost (AUD)
12,960	38.50	0.0827	989.09	1,027.59
			Total (AUD)	3,277.75
			Total (x 3)	9,983.26

time not exceeding the cost or power budget was used to determine the altitude the operation mode will enable. This was achieved using the ESA Debris Risk Assessment and Mitigation Analysis (DRAMA) software [145]. By inputting the final TLEs of the Binar-1 orbit into both the DRAMA Orbital Spacecraft Active Removal (OSCAR) and DRAMA Survival and Risk Analysis (SARA) tool the altitude at which the operation mode can be enabled was determined. The OSCAR tool is first used to propagate a satellite object until it enters the Earths atmosphere. At this point the SARA tool is used to determine how far the satellite object can travel through the atmosphere until it is expected to disintegrate.

First, the cost of using each service was determined. For SatNOGS, the service is free to use. However, it will require software development to set up the passes to receive the re-entry telemetry. For Iridium and Globalstar, the size of the telemetry message being transmitted was needed. This was determined to be 80 bytes by the software team of the Binar Space Program and would contain the GPS location and basic telemetry of the CubeSat. Using a transmission period of 10 seconds over a day and a half met the AUD$10,000 cost criteria for the three CubeSats. A summary of the calculations is presented in Table 4.11. The initial set-up cost is excluded from the total cost as it will be covered during assembly and testing.

As the cost of the system limited the operation to a day and a half, the power analysis was performed for a matching timeline. The combined peak transmission power of all three radios was calculated to be 10.5675W, being nearly half the maximum power delivery of the Binar power system batteries. This was considered acceptable as the the remaining systems would still be able to operate along side the radios without triggering the battery protection circuitry. Next, the total energy usage of the system was measured to prevent the CubeSat from flattening its battery before re-entry occurred. The total energy usage was calculated using an over approximate transmission time of 150ms and the power consumption information provided in the datasheets. The results are presented in Table 4.12. The total energy consumption for 1.5 days of system operations was calculated to be 23.70Whr. This was considered acceptable as it is under half of the battery capacity, and the solar panels will still be active.

With cost limiting the system operation time to one and a half days, the enable altitude was determined from the historical TLE data of Binar-1. Although TLEs are not accurate at lower altitudes for precise positioning, the results are still suitable for approximating the enable time of the system. Using DRAMA [145], the re-entry time prediction for a Binar-shaped object was estimated. Assumptions were necessary to use the software and create a Binar-shaped object. The shape was assumed to take the form of a 1U Cube made entirely of space grade aluminium, with wings made of FR4 PCB material acting as simplified deployable solar panels. The shape and material of the satellite in the simulations impact the simulations orbital decay rate, the satellites drag coefficient, and the expected re-entry point. The antennas were neglected from the design due to having a minimal aerodynamic impact on the satellite as it re-enters the atmosphere. The orientation of the CubeSat was assumed to be fixed with the

Table 4.12: System power consumption.

	Idle (W)	Idle (Whr)	Transmitting (W)	Transmitting (Whr)
Iridium	0.1700	6.1200	6.5000	3.5100
Globalstar	0.0099	0.3564	1.5675	0.8465
UHF	0.3200	11.5200	2.5000	1.3500
Total	0.4999	17.9964	10.5675	5.70645
			Total (Idle + Transmit)	23.7029

antenna of the UHF system pointing towards the earth (nadir pointing). The re-entry point was determined in the simulation as the point where the CubeSat loses attitude control and begins tumbling rapidly or the point at which plasma blocks communications. To identify this point, the OSCAR tool was used to propagate the orbit forward until the SARA tool could be used to predict the re-entry time. The final re-entry altitude to enable the system was 180km. The legacy TLEs of Binar-1 used for the propagation were sourced from CelesTrak [146].

4.3 Simulation Methodology

Simulations at re-entry altitudes, combining the selected services, were performed to calculate the total theoretical coverage and identify communication gaps. These communication gaps were then able to be used to predict the accuracy of the re-entry tracking system at correctly determining the re-entry location. The main variables considered were each service's single and combined availability, the system's communication gap size and frequency, and the system's accuracy in determining the re-entry location. The simulations were performed using Python and the open-source packages Cartopy [147] and Skyfield [148]. Cartopy offers tools for projecting shapes and images onto the Earth's surface, this was used for visualisations and availability simulations. Skyfield is a library that can import satellite positional information from TLEs and propagate them using the Simplified General Perturbations 4 (SGP4) algorithm. All the TLEs that were used were imported from CelesTrak [146] on the day of performing the simulations.

4.3.1 Total Availability

To determine the total system availability or the total system up-time, each service's availability at an altitude of 110km was first visualised for a single time step. This preliminary check was used to verify the method for determining the total availability and provide a visual tool which could be used to observe which service was the most effective. Next, the total availability simulation was performed used a matching approach to the visualisations where the figures were converted to black and white images corresponding to available and not available. From the images, the black and white pixels were counted to determine the total availability of the service at each time step. The total availability simulation was

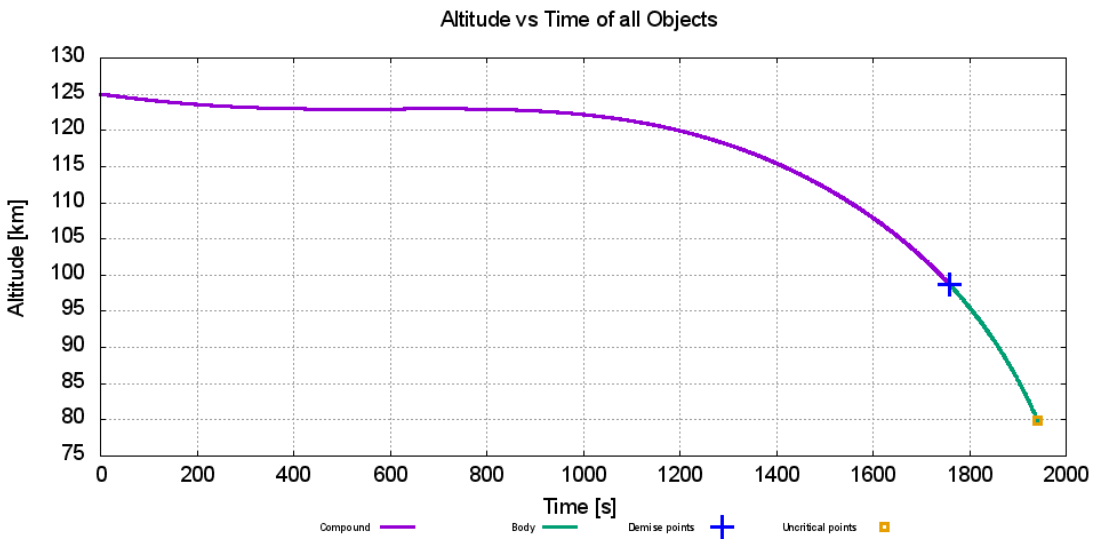

Figure 4.5: Output of the SARA simulation tool showing the altitude and demise point of the simulated CubeSat over time. This simulation was used to determine a suitable re-entry altitude of 110km for the remaining simulations.

performed for one day at 10-second time steps. The final total availability was calculated by taking the average total availability across all time steps. The total availability was also separated into different latitudes for further evaluation of the services if different orbits are used on future Binar missions.

An assumption made in the simulations was the re-entry altitude of 110km. This altitude was used based on the TLE information of Binar-1 and the results of the DRAMA simulations performed in Section 4.2. The simulations showed that the approximated demise point of the CubeSat was 98km altitude. As these simulations used a solid block of aluminium as a reference cube for the CubeSat, it is highly likely the CubeSat would begin re-entry earlier. As such, an altitude 200 seconds earlier was used which was 110km. This can be seen in Figure 4.5.

Cartopy was used to project the cone of a satellite or ground station antenna to the altitude of 110km in a 3D reference frame before converting it to the 2D reference frame used by the visualisation and total availability simulation. To create the 3D projection, the radius angle from the Earth's centre was required to map the availability to the ground image. For the Iridium constellation, this was determined using the sine rule and the altitudes and cone angle of each satellite in the constellation. The radius angle θ_E was calculated using Equations 4.1 and

Figure 4.6.

$$\theta_E = 180 - \theta_B - \theta_C \tag{4.1}$$

Where:

$$\theta_B = \sin^{-1}(\frac{R_E + A_C}{R_E + A_R} \sin \theta_C) \tag{4.2}$$

For Globalstar, the process was similar, except an additional check had to be made to determine if the satellite was actively connected to a Globalstar Gateway. The service is only usable if a satellite in the constellation can connect to the Gateway. This check was made at every time step for every Globalstar satellite. If the satellite was not connected to a Gateway, its connection was removed from the total availability.

For SatNOGS, the equation for the radius angle changes to be the satellite passing through the cone from above. This was calculated using Equation 4.3 and Figure 4.7.

$$\theta_E = \theta_C - \theta_B \tag{4.3}$$

Where:

$$\theta_B = \sin^{-1}(\frac{R_E}{R_E + A_R} \sin(180 - \theta_C)) \tag{4.4}$$

All equations assume that the satellite passing through the cone projection is facing its antennas towards the zenith and nadir, respectively, and that the antenna gain is suitable at the edge of the cone angle to make a connection. For the SatNOGS availability, the elevation angle of the service was assumed to be 15°. This meant the effective cone angle was 75°.

To determine each satellite position at each time step, Skyfield was used to propagate the orbit. After each black-and-white image was created, the total availability of the time step was calculated for different latitudes and then averaged. The parameters used to calculate the Earth radius angles can be found in Table 4.1 and Table 4.4. A summary is also provided in Table 4.13.

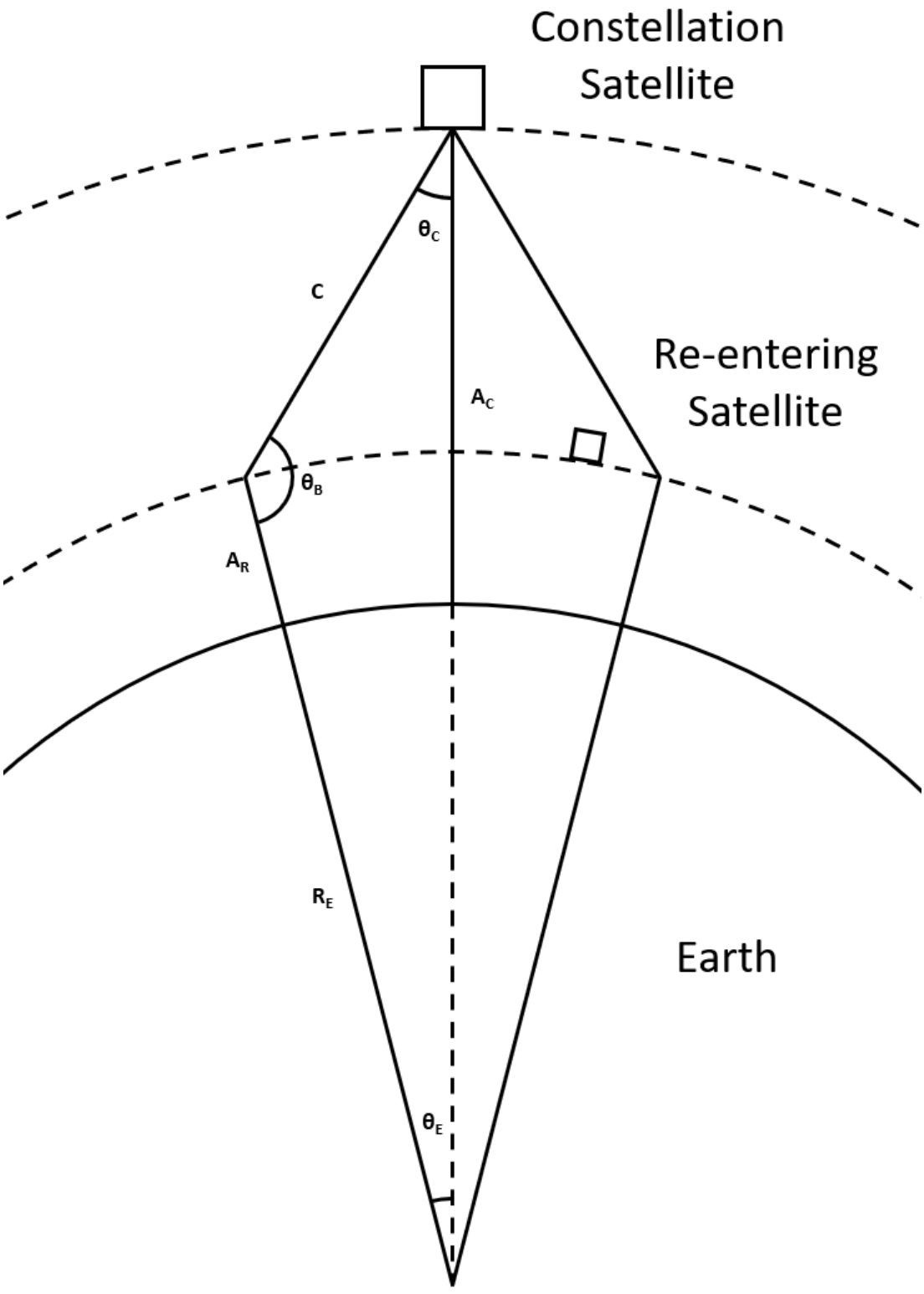

Figure 4.6: Communication satellite constellation cone of influence on satellites at re-entry altitudes in 2D.

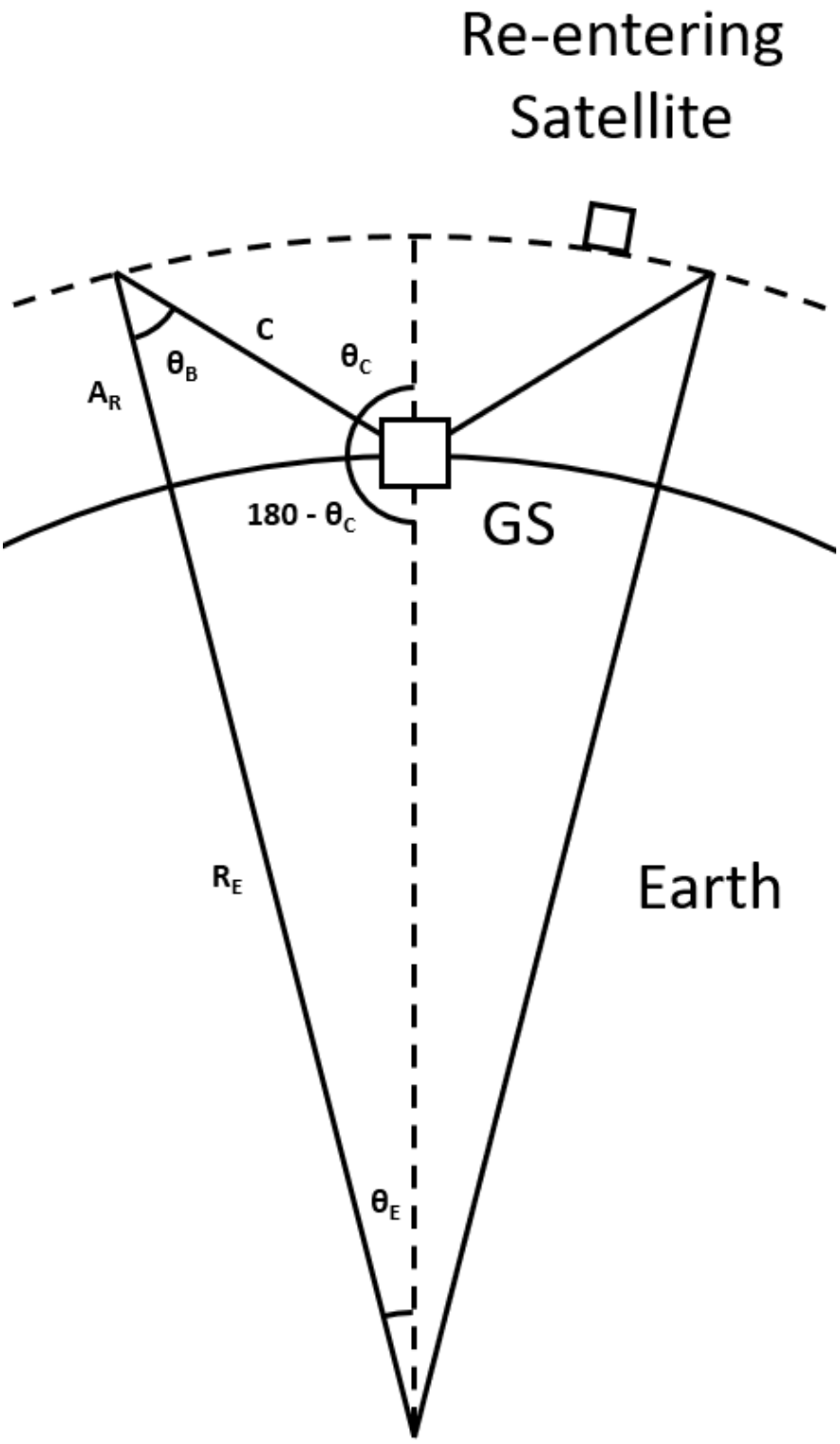

Figure 4.7: Cone of influence represented in 2D for the ground station network. θ_E is used by Cartopy in the simulations to generate the total availability images.

Table 4.13: Parameters used for the total availability simulation.

Service	Constellation Altitude (Km)	Service Cone Angle	Earth Radius Angle (θ_E)
SatNOGS	0	75.00	6.68
Iridium	780	61.30	14.10
Globalstar	1414	53.72	21.78

4.3.2 Communication Gaps

To determine the accuracy of the re-entry tracking system, the size and frequency of any communication gaps were required. This was determined using another simulation that propagated a satellite with an International Space Station (ISS) orbit through the communication satellite constellations and ground station network. The ISS orbit was selected as the test case as the upcoming Binar mission will be deployed from the ISS and have a matching inclination. The satellite positions were altered after being propagated to have an altitude of 110km, imitating the CubeSats at re-entry altitudes. One limitation of the total availability simulation was the inability to measure the effects of doppler shift on the Iridium constellation. This was measured in this simulation as Skyfield provides the velocity information of the satellites as it propagates. Due to the Iridium constellation having six planes covering only half the globe, the Right Ascension of the Ascending Node (RAAN) of the ISS orbit satellite will impact the system performance. As such, four ISS orbit satellites were used in the simulations to analyse the effects of different RAANs.

The displacement between the ISS orbit satellite and communication services was first compared to the connection distance limits to determine if a connection was present in the simulation. The connection distance limits for both services were calculated using Equations 4.5 and 4.6, where C is the respective connection distance seen in Figure 4.6 and Figure 4.7. If the displacement magnitude was larger than this limit, a connection was not made as the ISS orbit satellite will not be within line-of-sight of the antenna. For the Globalstar constellation, the same approach for determining the link to the ISS orbit satellite was applied to the connection with Globalstar Gateways.

For the communication satellite constellations:

$$C = (R_E + A_E)\frac{\sin\theta_E}{\sin\theta_C} \tag{4.5}$$

And for the ground station network:

$$C = (R_E + A_E)\frac{\sin\theta_E}{\sin(180 - \theta_C)} \tag{4.6}$$

For the Iridium service, the effects of the doppler shift needed to be included in the connection check. The velocity information provided by Skyfield was applied to the doppler shift equation (Equation 4.7) to determine the range rate limit.

The doppler shift equation used was:

$$\Delta f = \frac{\rho f}{c} \tag{4.7}$$

Where:

$$\rho = v\cos\theta \tag{4.8}$$

Where Δf is the maximum allowable doppler shift, f is the central frequency, c is the speed of light, ρ is the range rate limit, v is the magnitude of the relative velocity vector, and θ is the angle between relative velocity vector and the displacement vector between the two satellites. If the ISS orbit satellite to constellation satellite range rate was greater than this limit, then a connection was not made as the doppler shift would be too large. The connection limits used for the simulation are provided in Table 4.14.

Table 4.14: Limits on a successful connection for the three communication services planned for use in the re-entry tracking system. All of the ranges were reasonable as the distance for ground usage of the network is far greater when compared to in orbit.

Iridium to ISS satellite connection distance limit	1802km
Iridium doppler shift limit	6.94km/s
Globalstar to ISS satellite connection distance limit	2986km
Globalstar to Gateway connection distance limit	3504km
SatNOGS to ISS satellite connection distance limit	757km

The values for the Iridium constellation connection distance and doppler shift limits are similar to those suggested by the MiniCarb CubeSat mission development team mentioned in the review [112]. No similar values could be found for simulating the Globalstar and SatNOGS services. The slight drop in parameters from the on-orbit performance of MiniCarb (2000km to 1802km and 7km/s to 6.94km/s) are likely due to the performance of the antennas in space. As the free space loss of the antennas is less at higher altitudes, the cone angle of the constellation can increase. The calculated values were still used in the simulation to account for any errors caused by other assumptions.

As identified in the review of the Iridium satellite constellation, the availability of communication satellite constellations was impacted by the RAAN of the connecting satellite orbit. Because of nodal precession, the RAAN of LEO satellites will change over time. This has implications as the rate of change of the RAAN is different for satellites at different altitudes and inclinations. In the case of the ISS orbit satellite, the RAAN would drift at a greater rate than the satellite constellations due to its lower altitude. This effectively means that the ISS orbit satellite RAAN will sweep under the orbital paths of the satellite constellations. This sweep would repeat each time it crosses under an orbit plane, being similar in connection gaps and doppler effects each time.

Six additional ISS orbit satellites were identified as necessary to evaluate the effects of nodal precession and different RAAN on the system accuracy. Two for both the Iridium and Globalstar constellation where the RAAN of the ISS orbit satellite would be equal and between the planes of each constellation, and another two for the Iridium constellation where the RAAN of the ISS orbit satellite would be equal and between planes plus 180° to make the orbits out of phase. This means that the satellites will be crossing orbit paths near the equator with the greatest relative velocity impacting the doppler shift. The RAAN of the constellations and the RAAN selected for the ISS orbit satellites can be seen in Table 4.15, Table 4.16, and Table 4.17. The additional ISS orbit satellites were merged when a similar RAAN between the Iridium and Globalstar constellations were found to reduce simulation time. This cut down the number of different satellite objects from six to four.

Table 4.15: Iridium orbital planes and the RAAN for each plane at the time of performing the simulation.

Iridium Orbit Plane	RAAN
1	130
2	162
3	193
4	225
5	256
6	288

Table 4.16: Globalstar orbital planes and the RAAN for each plane at the time of performing the simulation.

Globalstar Orbit Plane	RAAN
1	40
2	87
3	135
4	182
5	226
6	269
7	314
8	359

Table 4.17: RAAN used for evaluating each RAAN condition in the simulations.

Simulated ISS Satellite	RAAN	Explanation
ISS RAAN at Simulation Time	92	-
Iridium and Globalstar Equal RAAN	225	Matches Iridium orbit 4 and Globalstar orbit 5.
RAAN Between Iridium RAAN	146	In between Iridium orbit 1 and 2.
Out of phase Iridium and between Globalstar RAAN	109	180° less than Iridium orbit 6 and between Globalstar orbit 2 and 3.
Out of phase Iridium between RAAN	29	180° less than in between Iridium orbit 3 and 4.

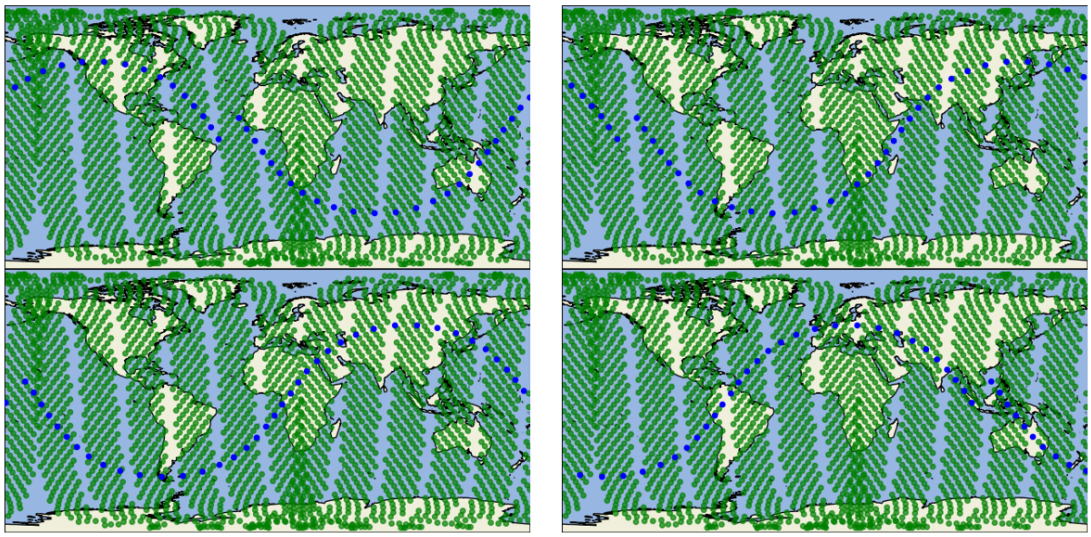

Figure 4.8: Demonstration of RAAN differences in the ISS orbit satellites. Out of phase satellites (bottom left and right) will move in the opposite direction to the constellation, increasing doppler shift. Meanwhile, the co-rotating satellites (top left and right) will move in the same direction, reducing the doppler shift.

In the case of the Iridium communication satellite constellation, RAAN was expected to have a more significant influence due to the out of phase orbits. The doppler shift is expected to be larger as the satellites pass with a larger velocity differential. Figure 4.8, shows the four ISS orbit RAAN paths. The out of phase orbits (bottom left and right) move against the trajectory of the Iridium satellite constellation, meaning the velocity difference will be more significant. Meanwhile, when the RAAN is near or equal (top left and right), the satellites move in a similar direction, reducing the differential velocity and impact of the doppler shift.

Performing this simulation over the same duration as the total availability simulation, the effects of doppler shift, nodal precession, and communication gaps were measured. The doppler shift effects and differing ISS orbit satellite RAAN were used to observe if there were any total availability losses. The connection gaps were used to calculate the ability of the system to track the re-entry position accurately. Additionally, the accuracy of a 550km ground track path was also measured to compare the system accuracy to an actual landing example. This path is the equivalent length of the longest trail in the Woomera test range, where other re-entry missions have landed in Australia [149]. The connection gap time of 80 seconds was included to estimate this accuracy.

4.4 Results and Discussion

The results of the accuracy simulations are detailed in this section. The simulations performed were separated into two parts. The first was an assessment to visualise and measure the total availability of the services at re-entry altitudes. The second was an analysis of the effects of doppler shift, nodal precession, and communication gaps on the ability of the system to determine the re-entry location.

4.4.1 Total Availability

The availability of each of the selected services was first visualised to verify the simulation setup. The starting availability visualisation for each of the three services is pictured in Figure 4.9.

The Globalstar network features availability circles of two different colours. The greyed-out rings are the Globalstar satellites which were not connected to a Gateway, meaning a modem cannot use them to transfer beacons during re-entry. The red circles highlight the satellites which are connected to Gateways. The black dots show the Gateways on the surface of the Earth.

Combining this availability, the total available area for the initial condition is presented in Figure 4.10. The initial results show that complete Earth availability is impossible at re-entry altitudes using these services. An observation made from these visualisations was that the coverage of Iridium is greater than the other two services.

For the total availability simulations, first, just SatNOGS was simulated, then Iridium was added, followed by Globalstar. Figure 4.11 is an example image of the three systems combined. The black represents the connected area, and the white represents the unconnected area.

The total availability of each system versus latitude is presented in Figure 4.12. As Binar missions are due to fly from the ISS, the latitude of 51.6° was used to measure the total availability. The average availability of the SatNOGS network

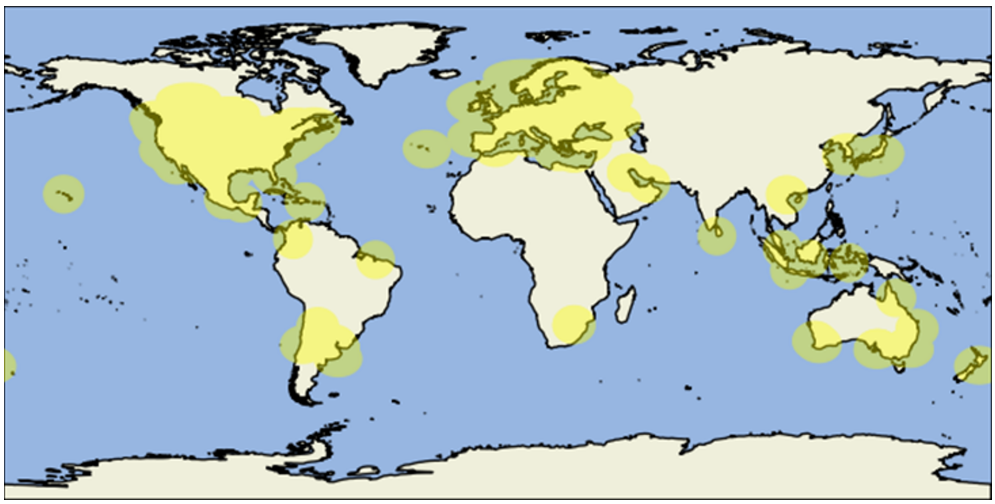

(a) SatNOGS.

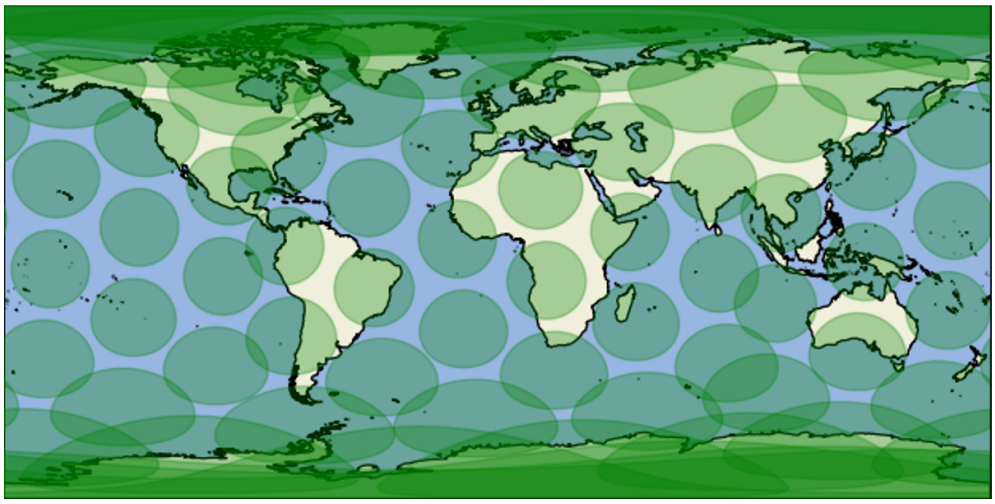

(b) Iridium.

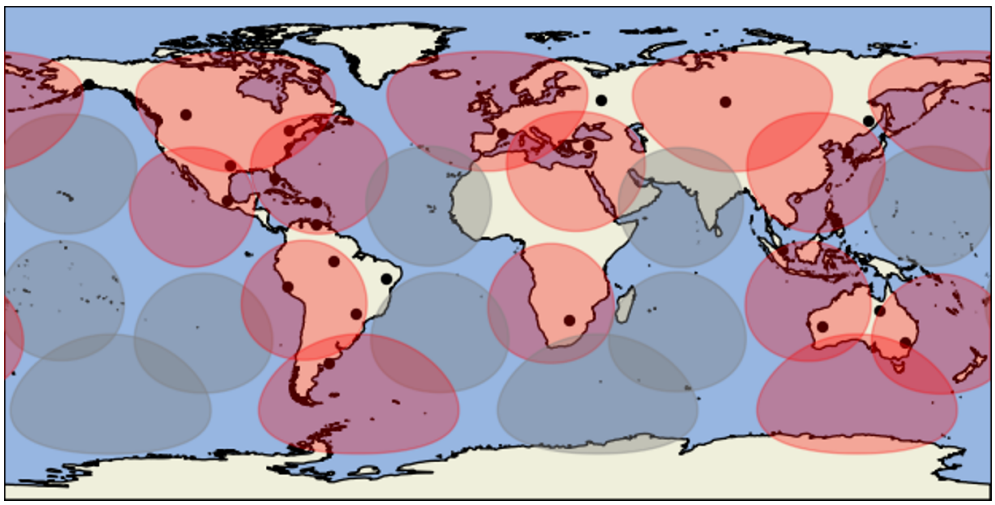

(c) Globalstar.

Figure 4.9: Initial availability images of each service selected. The availability altitude was 110km above sea level, projected proportionally onto the surface of the Earth.

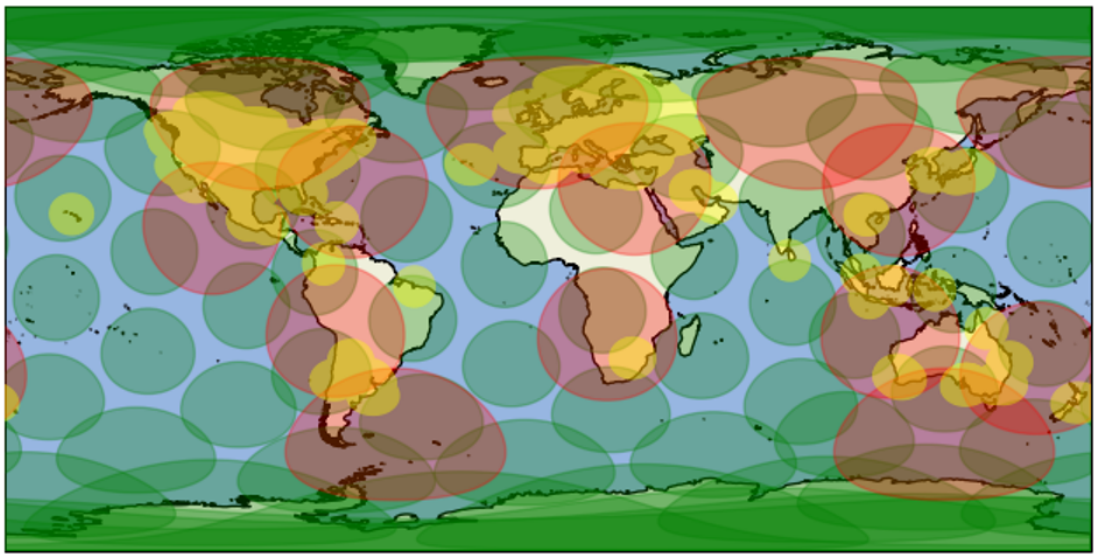

Figure 4.10: Combined initial availability map showing only the available services. Iridium is noted as having a higher availability due to its ability to operate at the poles and over oceans.

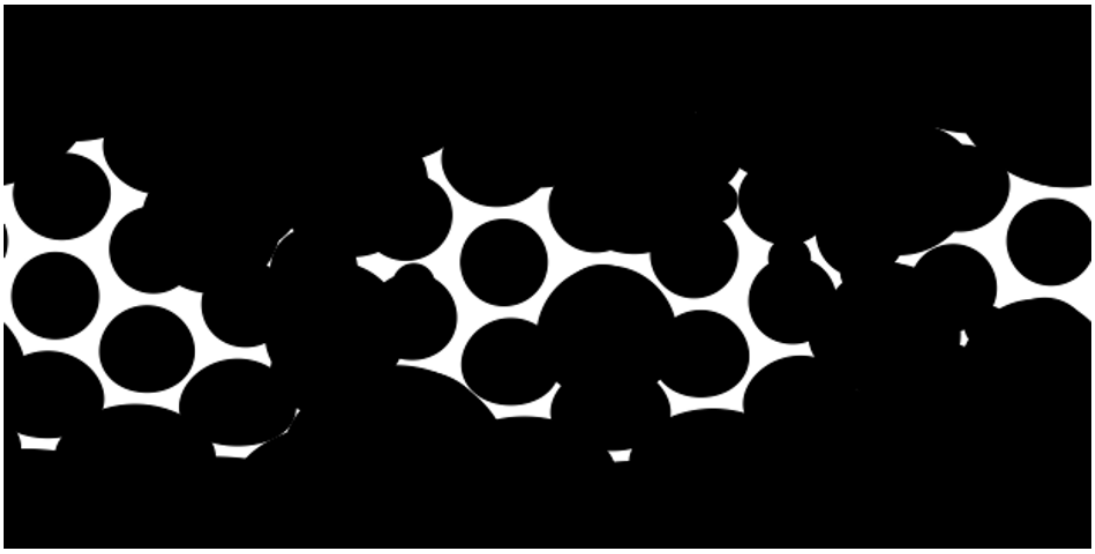

Figure 4.11: An example of the black and white visualisations used to measure the availability of the three systems combined.

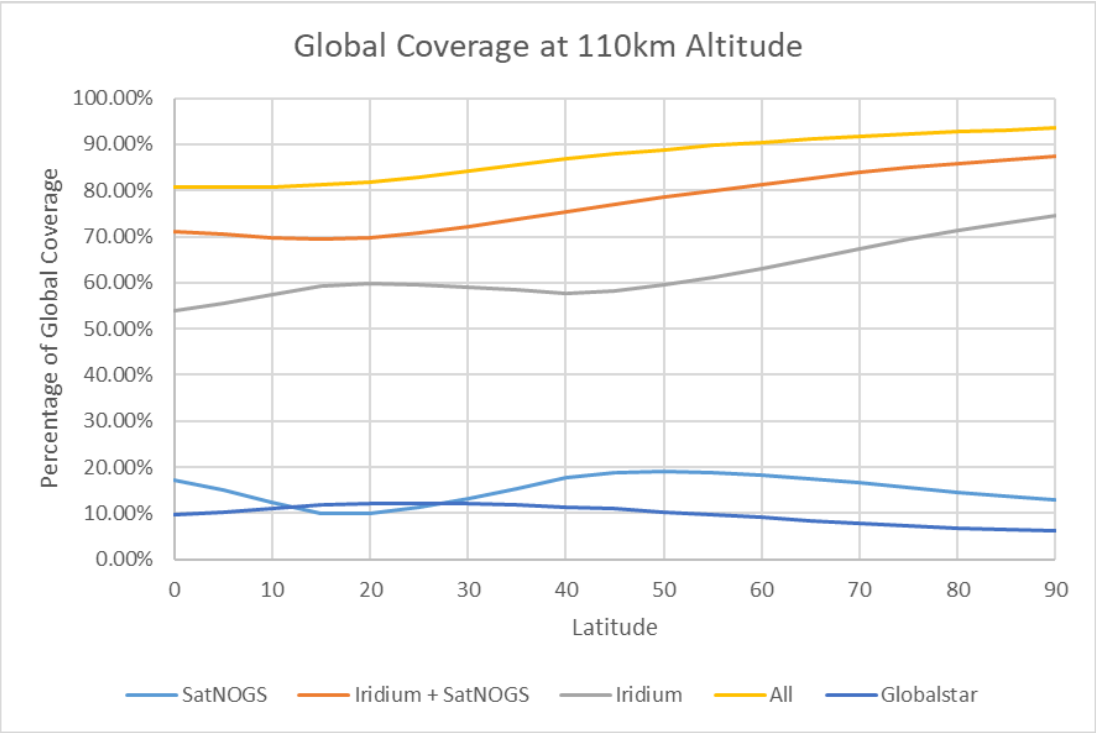

Figure 4.12: Percentage availability of each system versus the latitude of the Earth.

at the time of performing the simulations was 19.03%. With the addition of Iridium, the availability increased to 78.50%, and with the addition of Globalstar, the availability increased to 88.86%. This equated to a total availability addition of 59.47% for Iridium and 10.36% for Globalstar.

The availability at each 10-second time step was plotted to observe any patterns in the data over the simulation period. The results showed that the average was periodic with the motion of the Iridium satellites. This periodicity was lost as the Globalstar constellation disconnected and re-connected with the Gateways. The plot is also linear, indicating that the system availability will not significantly change unless changes are made to the services. Figure 4.13 demonstrates the periodic cycle. The average availability was used for measuring the total availability, as seen in the percentage availability of Figure 4.12.

4.4.2 Communication Gaps

The resulting communication gaps are presented in Figure 4.14, and the combined results are in Table 4.18.

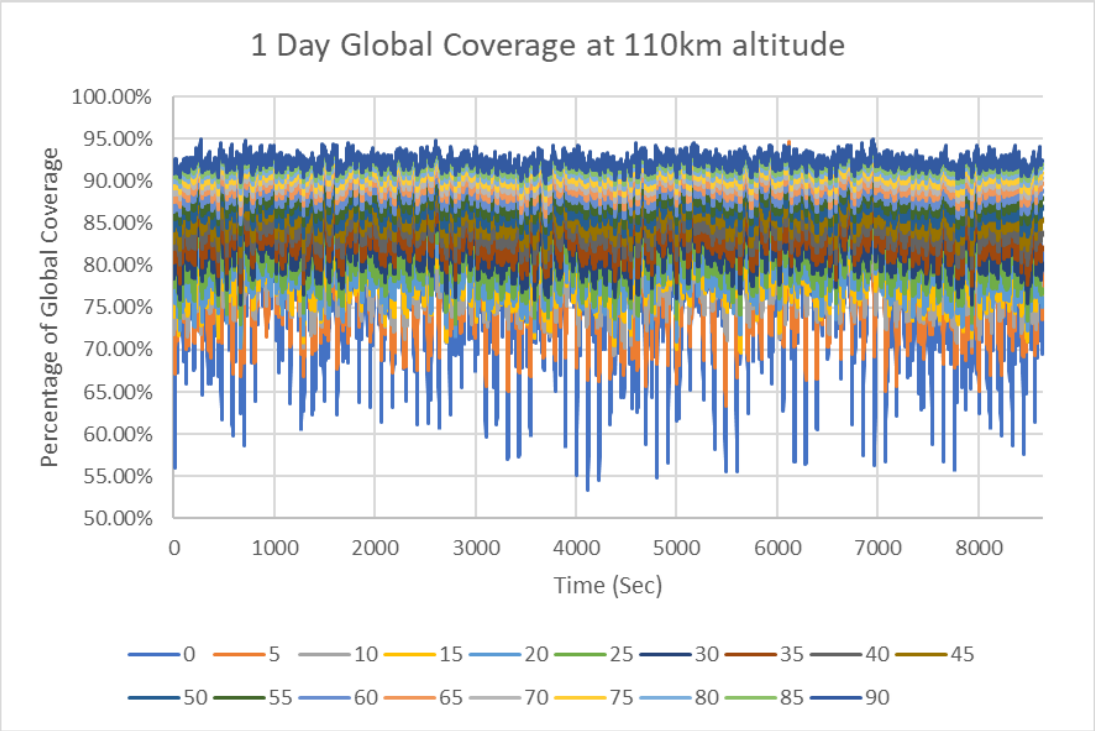

Figure 4.13: Assessment of the effects of nodal precession and if any patterns are present in the data. No changes were observed in the data indicating that the performance of the services will remain the same. The 19 lines mirror the availability at different latitudes.

Table 4.18: Simulation results for each RAAN. The SatNOGS and Globalstar connection stayed consistent at all RAAN. However, Iridium dropped as it approached the out of phase orbits. This was due to the doppler shift effects being greater when out of phase.

RAAN	SatNOGS Connection Time (%)	Iridium Connection Time (%)	Globalstar Connection Time (%)	Total Connection Time	Average Gap Time (seconds)	Median Gap Time (seconds)
92	18.9%	46.3%	59.5%	77.2%	142	130
225	19.0%	69.3%	60.0%	86.9%	131	110
146	18.7%	64.9%	58.7%	85.5%	142	100
109	18.5%	53.8%	60.6%	82.1%	114	110
29	19.3%	37.1%	60.9%	76.0%	139	130

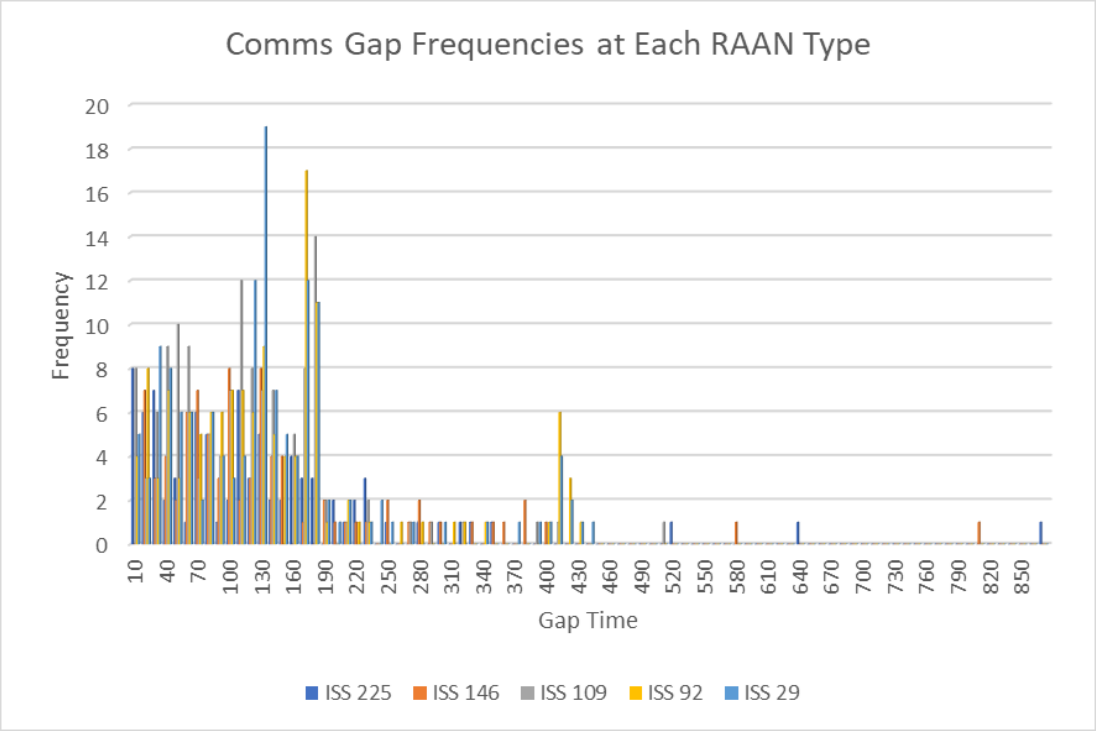

Figure 4.14: Communication gap size and frequency for the five simulated orbits. The orbits which rotated with the Iridium constellation had the most significant gaps, while the orbits that were out of phase with Iridium had more frequent smaller gaps.

A notable trend in the results is the minimal change in the connection time of SatNOGS and Globalstar. This shows that the availability of the services was not affected by changing the RAAN of the ISS orbit satellite. This trend is plotted in Figure 4.15, showing the horizontal points of both the SatNOGS and Globalstar services. For Iridium, there is a noticeable drop in performance for the out of phase orbits, where the in-between RAAN satellite performed the worst. However, the effect on the overall connection time was reduced as the Globalstar and SatNOGS services were able to fill in the gaps. Another notable trend is the nature of the communication gaps. All the averages and medians show that the communication gaps are skewed to a shorter length. This indicates that a more temporary communication gap is more likely than a larger one at the re-entry time.

The effects of the doppler shift are primarily responsible for the difference in connection time presented in Figure 4.15. The losses due to the range rate being too large between the Iridium satellite and ISS orbit satellite are shown in Table 4.19. A significant range rate means the doppler shift for a successful connection

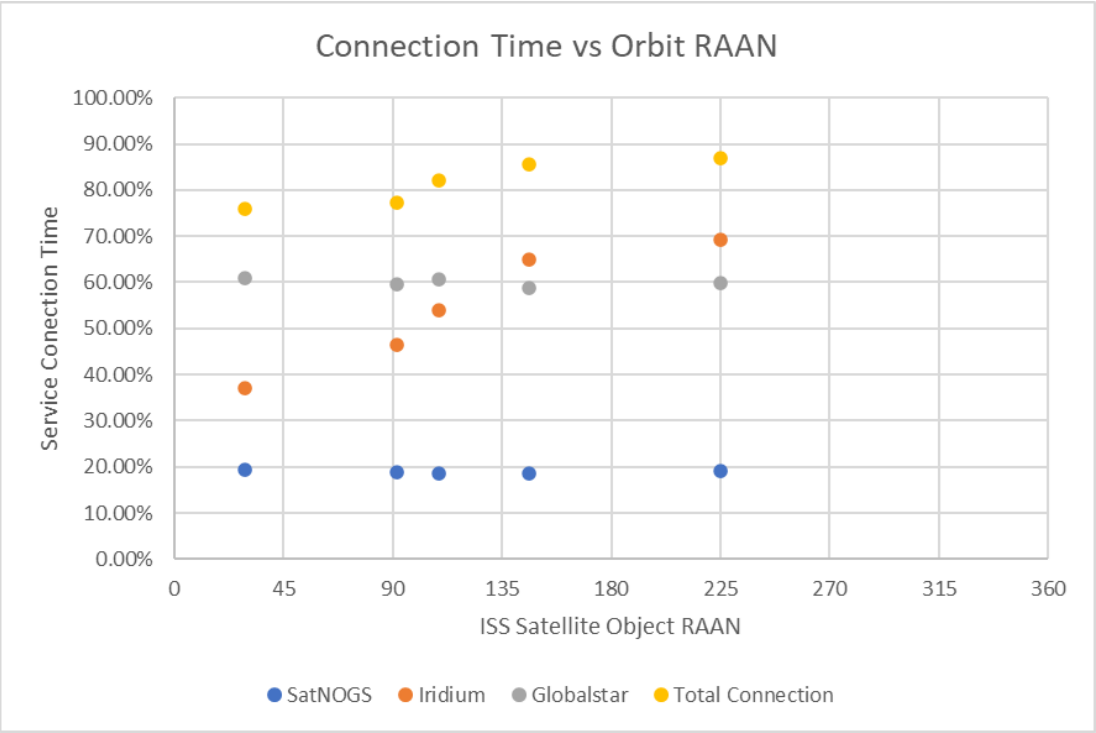

Figure 4.15: Service connection time and total connection time for the combined services. All the services except Iridium did not change. The Iridium services performed worse when the ISS orbit satellite had a out of phase RAAN to the Iridium constellation.

is too large.

The resulting final accuracy of the system was evaluated by observing the ground track of each communication gap. Figure 4.16 presents the accuracy of the different RAAN orbits to the ground track travelled between the final communication and the actual re-entry location. All RAAN was shown to be able to transmit at the exact re-entry location 76.0% of the time. For all systems at a ground track of 550km, the approximate length of the longest stretch of the Woomera range, the transmit location raised to 78.3%. If the re-entry occurs when the CubeSat RAAN matches an Iridium constellation orbit, this increases to 88.6%.

The resulting re-entry tracking system will use the Iridium, Globalstar, and SatNOGS services for its global communications solution. Once the CubeSat altitudes reach 180km, the re-entry tracking operation mode will enable. The mode will attempt to hold the satellites in a nadir point and transmit on all the communication services at 10-second intervals. As the CubeSats re-enter the

Table 4.19: The effects of the doppler shift on the performance of the Iridium service are presented in this table. The out of phase orbit losses were 4 to 6 times greater than those with equal RAAN. The orbit with the RAAN in between had double the losses.

RAAN	Range Rate Too Large, In Range (Sec)	Iridium Total Connection (Sec)
92	25770	40020
225	5520	59850
146	10860	56060
109	21400	46510
29	31690	32030

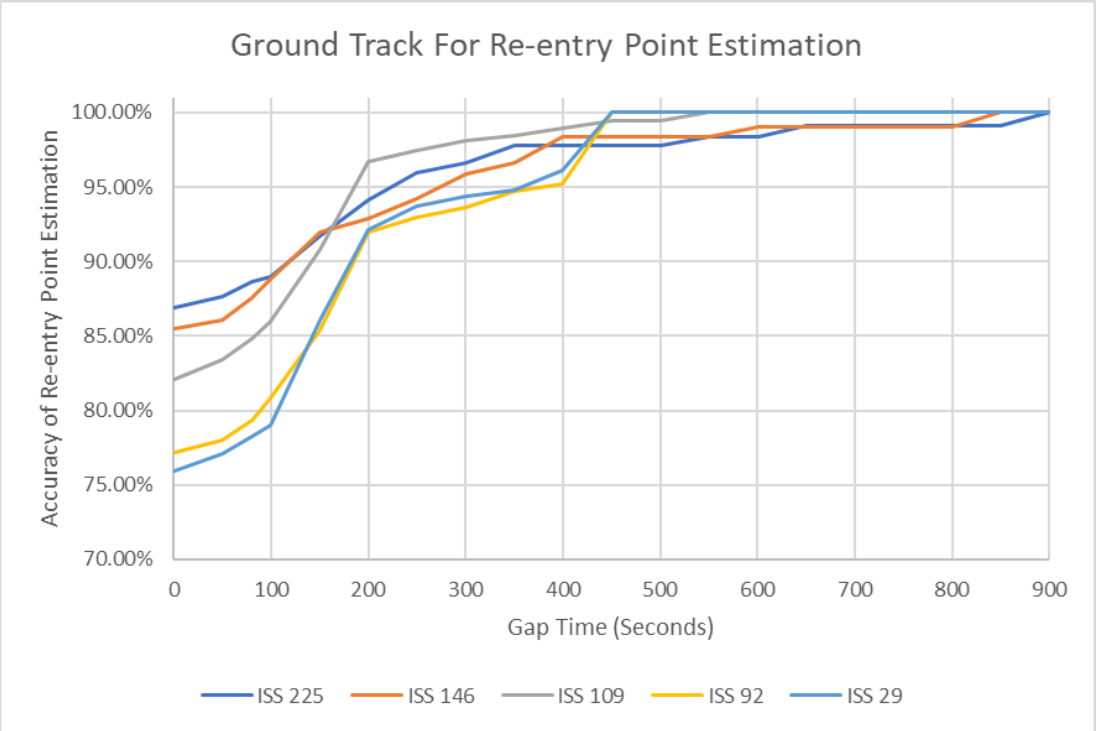

Figure 4.16: Accuracy of the re-entry location final transmit location. The results show that the re-entry tracking system can send the final transmission location within 80 seconds, 78.3% of the time.

Earth's atmosphere, the final transmission received will determine the re-entry location. The simulations indicate that the final re-entry location will be correctly transmitted 76% of the time due to gaps in the combined connection. This accuracy can be further improved by collecting the TLEs of the Iridium constellation during re-entry.

4.4.3 Discussion

Although the simulations are similar to those performed in the past, they are the first to be performed using freely available software. CubeSat developers have widely used the Iridium and Globalstar communication constellations for various applications. Besides the global availability, the main benefit of using these systems is the small size and power consumption. Claybrook presented a detailed model using the Iridium constellation for communications at altitudes greater than re-entry using the Ansys Systems Tool Kit (STK) [150]. Similar results to Claybrook were achieved by adapting the simulations presented in this chapter to simulate the ISS. By changing the re-entry altitude of the simulation to 419km for the altitude of the ISS, the available time for a single day was found to be within the boundaries presented in the thesis [111]. For Globalstar, matching simulations representing the current state of the Globalstar network were not found. In recent years the number of active Globalstar satellites and Gateways have changed, making previous simulations out of date. However, given the extensive reporting of Near Space Launch and the success of the EyeStar radio [123][126][128][135], the performance of the service for CubeSats is still well-proven. Many university CubeSat developers use the SatNOGS project for debugging and telemetry observations. The project assists many teams limited to a single ground station in collecting mission data.

Limitations are present in the simulations as assumptions. The simulations assume that the re-entry tracking system will have the Iridium and Globalstar antennas directed towards the satellite zenith and have a suitable gain angle to receive at specified angles. While the latter is an appropriate assumption given that most antennas are designed to operate on the Earth's surface, where the free space loss will be more significant, the satellite will likely not be able to hold a perfect nadir point for an extended period. This may add some differences to the real-world availability, and communication gap size and frequency depend on the

performance of the attitude control system. Another assumption is the SatNOGS ground station elevation angle. While not an appropriate assumption for some of the isolated stations in the network, assuming a constant elevation angle for densely populated areas with numerous ground stations is. Alongside this, as the Binar CubeSats are due to be launched a year later than when the simulations were performed, the number of SatNOGS stations will likely have grown [108], meaning the network will improve its ability to track re-entry.

The re-entry tracking system will use the CubeSats existing UHF radio and include an Iridium 9603 and Globalstar STX3 modem for use with the respective satellite constellations. By mounting the antennas for both modems on the zenith of the CubeSat, the antennas will maximise the line of sight of the satellite constellations. The UHF antenna will be at the nadir of the CubeSat for communicating with the ground. The two communication satellite constellation modems will be integrated and either implemented in the new modular payload bay featured in the upgraded BCB design or be made part of the Binar CubeSat Core (BCC) if the functionality is deemed necessary for other parts of the mission. For the Iridium modem, this is an expected additional application of the research due to the reported successful two-way communication. Using the service as a secondary communication system can support other mission objectives.

The simulations also justify the use of the services by other CubeSat operators who require a communications system with near real-time availability. It offers a high-availability communication solution in LEO for a low operation cost. The system will only improve in its availability as the altitude of the satellite drops. The simulations are a first of its kind being performed using Python and open-source packages rather than STK. This repeatability and ease of access can make the software usable for mission planning on other CubeSat missions. With slight modification, other CubeSat teams can determine their expected coverage with SatNOGS and even test the performance of Iridium and Globalstar with minimal alteration to the code.

Although the simulations do not provide a 100% accurate solution for tracking the re-entry of the CubeSats, the precision can be improved by collecting the constellation TLEs at the time of the final transmission. By observing if the

last communication was made within the range of a SatNOGS ground station or under the beam cone of a constellation satellite, the re-entry location accuracy can be improved. This data collection is currently planned for further analysis and publication after the following Binar CubeSats re-enter Earth's atmosphere.

Future re-entry tracking systems should consider upgrades to existing and new constellations that may become usable. This would include upgrades to the Inmarsat modems and antennas. If they can compete with the size of the Iridium and Globalstar systems, the global availability of Inmarsat would surpass that of the others combined. Furthermore, as the use of space and small satellites continue to be developed, other services will emerge that may be able to provide better availability. The continued improvement of these systems should be monitored for the potential of improving re-entry tracking accuracy and real-time re-entry control in the future.

4.5 Concluding Remarks

This chapter documents the design of a re-entry tracking system capable of being integrated with the BCB without compromising the available payload power and space. Completing the system design and simulations demonstrate that the trade-off between size and functionality provides a suitable solution for tracking CubeSat re-entry. The first test of the system and its ability to reflect the simulations will be performed on the next Binar mission, Binar-2, 3, and 4. The CubeSats will use the Iridium and SatNOGS services once reaching 180km altitude and begin to transmit at 10-second intervals the CubeSat location and telemetry. Although the design simulations demonstrated that the Globalstar service would also be effective, unfortunately, due to licensing constraints discovered after completing this work, it could not be included on the Binar-2, 3, and 4 mission. The results of this mission will determine if it is required and determine if any improvements should be made to the system for the first CubeSat controlled re-entry technology demonstration.

References

[7] "State-of-the-Art of Small Spacecraft Technology," English, Oct. 2021. [Online]. Available: http://www.nasa.gov/smallsat-institute/sst-soa.

[53] E. Kulu, *Nanosats Database*, en. [Online]. Available: https://www.nanosats.eu/index.html (visited on 12/19/2022).

[72] M. Murbach, R. Alena, and A. Luna, "The TechEdSat/PhoneSat Missions for Small Payload Quick Return," *Small Satellite Conference*, Aug. 2016. [Online]. Available: https://digitalcommons.usu.edu/smallsat/2016/S7Comm/6.

[73] F. Tavares, *TechEdSat-10 Deploys from the Space Station*, und, Text, Aug. 2020. [Online]. Available: http://www.nasa.gov/image-feature/ames/techedsat-10-deploys (visited on 12/19/2022).

[74] M. S. P. Murbach, *Modeling the Exo-Brake and the Development of Strategies for De-Orbit Drag Modulation*, Library Catalog: NASA NTRS, Jun. 2016. [Online]. Available: https://ntrs.nasa.gov/search.jsp?R=20160008903.

[75] M. S. P. Murbach, *Modulated Exo-Brake Flight Testing - Modeling and Test Results - Successes with Exo-Brake Development and Targeting for Future Sample Return Capability: TES-6,7,8 Flight Experiments*, Library Catalog: NASA NTRS, Jun. 2019. [Online]. Available: https://ntrs.nasa.gov/search.jsp?R=20190028931.

[98] D. J. White, I. Giannelos, A. Zissimatos, E. Kosmas, and D. Papadeas, "SatNOGS: Satellite Networked Open Ground Station," en, Oct. 2015. [Online]. Available: https://scholar.valpo.edu/cgi/viewcontent.cgi?article=1039&context=engineering_fac_pub.

[102] P. Kovář, P. Puričer, and K. Kovářová, "Study of the Two-Line Element Accuracy by 1U CubeSat with a GPS Receiver," en, *Sensors*, vol. 22, no. 8, p. 2902, Jan. 2022, ISSN: 1424-8220. DOI: 10.3390/s22082902. [Online]. Available: https://www.mdpi.com/1424-8220/22/8/2902.

[103] K. Riesing, "Orbit Determination from Two Line Element Sets of ISS-Deployed CubeSats," *Small Satellite Conference*, Aug. 2015. [Online]. Available: https://digitalcommons.usu.edu/smallsat/2015/all2015/58.

[104] G. D. Krebs, *Gunter's Space Page - Information on spaceflight, launch vehicles and satellites*. [Online]. Available: https://space.skyrocket.de/ (visited on 01/10/2023).

[105] *Sweedish space corporation - satellite Ground Station Services*, en-US. [Online]. Available: https://sscspace.com/services/satellite-ground-stations/ (visited on 01/12/2023).

[106] *Ksat - ground Network Services*, en. [Online]. Available: https://www.ksat.no/ground-network-services/ (visited on 01/12/2023).

[107] D. White, C. Shields, P. Papadeas, *et al.*, "Overview of the Satellite Networked Open Ground Stations (SatNOGS) Project," *Small Satellite Conference*, Aug. 2018. [Online]. Available: https://digitalcommons.usu.edu/smallsat/2018/all2018/313.

[108] K. Croissant, D. White, X. Álvarez, *et al.*, "An Updated Overview of the Satellite Networked Open Ground Stations (SatNOGS) Project," *Small Satellite Conference*, Aug. 2022. [Online]. Available: https://digitalcommons.usu.edu/smallsat/2022/all2022/172.

[109] J. Bordalo Monteiro, J. Santos, P. Antunes, A. Guerman, and F. Jorge, "A review of small satellite constellations for IoT connectivity," Sep. 2022. [Online]. Available: https://www.researchgate.net/publication/364213241_A_review_of_small_satellite_constellations_for_IoT_connectivity.

[110] *Iridium 9603 Module | Iridium Satellite Communications*. [Online]. Available: https://www.iridium.com/products/iridium-9603/ (visited on 01/10/2023).

[111] J. Claybrook, "Feasibility Analysis on the Utilization of the Iridium Satellite Communications Network for Resident Space Objects in Low Earth Orbit," *Theses and Dissertations*, Mar. 2013. [Online]. Available: https://scholar.afit.edu/etd/819.

[112] V. J. Riot, L. M. Simms, and D. Carter, "Lessons Learned Using Iridium to Communicate with a CubeSat in Low Earth Orbit," English, *Journal of Small Satellites*, vol. 10, no. 1, Feb. 2021, ISSN: 2327-4123. [Online]. Available: https://www.osti.gov/pages/biblio/1770026.

[113] R. Shimmin, R. Alena, C. Priscal, *et al.*, "The successful PhoneSat wifi experiment on the Soarex-8 flight," in *2016 IEEE Aerospace Conference*, Mar. 2016, pp. 1–9. DOI: 10.1109/AERO.2016.7500826.

[114] K. Alexandrou, "Ionizing Radiation Effects on Graphene Based Field Effects Transistors," en, Ph.D. dissertation, Columbia University, 2016. DOI: 10.7916/D86D5T53. [Online]. Available: https://doi.org/10.7916/D86D5T53.

[115] N. Enoki, Y. Takahashi, N. Oshima, K. Yamada, and K. Suzuki, "Aerodynamics of inflatable nano-satellite "EGG" in low earth orbit and reentry duration," en, *AIP Conference Proceedings*, vol. 2132, no. 1, p. 100 002, Aug. 2019, ISSN: 0094-243X. DOI: 10.1063/1.5119597. [Online]. Available: https://aip.scitation.org/doi/abs/10.1063/1.5119597.

[116] Y. Prevereaud, F. Sourgen, D. Mimoun, A. Gaboriaud, J.-L. Vérant, and J.-M. Moschetta, "Predicting the Atmospheric Re-entry of Space Debris Through the QB50 EntrySat Mission," Apr. 2013. [Online]. Available: https://www.researchgate.net/publication/265139721_Predicting_the_Atmospheric_Re-entry_of_Space_Debris_Through_the_QB50_EntrySat_Mission.

[117] M. Murbach, R. Ntone-Johansen, A. Salas, *et al.*, *TECHEDSAT-7 and 10: The Little Spacecraft That Could*, NTRS Author Affiliations: Ames Research Center, Millennium Engineering and Integration (United States), Wyle (United States) NTRS Meeting Information: Interplanetary Small Satellite Conference; 2021-05-03 to 2021-05-04; undefined NTRS Document ID: 20210014950 NTRS Research Center: Ames Research Center (ARC), 2021. [Online]. Available: https://ntrs.nasa.gov/citations/20210014950.

[118] *CACTUS-1: Mission Complete!* en. [Online]. Available: https://www.captechu.edu/news-events/cactus-1-mission-complete (visited on 01/10/2023).

[119] G. Morelli, G. Parissenti, R. Navoni, *et al.*, "FLEXIBLE EXPERIMENTAL EMBEDDED SATELLITE," en, 2019. [Online]. Available: https://icubesat.org/papers/2019-2/2019-b-1-3-fees-flexible-experimental-embedded-satellite/.

[120] *Hatchling Veery "Clay" Mission Detail*, en. [Online]. Available: https://careweather.com/mission/veery-rl1-1615347564369x827669778420672500 (visited on 01/10/2023).

[121] T. Sakamoto, *Get clues about sudden celestial gamma-ray bursts with the micro-miniature "ARICA"!* ja, 2022. [Online]. Available: https://academist-cf.com/projects/234/progresses?lang=ja (visited on 01/10/2023).

[122] M. Murbach, A. Salas, M. Lowry, *et al.*, *TechEdSat-13: The First Flight of a Neuromorphic Processor*, Apr. 2022. [Online]. Available: https://ntrs.nasa.gov/citations/20220005780.

[123] H. Voss, J. Dailey, M. Orvis, and M. Voss, "Thin CubeSats and Compact Sensors for Constellations in VLEO to Deep Space," *Small Satellite Conference*, Aug. 2022. [Online]. Available: https://digitalcommons.usu.edu/smallsat/2022/all2022/8.

[124] *STX3 | Globalstar AP*, en-ap. [Online]. Available: https://www.globalstar.com/en-ap/products/iot/stx3 (visited on 01/10/2023).

[125] M. O'Connell, *STX3 Declanation of Conformity*, English, 2017. [Online]. Available: https://www.globalstar.com/Globalstar/media/Globalstar/Downloads/Regulatory/Declaration_of_Conformity_STX3.pdf (visited on 01/10/2023).

[126] H. Voss, J. Dailey, M. Orvis, A. White, and S. Brandle, "Globalstar Link: From Reentry Altitude and Beyond," *Small Satellite Conference*, Aug. 2016. [Online]. Available: https://digitalcommons.usu.edu/smallsat/2016/S7Comm/1.

[127] M. Ovchinnikov, D. Ivanov, O. Pansyrnyi, *et al.*, "Flight Results of the Mission of TNS-0 #2 Nanosatellite Connected via Global Communication System," Oct. 2018. [Online]. Available: https://www.researchgate.net/publication/328102767_Flight_Results_of_the_Mission_of_TNS-0_2_Nanosatellite_Connected_via_Global_Communication_System.

[128] H. Voss, J. Dailey, J. Crowley, B. Bennett, and A. White, "TSAT Globalstar ELaNa-5 Extremely Low-Earth Orbit (ELEO) Satellite," *Small Satellite Conference*, Aug. 2014. [Online]. Available: https://digitalcommons.usu.edu/smallsat/2014/Workshop/3.

[129] C. Nogales, B. Grim, M. Kamstra, *et al.*, "MakerSat-0: 3D-Printed Polymer Degradation First Data from Orbit," *Small Satellite Conference*, Aug. 2018. [Online]. Available: https://digitalcommons.usu.edu/smallsat/2018/all2018/434.

[130] *HSAT-1 Experiment Description Document for FCC Application*, English, Aug. 2016. [Online]. Available: https://apps.fcc.gov/els/GetAtt.html?id=185034&x=..

[131] D. Werner, *Harris says first cubesat performing well in orbit*, en-US, Dec. 2018. [Online]. Available: https://spacenews.com/harris-hsat/ (visited on 01/10/2023).

[132] G. Kissel, R. Loehrlein, N. Kalsch, W. Helms, Z. Snyder, and S. Kaphle, "UNITE CubeSat: From Inception to Early Orbital Operations," *Small Satellite Conference*, Aug. 2019. [Online]. Available: https://digitalcommons.usu.edu/smallsat/2019/all2019/50.

[133] M. Goggin, S. Tamrazian, R. Carlson, A. Tidwell, and D. Parkos, "CubeSat Sensor Platform for Reentry Aerothermodynamics," *Small Satellite Conference*, Aug. 2017. [Online]. Available: https://digitalcommons.usu.edu/smallsat/2017/all2017/132.

[134] R. Twiggs, A. Zucherman, E. Bujold, *et al.*, "The ThinSat Program: Flight Opportunities for Education, Research and Industry," *Small Satellite Conference*, Aug. 2018. [Online]. Available: https://digitalcommons.usu.edu/smallsat/2018/all2018/475.

[135] H. Voss, J. Dailey, M. Orvis, *et al.*, "Architecture & Manufacture for 1/7U to 27U 60 ThinSat Constellations: Flight Results," *Small Satellite Conference*, Aug. 2019. [Online]. Available: https://digitalcommons.usu.edu/smallsat/2019/all2019/298.

[136] A. Martinez and C. Munoz, "AztechSat-1, a First Collaborative CubeSat Between NASA and Mexico," Brasilia, Dec. 2014. [Online]. Available: https://ntrs.nasa.gov/citations/20190001961 (visited on 01/10/2023).

[137] B. Campbell, C. Nogales, B. Grim, M. Kamstra, J. Griffin, and S. Parke, "On-Orbit Polymer Degradation Results from MakerSat-1: First Satellite Designed to be Additively Manufactured in Space," *Small Satellite Conference*, Aug. 2020. [Online]. Available: https://digitalcommons.usu.edu/smallsat/2020/all2020/45.

[138] T. Gies, T. Rodriquez, G. Holt, *et al.*, "Very Low Frequency Propagation Mapper (VPM) Experience and Results from the Systems Engineering Cycle of a Small Satellite," *Small Satellite Conference*, Aug. 2020. [Online]. Available: https://digitalcommons.usu.edu/smallsat/2020/all2020/114.

[139] M. Nunes, L. French, P. Englert, *et al.*, "NEUTRON-1 Mission: Low Earth Orbit Neutron Flux Detection and COSMOS Mission Operations Technology Demonstration," *Small Satellite Conference*, Aug. 2019. [Online]. Available: https://digitalcommons.usu.edu/smallsat/2019/all2019/124.

[140] J. Hanson, "PTD Management and Governance," en, *CubeSat Developers Workshop 2019*, Apr. 2019. [Online]. Available: http://mstl.atl.calpoly.edu/~workshop/archive/2019/Spring/Day%201/Session%202/John Hanson.pdf.

[141] M. B. Orvis, J. F. Dailey, H. D. Voss, and J. N. Fritsch, "Flight Results Including the ThinSat-2 Constellation, TROOP Payload Host, and Miniaturized GPS Integrated into the EyeStar-S3," en, 2021. [Online]. Available: http://mstl.atl.calpoly.edu/~workshop/archive/2021/presentations/Day%203/Subsytems%20Part%202/Matthew%20Orvis.pdf.

[142] S. T. Goh, L. Lim, V. Bui, *et al.*, "VELOX-II: Summary of One Year in Operation," Jun. 2017. [Online]. Available: https://www.researchgate.net/publication/317589990_VELOX-II_Summary_of_One_Year_in_Operation.

[143] *OG2 AND OGi MODEMS*. [Online]. Available: https://www.orbcomm.com/PDF/datasheet/OG2-OG-ISAT-Satellite-Modems.pdf (visited on 01/10/2023).

[144] D. F. Bruhn, "TechEdSat – CubeSat Technology demonstration mission featuring Plug- and-play and radiation hardened electronics," en, [Online].

Available: http://mstl.atl.calpoly.edu/~workshop/archive/2012/Spring/43-Bruhn-TechEdSat.pdf.

[145] V. Braun, Q. Funke, S. Lemmens, and S. Sanvido, "DRAMA 3.0 - Upgrade of ESA's debris risk assessment and mitigation analysis tool suite," en, *Journal of Space Safety Engineering*, Space Debris: The State of Art, vol. 7, no. 3, pp. 206–212, Sep. 2020, ISSN: 2468-8967. DOI: 10.1016/j.jsse.2020.07.020. [Online]. Available: https://www.sciencedirect.com/science/article/pii/S2468896720300847 (visited on 01/10/2023).

[146] T. Kelso, *CelesTrak*. [Online]. Available: https://celestrak.org/ (visited on 01/10/2023).

[147] *Cartopy: A cartographic python library with Matplotlib support for visualisation*. [Online]. Available: https://scitools.org.uk/cartopy/docs/latest/ (visited on 01/10/2023).

[148] B. Rhodes, *Skyfield: Elegant astronomy for Python*. [Online]. Available: http://github.com/brandon-rhodes/python-skyfield/ (visited on 01/10/2023).

[149] M. Fairclough and R. Dutch, *Mineralisation and mineral potential of the Woomera Prohibited Area, central Gawler Province, South Australia. Davies, M., Fairclough, M., Dutch, R., Katona, L., South, R. and McGeough, M.: 2008.South Australia. Department of Primary Industries and Resources. Report Book 2008/18.* Sep. 2008.

[150] *Ansys STK | Digital Mission Engineering Software*. [Online]. Available: https://www.ansys.com/products/missions/ansys-stk (visited on 01/10/2023).

Chapter 5

Improving the Reusability of the Binar CubeSat Bus

The CubeSat standard was developed over two decades ago as an educational tool for training the next generation of space scientists and engineers. In recent years, the platform has grown, beginning to perform valuable space missions outside Low Earth Orbit (LEO), heading further into the Solar System. The MarCO A and B CubeSats were the trailblazers, travelling to Mars alongside the InSight lander and providing a redundant communications link during its Entry, Descent, and Landing (EDL) [13]. Since then, CubeSats have assisted other large missions such as DART with LICIACube [14], and Artemis 1, which carried ten secondary CubeSats with Lunar science and Near Earth Asteroid (NEA) research objectives [15]. Although these CubeSats were not mission-critical or launched solely on their own, including low-cost CubeSats with a high acceptance of risk on large-scale planetary science missions is becoming a default component of a missions architecture when factored against the value they can provide.

Demonstrating the novel Binar CubeSat Core (BCC) was the primary objective of the maiden Western Australian space mission, Binar-1. The BCC design objectives of reducing hardware costs and maximising payload space without limiting the system capabilities were motivated by the need to improve the efficiency of CubeSat technologies for performing planetary science. Controlled re-entry and

recovery technologies were some of these targeted improvements, as they can offer countless opportunities to explore the Solar System. CubeSats capable of returning samples from asteroids or landing on the surface of Mars and Titan as part of larger space missions can provide precious additional science for a minimal added cost.

The BCC was the main design effort of the Binar CubeSat Bus (BCB) version used on Binar-1. The work provided many lessons learned and delivered successful results, demonstrating that the integrated BCC design was suitable for the CubeSat platform. However, due to the small development team, the design could not focus on another crucial design objective, platform reusability. This objective refers to the ability of the platform to be replicated and reused on future space missions. Targeting a low-cost design, the affordable BCB still required some additional work to improve reusability. The next Western Australian space mission, Binar-2, 3, and 4, offered an opportunity to include this design objective and the lessons learned from Binar-1, improving the Binar CubeSat Bus to where it can begin to demonstrate controlled re-entry and recovery technologies.

Although one of the significant motivators for performing a custom design on Binar-1 was the hardware cost savings, it could only be partially custom-designed as a focus was put on the design of the BCC. With the BCC now completed for Binar-2, 3, and 4, the custom design has been finalised, maximising the platform reusability. The BCC has included a communications system, utilising three communication methods for improved system capability and redundancy. The custom payload system inclusion was more complex, needing to consider all future applications of the BCB and the payloads it may carry. The resulting design features a modular payload bay with a single interface connector board that can be adapted depending on the mission objectives. The resulting novel payload bay design is unique as it allows high school, university, research, and industry payloads to interface with the BCB requiring minimal intervention to the platform.

Similar to the justification for only partially completing the custom design, the design, assembly, integration, and testing of the BCB on Binar-1 was not easy to understand. With a large effort put into the development of the BCC, some assumptions were left outstanding for the remainder of the BCB. Tying in with the

Binar-1 lessons learned, this resulted in new documentation for testing and further minor design improvements targeted at making all parts of the mission lifecycle process easy to understand and complete. This has improved the reusability of the BCB and its mission lifecycle process.

This chapter presents the improved and reusable BCB and mission lifecycle process that enables the development of controlled re-entry and recovery technologies for CubeSats. Also included in this chapter is an introduction to the Binar-2, 3, and 4 mission. This mission is the first implementation of the Binar-1 lessons learned and the reusability design objective. Its context is essential for understanding how the improved BCB meets the aim of this thesis. First, the Binar-2, 3, and 4 mission is presented, including a summary of its eight mission objectives. Second, the methodology for improving the BCB design and mission lifecycle process is explained. Finally, an overview section summarises how the improvements compare to the previous Binar-1 BCB and other existing integration methods, and how the lessons learned from Binar-1 have been successfully implemented.

5.1 The Binar-2, 3, and 4 Mission

Binar-2, 3, and 4 is the second mission to use the BCB. The mission will be launched and deployed into orbit using the same method as Binar-1. However, this time the team will be assembling, integrating, and testing three 1U CubeSats (Figure 5.1) for flight, which will be identical except for slight material changes in one of the payloads. A singular engineering model will also be built. This model will test the improved design deployables and assembly and testing processes before being performed on the flight models. Additionally, the engineering model will be used during operations to identify potential failures and test recovery options. By flying three CubeSats, the team can increase the chance of mission success, maximise the amount of platform data collected, and prepare for flying multiple 1U CubeSats with different payloads in the future. With the planned usage of the platform for providing valuable research, technology demonstration, and education, this mission is critical to ensure the platform is suitable for its purpose. The Binar-2, 3, and 4 mission objectives are to:

- Demonstrate the improvements made to the BCB design and mission life-

cycle process following Binar-1,

- Test two radiation shielding materials for the CSIRO (one control and two different materials on three CubeSats),

- Test a re-entry tracking system for validating controlled re-entry technologies on future Binar CubeSats (Chapter 4),

- Test an on-board intelligence algorithm for the development of a digital satellite twin,

- Test a novel deployable solar panel method,

- Test an improved star tracker camera payload designed and assembled by undergraduate students at Curtin University,

- Test a robotic arm solar panel deployment failure simulation to demonstrate the capabilities of the Fugro SpAARC, and

- Provide amateur radio operators with the ability to command a CubeSat creating interest in amateur radio.

Binar CubeSat Bus Improvements

Improvements were made to the BCB to maximise design reusability. The primary design improvement was the completion of the custom design, reducing further the total platform cost. On Binar-1, the communications and payload systems were primarily made of COTS components or not designed to be reusable. As such, a custom communications system and payload system were designed and included in the BCB. Completion of this custom design has further reduced the hardware costs and increased the payload space of the platform.

The secondary design improvements included additions to the system capabilities. The available payload power, pointing accuracy, and mass increased by includ-

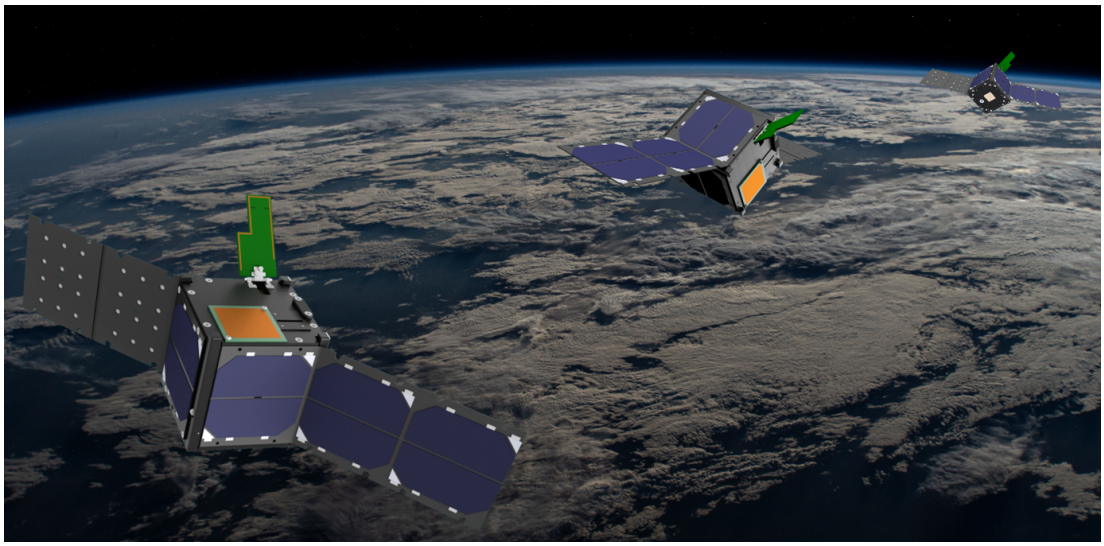

Figure 5.1: Render of the Binar-2, 3, and 4 CubeSats flying over Earth. The CubeSats will match internally except for the three different radiation shielding materials surrounding the radiation sensor payload.

ing deployable solar panels, additional attitude control algorithms, and better thermal management techniques in the design. When combined with the additional payload space created by completing the custom design, the range of future payloads have been expanded, broadening the payload options the platform can carry.

To implement one of the lessons learned from Binar-1 several other detailed design improvements were made. By simplifying elements of the BCC and how it integrates with the remainder of the BCB, its assembly, integration, and testing can be better understood. This is referred to as the design understandability which aims to make the Binar design more available to new Binar team members and students who get involved in the project.

Outside of the BCB design, its mission lifecycle process also needed to be improved to increase mission repeatability and improve the design understandability. These improvements matched the remaining lessons learned from the Binar-1 mission. These lessons were:

- Lockdown high-level mission requirements early,

- Test as you fly,
- Plan for delays, and
- Include an operations plan.

Streamlining the Binar mission lifecycle and documenting the process has made meeting launch requirements simpler. Implementing the lessons learned from Binar-1 has improved the repeatability of Binar missions, making them more accessible to the next generation of Binar students and easier to execute and complete. Successful completion of the remaining mission objectives will demonstrate the BCB design modifications and confirm the suitability of the improved mission lifecycle for future Binar missions.

Radiation Shielding

An on-orbit radiation shielding test for the CSIRO will include a payload with different materials on each CubeSat. The sensors at the centre of the payload include a scintillation crystal, radFET, and floating gate dosimeter for measuring different energy levels of radiation. On Binar-2, the payload will have regular space-grade aluminium (7075) shielding, while Binar-3 and Binar-4 will have shielding manufactured by the CSIRO using a new manufacturing technique [151]. The payload results will provide flight heritage to the material and an analysis of the performance compared to regular space-grade aluminium.

Re-entry Tracking

A re-entry tracking system will be used to locate the CubeSats as they re-enter Earth's atmosphere. With solar activity increasing in the 11-year cycle [152] and the increased surface area of the CubeSat bus due to the deployable panels, the three CubeSats are expected to de-orbit faster than Binar-1, which de-orbited after almost a year. This provides a valuable opportunity to test the re-entry tracking system developed in Chapter 4. The final recorded CubeSat location can be used as the approximate re-entry location and using some post-analysis techniques the accuracy of this re-entry location approximation can be determined. The results can demonstrate the suitability of the system for verifying

controlled re-entry technologies.

Onboard Intelligence

An onboard intelligence simulation will be performed, testing an algorithm for power management of systems not directly controlled by the flight computer. On Binar-1 and the now improved BCB, only the battery heating system is not controlled by the flight computer. Controlled by an automatic analogue temperature sensor switch, the battery heaters cannot be disabled or enabled by the flight computer. This protects the integrity of the batteries. The resulting circuitry, although reliable and independent of the performance of the primary flight computer, can result in the power state of the CubeSat being compromised if the heaters enable unexpectedly. Although the temperature state of the CubeSats during the mission will be well known, the test is being performed to verify the algorithm's performance so that it may be used on satellites operating in communication-denied environments. Observing the capability of the CubeSat to reschedule or cancel tasks due to clashing with heater operation will demonstrate the importance of onboard intelligence for larger deep space missions.

Deployable Solar Panels

Deployable solar panels have been included in the design of the BCB for the Binar-2, 3, and 4 mission. The addition was made after the team identified the need for more payload power. The deployment mechanism is part of a doctoral project at Curtin University investigating the performance and use of compliant mechanisms in space. The panels will be deployed using Shape Memory Alloy (SMA) to extend after a burn wire hold-down release mechanism is used to make the initial deployment. The final design has included changes to the Binar CubeSat Core (BCC), including more Maximum Power Point Controllers (MPPCs) and temperature sensor lines. As the deployable panel has no flight heritage, significant work has been performed to ensure that if the solar panel deployment fails, the CubeSats can still meet the mission objectives.

Star Tracker

On Binar-1, a camera for star tracking was selected and flown by a team of Curtin University undergraduate students. Due to the only partial success of Binar-1, the camera could never be tested. However, the team has since expanded and,

as a result, developed a custom camera for star tracking. The objectives of the payload remain the same, to capture an image and determine the attitude of the CubeSat on the ground. The payload design project was also used as a modular payload bay case study. The Binar team used the integration and testing process of the payload to understand and improve the procedure. This assisted in the payload bay design, resulting in an easy-to-manufacture and integrate solution.

Fugro SpAARC Simulation

Similar to the star tracker camera, the Binar-1 mission software will also contain the Fugro SpAARC robotic arm simulation. As the payload was not successfully able to be evaluated on Binar-1, it will attempt to be performed on one of the CubeSats during the Binar-2, 3, and 4 mission. The payload is important for demonstrating the remote operations capability of the centre and Western Australia.

Amateur Radio Communications

Finally, an amateur radio communications payload will be demonstrated using the new UHF communications system included as part of the hardware improvements for the mission. The payload will consist of a separate operation mode where the CubeSat can receive a command from amateur radio ground stations worldwide. The payload will be used to play a game of capture the flag or "Capture the CubeSat". Amateur radio enthusiasts will be able to attempt to send the special command to the CubeSat containing their six-character call sign, which will then be broadcast as part of the standard telemetry beacon. The amateur with their call sign as part of the beacon the longest will have captured the CubeSat and receive a reward from the Binar CubeSat Program. The payload is a new development attempting to gain more interest in amateur radio, enticing younger generations to get involved.

The mission is designed so that for 7 of the 8 objectives to be completed, only one of the CubeSats needs to be successful. The remaining objective, the radiation shielding payload, will be tested first. The remainder of this chapter targets the changes to the hardware design, software design, and mission lifecycle to meet the existing and new objectives of the BCB. Further information on the design of payloads out-of-scope to this thesis have been omitted.

How to Read the Following Two Sections

Similar to the work performed during the delivery of Binar-1, designing, assembling, integrating, and testing the Binar-2, 3, and 4 CubeSats was not completed by an individual but rather by the team of engineers and PhD students at the Binar Space Program. Since the delivery of Binar-1, a large portion of the work that has gone towards Binar-2, 3, and 4 has been completed as part of this PhD. To provide context to the rest of the methodology changes, sections are included that were not solely completed by the author. To identify what work was completed by the author, percentage contributions are included at the heading of each section to recognise the contributions of others to the Binar 2, 3, and 4 mission.

5.2 Design Improvements

Improvements to the BCB design were necessary to improve reusability and understandability. These improvements aimed at using the expertise developed from the Binar-1 mission to further lower costs and increase payload space and system capabilities. Additionally, included in the methodology are measures to combat the impacts of the COVID-19 pandemic. Supply chain challenges incurred due to the resulting economic effects of COVID-19 have left many of the parts used on Binar-1 in short supply [153]. Components have been swapped out to similar parts with available stock. The other changes included additional power generation, battery protection, a new communications system, and a modular payload bay.

5.2.1 Design Requirements

Similar to Binar-1 a set of design requirements were developed alongside the mission objectives. Although these design requirement were more established for for the Binar-2, 3, and 4 mission, most of the requirements overlap with the functionality of the already established parts of the Binar-1 BCB. As such, only a shortened list of the second level requirements are provided to give context to some of the design improvements mentioned in this section. Additionally, the same safety requirements specified in the JEM Payload Accommodation Handbook [88] needed to be met. The shortened list contains:

- The CubeSat shall have a mass of less than 1.33kg as specified by the CubeSat handbook.

- The CubeSat shall operate in LEO with similar conditions to the ISS were it will be deployed from.

- The CubeSat shall be operational until the end of its life when it re-enters the Earth's atmosphere.

- The CubeSat EPS shall operate with a power surplus for the duration of its mission life.

- The CubeSat EPS shall have a power storage subsystem cable of operating the CubeSat when solar power is not available.

- The CubeSat communication system shall be operational when nadir pointing.

- The CubeSat communications system shall have a reliable link for remote operations and telemetry downlink.

- The CubeSat ADCS shall be able to slow the CubeSat rotation after deployment to 2 rpm for thermal regulation.

- The CubeSat ADCS shall be able to nadir point the CubeSat with the UHF antenna CubeSat face directed towards the Earth.

- The CubeSat thermal budget shall have a steady state between operational limits when nadir pointing.

5.2.2 Deployable Solar Panels (40%)

To expand the ability of the BCB to carry certain additional payloads, more payload power was required. To provide this additional power, the power generation

subsystem could be enhanced by replacing a set of regular panels with deployable ones. Deployable panels could provide more surface area to carry solar cells, thus increasing the power-generating capability. By making this change, the team was able to double the available solar cells from 8 to 16 using a double-deployed solar panel system. Alongside this, additional temperature sensors and MPPC circuits were included to understand the thermal performance and supply the additional generated power to the battery. The resulting design was achieved using a rigid-flex Printed Circuit Board (PCB) for the solar panel structure and a burn wire and thermally activated SMA strips for the deployment system.

The deployable panel structure was a single rigid-flex PCB which, when folded, could fit within the allowable solar panel envelope of a 1U CubeSat (100 x 83 x 6.5 mm). The thickness of the rigid sections was 1mm and contained three internal copper layers to accommodate the necessary electrical connections. The resulting PCB was able to have a flex bend radius of 0.75mm to meet the 6.5mm thickness requirement with sufficient room for the top-side solar cells. The panel also included four temperature sensors for measuring operating temperatures in orbit and during thermal vacuum testing. Assembling the solar panel used a similar approach to the original 1U solar panels. First, the backside components were mounted using a stencil, solder paste, and a reflow oven. Next, the solar cells were attached using double-sided Kapton tape before being soldered on the back side using solder paste and on the top side using regular solder. Finally, the electrical components were soldered by hand to the top side of the panel before the SMA was connected to the PCB via spot welding. Finally, the new deployable solar panels were mounted with aluminium spacers to align the folding for the tying of the burn wires.

The solar panel deployment method consists of a burn wire circuit and an SMA setting system. The SMA setting system design is part of another doctoral project investigating the use of compliant mechanisms for space applications. The burn wire circuit was designed with two wires to meet the safety review requirements. Both are cut using a single resistor and activated via General Purpose Output (GPO) from the flight computer. The burn wire circuit was tested and successfully burnt through the wire efficiently and quickly, conserving power. The benefit of custom designing the deployment system was the ability to repeat the

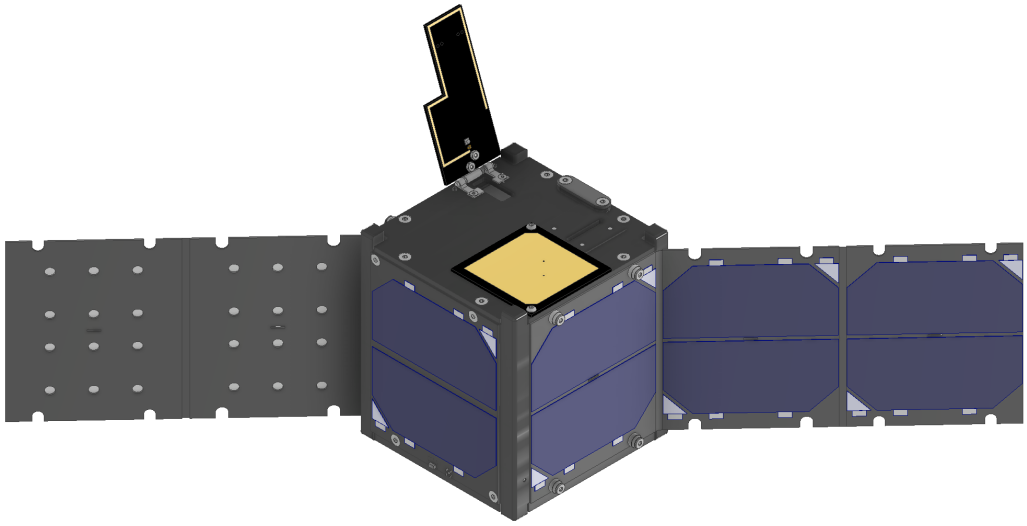

Figure 5.2: Deployable solar panels extending 45° from the mounting face seen in the Computer-Aided Design (CAD) for Binar-2, 3, and 4.

deployment tests easily, unlike Binar-1.

Following the burn wire activation, the solar panels would be set to the final deployed state using SMA actuators. Training of the SMA is performed using electrical heating and a mechanical fixing device. Two strips of SMA are located at each of the two hinges on the deployable solar panel. The two strips on the first hinge were trained to return to a 45° bend once heated to activation temperature, while the other strips on the second hinge would return to a straight 0° bend position. The resulting panel, once deployed, would extend at 45° from the face of the deployable panel, as seen in Figure 5.2.

The panel was designed so that failed deployments do not prevent meeting the mission objectives. If the panels cannot deploy after start-up or during repeat attempts in commissioning, the external solar panel will still be able to operate independently. This design effectively means the success of the Binar-2, 3, and 4 mission is independent of the performance of the un-demonstrated deployment method. If the panels cannot be deployed, the CubeSats will still be able to perform mission tasks at reduced repeatability while still meeting the mission objectives. This scenario will be accounted for in the mission operations plan to prepare the team. This was implemented to reduce the risk of using untested deployable solar panels.

The final compact deployable panels enable the BCB to increase its power generation by doubling the number of cells available. Assuming the panels deploy correctly and the CubeSats can successfully nadir point and rotate about the Z-axis, the additional panels will approximately double the power generation per orbit to 3.2Whr. This extra power will be used to power the numerous payloads on Binar-2, 3, and 4 at increased frequency and provide more opportunities to fly higher-powered payloads in the future. This was noted in the power budget where the budget was balanced around the operation times of certain payloads. In the future this increase power generation will allow for more dynamic power budgeting, optimising payload operation time and payload priority order.

5.2.3 Binar CubeSat Core Improvements (80%)

Multiple design changes were made to the BCC to remove assumptions and improve the platform's reusability. Additional MPPCs, an inrush current limiter, a new communication system, and a modular payload bay were included in the design. Due to COVID-19 and the resulting supply chain challenges, some of the parts used on Binar-1 were swapped. Although these parts needed to be exchanged, no functionality was removed from the design, maintaining capability.

Additional MPPC (100%)

To account for double the solar cells on the BCB, the core needed to include double the MPPCs. The additional controllers were added to the core using a matching method to the original controllers. However, the functionality of the controllers together needed to be considered. The original MPPCs were added for each axis of Binar-1 with solar panels, where the parallel faces of solar panels never faced the sun together, so a MPPC was shared. For the new design, the other solar cells will also be parallel and facing in opposite directions when deployed. As such, a single MPPC could be used for all of the other cells if deployed correctly. However, if the cells do not deploy correctly, or not at all, then using one MPPC is not possible because if the face of the deployable cell is shaded, then the performance of all the other cells together would be significantly reduced. As such, two MPPCs were added for each of the deployable faces. If the deployment fails, then the MPPC which is connected to the outer deployable cells, will be able to operate. If the panels deploy correctly, the MPPC will still generate the same amount of power as the combined solution. The design block diagram

and examples of the deployment states are provided in Figure 5.3. The two deployment states show why each MPPC is necessary for each rigid face of solar cells.

The addition of two more MPPCs on the BCC has improved the system capabilities as discussed in Section 2.4.3. This improvement is important to recognise, as it demonstrates the ability of the BCC to maintain its capabilities without compromising the available payload space. Additionally, the ability to add MPPC demonstrates the benefits of performing a custom design. The customizability of the BCC and the ability of the Binar Space Program to improve the design when necessary is a vital advantage of the design decision mentioned in Chapter 2.

Inrush Current Limiter (100%)

An inrush current limiter was included in the design to prevent unintended current spikes when powering on the magnetorquer system. On Binar-1, the team initially attempted to have an additional Binar CubeSat Motherboard (BCM) PCB for further technology qualification. Before launch, it was removed primarily due to challenges with managing the software and the risk of tripping the battery protection circuitry when the deployment switches were released. During the testing of Binar-1, when every device was connected to the main BCC, it was assumed that the battery safety circuit would be able to handle the inrush current. This was not the case, as the battery protection circuit would sometimes trigger after releasing the deployment switches. To mitigate this on Binar-1, the magnetorquers were found to be the cause and were removed on the additional BCM PCB, but not on the main BCC PCB. Resulting from this observation, an inrush current limiter was added to the magnetorquer circuits for Binar-2, 3, and 4 to conserve battery health. This also allowed the flight computer to control the power input to the magnetorquers directly. The simple inrush current circuit is presented in Figure 5.4. The design will reduce the risk of accidentally triggering the battery protection when using the magnetorquers and conserve battery health, removing a design assumption and implementing the lesson learned from Binar-1.

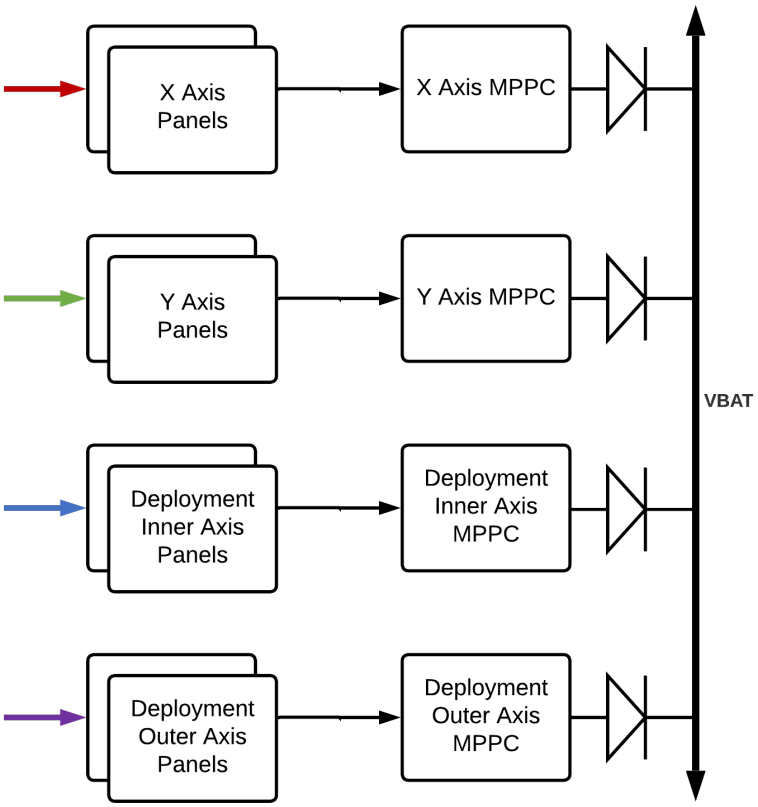

(a) MPPC simplified schematic.

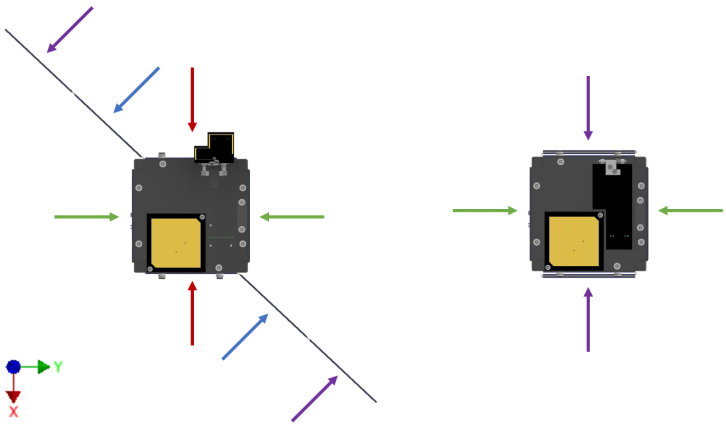

(b) Solar panel illumination directions.

Figure 5.3: MPPC simplified block diagram and solar cell illumination directions. The two deployment examples show how more MPPCs allow the solar panels to operate at maximum efficiency regardless of position. If the inner axis and outer axis solar panels shared an MPPC and the solar panels were to not deploy correctly, then the inner axis panels would be shaded, reducing the efficiency of the outer axis panels. To prevent this from occurring, two MPPC were included instead. An explanation of how the MPPCs are able to support two sets of solar panels is provided in Section 2.2.2.

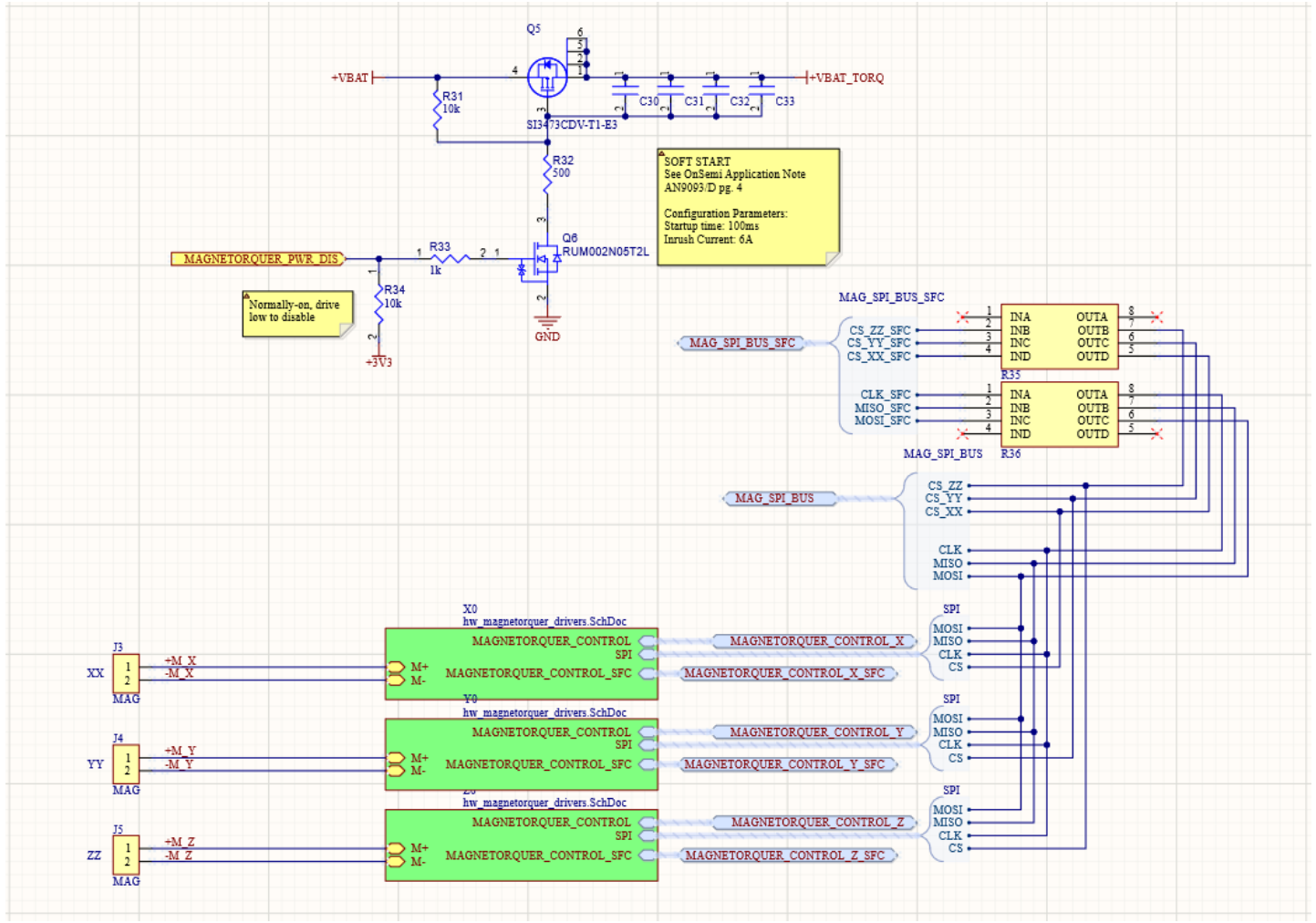

Figure 5.4: Altium schematic of the inrush current limiter upgrade for the BCC. The limiter will prevent the inrush current from spiking past the battery protection limit when the magnetorquers are powered on.

Custom Communication System (20%)

For the Binar-1 mission, the communications system was excluded from the custom-designed core due to design time constraints. With the BCC and structure design predominantly being reused for the Binar-2, 3, and 4 mission, the team could now allocate time for integrating a custom communication system. The system combines three independent communication systems for redundancy. However, only two are duplex and will be permanently included in the core. First, a UHF transceiver and antenna were added to the core as the primary communication system. Second, during the development of the re-entry tracking system, the Iridium 9603 transceiver and antenna were identified as suitable candidates for a secondary communication system if space was available. With minor remapping of the BCM PCB, the 9603 transceiver could be added. The dual duplex communication systems will provide the mission with multiple methods for gathering telemetry and controlling the CubeSats.

Like the payload power concern resulting in extra solar cells, future Binar missions may require high data downlink to collect results. The team has collaborated with AVI, a Perth-based technology company, to develop an S-band transmitter that will fit within the 1U platform. The transmitter is the third communication system that will be flown on all three CubeSats improving its flight heritage and demonstrating its usability for future missions where high data downlink is required.

The UHF transceiver was based on the OpenLST. The Planet team developed the open-source design and has flown it on 100% of Planet's Dove CubeSats [154]. Before being integrated with the BCC, the transceiver was modified. Due to the supply chain challenges associated with COVID-19, certain parts of the design were no longer available. Combining this with the Binar ethos for design compaction, new parts were sourced and the design was compressed. The design was separated from the central core PCB to limit noise. By mounting the transceiver on top of the core, as seen in Figure 5.5, the design could be compacted and easily interfaced with the antenna.

The antenna was custom designed from lessons learned during the modification

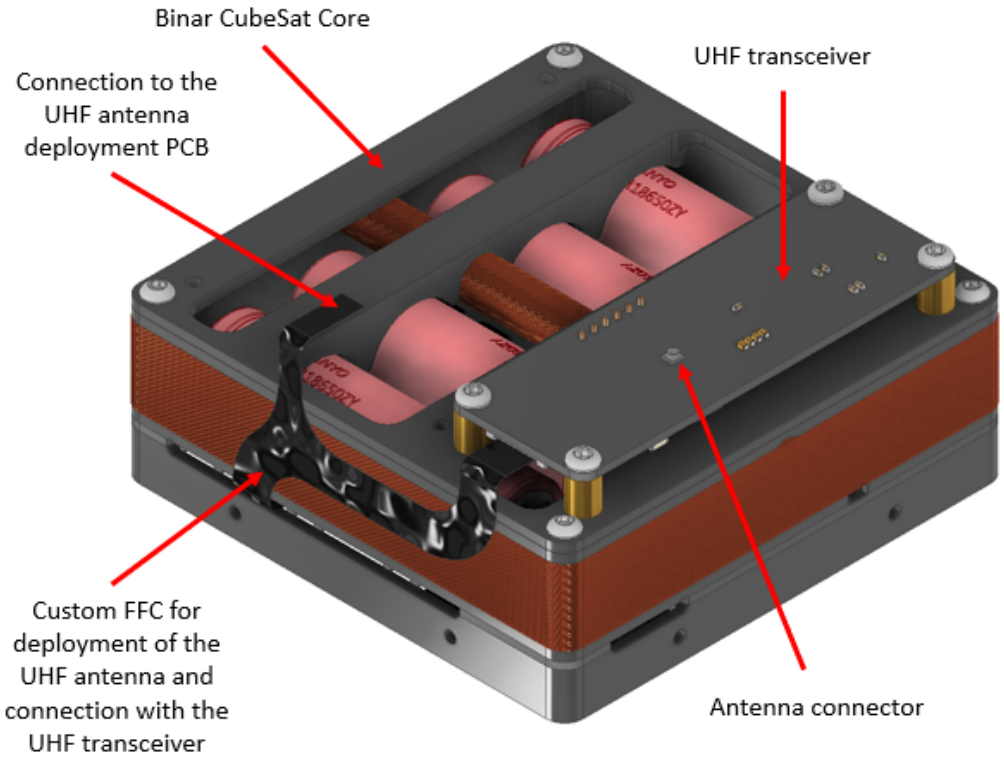

Figure 5.5: The OpenLST-based design is mounted to the BCCs top. The connections are made using a Flat Flexible Connector (FFC) which can run along the side of the CubeSat behind the 1U solar panels.

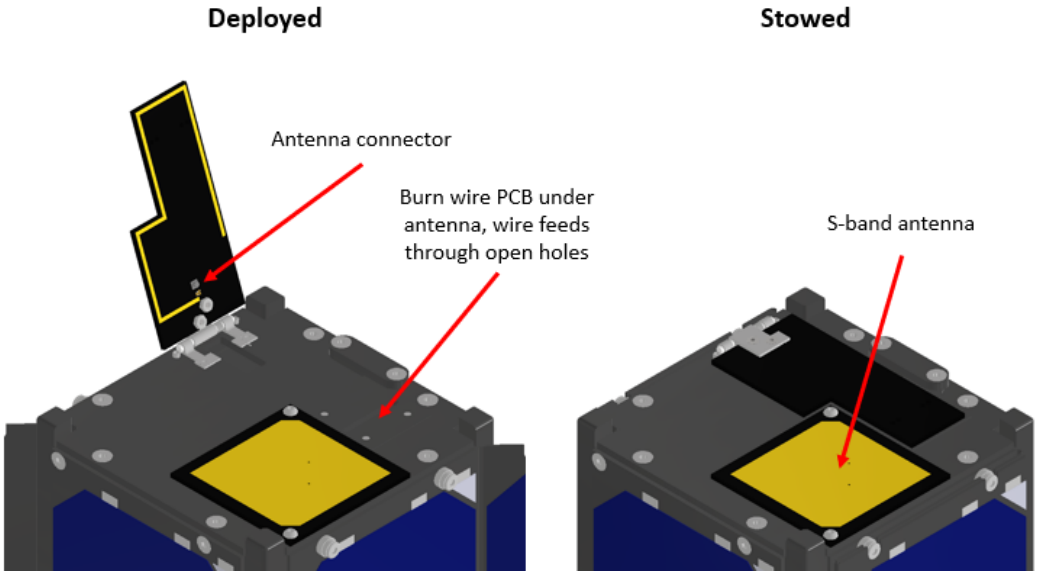

Figure 5.6: Deployed and stowed state of the planar monopole antenna being flown on Binar-2, 3, and 4. The rigid design makes resetting the deployment mechanism easy to perform.

of the Commercial Off The Shelf (COTS) UHF antenna on Binar-1. The planar monopole antenna is rigid to improve the structural performance of the design and simplify the deployment mechanism. Using a spring and hinge system along with a burn wire, the antenna can be stowed and deployed simply without having to take the antenna apart. Removing the antenna from the CubeSat and disconnecting the connectors found in convenient locations allows the antenna to be reset and remounted to test the deployment system. This improved the repeatability of the design when performing the final system tests and built confidence in its performance in space. The deployed and stowed antenna is illustrated in Figure 5.6.

The Iridium secondary and re-entry communication system comprises an Iridium 9603 transceiver and patch antenna. Selected initially for the re-entry tracking payload, the Iridium system was found to be suitable as a secondary communications system for the BCC. The Iridium 9603 transceiver modem is compact and could be mounted to the BCM PCB, requiring only an additional 5V distribution system. The modem will be used as a secondary beacon on all three satellites and be investigated for its ability to perform two-way communications. The antenna, needing to communicate with the Iridium satellite constellation, was attached to the zenith face of the CubeSat on the opposite end to the UHF

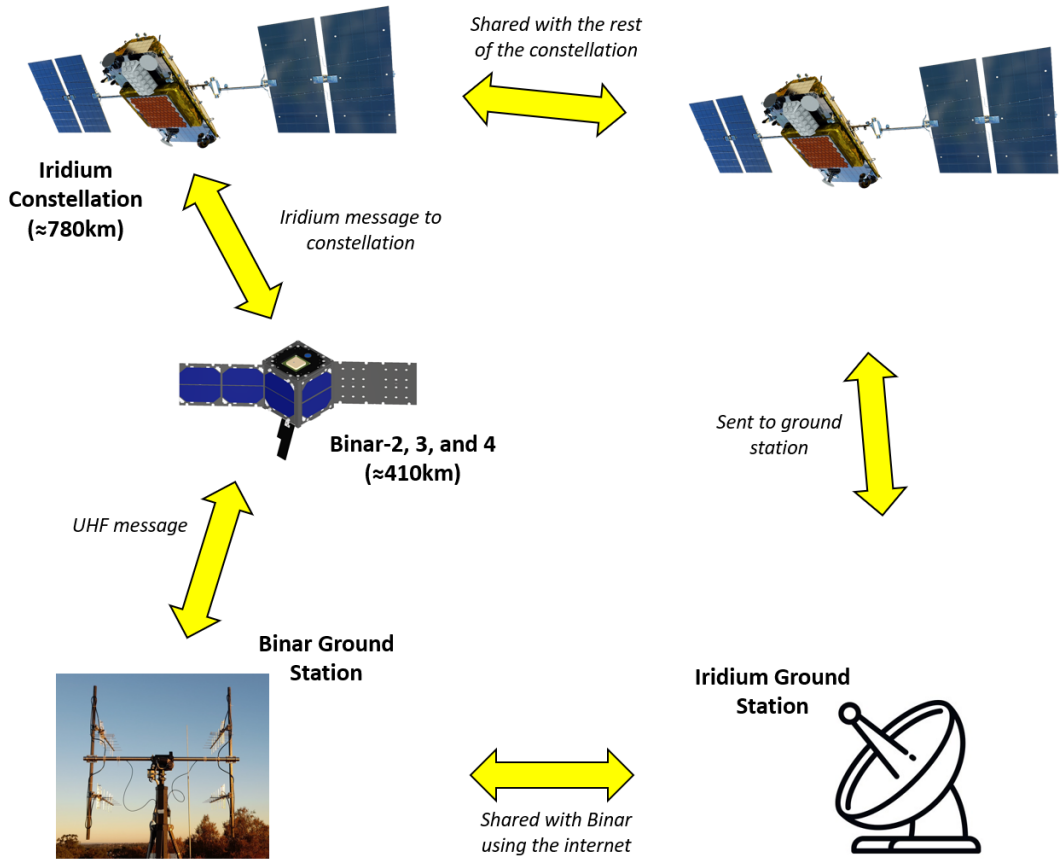

Figure 5.7: Antenna communication diagram containing ground stations and the Iridium constellation.

and S-band antennas. If the improvements to the Attitude Determination and Control System (ADCS) can successfully nadir point, then all the communication systems will be able to operate successfully. Additionally, as the communication system now depends on the CubeSat ADCS, the ADCS is now used when the CubeSat enters safe mode. However, to save power, the ADCS will only operate at reduced frequency causing a loss of pointing accuracy. This may affect the ability of the CubeSat to maintain extended communications, but will allow for basic debugging and error determination before re-enabling the ADCS for an attempted recovery or firmware update. Figure 5.7 illustrates the antenna locations for all three systems and shows how each antenna communicates in space.

The S-band transmitter was designed by a Perth-based technology company AVI. The company has a history of creating radio solutions for defence and mine site applications. Attempting to diversify its market opportunities, the company is

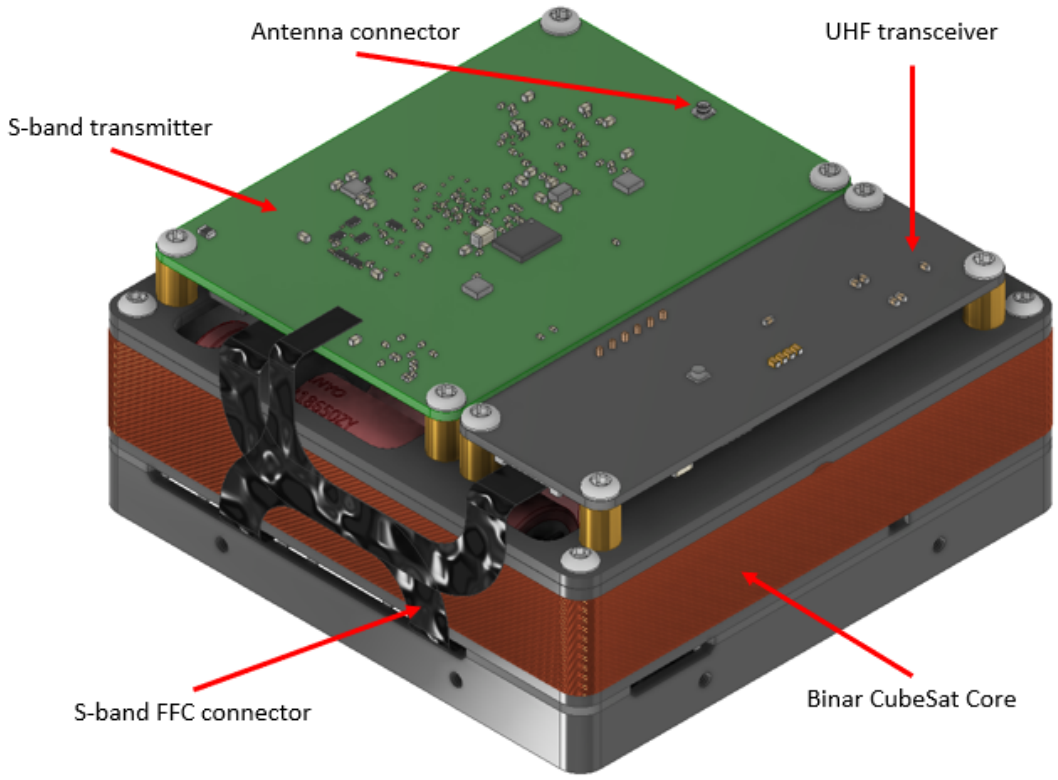

Figure 5.8: The S-band transmitter located at the top of the BCC next to the UHF transceiver.

now interested in developing space communications systems. After engaging with the Binar team, it was put forward that an S-band radio would improve payload possibilities for future Binar missions as the platform would be able to transmit more data. The S-band transmitter is located at the top of the BCC next to the UHF transceiver and interfaces with the rest of the BCC similarly to the UHF transceiver. This can be seen in Figure 5.8. The radio will be tested on the Binar-2, 3, and 4 mission by attempting to transmit the complete 1 Gbit of external storage on the BCC. If the radio is unsuccessful, the data will still be collected using the other two communication systems. The antenna is located at the top of the satellite next to the deployable UHF antenna (Figure 5.6). The patch S-band antenna was designed at the same time as the UHF antenna to optimise space usage at the satellite's nadir. If the entire 1 Gbit of storage can be received by the S-band ground station used for the mission, then the S-band transmitter will be successful and usable on future Binar missions with high data rate payloads.

Link budgets were analysed for all of the new antennas on the Binar-2, 3, and 4 mission. Of the three, two were custom designed and simulated at Curtin University and shown to provide a 3dB margin. These two antennas were the UHF antenna which has a cone angle of 120°, and the S-band antenna which has a cone angle of 60° at this gain margin. This met the design requirements as both would be able to operate when nadir pointing and be able to provide a reliable connection in this condition. The final antenna is the Iridium antenna which did not have a direct link budget performed as the antenna was bought off the shelf for ground applications. As free space losses are greater for ground communications, its gain will be very suitable for applications in space where the free space loss is less.

The final combined communication system comprises three transmission methods and two receiving methods. Redundancy has been implemented in the design to reduce mission risk and increase the platform's capability. Completing the custom design, the ability to merge the communication system with the BCC has improved the reusability of the BCB. The design, once successfully demonstrated, will enable a multitude of payloads to be tested including controlled re-entry and recovery systems.

Deployment Switch Improvements (100%)

The deployment switches and wires were modified to improve the assembly procedure and remove assumptions present in their design. On Binar-1, the deployment switch wires were soldered directly to the BCM PCB before being soldered to the deployment switches. This created many challenges, especially when trying to include double insulation on the PCB soldered ends to meet the safety review requirements. A connector was added to the main BCM PCB to improve the assembly method for connecting the deployment switches. The deployment switch assembly was then able to be built and mounted to the rail halves before being connected to the BCC. The final design simplified the approach to managing double insulation and installing the deployment switches onto the rail halves, improving the design understandability by reducing complexion and removing assumptions associated with soldering and insulation lengths.

On Binar-1, only two deployment switches could be placed on the -Z-axis ends

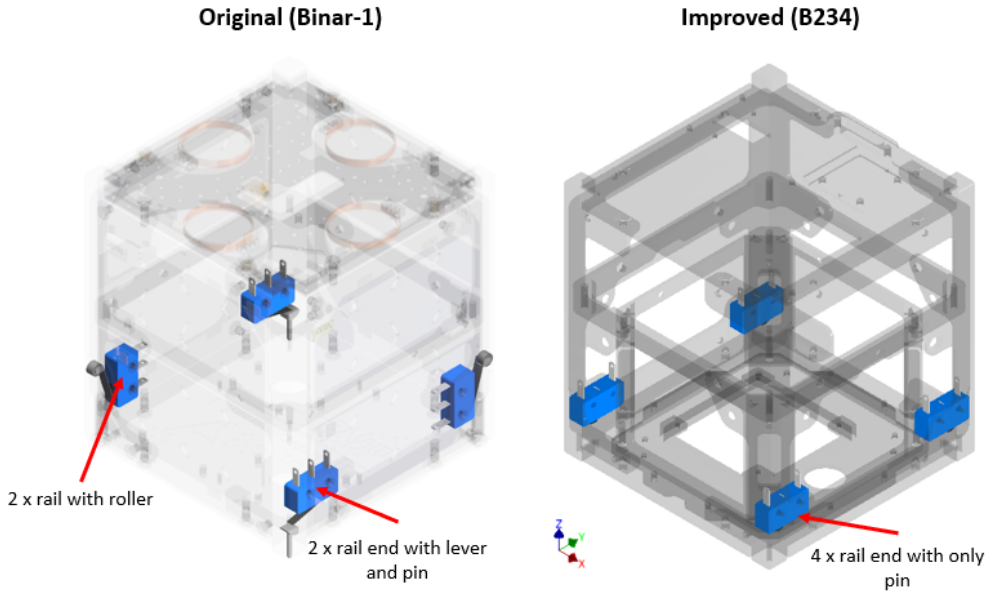

Figure 5.9: The differences between the deployment switches on Binar-1 and Binar-2, 3, and 4. The levers are not included on Binar-2, 3, and 4 to remove the flexing experienced on Binar-1. Instead, the pins interface directly with the switch button.

of the rails due to the deployment springs necessary to meet the safety review requirements. This was changed for the Binar-2, 3, and 4 design as the deployment spring requirement was removed. As such, four deployment switches could be mounted on the rail ends to meet the safety review requirements. This simplified the design and removed the rail switches, which required a safety review waiver for qualification on Binar-1 due to exerting too much force on the internal rails of the deployment pod. The levers were also removed as the lever bending rate and switch stroke caused the switches to be inconsistent. The deployment switch changes have simplified the assembly of the Binar-2, 3, and 4 CubeSats. Figure 5.9 demonstrates the differences between the deployment switch set-up for Binar-1 and Binar-2, 3, and 4.

Component Exchange

Some components needed to be exchanged as they were unavailable due to the COVID-19 pandemic. A list of the components that were unavailable and needed to be replaced is provided in Table 5.1. Datasheets and preliminary testing demonstrated that no functionality was lost because of the changes, and the board could still be assembled using the same method as Binar-1.

Table 5.1: List of parts exchanged on the BCC due to the COVID-19 pandemic supply chain issues.

System	Original Part	New Part(s)
Global Positioning System (GPS)	Venus838	OrionB16
ADCS	LSM9DS1	MPU-6881 & MMC5983MA
Electrical Power System (EPS)	ACS70331	TMCS1108-Q1
EPS	TPS2121RUX	LTC4415EMSE
EPS	LTC4376	LTC4359
Flight Computer System	MTFC4GMWDQ	W25N01GVZEIG

5.2.4 Modular Payload Bay (20%)

A significant design improvement for Binar-2, 3, and 4 was the addition of a modular payload bay. The payload bay can be easily inserted and removed from the BCB, enabling different payload designs to be tested in parallel with the CubeSat mission lifecycle. The payload is connected to the BCC through a single board-to-board connector. This makes developing payloads easier and allows the Binar Space Program to simulate part of the BCCs functionality with a simplified microcontroller board. The Binar-2, 3, and 4 payloads have been used to improve the payload bay and its ability to provide a payload development platform. The integration process evaluated the payload bay design and its suitability.

Changing from the Binar-1 design, instead of using a Flat Flexible Connector (FFC) to interface the payload with the payload adapter board, the payload bay now rigidly fixes to the payload connector board. The distance from the base of the CubeSat to the connector on the BCC defines the height of the payload. The resulting payload bay space is now approximately 0.55U. The design is also significantly more robust than the previous one, rigidly fixing from the bottom and middle of the CubeSat. The payload bay Computer-Aided Design (CAD) is illustrated in Figure 5.10, showing the inserted and removed set-up, demonstrating the complete design.

The sides of the payload bay are made from matching parts to reduce the total design part count. The base is separated into two parts, the outer edge, which is fastened to the two rail halves, and the inner edge, which is part of the payload

bay. When the payload is ready to be integrated, the inner edge is connected to the outer edge using eight M2 machine screws. Eight M3 screws also support the payload at the top of the payload bay to prevent movement on the X and Y axes. The final design is more robust and modular than the Binar-1 approach and will make the platform more reusable, only being defined by the payload inserted into the CubeSat.

5.2.5 Attitude Control Algorithms (0%)

Due to the assembly challenges and omnidirectionality of the antenna on Binar-1, only a detumble algorithm was developed for the mission. To improve the opportunities for payloads on future Binar missions and meet the new communication system pointing requirements, an additional ADCS algorithm was developed for Binar-2, 3, and 4. The new algorithm developed was a nadir pointing algorithm that can point the CubeSat +Z-axis towards the Earth. On the +Z-axis is the antenna for the S-band and UHF communication system. The payload bay, located at the -Z-axis of the CubeSat, includes the Iridium antenna and the star tracker camera payload. The developed algorithm takes inputs from the magnetometer and GPS. Then using a simplified International Geomagnetic Reference Field (IGRF) model and the GPS coordinates, the control algorithm determines the location of the Earth. The magnetorquers are then actuated to maintain a stable nadir point and balance the power of the CubeSats.

Although there have been no changes made to the design and abilities of the ADCS, new software pointing algorithms will be needed to meet the mission objectives. This objective is constrained by the directionality requirements of the Iridium and UHF antenna which both have cone angles of greater than 120°. This means that the ability of the CubeSat to nadir point does not need to be extremely precise, acting as a suitable stepping stone for the Binar Space Program to learn about attitude control algorithms.

The development of more attitude control algorithms is important for the development of controlled re-entry and recovery payloads. More advanced attitude control algorithms are necessary for the re-entry tracking system and pointing controlled re-entry technologies. As such, leaning to develop basic systems first assists the Binar Space Program in reaching its long term objectives. This design

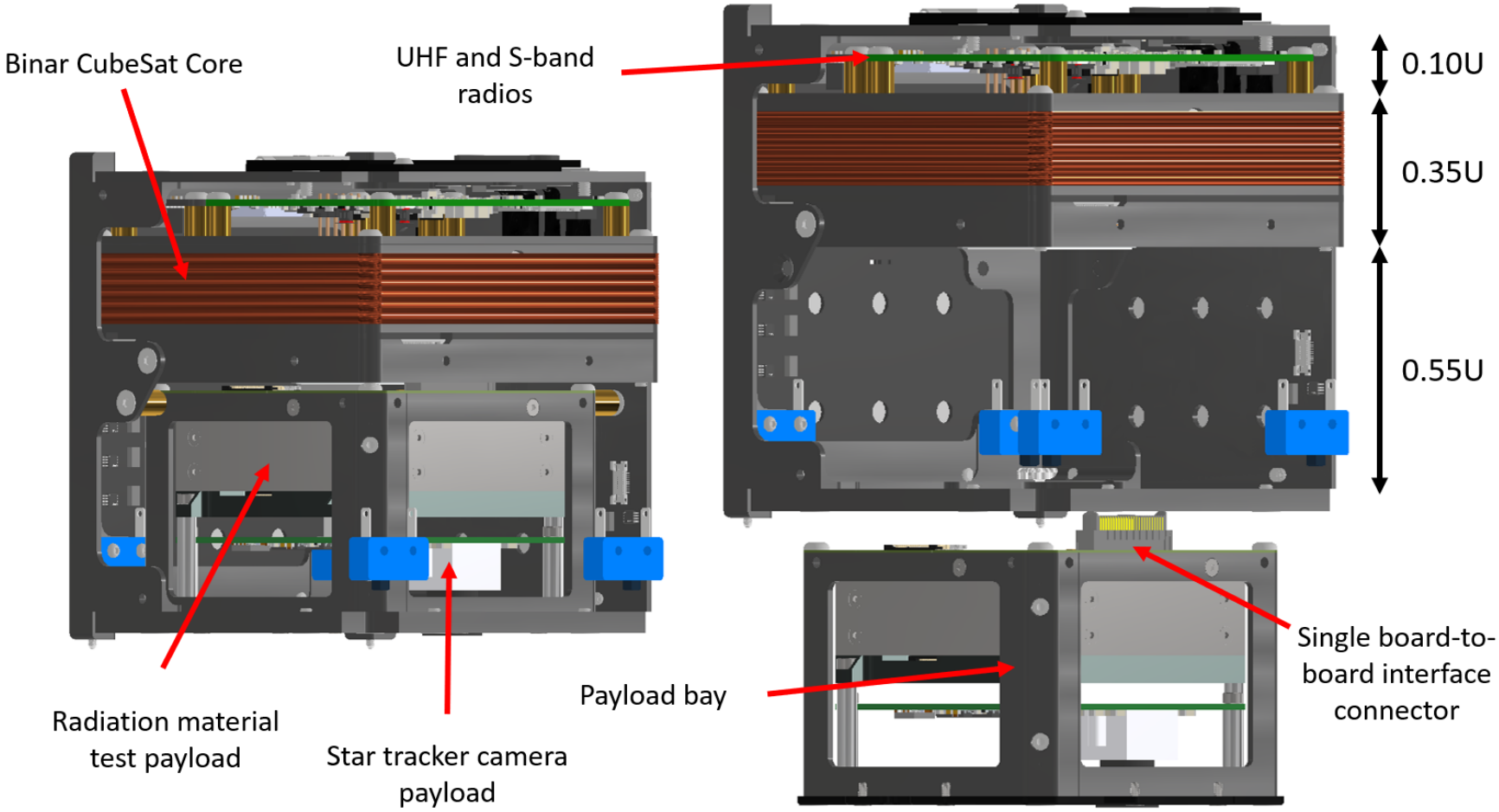

Figure 5.10: The new modular Binar CubeSat Bus (BCB) payload bay. The modular design improves the reusability of the design and enables missions to be flown more frequently.

improvement has contributed to the reusability of the platform significantly.

5.2.6 Thermal Modelling (80%)

Thermal modelling and balancing was an aspect of Binar-1 that was overlooked due to schedule constraints. From the understanding gained during the Binar-1 mission and the testing performed using the Wombat XL at the National Space Test Facility in Canberra, the team has created a CubeSat thermal model for Binar-2, 3, and 4. The purpose of this model was to see if any design modifications would improve the thermal performance of the CubeSat.

The development of the thermal model was done using the historical data collected during the testing of Binar-1. Using this historical data and a thermal property constrained CAD model of the Binar-1 CubeSat, the Ansys thermal software suite was able to simulate the thermal response of the Binar-1 CubeSat. The thermal response observes the CubeSat at its expected minimum and maximum temperatures (mentioned in Chapter 2), and at its thermal steady state between these conditions while on orbit. During nominal operations, the CubeSat will be rotating about its nadir point and as such the CubeSat is never expected to reach these temperatures. However, it may experience these temperatures if the ADCS malfunctions.

The resulting model was then applied to a Binar-2, 3, and 4 CAD design, identifying aspects of the design that were able to have thermal design improvements and to observe the thermal balance. In optimising the design, some insulating aluminium has been removed from the top cap structure. This enables the battery heaters to perform more efficiently and conserve power. Additionally it assisted in meeting the mass design requirement of 1.33kg as now heavier payloads can be used with the platform. The thermal balance of the CubeSat was observed in the steady state operations of the thermal model. This demonstrated the response of the CubeSat to the temperature fluctuations experienced during orbit was adequate and that none of the temperature critical components would reach the limits. The model was also used to improve the power budgeting of the CubeSat by predicting the enable time of the heaters. This prediction algorithm is a critical part of the onboard intelligence payload, creating a simplified thermal model for predicting the battery heater on time while in space.

5.3 Mission Life Cycle Improvements

Alongside the changes to the CubeSat design, improvements were made to the mission lifecycle. The improvements were based on the lessons learned from the Binar-1 mission and the need to improve the design understandability. The lessons learned that caused the changes to be implemented were: locking down high-level requirements early, testing as you fly, planning for operations, and planning for delays. The fundamental changes highlighted in this section are an improved review process, system verification documentation, test planning, operations planning, and de-scope planning.

The Binar-1 mission lifecycle was based on a modified NASA Systems Engineering Handbook [155] and NASA Procedural Requirements document NPR 7123.1C NASA Systems Engineering Processes and Requirements [156]. Typically used to manage large NASA missions, the procedures were modified to suit the size and structure of the Binar team. For the improvements being made to the mission lifecycle for Binar-2, 3, and 4, the same documents were used as a reference. After completing Binar-1, the team better understood how to complete the mission lifecycle. This knowledge learned through the Binar-1 experience has improved the processes for Binar-2, 3, and 4.

5.3.1 Improved Review Process (20%)

A review process structure was implemented to improve the method of locking down high-level requirements and increasing the understandability of the BCB design decisions. The Binar-1 mission, although attempting to follow parts of the NASA procedural requirements, was unable to complete every step due to a lack of team size and experience. A hybrid approach was taken, and only specific lifecycle steps were completed. As the mission was a learning process as well as a technology demonstrator, the mission lifecycle of Binar-1 was performed with a trial-and-error approach to determine what was necessary. As a result, the team decided to improve the mission review process by implementing more design reviews and progress gates. Due to the team size, the number of reviews needed to be restricted while still being effective. It was decided that a Preliminary Design Review (PDR), Critical Design Review (CDR), and Flight Readiness Review (FRR) would be performed.

The PDR was based on the NASA procedural requirements and modified based on lessons learned from Binar-1. Review processes can be long and technical, so limiting the scope of the review to be more directly involved with mission planning and payload design was beneficial. Being a PDR, the mission concept was presented in a more theoretical format rather than as a complete and finalised mission design. The review was presented to a panel of engineers and scientists with backgrounds in space mission designs from different parts of the world. This gave the newer engineers and scientists in the Binar team a chance to get feedback on the preliminary design and payload operation plan. This feedback was then implemented as part of the progress towards the CDR. The PDR provided a design gate where a detailed design was performed when feedback was provided. The Binar-2, 3, and 4 PDR process included a mission description and high-level requirement lockdown, a preliminary operations plan, a system description including the planned changes to the BCB mentioned in Section 5.2, a detailed test plan, a payload description, a regulation requirements summary, and a schedule. After completing the PDR, the progress gate allowing detailed design was passed, and work started towards the CDR.

The CDR was based on and modified similarly to the PDR to be more understandable and in line with the scale of Binar missions. Completion of the CDR for Binar-2, 3, and 4 occurred after the detailed design had been completed and the engineering model had been successfully assembled and tested. This allowed the team to complete and use the newly developed System Verification Documents (SVDs) and test documents, demonstrating how the flight requirements would be met. The review was also presented in front of a panel of engineers and scientists, similar to the PDR. The review included a detailed list of the mission requirements, a mission overview, a detailed operation, assembly, integration, and test plan, a system overview, a command and telemetry breakdown, an updated technology maturity assessment, and an updated regulation requirements report. Completing the CDR, the team implemented feedback into the assembly, integration, and testing procedures preparing the team for flight model assembly. The CDR formed the progress gate for beginning the assembly, integration, and testing of the flight model CubeSats. Thus far, the PDR and CDR for Binar-2, 3, and 4 have been completed. The FRR is planned for completion after the assembly of the flight model CubeSats.

The final review being implemented is the FRR. The team will perform the review to present the assembly, integration, and testing results and the final operations plan. The review is essential to close out requirements and remove oversight from the operations plan. The review will include the final operations plan, the completed integration and test results, a requirement completion analysis, and a shipping, launch and deployment schedule. Once the FRR is completed, the progress gate for shipping the CubeSats will be passed, moving the mission to its operational phase. In completing the three reviews, the team has put mission lifecycle progress gates in place and locked down high-level requirements. These changes aim to assist the Binar Space program in improving the understandability of the mission lifecycle process while also implementing the lessons learned from the Binar-1 mission lifecycle. Figure 5.11 presents a flow chart demonstrating the current mission lifecycle for Binar-2, 3, and 4. The lifecycle will be reused on future Binar missions.

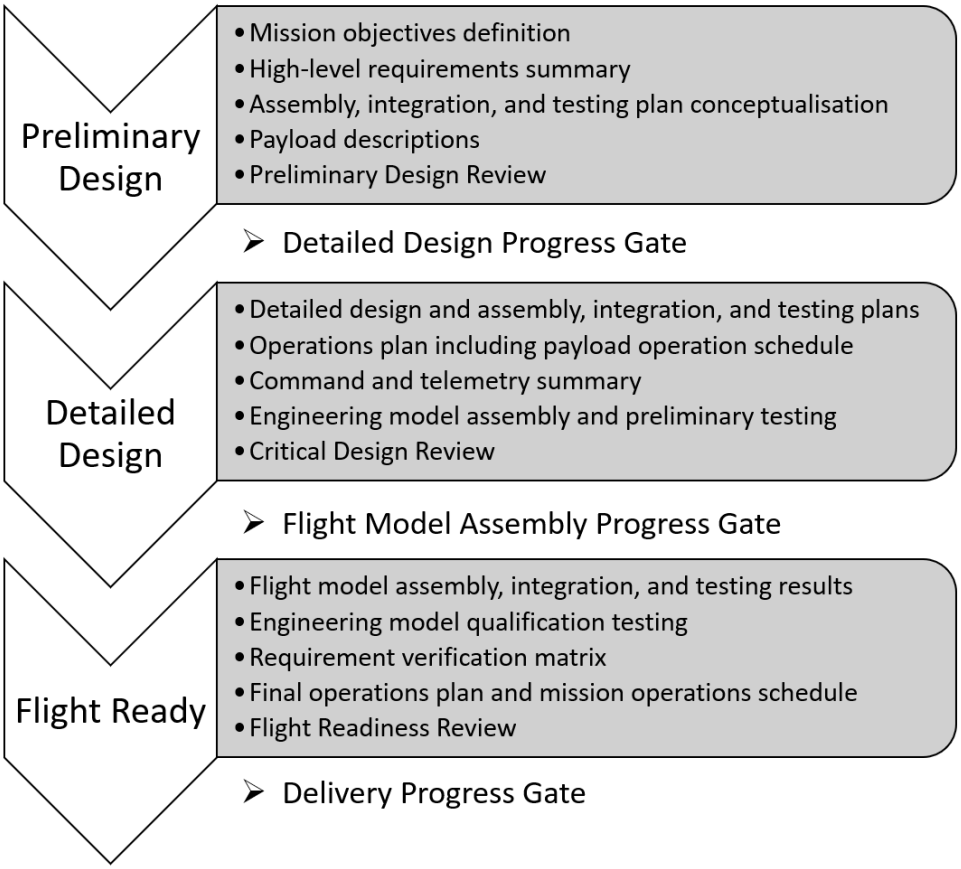

Figure 5.11: Binar Space Program mission lifecycle and progress gates. The new design process aims to improve the understandability of the mission lifecycle to better involve students.

5.3.2 System Verification Documentation (100%)

One significant addition to the assembly and integration process was the System Verification Documents (SVDs). These newly created documents serve as a verification plan for each critical component in the BCB and implements the Systems Engineering Engine from the NASA Systems Engineering Handbook [155] and NPR 7123.1C document [156]. The engine, seen in Figure 5.12, has been simplified to suit the Binar mission scale, similar to other implementations. The documents manage the relationship between the mid-level and low-level requirements, named the "system design process" in the engine. The documents also perform the product realisation process containing the subsystem integration and testing processes required for "product validation". In total, 17 SVDs were created for verification of the BCB subcomponents. Confirming the ability of the document to meet the system requirements was an essential element of the work completed between the PDR and CDR.

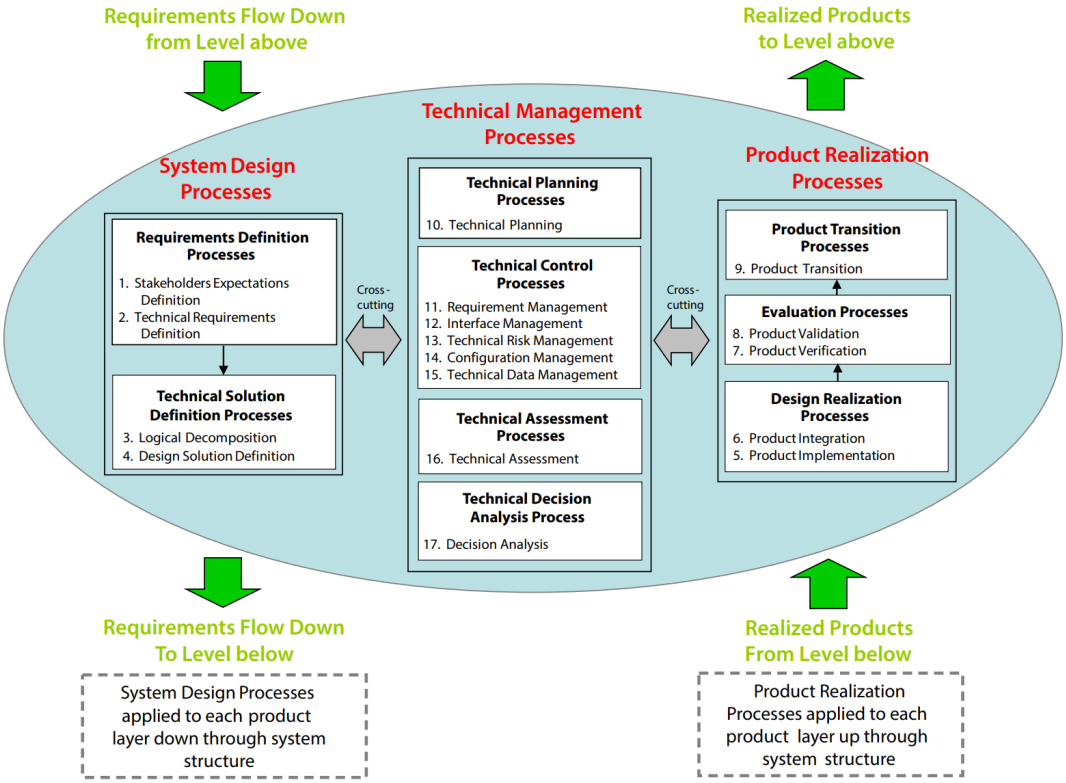

Figure 5.12: The systems engineering engine defined in the NASA Systems Engineering Handbook [155].

The technical management process is the final part of the engine that is not managed directly through the SVDs. To manage change and plan the development of the SVDs and requirements, the team used a tasking tool to keep track of and lock down requirements. The Microsoft Teams Tasks manager was used to create a bucket list of tasks for each SVD and recorded the completion progress through each document. This includes creating, changing, and completing the documents for all three CubeSats on the Binar-2, 3, and 4 mission.

The structure of the SVDs was set to be consistent to assist with understandability. Each document contained the following sections:

- Purpose,
- Requirements,
- Assembly procedure (if applicable),
- Verification Test Methodology, and
- Verification Results.

The purpose section summarises the necessary verification performed in each document. The requirements section is implemented to demonstrate how the requirements process is completed and provide further recognition of the verification process. Some of the SVDs for components requiring low-level assembly include an assembly procedure. This includes an assembly procedure with integrated verification tests for components such as solar panels. Verification test methodology and results are the processes performed for verifying each requirement. The testing includes basic functional testing and power consumption measurements for electronic components such as the BCM, UHF transceiver, and solar panels. By verifying the functionality at each component level before assembly and integration, confidence in completing the final system tests without unexpected challenges is built. For structural components, dimension checks are performed to verify the ability of the CubeSat to meet the launch requirements. By com-

pleting this check, the team will remove assumptions and unexpected challenges with the structural testing performed in the safety review.

To assist in managing the completion of the SVDs for Binar-2, 3, and 4, when each of the documents will be completed in the assembly and integration process was included in the assembly procedure document (Figure 5.13). The assembly procedure was used as the master document for managing the safety review verification testing on Binar-1. By adding detail to this master document, the team will be able to meet and manage the mission requirements, locking them down and limiting scope creep.

5.3.3 Test Plan Documentation (50%)

The Binar-1 test plan was limited to the safety review and thermal vacuum testing. Although this demonstrated the functionality of the design, better documentation could have improved it. Additionally, the software testing practice for Binar-1 was limited to development on bench models rather than with the complete system. Learning from this, the team aimed to test as you fly by testing the software on a completely assembled engineering model rather than just the integrated BCM PCB. Implementing this practice into the Binar mission lifecycle, an improved test schedule and additional test planning documentation were developed. The documents included a day-in-the-life test plan, thermal vacuum test plan, ground station test plan, and ADCS test plan.

The primary test document developed was the day-in-the-life test plan. To improve the practices of Binar-1, a complete report on the performance of the combined systems was necessary. Due to the time constraints imposed on the assembly, integration, and testing of Binar-1, the final testing program was limited. The only method of software integration testing the team implemented was to try all possible commands using the external Universal Serial Bus (USB) connection. Although this showed that all the commands worked correctly, it failed to verify the interface between the communications system and payloads on Binar-1.

To improve the process and test as you fly, a day-in-the-life test plan document has been developed to simulate the actual operations phase as closely as possible

Figure 5.13: The assembly procedure flow chart includes the completion of each system verification and safety review document. The SVDs have been formed following the Binar-1 mission to better manage the close-out of mission requirements.

when integrating the software. The objective is to step through mission operations from deployment to nominal operations. The deployment consists of the initial release process after being ejected from the International Space Station (ISS). After the deployment switches are released, a 30-minute timer will count down until the deployable panels and antenna are deployed. If successful, the CubeSats will move into the find me mode of operation, where the team can begin to simulate commissioning command and control. The commissioning test includes transmitting all possible commands and checking the expected responses from the Iridium and UHF communication systems. Next, the CubeSat is forced into safe mode to validate the ability of the satellite to recover from an unexpected condition before testing the firmware update functionality and then testing the payloads. Successful completion of the test on all three CubeSats will be presented at the FRR to validate the CubeSats ability to meet the mission objectives.

The thermal vacuum, ground station, and ADCS test plan documents were also all developed for the Binar-2, 3, and 4 mission. Although all were performed for Binar-1, a lack of proper documentation meant that none were recorded or verified appropriately. To improve the understandability of the mission life cycle and implement lessons learned, better documenting of these tests was required. Predominantly, by imposing a strict test plan, the test as you fly lesson learned can increase confidence in the performance of the CubeSats to meet the mission objectives. The thermal vacuum test plan document includes a test plan for using the WOMBAT XL similar to the engineering model of Binar-1. Now, the team plans to test all three CubeSats simultaneously and perform a combined vibration test using the larger vibration test platform in the facility. The vibration test is still included as part of the safety review process as it was in Binar-1. The ground station test plan is performed to validate the hardware and software compatibility with the complete system. The Iridium and UHF communications systems will be operated from the Curtin University ground station computer. To perform the ADCS test plan, the team has had assistance from undergraduate students to assemble an open-source Helmholtz cage for testing CubeSats. The final design will verify the nadir pointing algorithm and pointing commands on Binar-1.

5.3.4 Operations Plan (100%)

One of the main lessons learned from Binar-1 was how to operate a satellite effectively. As the team had not operated a satellite before, better preparation for the operations phase of Binar-1 could have been done. Learning from this, the team has implemented an operations plan for the Binar-2, 3, and 4 mission to manage meeting the mission objectives. Given that this time the team will be operating three CubeSats instead of one, this was essential.

The plan includes details on the commissioning process, how each CubeSat will be prioritised and commanded while in orbit, and strategies for worst-case scenarios assisting in a quick recovery. The objective of the documentation is to ensure that the mission payloads can all be used and collect sufficient data while not compromising the performance of the CubeSats. This includes a set of operation times and plans for the entire mission duration, including how long each payload will operate. This is especially important for Binar-2, 3, and 4 due to the large number of payloads on board. The operation time of each payload needs to be managed efficiently to maximise the data collected. The radiation payload is the most challenging due to the continuous operation requirement for collecting the data. As such, the plan includes priority compromises based on the power consumption of each payload. Once the SVDs were completed, this process was more accurate, as all power consumption data was collected.

5.3.5 Delay De-scoping Plan (20%)

The last implemented change to the mission lifecycle was a de-scoping document to plan for schedule delays. During the assembly, integration, and testing of Binar-1, many delays occurred due to challenges with the COTS transceiver and antenna. As a result, the team learned a valuable lesson about the need to plan for delays. The plan includes a mission criticality and risk ranking scale for identifying steps in the assembly, integration, and testing process that can be excluded in the event of a delay. By signifying the mission risk of not performing each of the verification and testing documents, the team was able to create a plan which can de-scope the appropriate work with a minimal impact on performance. The document can also convey the risk of de-scoping to stakeholders if the launch schedule is severely delayed. The de-scoping document included all processes

in the master assembly procedure document, including the system verification, safety review, and test plan documents mentioned previously. By implementing this procedure and creating the documentation for future missions, the Binar team will be ready to manage mission risks associated with schedule delays. Given the aforementioned impact of COVID-19 on the electronics supply chain, this de-scoping plan is even more critical due to the uncertainty in the electronics market.

5.4 Results and Discussion

5.4.1 Results

Comparing the design improvements to the results from Chapter 2 can show how the Binar-2, 3, and 4 BCB has improved on its initial design objectives to accommodate for platform reusability. The previous design objectives were to reduce hardware costs and increase payload space without compromising the system capabilities.

As the flight models still need to be built, the total hardware cost of the improved BCB is not yet accurate. However, using some estimates, a comparison can be made. Table 2.2 presented in Chapter 2 is a complete cost breakdown of the Binar-1 BCB hardware. In this list, three items stand out as being the most expensive. The first two were the EnduroSat transceiver and antenna. Their removal from the design has contributed to a significant cost reduction, as the new custom-designed communications system is estimated to cost <AUD$500. The other expensive item in Table 2.2 was the solar cells used for power generation. With the addition of two deployable solar panels on Binar-2, 3, and 4, the number of solar cells has doubled, meaning the cost also has. The other new design features include the rigid-flex deployable solar panels and the modular payload bay. This has slightly increased the cost of the BCB, adding approximately AUD$1000. Using these estimates, the approximate cost of the BCB has reduced from AUD$17,567 to approximately AUD$12,035, a reduction of just over AUD$5,500. A summary is provided in Table 5.2.

The available payload space has increased in size with the removal of the COTS

Table 5.2: A summary of the hardware cost reductions caused by the improvements to the BCB. The total cost reduction is approximately AUD$5,500.

Component	Cost (AUD)
Binar-1 BCB	+17,567.00
COTS Communication System	-10,473.00
Custom Communication System	+500.00
Double Solar Cells	+3,442.00
New Design Features	+1000.00
Binar-2, 3, and 4 BCB	$12,035.00

communication system and the addition of the optimised modular payload bay. Two hardware payloads heavily utilise this increase in space on the Binar-2, 3, and 4 CubeSats. Updating the previous comparison table (Table 2.3) from Chapter 2, the performance of the BCB can be evaluated when combined with the system capabilities. The updated table (Table 5.3) shows that while the BCB does still not quite have the greatest payload space, when merged with system capabilities, it far outperforms the remainder of the COTS solutions.

The capabilities of the BCB have improved by including two deployable panels, two communication systems, more attitude control algorithms, and better thermal design. The results allow higher power consumption payloads to be flown, and more opportunities for payload data collection. Compared to the other COTS solutions with similar payload space, EnduroSat (0.53U) and Near Space Launch (0.58U), neither include deployable panels or a dual communication system. Although the BCB still does not include an advanced ADCS like the AAC Clyde solution, it has increased its MPPC number to four, making it more capable than the other solutions when considering power generation. These improvements are essential to making sure the BCB is reusable and able to support as many payload opportunities as possible.

Table 5.3: An updated payload space comparison table. The BCB is now the second largest, with only Near Space Launch still being larger. However, this platform is highly limited in capabilities when compared to the BCB.

Supplier	EnduroSat	AAC Clyde	ISISpace	Near Space Launch	Binar-1
Payload Space (U)	0.53	0.3	0.4	0.588	0.55

5.4.2 Discussion

Improvements to the BCB design and Binar mission lifecycle have assisted in increasing the reusability of the platform. The modular payload bay design has been integrated and validated on the Binar-2, 3, and 4 engineering model. Using the undergraduate-designed and assembled star tracker payload as a test case for payload integration, the usability of the design has been evaluated. The BCB design understandability was improved by removing assumptions from the hardware design and by improving the verification and testing documentation. By creating the SVDs, new team members have been able to repeat testing and design practices performed for the Binar-1 mission with limited intervention. The combined documentation provides a clear step-by-step guide to assemble, integrate, and test a BCB, verifying the requirements and validating the ability of the platform to meet its mission objectives. Combining these improvements together, the repeatability of Binar missions has been greatly increased. Already the mission execution time for Binar-2, 3, and 4 is forecast to be nearly half the time as Binar-1. With this reduction in delivery time, more opportunities have been created to test and develop controlled re-entry and recovery systems.

The initial motivation for including a modular payload bay was to improve the reusability of the platform. By enabling more payload possibilities and parallel payload design opportunities, this was achieved. The BCB can be prepared for launch and integrated with available payloads once passing the required testing. This separation is vital when considering the design of different phases of controlled re-entry and recovery technologies and the many possibilities to test.

Although initially included for reusability, the modular payload bay was found to provide many other benefits when compared to existing payload integration methods. Being a new concept, a comparison to other modular CubeSat integration methods can demonstrate its significance to other CubeSat developers who are interested in a modular approach to payload design.

Many CubeSat designs use the PC104 standard headers to integrate subsystems, including the payload. As mentioned in the motivation for performing a custom design (Section 2.1), this is considered by many to be space inefficient and

outdated [83][84][157]. Comparing the BCB modular payload bay integration method to the PC104 headers, a single compact connector makes the connection and mates precisely to the base of the BCC. No screw or double header alignment is required as the alignment is handled by the dual base plate design. This interfacing method is demonstrated in Figure 5.10. This integration method also removed the stack mounting system commonly associated with the PC104 headers. This stack mounting system would require the whole CubeSat to be disassembled if challenges occurred with the payload during full system testing. By being able to easily remove the payload, it can avoid this as it can be tested and modified without disassembling the entire CubeSat. The BCB payload bay also benefits by including an external CubeSat face. The PC104 integration method requires tight tolerances to ensure the stack lines up correctly and the payload can face externally. By connecting directly to an external face, the design is simplified. All these factors make integrating and testing the payload easier as the connections are more defined and easy to access than the PC104 alternative.

Other newly proposed CubeSat designs use single backplane PCBs and edge card connectors to integrate CubeSat payloads and subsystems [158][159]. This method has been highly successful for the BIRDS satellite program, operated by the Kyushu Institute of Technology in Japan since 2015 [160][161][162][163][164]. Although the design is highly reusable and suited to rapid mission lifecycles, the 1U CubeSats have significantly smaller payload opportunities when compared to the BCB. The design also depends on the payload design completion for assembly and integration, similar to the PC104 method. This requires the payload to be highly defined before the CubeSat can be assembled, integrated, and tested. Compared to other existing solutions for payload integration, the modular payload bay is advantageous as it allows the CubeSat to be verified and then defined by the selected payload with only software implementation required.

Locking down high-level requirements was implemented through the improved review process. By including strict mission lifecycle progress gates and detailed review processes, the high-level requirements could be tracked, approved, and locked down at the PDR of the Binar-2, 3, and 4 mission. Carrying this forward to the CDR, the lower-level requirements could be specified easier than with the Binar-1 missions removing a considerable workload. This additional time

could be focused on the design improvements and new verification and test plan documentation. The team is now preparing to take these document templates and the review process forward to the next mission using the same requirement and objective development process.

The improved verification and test plan documentation provided a suitable method to implement the test as you fly lesson learned from Binar-1. All verification methods are being performed in as similar to operating conditions as possible. Examples include the day-in-the-life test and the thermal vacuum test. The day-in-the-life test will be conducted solely using the UHF and Iridium communication systems rather than through a USB connection, as done on Binar-1. This simulates the flight environment where all commands must travel through the complete system, verifying the process. To properly simulate the flight environment, the test will be performed by following the command sequences that will occur during actual operations. The thermal vacuum testing will include a solar heater simulator to simulate thermal gradients through the CubeSat better and replicate the on-orbit performance. Unlike Binar-1, which was just tested at its expected maximum and minimum temperatures, the thermal gradients will better simulate the flight environment.

The team developed and reviewed a de-scoping and operation plan to implement the lessons learned from Binar-1. The de-scoping plan document enables the Binar team to manage the risks of not performing specific testing in the mission lifecycle and convey this risk to stakeholders more effectively. If an unexpected delay occurs during the assembly of Binar-2, 3, and 4, the team can determine the most appropriate course of action. This may include delaying the launch if the risks are considered too great by the stakeholders. An operation plan has been developed to manage the workload of operating three CubeSats while still achieving the objectives of the payloads. The team and payload developers can better manage data and plan research by scheduling the relevant workforce and including payload operation plans.

Assumptions previously present in the Binar-1 design were removed. This was largely achieved by developing the SVDs and by improving the design understandability. The assumptions eliminated include correct dimensioning, power

consumption, interface methods, and communication protocols. In some cases, the assumptions were found to be accurate. However, the additional verification has reduced risk and increased design confidence. Cases, where the assumptions were inaccurate, have added value to the verification process reducing the risk of assembly and integration delays. Additionally, improving the design understandability has removed assumptions entirely. This has only been achievable due to the understanding gained throughout the Binar-1 mission.

5.5 Concluding Remarks

Binar-2, 3, and 4 will be the first implementation of the new Binar mission lifecycle and flight of the improved BCB. Learning from the Binar-1 mission, the BCB design and mission lifecycle have been improved. Additionally, the reusability of the platform has been increased by completing the custom design and improving the platform understandability. The inclusion of a modular payload bay was the most significant aspect of this improvement. The unique design allows many payloads to be designed and tested with the BCB in parallel to the mission lifecycle. Successfully demonstrating these improvements creates a pathway towards regular CubeSat missions demonstrating controlled re-entry and recovery technologies, eventually providing a platform that can be used to perform sample collection and return or Entry, Descent, and Landings (EDLs) on the surface of extra-terrestrial planets.

References

[13] A. Klesh, B. Clement, C. Colley, *et al.*, "MarCO: Early Operations of the First CubeSats to Mars," *Small Satellite Conference*, Aug. 2018. [Online]. Available: https://digitalcommons.usu.edu/smallsat/2018/all2018/474.

[14] E. Dotto, V. Della Corte, M. Amoroso, *et al.*, "LICIACube - The Light Italian Cubesat for Imaging of Asteroids In support of the NASA DART mission towards asteroid (65803) Didymos," en, *Planetary and Space Science*, vol. 199, p. 105 185, May 2021, ISSN: 0032-0633. DOI: 10.1016/j.pss.2021.105185. [Online]. Available: https://www.sciencedirect.com/science/article/pii/S0032063321000246.

[15] T. R. Lockett, J. Castillo-Rogez, L. Johnson, *et al.*, "Near-Earth Asteroid Scout Flight Mission," *IEEE Aerospace and Electronic Systems Magazine*, vol. 35, no. 3, pp. 20–29, Mar. 2020, Conference Name: IEEE Aerospace and Electronic Systems Magazine, ISSN: 1557-959X. DOI: 10.1109/MAES.2019.2958729.

[83] S. Wu, W. Chen, and C. Chao, "The STU-2 CubeSat Mission and In-Orbit Test Results," *Small Satellite Conference*, Aug. 2016. [Online]. Available: https://digitalcommons.usu.edu/smallsat/2016/TS3YearInReview/8.

[84] A. Greenberg, D. Lay, G. Lebrasseur, *et al.*, "OreSat: A Student Team-Based Approach to an Inexpensive, Open, and Modular (1-3U) CubeSat Bus," *Small Satellite Conference*, Aug. 2021. [Online]. Available: https://digitalcommons.usu.edu/smallsat/2021/all2021/236.

[88] *JEM Payload Accomodation Handbook - Vol. 8 - Small Satellite Deployment Interface Control Document - Rev. D*, Jul. 2020. [Online]. Available: https://iss.jaxa.jp/kibouser/library/item/jx-espc_8d_en.pdf (visited on 12/21/2022).

[151] S. Yan, L. Chen, A. Yob, *et al.*, "Multifunctional Metal Matrix Composites by Friction Stir Additive Manufacturing," en, *Journal of Materials Engineering and Performance*, vol. 31, no. 8, pp. 6183–6195, Aug. 2022, ISSN: 1544-1024. DOI: 10.1007/s11665-022-07114-7. [Online]. Available: https://doi.org/10.1007/s11665-022-07114-7.

[152] K. Petrovay, "Solar cycle prediction," en, *Living Reviews in Solar Physics*, vol. 17, no. 1, p. 2, Mar. 2020, ISSN: 1614-4961. DOI: 10.1007/s41116-020-0022-z. [Online]. Available: https://doi.org/10.1007/s41116-020-0022-z.

[153] B. Frieske and S. Stieler, "The "Semiconductor Crisis" as a Result of the COVID-19 Pandemic and Impacts on the Automotive Industry and Its Supply Chains," en, *World Electric Vehicle Journal*, vol. 13, no. 10, p. 189, Oct. 2022, ISSN: 2032-6653. DOI: 10.3390/wevj13100189. [Online]. Available: https://www.mdpi.com/2032-6653/13/10/189.

[154] *Planet Releases OpenLST, an Open Radio Solution.* [Online]. Available: https://www.planet.com/pulse/planet-openlst-radio-solution-for-cubesats/ (visited on 01/11/2023).

[155] *NASA Systems Engineering Handbook Revision 2*, en, Jun. 2017. [Online]. Available: http://www.nasa.gov/connect/ebooks/nasa-systems-engineering-handbook (visited on 01/24/2023).

[156] *NPR 7123.1C - main.* [Online]. Available: https://nodis3.gsfc.nasa.gov/displayDir.cfm?t=NPR&c=7123&s=1B (visited on 01/11/2023).

[157] S. Song, H. Kim, and Y.-K. Chang, "Design and Implementation of 3U CubeSat Platform Architecture," en, *International Journal of Aerospace Engineering*, vol. 2018, e2079219, Dec. 2018, ISSN: 1687-5966. DOI: 10.1155/2018/2079219. [Online]. Available: https://www.hindawi.com/journals/ijae/2018/2079219/.

[158] S. Busch, P. Bangert, S. Dombrovski, and K. Schilling, "UWE-3, in-orbit performance and lessons learned of a modular and flexible satellite bus for future pico-satellite formations," en, *Acta Astronautica*, vol. 117, pp. 73–89, Dec. 2015, ISSN: 0094-5765. DOI: 10.1016/j.actaastro.2015.08.002. [Online]. Available: https://www.sciencedirect.com/science/article/pii/S0094576515003185.

[159] M. Sejera, T. Yamauchi, N. C. Orger, Y. Otani, and M. Cho, "Scalable and Configurable Electrical Interface Board for Bus System Development of Different CubeSat Platforms," en, *Applied Sciences*, vol. 12, no. 18, p. 8964, Jan. 2022, ISSN: 2076-3417. DOI: 10.3390/app12188964. [Online]. Available: https://www.mdpi.com/2076-3417/12/18/8964.

[160] M. Samsuzzaman, M. T. Islam, S. Kibria, and M. Cho, "BIRDS-1 CubeSat Constellation Using Compact UHF Patch Antenna," *IEEE Access*, vol. 6, pp. 54 282–54 294, 2018, ISSN: 2169-3536. DOI: 10.1109/ACCESS.2018.2871209.

[161] M. H. Azami, B.-2. P. M. BIRDS Partners, G. Maeda, *et al.*, "BIRDS-2: A Constellation of Joint Global Multi-Nation 1U CubeSats," en, *Journal of Physics: Conference Series*, vol. 1152, no. 1, p. 012 008, Jan. 2019, ISSN: 1742-6596. DOI: 10.1088/1742-6596/1152/1/012008. [Online]. Available: https://dx.doi.org/10.1088/1742-6596/1152/1/012008.

[162] S. B. M. Zaki, M. H. Azami, B.-2. P. Members, *et al.*, "Design, Analysis and Testing of Monopole Antenna Deployment Mechanism for BIRDS-2 CubeSat Applications," en, *Journal of Physics: Conference Series*, vol. 1152, no. 1, p. 012 007, Jan. 2019, ISSN: 1742-6596. DOI: 10.1088/1742-6596/1152/1/012007. [Online]. Available: https://dx.doi.org/10.1088/1742-6596/1152/1/012007.

[163] S. Kim, T. Yamauchi, H. Masui, and M. Cho, "BIRDS BUS: A Standard CubeSat BUS for an Annual Educational Satellite Project," en, *Journal of Small Satellites*, vol. 10, no. 2, pp. 1015–1034, Jul. 2021. [Online]. Available: https://jossonline.com/wp-content/uploads/2021/07/Kim-first-pg.pdf.

[164] A. Cespedes, I. Bautista, G. Maeda, *et al.*, "An Overview of the BIRDS-4 Satellite Project and the First Satellite of Paraguay," *Small Satellite Conference*, Aug. 2021. [Online]. Available: https://digitalcommons.usu.edu/smallsat/2021/all2021/245.

Chapter 6

Conclusions and Future Work

The primary objective of this work was to progress towards performing controlled re-entry and recovery missions using CubeSats to increase the frequency of Solar System exploration missions such as extra-terrestrial sample collection and return and planetary Entry, Descent, and Landing (EDL).

Additional applications of controlled re-entry and recovery of CubeSats were also discovered in the existing literature. These applications included space station payload return, global disaster response, space debris prevention, thermal protection system testing for larger spacecraft, and upper atmosphere data collection. These applications can all benefit from the increased reliability and reduced cost of controlled re-entry and recovery. This makes the application of controlled re-entry and recovery for CubeSats important to other science specialities and the general population.

Progress towards controlled re-entry and recovery of CubeSats began with the development of a CubeSat capable of completing the process. This CubeSat platform, the Binar CubeSat Bus (BCB), has further reduced the cost to launch payloads and test new technologies by compressing the core subsystems into a single integrated stack called the Binar CubeSat Core (BCC). The 0.45U size core contains an Electrical Power System (EPS), Attitude Determination and

Control System (ADCS), flight computer system, and communication system. This size compression and power optimisation allows the 1U BCB to contain a 0.55U modular payload bay with the capabilities to demonstrate technologies for each phase of controlled re-entry and recovery of CubeSats.

The maiden Western Australian space mission, Binar-1, was the first test of the BCB. Lessons learned as a result of the mission improved the BCB design and mission lifecycle process. The reusability of the platform was the focus of the design improvements. The platform's hardware cost, payload space, and system capabilities were optimised by completing the custom design and removing the remaining design assumptions. The resulting design has more available payload space than the previous iteration, making it an ideal platform for developing controlled re-entry and recovery technologies.

Improvements to the Binar mission lifecycle prepared the Binar Space Program for the Binar-2, 3, and 4 mission. The lessons learned from Binar-1 were linked closely to improving documentation and verifying the mission requirements. The improvements included a streamlined review process, system verification documents, and better test, operations, and de-scope plans. The improved process will ensure the Binar-2, 3, and 4 mission is successful and prepare the Binar Space Program for performing more missions in the future.

The development of a CubeSat re-entry tracking system continued the progress towards controlled re-entry and recovery of CubeSats. Existing CubeSat tracking methods were unsuitable for the global coverage necessary for observing CubeSat re-entry. Open-source ground station networks and communication satellite constellations provided a solution. A review of these services found that the open-source SatNOGS network and the Globalstar and Iridium constellations had sufficient CubeSat flight heritage and were affordable, size, and power compatible with the BCB. Simulations determined that the services could communicate at the final re-entry location at 110km to an accuracy of 78.3% of the time. If the Iridium constellation and the re-entering CubeSat match RAAN, this increased to 88.6%. Testing of the system will occur on the upcoming Binar mission, Binar-2, 3, and 4. Its successful demonstration will improve the ability of the BCB to test controlled re-entry technologies.

The significant outcome of the work completed during this doctoral thesis was the BCB. Its first implementation, the successful Binar-1 mission, provided many lessons learned that improved the platform and mission lifecycle process. These improvements included a re-entry tracking system to demonstrate controlled re-entry technologies on future missions. The groundwork has allowed the progress towards controlled re-entry and recovery of CubeSats to continue into technology development. Once completed, a controlled re-entry and recovery system will enable a more systematic exploration of the Solar System. With more opportunities to return samples from extra-terrestrial sources and land on the surface of planets and moons, the formation and evolution of the Solar System can be better understood.

6.1 Contributions

The work described throughout this thesis has documented contributions to the fields of planetary science and small satellite engineering by developing a low-cost and integrated CubeSat platform capable of demonstrating and testing controlled re-entry and recovery technologies for CubeSats. These contributions are separated into three primary components being the BCB platform development, the Binar-1 demonstration mission, and the re-entry tracking system capability.

The design of the BCB and the internal BCC has created a platform capable of testing and developing controlled re-entry and recovery systems. The unique, single Printed Circuit Board (PCB) design has enabled a reusable and modular payload bay to be included in the platform without increasing cost or reducing system capabilities. This novel approach to small satellite design significantly contributes to the fields of small satellite engineering and planetary science as it has increased the number of possible applications of the platform. Improved through the delivery of Binar-1 for the Binar-2, 3, and 4 mission, the BCB can now include a variety of payloads for a reduced cost compared to previous existing designs. This provides more opportunities to test instruments for planetary science and study the solar system. My principal contributions to the development of the platform include being one of two full-time developers for the Binar-1 CubeSat as well as advising and assisting in making the improvements to the platform for Binar-2, 3, and 4. This contribution is recognised as percentage indicators in the headings of Chapter 2 and 5. How the Binar CubeSat designs compare to other

Table 6.1: A summary of the final Binar CubeSat and how it compares to its previous iteration and other COTS CubeSats.

Supplier	EnduroSat	AAC Clyde	Binar-1	Binar-234
Price	USD$37,200	Unknown	AUD$17,500	AUD$12,000
Payload Volume	0.53	0.3	0.5	0.55
Total Mass (kg)	1.33	1.33	1.33	1.33
Communication Systems	UHF	UHF	UHF	Iridium, UHF & S-Band
Attitude Control	Magnetorquers	Magnetorquers & Reaction Wheels	Magnetorquers	Magnetorquers
Attitude Determination	Gyroscope & Sun Sensor	Gyroscope, Magnetometer & Star Tracker	Gyroscope & Magnetometer	Gyroscope & Magnetometer
GPS	Yes	Yes	Yes	Yes
Solar Cells	8 or 10	8	8	16
Number of MPPC	3	2	2	4
Power Storage (Whr)	20.4	20	48.1	48.1
Power Distribution (V)	3.3, 3.7 & 5	3.3, 5 & 7.4	3.3, 5 & 7.4	3.3, 5 & 7.4
Flight Computer	Yes	Yes	Yes	Yes

COTS CubeSat designs mentioned in Chapter 2 and Chapter 5.2 are summarised in Table 6.1.

The delivery and operations of the Binar-1 CubeSat significantly contributed to small satellite engineering. The mission results and lessons learned were shared at the 2022 SmallSat conference and provided five critical lessons learned (Appendix A.1). These lessons improved the BCB design for the subsequent launch of Binar-2, 3, and 4 and also provided insight to new CubeSat developers hoping to learn from the Binar-1 mission. Additionally, the Binar-1 mission contributed to planetary science by creating awareness about its importance in the West Australian community. Through the development of the CubeSat, the Binar Space Program has received tremendous support for its planetary science objectives.

Research into the usage of open-source ground station networks and communication satellite constellations as methods for tracking the re-entry of CubeSats has contributed to small satellite engineering. The simulations performed as part of this work were the first to use open-source software packages to simulate global communication solutions. This novel simulation approach can assist other devel-

opers in selecting global communication systems for CubeSats at a reduced cost. Using the newly developed tool the design of the re-entry tracking system for the BCB was able to be completed. The results showed that the tracking system provides the necessary capability to demonstrate controlled re-entry and recovery technologies and successfully track CubeSat re-entry. After being implemented with the BCB, the platform is now able to test controlled re-entry and recovery technologies for CubeSats.

6.2 Future Work

To continue the progress towards controlled re-entry and recovery of CubeSats, first, the Binar-2, 3, and 4 mission must be delivered for launch. This critical engineering work, including the assembly, integration, and testing of the flight model CubeSats, is vital for demonstrating the re-entry tracking system and validating the improvements to the BCB design and Binar mission lifecycle.

The re-entry tracking system could not include Globalstar alongside Iridium due to communication licensing concerns. As a result, the tracking system will only operate using the SatNOGS and Iridium services. Making up for the loss of Globalstar, the re-entry location accuracy can be improved by comparing the final transmission path to the location of Iridium satellites and active SatNOGs ground stations. Following the re-entry of Binar-2, 3, and 4, an evaluation of the ability of the system to track re-entry will be completed. The results will be published along with the accuracy of the simulations when compared to the real-world scenario.

Expanding the SatNOGS ground station network outside major Australian cities can improve the re-entry tracking system. Through a collaboration with the Desert Fireball Network (DFN), a proposal to include SatNOGS ground stations at DFN camera sites has been put forward. This will improve SatNOGS coverage across the Australian outback and increase the opportunities for collecting final transmission data over Australia. As controlled re-entry and recovery missions operated by the Binar Space Program will all aim to land in Australia, this future work will provide greater re-entry location accuracy when targeting landings over the Australian outback. Additionally, a resulting technology from the DFN,

FireOPAL, provides another possibility for tracking CubeSat sized objects over Australia. The advanced system was developed as a space situational awareness tool that could track satellites as small as 1U. Using this technology as a method for tracking CubeSat re-entry demonstrations, additional data can be provided for technology validation.

Completing the Binar-2, 3, and 4 mission will determine the suitability of the BCB design and mission lifecycle improvements. However, following mission completion, a review of the platform updates and mission lifecycle will need to be completed. The review will likely identify necessary platform upgrades and mission lifecycle changes that can further optimise the Binar Space Program's ability to deliver space missions successfully. Completing this review will be necessary to ensure the success of controlled re-entry and recovery missions on future platform applications.

Beyond the future work required for the Binar-2, 3, and 4 mission, developing new technologies for controlled re-entry and recovery can continue the progress towards a complete mission. New projects can begin to investigate and test methods for all three phases of the controlled re-entry process. The first phase is the most critical of these projects and is the primary benefactor of the BCB development. It is the most critical because if the CubeSat enters the atmosphere at the incorrect location, the remaining phases may never be recovered or tested on an actual mission due to the associated landing risks. Successfully controlling CubeSat re-entry and validating it using the re-entry tracking system described in this thesis, the development of the remaining phases can be tested in flight conditions. Methods of controlled re-entry to investigate include new small CubeSat propulsion methods and varying drag de-orbit systems. These solutions were shown in the literature review to be the most favourable in existing designs. However, with the fast rate technology can improve, better implementations are possible. Forming the most significant part of the future work for this thesis, the BCB is an ideal test platform to begin testing these technologies. Its highly reusable design means that many launches with multiple CubeSats can test different systems and collect data on their performance. This data includes de-orbit speed, controlled re-entry accuracy, and platform stability. With a platform developed and a method to track the performance of new controlled re-entry technologies,

controlled re-entry and recovery from a Binar CubeSat will soon be achieved.

Appendices

Appendix A

First Author Abstracts and Publications

A.1 Binar Space Program: Binar-1 Results and Lessons Learned

Fergus W. Downey[1], Stuart Buchan[1], Benjamin Hartig[1], Daniel Busan[1], Jacob Cook[1], Robert Howie [1], Philip A. Bland[1] and Jonathan Paxman[2]

[1]Space Science and Technology Centre, Department of Earth and Planetary Science, Curtin University, Perth, Australia

[2]Department of Mechanical Engineering, Curtin University, Perth, Australia

This conference proceeding was presented at the 36th Annual Small Satellite Conference at Utah State University in Logan, Utah, USA.

SSC22-WKII-06

Binar Space Program: Binar-1 Results and Lessons Learned

Fergus Downey, Stuart Buchan, Benjamin Hartig, Daniel Busan, Jacob Cook, Robert Howie, Phil Bland, Jonathan Paxman
Curtin University
Space Science and Technology Centre, School of Earth and Planetary Sciences, Curtin University, GPO Box U1987, 6845 WA, Perth, Australia; (+61) 0488 442 133
Fergus.downey@curtin.edu.au

ABSTRACT

The Binar Space Program is a recently formed space research and education group part of the Space Science and Technology Center at Curtin University in Western Australia. Recently launching the first CubeSat from the state, Binar-1, the team is making steps towards creating a sustainable mission schedule for research and education. The Binar-1 mission primary objective was to demonstrate the custom designed systems made by PhD students and engineers at the university. The main technology being demonstrated was the integrated Binar CubeSat Core, which compacted the Electrical Power System, Attitude Determination and Control System, and flight computer system into 0.25U. Alongside this, the team also aimed to learn about end-to-end spacecraft mission design and engage with the public to build an understanding of the importance of space industry and research in the country. Binar-1 was deployed from the International Space Station on the 6th of October 2021, and initially was silent for 15 days until the Binar team was able to make contact by enabling a secondary beacon. This paper will present the Binar-1 mission including the custom design, operations, failure analysis, and results before finally summarizing the lessons learned by the team while flying Western Australia's first space capability.

INTRODUCTION

With the foundation of the Australian Space Agency (ASA), a new wave of space industry and research has begun in the country. One of the research groups is the Space Science and Technology Center (SSTC) located at Curtin University in Western Australia. With a history in global fireball entry tracking and space situational awareness technologies[1], the research center formed a new branch in the Binar Space Program. This program aims to help develop the skills necessary for working in the space industry by performing valuable space research at the university with frequent CubeSat missions. The first mission performed by the Program, Binar-1, was a technology demonstrator mission that tested the custom designed systems put together by a team of PhD students and engineers.

The design of Binar-1 took inspiration from the first CubeSats developed and launched by universities, focusing on using custom design systems rather than purchasing Commercial Off the Shelf (COTS) solutions. This design decision was made for many reasons; however, the main purpose was to reduce the cost of future missions and build capabilities which can be upscaled to more complex space missions. This technology skill growth has been vital for the team as it now works towards its future missions in Binar-2, Binar-3, and Binar-4.

Having first been conceptualized in the middle of 2018, this paper will present the complete lifecycle of Binar-1. First, the Binar-1 mission goals and design will be detailed. Next, it will discuss the operations, recovery process, and results of the mission. Finally, it will provide a summary of the lessons learned and how these lessons will be implemented into future Binar missions.

BINAR-1 MISSION

Binar-1 was launched from cape Canaveral on the 29th of August 2021 onboard a SpaceX Falcon 9 rocket as a ride share on the International Space Station (ISS) commercial resupply mission CRS-23. The CubeSat was then deployed along with 2 others (Maya-3 and Maya-4) on the 5th of October from the Kibo module and JEM Small Satellite Orbital Deployer (J-SSOD). The launch was coordinated with the Japanese Aerospace Exploration Agency (JAXA) through SpaceBD, a commercial space company in Japan. Figure 1 is a photo taken from on-board the ISS of the CubeSat deployment. Binar-1 can be seen in the top right of the image with the Earth and ISS solar panels seen in the background.

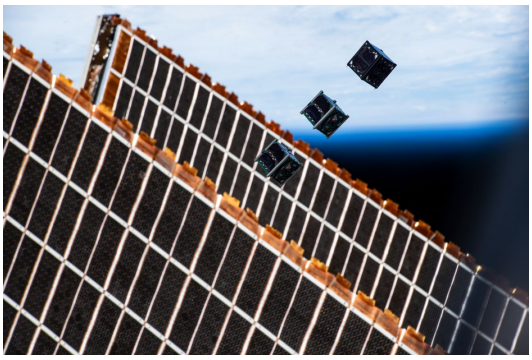

Figure 1: Binar-1, Maya-3, and Maya-4 just after deployment from the J-SSOD with the ISS solar arrays and Earth pictured in the background.

The main objectives of the Binar-1 mission were to:

- Demonstrate the custom designed systems created by the Binar Space Program,
- Educate staff and students about end-to-end spacecraft mission design, and
- Spread awareness about the importance of a space sector in Western Australia.

Alongside these objectives, the CubeSat was also flown with two secondary payloads: an undergraduate student led star tracker, and a high-resolution Earth imagery camera.

Of the custom designed systems being tested, the primary novel system is the integrated Binar CubeSat Core (BCC). Contained inside the 0.25U package is an Electrical Power System (EPS), Attitude Determination and Control System (ADCS), and flight computer system. Also, custom designed by the team was the Binar structure, the Binar Software Framework, and integration method for the communications system and payload cameras.

BINAR-1 DESIGN

The design, testing and integration of Binar-1 took place over the course of 3 years at Curtin University. The initial concept for the design was to make up the satellite from CubeSat COTS systems to meet the mission objectives. This process educated the team on what was typical for CubeSat missions and how to start its own design process. The decision to move to a custom design was made from observations of the COTS solutions architectures and the benefits that could be achieved from a custom designed system. While the systems were modular and made to work together across suppliers, the team noticed that the systems available were not able to achieve the team goals. The system solutions are larger than needed and limited to the design, making it hard for modification to be made without major intervention. Also, the cost of purchasing the systems is greater than if the hardware is custom designed. Moreover, this benefit of custom designing the systems will help the Binar team to reduce future cost and build skills for designing more complex systems in future missions. As such, the team decided to go forward with a custom design due to the many benefits it had alongside the ability to modify and compact the design.

As a result, the custom design of Binar-1 included the BCC, Binar structure, Binar Software Framework, and the payloads. Alongside these systems was a COTS communication system. The system block diagrams for Binar-1 are presented in Figure 2, separated into its power and signal connections.

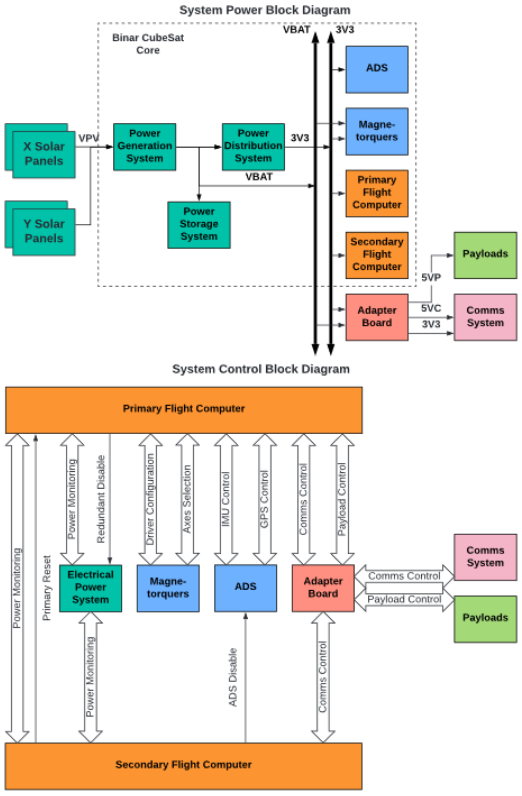

Figure 2: Simplified Binar-1 system block diagrams.

Binar CubeSat Core

The integrated BCC is the primary technology demonstrator objective of Binar-1. Containing the

integrated EPS, ADCS, and flight computer system, the goal of the design was to compact these systems to make more space for payloads. Learning from the initial Binar-1 design which used COTS systems, the primary requirements for the BCC were based around compactness, safety, reusability, reliability, and testability. The complete design was achieved using computer aided design software, allowing for optimal placement of electronic parts and mechanical structures.

The EPS found on the BCC contains the typical subsystems of an EPS including a power generation subsystem, power storage subsystem, and power distribution subsystem. The power generation subsystem consisted of two Maximum Peak Power Controllers (MPPC) which are supplied from solar panels on the X and Y faces of the CubeSat. The solar panels were assembled by the Binar Space Program, making modifications to existing assembly methods to optimize and simplify the process for 1U panels[2]. Connected to the power generation subsystem, the power storage subsystem consisted of four lithium-ion 18650 battery cells in a 2S2P configuration. To meet the mission and launch safety requirements, the power storage subsystem also included battery heating and an ISS launch qualified battery protection system. Finally, the distribution subsystem consisted of a dual redundant 3.3V converter to power the remaining systems on the BCC. The distribution subsystems for the payloads and communications system were found on the adapter board which connected the BCC to the PC104 connectors used by the COTS communication system.

The ADCS contained on the BCC consisted of an Inertial Measurement Unit (IMU), Magnetometer, Global Positioning System (GPS), and a 3-axes magnetorquer. Combining the complete system into the BCC, the EPS and flight computer system were able to integrate with the ADCS from the beginning of development. This process helped to remove integration issues and increase confidence in the design. The IMU and magnetometer were used for feedback in the attitude control system and operation of the magnetorquers. Integrated with the batteries inside the 0.25U BCC, the magnetorquers consisted of two X and Y axes iron core magnetorquers and one large Z axis vacuum core magnetorquer. These coils are all operated by driver circuits located on the BCC.

The flight computer system consists of two flight computers, one primary and one secondary, as well as an external memory device. The system uses the primary flight computer for all flight operations and control, relying on the secondary flight computer only if the primary flight computer fails. The external memory device provides 4GB of on-board payload and system log storage for the primary flight computer which can be requested from the ground via telecommand. Housed around the BCC is part of the Binar structure including the RBF bracket, magnetorquer mount and top cap. These all fit inside the rest of the Binar structure detailed in the following section. A BCC that was used for lab testing is presented in Figure 3. Due to the reduced hardware cost of the BCC, the team was able to assemble multiple versions of the core for integration testing and verification.

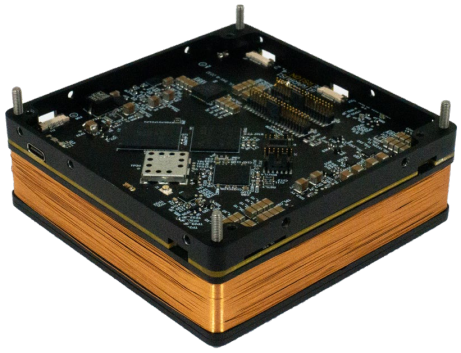

Figure 3: A flight model equivalent of the Binar CubeSat Core (BCC) that was used for lab testing.

By combining three of the main systems of a CubeSat into a single core, the Binar team was able to meet its design requirements. The compact design compared to the original COTS Binar design has allowed the team to increase its payload space, which in turn will benefit the team in future missions when reused. Safety has been implemented, protecting the batteries from accidental shorts or over charge and over discharge conditions. Reliability was implemented with extensive integration testing during design iterations, and simple additions of redundancy were possible. The testability of the design is also made easier through the combination of the Binar Software Framework which was designed to work with the BCC. This direct access to BCC is what will enable the Binar Space Program to fly more complex payloads on future missions.

Binar Structure

The Binar structure was designed by the Binar team to meet the launch requirements of the JEM Payload Accommodation Handbook Vol 8. Rev D[3]. The structural design consisted of two rail halves which were connected to the BCC in the center. The antenna and payload were then used to constrain the satellite at

the top and bottom. This design was able to meet the launch requirements due to the tight tolerancing of the BCC holding the satellite together. Other parts of the structure included those found in the BCC and the payload mounting plate. The mounting plate was designed to also act as a counter mass for the BCC to move the center of gravity as close to the geometric center of the satellite as possible, assisting with the attitude control system. The exploded view (Figure 4) presents the structural design of Binar-1. The exploded BCC seen in the center connects to the adapter board and transceiver forming the stack. This was then fastened to the two main rail halves which form the structure. The antenna, payload and solar panels were then fastened to the six sides of the CubeSat.

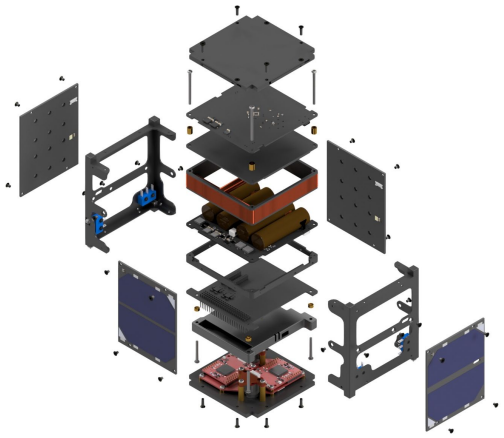

Figure 4: Exploded view of Binar-1

Binar Software Framework

Matching the hardware design goals of creating a safe, reusable, reliable, and testable platform, the Binar Software Framework was written to enable rapid mission concept-to-orbit. Specifically structured around areas that commonly contribute to software related mission failures, namely insufficient software testing, lack of documentation, unsafe code reuse and cursory code review, the Binar Software Framework has provided the Program with a reliable code base that can be reused on future Binar missions.

Comprising of flight application code, a hardware abstraction layer, utilities, resource manager, and board support layer, the codebase adheres to an abstracted software design that enables hardware to be changed with only minor modifications to the software. Moreover, the loose module coupling within the abstracted design allows hardware dependencies to be broken during unit testing to increase the testability of the code base.

Communications System

The communications system on Binar-1 was the only system that was supplied by a COTS provider. The decision to use COTS for this part of the satellite was based on the team size and amount of experience. At the time of decision, the small team was only made up of PhD students and part-time engineers. With significant focus on developing the BCC, Binar structure, and Binar Software Framework, the team was unable to commit the time to learn about communications design. As such it was decided that the best course of action for the success of Binar-1 was to purchase a COTS communications system.

The data requirements for transmitting the flight logs and payload images were achievable with a UHF communications system. The team decided to use the COTS system recommended in the initial COTS design of Binar-1 to meet this requirement. The deployed antenna can be observed in Figure 5. As the BCC was not based on the PC104 standard to optimize its space efficiency the team used an adapter board to connect the two together. This board was also used to adapt the BCC to the payloads.

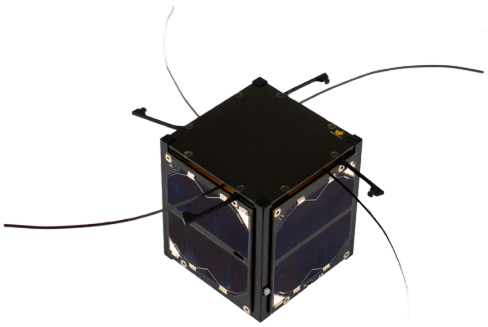

Figure 5: The Binar-1 engineering model with the antennas deployed.

Payloads

Two payloads were flown on Binar-1 including a high-resolution camera for Earth imagery of Western Australia and a student led star tracker camera for developing more precise attitude determination capabilities at the Binar Space Program. Both payloads were originally planned as primary mission objectives, however, after the change to a custom design, the purpose of the payloads shifted to demonstrating the

functionality of the BCC and its ability to operate payloads. The payloads were integrated together with a custom PCB that connected to the same adapter board used by the communications system. The two cameras were both COTS cameras, the first being selected by the Binar team to give the best resolution for Earth imagery in the available payload space (80m/pixel), and the other being a low-resolution camera that was selected from a range of cameras tested by the team of undergraduate students. The final payload system was mounted to the bottom of the satellite.

Ground Segment

As part of the mission plan for Binar-1, the team also needed to develop its own ground station (Figure 6) and operation software for the Binar-1 mission. Made from a combination of custom and COTS components the Binar ground station was built and placed on top of the engineering building on the Curtin University Bentley campus. The operating software was designed as part of a collaboration with Fugro Space Automation, AI, and Robotics Control Complex (SpAARC). The complete design was tested on existing satellites in LEO in preparation for the deployment of Binar-1.

Figure 6: The Binar ground station located at the Curtin University Bentley campus in Western Australia.

INTEGRATION AND TESTING

Integration and testing of the Binar-1 flight model was conducted using the facilities available at Curtin University. Testing was separated into two parts, being the integration and testing performed on the custom designed systems and the testing performed to meet the launch requirements. The regulatory requirements necessary for launch are documented in the JEM Payload Accommodation Handbook Vol 8. Rev D. which included battery safety testing, vibration testing, and interface verification testing.

Binar Testing Procedures

To verify the functionality of the custom Binar-1 platform the team developed testing processes throughout the course of the design. One of the main testing processes that was developed was the integration testing process of the BCC. A benefit of the integrated design was the straightforward process of verifying the connections and operation software for each system on the integrated core. This helped to build confidence in the hardware and software design as faults were identified and removed early in the custom design process.

Typical to CubeSat testing programs, the team performed thermal vacuum testing using a modified vacuum chamber at Curtin University (Figure 7). The modification included a liquid nitrogen shroud and electric heater which can reach surface temperatures of -100°C to +150°C. Testing in this chamber was also verified with a test using the Wombat XL located at the National Space Test Facility (NSTF), Australian National University (ANU), in Canberra. The verification test was done before the assembly of the flight model using the Binar-1 engineering model. Results from this testing was important to verify the modified vacuum chamber due to the COVID-19 pandemic restricting the ability of West Australians to travel without quarantine. This meant the team could not return to Canberra to perform the vacuum testing again with the flight model.

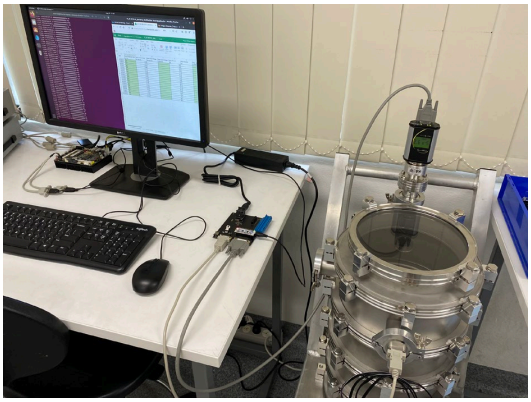

Figure 7: Vacuum testing performed at Curtin University.

Although the team would have liked to have performed more testing on the BCC and Binar-1, challenges with the communication system and a misunderstanding of changes in the regulatory requirements led to delays in the design and integration process, reducing the available testing time of Binar-1. Changes in the launch regulations meant that the antenna needed to be

modified and re-tested to include two burn wires. This change was necessary due to the requirement for inadvertent antenna deployment inside the J-SSOD having its maximum allowable force reduced to below the force exerted by the COTS antenna. The schedule was also affected by a difference in the engineering model COTS UHF transceiver and the flight model COTS UHF transceiver. To reduce cost the team purchased a 1W variant of the transceiver for the engineering model and a 2W variant for the flight model. Due to a misunderstanding of documentation, it was unknown to the team until the beginning of testing the flight model transceiver that I2C was not usable on the 2W variant. This added to the delays as a new adapter board had to be made to change the connection to the transceiver.

As a result, only the very basic system level verification was performed on Binar-1 between the BCC and the transceiver alongside the necessary regulatory testing requirements. This means that only the beacon, detumble, and basic telecommands of Binar-1 was tested before launch, and no full Day-In-The-Life (DIL) testing could be completed as planned. One observation that was noted in the basic system testing was another challenge involving the UHF transceiver. A difference in receiving power usage from the datasheet was noticed which effected the power budget. The team decided that it was still in the best interest of the program to continue with the launch and perform a system update early in the mission to reduce the power usage of some of the other systems.

Regulatory Testing Requirements

The main regulatory testing requirements necessary for Binar-1 to meet were included in the safety review process. This included testing all the systems of Binar-1 that could cause damage to the launch vehicle, ISS, or astronauts on-board. The most significant of these tests was the battery verification testing, safety inhibit testing, and the vibration testing.

The battery verification and safety inhibit testing was the critical path of the Binar-1 assembly and testing process. Requiring a batch qualification of the lithium-ion cells on Binar-1, the process was time consuming due to the lack of resources able to perform the tests. After qualification, with flight model cells approved, the battery safety inhibits required testing as well. This included a short-circuit test, over-charge test, over-discharge test, switch inhibit test, and insulation test. These tests were performed at various stages of the assembly and integration procedure. After the complete assembly, a final battery cycle test was required before and after the vibration testing to finally verify the structural integrity of the battery cells and qualify for launch.

Vibration testing was performed at Curtin University using the available facilities. Similar to other CubeSat launches to the ISS, Binar-1 was qualified to all possible ISS resupply mission launch vehicles. The final testing before delivery was important to ensure that the satellite had been assembled correctly and that the antenna modification would not inadvertently deploy inside the J-SSOD.

MISSION OPERATIONS AND RESULTS

Deployed from the ISS at approximately 5:20pm (AWST) on the 6th of October, Binar-1 was required to wait 30 minutes before deploying its antennas and starting to beacon. The first possible attempt at receiving from the ground station in Western Australia was expected at approximately 11:00pm (AWST) however, the team also planned to use the SatNOGS[4] service to look for signals earlier. The beacon string contained the satellite name, GPS data, critical power and temperature information, and a unique message from the Binar team. Unfortunately, no communications were received on the first pass, or on any of the SatNOGS passes. This prompted the team to start attempting to communicate with the satellite and search the sky for its location. However, these attempts soon ended as the other two CubeSats launched along with Binar-1, Maya-3 and Maya-4, successfully established contact within the first day of operations, successfully confirming the expected location of Binar-1. As such, this prompted the team to start a failure mode analysis to determine if a recovery could be made.

Failure Mode Analysis

A benefit of the Binar-1 custom design was the knowledge of the system available to the team. By stepping through how the satellite would behave after deployment, the team was able to closely analyze the possible operation paths and determine if any possible software bugs or hardware failures could have caused the communication silence.

The first step of the failure analysis and the starting point for operation was the EPS. Being one of the most common reasons to failure[5], and necessary for powering the rest of the Binar systems, the EPS had been heavily tested throughout the design process. One possible failure point was found involving an interaction between the power distribution subsystem and the flight computer system. When the flight computer booted, one of the first actions it performs was to disable the secondary distribution subsystem. Before performing the task, the flight computer sets a system flag into

memory and then resets it after the task is complete. If the system power cycles after disabling the redundant distribution subsystem, then at re-boot the system flag should still be set, and the flight computer will know that the redundant distribution subsystem is being used. However, a flaw was found in that the flag was being set in volatile memory causing it to reset if power was lost to the flight computer. This would have resulted in a flight computer power cycling event where it would continuously disable the redundant distribution subsystem. This flaw was found to not be the reason for failure due to the next attempts made by the team, however it was still an error that needed to be corrected in future implementations of the BCC.

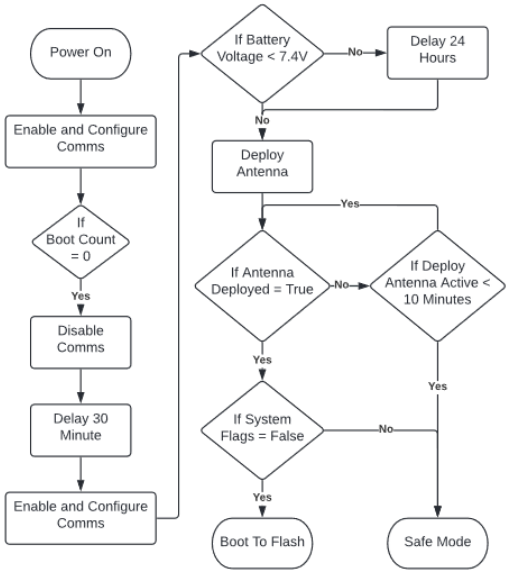

Figure 8: Binar bootloader software flow chart.

To continue the failure analysis process, the team assumed the flight computer system still had power. From here the team analyzed the flight software to determine if any logic errors or bugs had gone unnoticed since delivery. First the 30-minute wait must occur after deployment where the communications system is powered off. After the 30-minutes, the communications system is powered on, and the antennas deployment circuit will activate if the satellite has over 50% battery. The deployment burn wires will be switched on until the successful deployment condition is met, or until the 10-minute timeout is reached. If the battery is less than 50% then the satellite will wait for 24 hours before attempting the deployment. After this, the bootloader makes two system checks before deciding to boot into application code or safe mode. The first check is the system critical checks. This check will scan the system flags for any reported faults. These flags are only set in the system critical check application in application mode or in safe mode. This means that during the first boot, this check will always pass. The other check that is performed is a check on the antenna deployment condition. If the antennas did not deploy correctly then the CubeSat would be put into safe mode, where a beacon would be broadcast at reduced frequency to conserve power. The flow chart for this process is summarized in Figure 8.

During testing, safe mode was tested by disabling the 30-minute wait time, disabling the 10-minute time out of the antenna deployment system, and holding down the deployment sensor switch. This was done to conserve time in the Binar testing program due to the schedule losses mentioned previously. As a result, when testing the satellite would boot directly into safe mode so that the functionality could be tested. In testing, these beacons were received correctly however, this was only observed when the delay timers were not enabled. In this state the software would enable and configure the communications system before jumping straight into safe mode. However, if the communications system doesn't receive any signals for 255 seconds, the configuration is reset to its default mode. This is where a software logic error was found as when the timers are enabled, and if the antennas didn't deploy within 255 seconds, then the communications system would not be configured properly. To test that the error existed, the team performed a test with the engineering model and verified that this was a possibility for failure on Binar-1.

Another theorized possibility is that the antenna did deploy correctly and boot into the flash application software operation mode. In the application mode, the communications system would have been configured again however, the theory was put forward that the poorly tested adapter board, that had a last-minute modification, had failed. Due to the nature of the last-minute modification, the board was not thermal vacuum tested or vibration tested correctly which could have caused a solder joint to break meaning that the flight computer was potentially not able to communicate with the communications system or power it.

Fortunately for the Binar team, if the COTS communications system was powered and in its default mode, it could be configured from the ground. As a result, the team concluded that the best action would be to attempt to send the configuration commands to the satellite and see if the beacon could be received. After first confirming with the engineering model that this was possible, the team attempted to communicate with

the communications system hoping that the adapter board was operating correctly.

Partial Recovery

To attempt the recovery, first the team attempted to configure the communications system in the required mode for the safe mode beacon to be received. These attempts were made over multiple passes to no success. It is still unclear as to the team on whether commands were received by the satellite or not as it depended on how many of the antennas were deployed, the attitude of the satellite during the passes, and if the adapter board was operating properly.

With these attempts not being successful, the team decided to attempt to put the COTS communication system into its own beacon mode. This beacon mode was built into the system and could be configured in a similar way to the desired configuration. The attempts to enable this mode were successful on the first attempt, partially recovering the location and status of Binar-1. The first beacon was received at approximately 5:21pm (AWST) on the 21st of October (Figure 9), almost exactly 15 days after the deployment from the ISS. The beacons enabled were operating with a shorter period and lower bit rate to try and help the team to locate the satellite on more ground station waterfall plots using the SatNOGS network.

One of the risks of enabling the shorter period beacon was that the power balance of Binar-1 would not be stable from the increased frequency of the beacon. As a result, the team needed to turn off the beacon as soon as possible. Unfortunately, the team was unable to turn off the beacon on the first attempt and was only able to switch the beacon into a shorter period mode 23 hours after the first signal had been heard. During this time, the beacon was seen around the world on the SatNOGS website before the beacons started to appear with a longer period. The longer period beacons were seen for another 11 and a half days until Binar-1 made its final recorded transmission at approximately 7:03am (AWST) on the 2nd of November. Although the team made many attempts to recover the satellite again after this date, it is suspected that the satellite ran out of charge at this point due to a combination of the compromised power budget and constant power cycling causing start-up applications to run regularly. The power cycling could be observed as the message contained in the beacon would revert to the default message. Another observation that was made was the bit rate of the beacons not being re-configured when the power cycle occurred. This led the team to believe that the cause of failure was likely due to the adapter board.

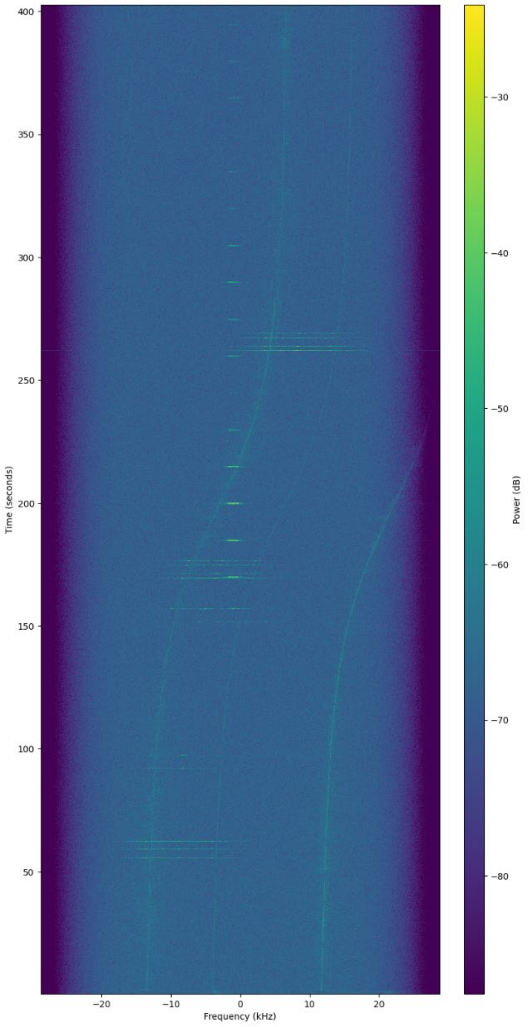

Figure 9: SatNOGS plot from the first observed communications with Binar-1. The wider signals are the transmissions from the ground station.

Results

From the failure analysis, the team believes that the last-minute adapter board modification was the cause of the lost communications with the flight computer. This belief comes from the beacon bit rate not being reset when the communications system was being power cycled, suggesting that the connection between the flight computer and the transceiver were not made correctly and likely broke during vibration testing, launch, or when exposed to the environment of space.

Although only a partial recovery was made, the Binar team was still able to infer some of the operations of the BCC from the beacon mode activated on the transceiver. It was clear to the team that the EPS was able to power the BCC until the final communication was made. Knowing the power budget problem before launch it is clear to the team that the solar panels, MPPTs, batteries, battery heaters, and the distribution subsystems were operational to some extent. The flight computer was also operating as expected as it was turning the communications system on. Alongside these two systems there was also valuable knowledge gained about the deployment switches and the performance of the structure during launch and in space. All of this could only be learnt by the team by delivering the mission.

LESSONS LEARNED

Although the mission was only considered a partial success in terms of the technology demonstration objective, the goal of educating staff and students was considered a success in terms of the many lessons that have been learned in the design process. Being a team starting with no knowledge about spacecraft design, the mission was always going to be challenging. The value of the lessons learned will help the team to overcome these challenges on the next launches from the Binar Space Program and be passed down to new students and staff beginning to work on the project. Although some of the lessons learned may not be new to more developed CubeSat design teams, the team believes that sharing the lessons learned will continue to build the literature around CubeSat design and hopes to help those who are yet to start the design process.

The first lesson learned by the team was the importance of locking down high-level mission objectives at the beginning of the design process. Although this is challenging when first starting the design, if possible, settle early on the budget and mission objectives. With these refined, defining requirements to meet the objectives is made easier. If the mission objectives are changed, start the process again and perform design reviews again if the objective changes are significant. One advantage of the decision to perform a custom design was the ability to easily adapt the design to some of these changing requirements, however this still meant that work needed to be repeated every time a change was made, significantly impacting the launch schedule.

Although power budgeting was performed in detail, the budget was only tested with the engineering model, and not to a suitable level of detail due to the missed DIL testing with the flight model. To improve its practices in the future the Binar team has learned to perform tests as you fly and not alter the engineering model to save costs. This costly operation may have been detrimental to the Binar-1 mission as the unbalanced power budget caused by the communication system was likely one of the reasons for communications loss.

Due to unexpected delays in the assembly process some testing was cut short. The team learned that it could be far better prepared for unexpected delays and prioritize its test program better if delays occur. Implementing this into the program will help to assess launch risk, and better manage the decision to either delay launch or remove some testing processes and assess the risks. Being able to present this plan to the mission leaders prior to the assembly can also help to better prepare the leadership team for delays and risk acceptance.

Although parts of the assembly and testing were shortened to make the launch, the team learnt important lessons about operation planning at the deployment of Binar-1. It was overlooked by the team the importance of putting in place an operations plan and setting up times for observations. This is something the team hopes to integrate into its DIL testing in the future to improve the performance of the operations plan and ready the team to operate the next set of Binar CubeSats.

The final lesson learnt relates to the goals of the Binar Space Program and the achievements observed by designing and assembling the satellite as a Program. Through the custom design, the Binar Space Program has learned and benefitted during the design and will continue to benefit in its future designs in different ways to how COTS comprised CubeSats benefit. This lesson will continue to be implemented by the Binar Space Program as it progresses into the future, aiming to work on its own payloads and platforms to continue building design experience at the university so that it will be able to deliver more complex space missions in the future.

CONCLUSION

Binar-1 was the first CubeSat launched by the Australian state of Western Australia. The custom designed CubeSat primary objective was to demonstrate the functionality of the integrated Binar CubeSat Core (BCC) which consisted of three of the satellites main systems including the Electrical Power System (EPS), Attitude Determination and Control System (ADCS), and flight computer system. The other objectives of the mission were to provide education to staff and students about end-to-end spacecraft design, and to spread awareness about the importance of space research and industry in the state.

After being deployed from the International Space Station (ISS) on the 5th of October 2021, Binar-1 was radio silent for almost exactly 15 days until a secondary beacon was enabled by the team. The secondary beacon was observed around the world by the SatNOGS network, until it stopped 11 and a half days later on the 2nd of November. This result has partially achieved the primary mission objective of the Binar-1 satellite demonstrating that the EPS and flight computer system on the BCC were operating in space, however no flight data could be collected to verify the systems completely.

Binar-1 has been successful at educating staff and students about end-to-end spacecraft design and provided a range of lessons learned which will be used in future Binar launches. These lessons include locking down mission requirements early, performing power budget testing with flight model systems, preparing for testing delays, planning for satellite operation, and the importance of using custom designed systems when aiming to perform consistent CubeSat missions.

Having learned these lessons and partially demonstrating the BCC, the team is now moving forward with implementing the lessons learned on its future missions. This will continue to grow the awareness of space in Western Australia as the team aims to deliver three 1U CubeSats, Binar-2, Binar-3, and Binar-4, in its next launch planned for 2023.

ACKNOWLEDGEMENTS

This research was supported by an Australian Government Research Training Program (RTP) Scholarship and received Strategic Research Investment support from Curtin University.

The authors would also like to acknowledge the continued support of AROSE and Fugro SpAARC, and thank them for their advice with ground station setup and operations planning.

REFERENCES

1. Robert M. Howie, Jonathan Paxman, Philip A. Bland, Martin C. Towner, Martin Cupak, Eleanor K. Sansom, and Hadrien A. R. Devillepoix. How to build a continental scale fireball camera network. Experimental Astronomy, 43(3):237–266, June 2017.
2. Andrew Dahir, Ariel Sandburg, and James Paul Mason. Advancement, Testing and Validation of an Innovative SmallSat Solar Panel Fabrication Process. SmallSat 2018, SSC17-WK-50.
3. JEM Payload Accommodation Handbook, Vol 8. Rev D. Small Satellite Deployment Interface Control Document. https://humans-in-space.jaxa.jp/kibouser/library/item/jx-espc_8d-d1_en.pdf
4. SatNOGS, Satellite Networked Open Ground Station. https://satnogs.org/
5. Raja Pandi Perumal, Holger Voos, Florio Dalla Vedova, Hubert Moser, and LuxSpace Sarl. Small Satellite Reliability: A decade in review. SmallSat 2021, SSC21-WKIII-02.

A.2 The Binar Space Program: Developing a reliable and efficient CubeSat Electronics Power System

Fergus W. Downey[1], Benjamin Hartig[1], Nathaniel Brough[1], Stuart Buchan[1], Martin Cupak[1], Daniel Busan[1], Philip A. Bland[1], Jonathan Paxman[2], and Robert Howie [1]

[1]Space Science and Technology Centre, Department of Earth and Planetary Science, Curtin University, Perth, Australia

[2]Department of Mechanical Engineering, Curtin University, Perth, Australia

This conference abstract was presented at the 19th Australian Space Research Conference (ASRC 2019) in Adelaide, Australia.

The Binar CubeSat Program: Developing a reliable and efficient CubeSat Electronics Power System

Fergus Downey, Benjamin Hartig, Nathaniel Brough, Stuart Buchan, Martin Cupak, Daniel Busan, Phil Bland, Jonathan Paxman and Robert Howie
Curtin University

CubeSats are fast becoming the new frontier for space science and exploration. The small low cost platform has key advantages in price and accessibility that make it optimal for many research groups and Universities. The Space Science and Technology Centre (SSTC) at Curtin University are beginning their own CubeSat program "The Binar CubeSat Program" which aims to develop CubeSats for its research purposes. The first CubeSat to be developed in this program is Binar-1 which will be a tech demonstration of the SSTC's new combined CubeSat bus. The bus will house all of the main CubeSat subsystems (excludes a payload) into 1/3U.

One of the main systems of the bus is the Electronics Power System (EPS). This system is one of the most important, as without it nothing else can function. As such, the system needs to be highly reliable and have redundancy in place to ensure that it can still operate if something is to go wrong. The system also has limited methods of generating and storing electricity. This challenge requires the system to be efficient, and to not use the limited power it has in the process of distributing it to other parts of the CubeSat bus. The final CubeSat bus to be tested on Binar-1 will verify the developed EPS as well as the other main subsystems. This will prepare the SSTC for future space research missions as well as offer a service to other interested parties looking to do space research and develop space hardware.

Presented by: Fergus Downey

A.3 Leveraging LEO Satellite Communication Constellations for Tracking the Targeted Re-entry of CubeSats

Fergus W. Downey[1], Benjamin Hartig[1], Stuart Buchan[1], Chelsea Tay[1], Jacob Cook[1], Daniel Busan[1], Philip A. Bland[1], Jonathan Paxman[2] and Robert Howie [1]

[1]Space Science and Technology Centre, Department of Earth and Planetary Science, Curtin University, Perth, Australia

[2]Department of Mechanical Engineering, Curtin University, Perth, Australia

This conference abstract was presented at the 20th Australian Space Research Conference (ASRC 2022) in Sydney, Australia.

Leveraging LEO Satellite Communication Constellations for Tracking the Targeted Re-entry of CubeSats

Fergus W. Downey[1], Benjamin Hartig[1], Stuart Buchan[1], Chelsea Tay[1], Jacob Cook[1], Daniel Busan[1], Philip A. Bland[1], Jonathan Paxman[2], and Robert Howie[1]

[1] *Space Science and Technology Centre, Department of Earth and Planetary Science, Curtin University, Perth, Australia*
[2] *Department of Mechanical Engineering, Curtin University, Perth, Australia*

One of the primary research outputs of the Space Science and Technology Centre (SSTC) at Curtin University has been its study of extra-terrestrial samples. The Centre has recovered meteorites for research using its custom designed and built Desert Fireball Network (DFN) and acquired asteroid samples from collaborations with international space agencies who have performed sample return missions such as CNSA (Chang'e 5) and JAXA (Hayabusa 2). Of these two sample collection methods, the latter is preferable due to the protection provided in the re-entry process. However, the cost of these missions is many times greater than the cost of operating the DFN.

As a long-term objective, and as part of the SSTCs new Binar Space Program (BSP), the Centre is researching new ways to perform sample return missions. One of the major phases of these missions is the Entry, Descent, and Landing (EDL). Currently under investigation at the BSP are methods for performing this process on a CubeSat platform. The first part of the EDL phase, re-entry for the case of the Earth, is being developed and planned for testing on the next Binar missions. In order to verify these systems a global communications system is necessary to maximise availability of the data link.

The proposed solution is to use global ground station networks and satellite communication constellations to communicate final location data before the satellite enters the atmosphere and burns up. By selecting the best systems on their performance against select criteria, the optimal solution for 1U CubeSats is determined. This presentation will provide a summary of the Binar-1 mission, an introduction to Binar-2, 3, and 4, an analysis into the design of the re-entry tracking payload on-board, and an overview of the plans for the Binar Space Program into the future.

Bibliography

[1] J. Puig-Suari, C. Turner, and W. Ahlgren, "Development of the standard CubeSat deployer and a CubeSat class PicoSatellite," in *2001 IEEE Aerospace Conference Proceedings (Cat. No.01TH8542)*, vol. 1, Mar. 2001, 1/347–1/353 vol.1. DOI: 10.1109/AERO.2001.931726.

[2] H. Heidt, J. Puig-Suari, A. Moore, S. Nakasuka, and R. Twiggs, "CubeSat: A New Generation of Picosatellite for Education and Industry Low-Cost Space Experimentation," *Small Satellite Conference*, Aug. 2000. [Online]. Available: https://digitalcommons.usu.edu/smallsat/2000/All2000/32.

[3] "CubeSat 101: Basic Concepts and Processes for First-Time CubeSat Developers," en, *NASA CubeSat Launch Initiative*, p. 96, Oct. 2017. [Online]. Available: https://www.nasa.gov/sites/default/files/atoms/files/nasa_csli_cubesat_101_508.pdf.

[4] H. Polat, J. Virgili-Llop, and M. Romano, "Survey, Statistical Analysis and Classification of Launched CubeSat Missions with Emphasis on the Attitude Control Method," *Journal of Small Satellites*, vol. 5, pp. 513–530, Jan. 2016.

[5] M. Swartwout, "The first one hundred CubeSats: A statistical look," *Journal of Small Satellites*, vol. 2, pp. 213–233, Jan. 2014.

[6] A. Poghosyan and A. Golkar, "CubeSat evolution: Analyzing CubeSat capabilities for conducting science missions," en, *Progress in Aerospace Sciences*, vol. 88, pp. 59–83, Jan. 2017, ISSN: 0376-0421. DOI: 10.1016/j.paerosci.2016.11.002. [Online]. Available: http://www.sciencedirect.com/science/article/pii/S0376042116300951.

[7] "State-of-the-Art of Small Spacecraft Technology," English, Oct. 2021. [Online]. Available: http://www.nasa.gov/smallsat-institute/sst-soa.

[8] J. Crusan and C. Galica, "NASA's CubeSat Launch Initiative: Enabling broad access to space," en, *Acta Astronautica*, vol. 157, pp. 51–60, Apr. 2019, ISSN: 0094-5765. DOI: 10.1016/j.actaastro.2018.08.048. [Online]. Available: http://www.sciencedirect.com/science/article/pii/S0094576517303107.

[9] S. Higginbotham, *CubeSat Launch Initiative*, Library Catalog: NASA NTRS, Jan. 2016. [Online]. Available: https://ntrs.nasa.gov/search.jsp?R=20160002253.

[10] G. L. Skrobot, *Project ELaNa and NASA's CubeSat Initiative*, Library Catalog: NASA NTRS, Aug. 2010. [Online]. Available: https://ntrs.nasa.gov/search.jsp?R=20110001319.

[11] B. Betts, B. Nye, J. Vaughn, *et al.*, "LightSail 1 Mission Results and Public Outreach Strategies," en, *Fourth International Symposium on Solar Sailing*, p. 5, 2017.

[12] D. A. Spencer, B. Betts, J. M. Bellardo, A. Diaz, B. Plante, and J. R. Mansell, "The LightSail 2 solar sailing technology demonstration," en, *Advances in Space Research*, Jun. 2020, ISSN: 0273-1177. DOI: 10.1016/j.asr.2020.06.029. [Online]. Available: http://www.sciencedirect.com/science/article/pii/S027311772030449X.

[13] A. Klesh, B. Clement, C. Colley, *et al.*, "MarCO: Early Operations of the First CubeSats to Mars," *Small Satellite Conference*, Aug. 2018. [Online]. Available: https://digitalcommons.usu.edu/smallsat/2018/all2018/474.

[14] E. Dotto, V. Della Corte, M. Amoroso, *et al.*, "LICIACube - The Light Italian Cubesat for Imaging of Asteroids In support of the NASA DART mission towards asteroid (65803) Didymos," en, *Planetary and Space Science*, vol. 199, p. 105 185, May 2021, ISSN: 0032-0633. DOI: 10.1016/j.pss.2021.105185. [Online]. Available: https://www.sciencedirect.com/science/article/pii/S0032063321000246.

[15] T. R. Lockett, J. Castillo-Rogez, L. Johnson, *et al.*, "Near-Earth Asteroid Scout Flight Mission," *IEEE Aerospace and Electronic Systems Magazine*, vol. 35, no. 3, pp. 20–29, Mar. 2020, Conference Name: IEEE Aerospace and Electronic Systems Magazine, ISSN: 1557-959X. DOI: 10.1109/MAES.2019.2958729.

[16] *CORONA: The First Recovery of Film from Space — Central Intelligence Agency*, 2012. [Online]. Available: https://www.cia.gov/news-information/featured-story-archive/2012-featured-story-archive/corona-the-first-recovery-of-film-from-space.html (visited on 07/31/2020).

[17] *CORONA: Declassified — Central Intelligence Agency*, 2015. [Online]. Available: https://www.cia.gov/news-information/featured-story-archive/2015-featured-story-archive/corona-declassified.html (visited on 07/31/2020).

[18] D. E. Brownlee, P. Tsou, J. D. Anderson, *et al.*, "Stardust: Comet and interstellar dust sample return mission," en, *Journal of Geophysical Research: Planets*, vol. 108, no. E10, 2003, ISSN: 2156-2202. DOI: 10.1029/2003JE002087. [Online]. Available: https://agupubs.onlinelibrary.wiley.com/doi/abs/10.1029/2003JE002087%4010.1002/%28ISSN%292169-9100.STARDUST1.

[19] P. Tsou, "Stardust encounters comet 81P/Wild 2," en, *Journal of Geophysical Research*, vol. 109, no. E12, E12S01, 2004, ISSN: 0148-0227. DOI: 10.1029/2004JE002317. [Online]. Available: http://doi.wiley.com/10.1029/2004JE002317.

[20] H. Yano, T. Kubota, H. Miyamoto, *et al.*, "Touchdown of the Hayabusa Spacecraft at the Muses Sea on Itokawa," *Science*, vol. 312, no. 5778, pp. 1350–1353, Jun. 2006, Publisher: American Association for the Advancement of Science. DOI: 10.1126/science.1126164. [Online]. Available: https://www.science.org/doi/10.1126/science.1126164.

[21] T. Yada, M. Abe, T. Okada, *et al.*, "Preliminary analysis of the Hayabusa2 samples returned from C-type asteroid Ryugu," en, *Nature Astronomy*, vol. 6, no. 2, pp. 214–220, Feb. 2022, Number: 2 Publisher: Nature Publishing Group, ISSN: 2397-3366. DOI: 10.1038/s41550-021-01550-6.

[Online]. Available: https://www.nature.com/articles/s41550-021-01550-6.

[22] Y. Tsuda, M. Yoshikawa, M. Abe, H. Minamino, and S. Nakazawa, "System design of the Hayabusa 2—Asteroid sample return mission to 1999 JU3," en, *Acta Astronautica*, vol. 91, pp. 356–362, Oct. 2013, ISSN: 0094-5765. DOI: 10.1016/j.actaastro.2013.06.028. [Online]. Available: https://www.sciencedirect.com/science/article/pii/S009457651300218X.

[23] D. S. Lauretta, S. S. Balram-Knutson, E. Beshore, *et al.*, "OSIRIS-REx: Sample Return from Asteroid (101955) Bennu," en, *Space Science Reviews*, vol. 212, no. 1, pp. 925–984, Oct. 2017, ISSN: 1572-9672. DOI: 10.1007/s11214-017-0405-1. [Online]. Available: https://doi.org/10.1007/s11214-017-0405-1.

[24] C. W. Hergenrother, C. K. Maleszewski, M. C. Nolan, *et al.*, "The operational environment and rotational acceleration of asteroid (101955) Bennu from OSIRIS-REx observations," en, *Nature Communications*, vol. 10, no. 1, p. 1291, Mar. 2019, Number: 1 Publisher: Nature Publishing Group, ISSN: 2041-1723. DOI: 10.1038/s41467-019-09213-x. [Online]. Available: https://www.nature.com/articles/s41467-019-09213-x.

[25] *NASA - NSSDCA - Hayabusa2 - Details*. [Online]. Available: https://nssdc.gsfc.nasa.gov/nmc/spacecraft/display.action?id=2014-076A (visited on 12/21/2022).

[26] *Cost of OSIRIS-REx*, en. [Online]. Available: https://www.planetary.org/space-policy/cost-of-osiris-rex (visited on 12/21/2022).

[27] I. Crawford, "The scientific legacy of Apollo," en, *Astronomy and Geophysics*, vol. 53, no. 6, pp. 6.24–6.28, Dec. 2012, ISSN: 1366-8781. DOI: 10.1111/j.1468-4004.2012.53624.x. [Online]. Available: https://ui.adsabs.harvard.edu/abs/2012A&G....53f..24C/abstract.

[28] *NASA: Apollo 50th Anniversary*. [Online]. Available: https://www.nasa.gov/specials/apollo50th/index.html (visited on 01/05/2023).

[29] D. S. Burnett, "NASA Returns Rocks from a Comet," *Science*, vol. 314, no. 5806, pp. 1709–1710, Dec. 2006, Publisher: American Association for the Advancement of Science. DOI: 10.1126/science.1137084. [Online]. Available: https://www.science.org/doi/10.1126/science.1137084.

[30] D. Kessler, N. Johnson, J.-C. Liou, and M. Matney, "The Kessler Syndrome: Implications to Future Space operations," *Advances in the Astronautical Sciences*, vol. 137, Jan. 2010.

[31] L. Qiao, C. Rizos, and A. G. Dempster, "Analysis and Comparison of CubeSat Lifetime," in *Proceedings of the 12th Australian Space Research Conference*, 2013, pp. 249–260.

[32] "FCC adopts new '5-year rule' for deorbiting satellites." (Sep. 29, 2022), [Online]. Available: https://www.fcc.gov/document/fcc-adopts-new-5-year-rule-deorbiting-satellites (visited on 08/03/2023).

[33] D. Masutti, E. Trifoni, E. Umit, *et al.*, *QARMAN re-entry CubeSat : Preliminary Results of SCIROCCO Plasma Wind Tunnel Testing*, en, Jun. 2018. [Online]. Available: https://www.colorado.edu/event/ippw2018/sites/default/files/attached-files/30_-_qarman_ippw_2018_v1.pdf.

[34] E. Gill, P. Sundaramoorthy, J. Bouwmeester, B. Zandbergen, and R. Reinhard, "Formation flying within a constellation of nano-satellites: The QB50 mission," en, *Acta Astronautica*, 6th International Workshop on Satellite Constellation and Formation Flying, vol. 82, no. 1, pp. 110–117, Jan. 2013, ISSN: 0094-5765. DOI: 10.1016/j.actaastro.2012.04.029. [Online]. Available: http://www.sciencedirect.com/science/article/pii/S0094576512001440 (visited on 07/30/2020).

[35] *QARMAN - QubeSat for Aerothermodynamic Research and Measurements on AblatioN*. [Online]. Available: https://www.vki.ac.be/index.php/qarman-home (visited on 12/16/2022).

[36] S. Wizemann, M. Ehresmann, A. Pagan, *et al.*, "MICRO-REENTRY-CAPSULE-2(MIRKA2) REXUS," Dec. 2015. [Online]. Available: https://www.researchgate.net/publication/305806796_MICRO-REENTRY-CAPSULE-2MIRKA2_REXUS#fullTextFileContent.

[37] S. F. Rafano Carná and R. Bevilacqua, "High fidelity model for the atmospheric re-entry of CubeSats equipped with the drag de-orbit device," *Acta Astronautica*, vol. 156, pp. 134–156, Mar. 1, 2019, ISSN: 0094-5765. DOI: 10.1016/j.actaastro.2018.05.049. [Online]. Available: https://www.sciencedirect.com/science/article/pii/S009457651731336X (visited on 08/17/2023).

[38] T. Liang, K. Nie, Q. Li, and J. Zhang, "Advanced analytical model for orbital aerodynamic prediction in LEO," *Advances in Space Research*, vol. 71, no. 1, pp. 507–524, Jan. 1, 2023, ISSN: 0273-1177. DOI: 10.1016/j.asr.2022.09.005. [Online]. Available: https://www.sciencedirect.com/science/article/pii/S027311772200847X (visited on 08/17/2023).

[39] G. E. Cook, "The effect of aerodynamic lift on satellite orbits," *Planetary and Space Science*, vol. 12, no. 11, pp. 1009–1020, Nov. 1, 1964, ISSN: 0032-0633. DOI: 10.1016/0032-0633(64)90077-7. [Online]. Available: https://www.sciencedirect.com/science/article/pii/0032063364900777 (visited on 08/18/2023).

[40] J. Ashenberg, "On the effects of time-varying aerodynamical coefficients on satellite orbits," *Acta Astronautica*, vol. 38, no. 2, pp. 75–86, Jan. 1, 1996, ISSN: 0094-5765. DOI: 10.1016/0094-5765(96)00002-1. [Online]. Available: https://www.sciencedirect.com/science/article/pii/0094576596000021 (visited on 08/18/2023).

[41] S. Ramjatan, N. Fitz-Coy, and A. Yew, "Magnus effect on a spinning satellite in low earth orbit," in *AIAA/AAS Astrodynamics Specialist Conference*, ser. AIAA SPACE Forum, American Institute of Aeronautics and Astronautics, Sep. 9, 2016. DOI: 10.2514/6.2016-5257. [Online]. Available: https://arc.aiaa.org/doi/10.2514/6.2016-5257 (visited on 08/18/2023).

[42] J. O. Murcia Piñeros, W. A. dos Santos, and A. F.B.A. Prado, "Analysis of the orbit lifetime of CubeSats in low earth orbits including periodic variation in drag due to attitude motion," *Advances in Space Research*, vol. 67, no. 2, pp. 902–918, Jan. 15, 2021, ISSN: 0273-1177. DOI: 10.1016/j.asr.2020.10.024. [Online]. Available: https://www.sciencedirect.com/science/article/pii/S0273117720307523 (visited on 08/17/2023).

[43] R. G. Wilmoth, R. A. Mitcheltree, and J. N. Moss, "Low-density aerodynamics of the stardust sample return capsule," *Journal of Spacecraft and Rockets*, vol. 36, no. 3, pp. 436–441, May 1999, Publisher: American Institute of Aeronautics and Astronautics, ISSN: 0022-4650. DOI: 10.2514/2.3464. [Online]. Available: https://arc.aiaa.org/doi/10.2514/2.3464 (visited on 08/18/2023).

[44] G. E. Cook, "Satellite drag coefficients," *Planetary and Space Science*, vol. 13, no. 10, pp. 929–946, Oct. 1, 1965, ISSN: 0032-0633. DOI: 10.1016/0032-0633(65)90150-9. [Online]. Available: https://www.sciencedirect.com/science/article/pii/0032063365901509 (visited on 08/18/2023).

[45] K. Moe and M. M. Moe, "Gas–surface interactions and satellite drag coefficients," *Planetary and Space Science*, vol. 53, no. 8, pp. 793–801, Jul. 1, 2005, ISSN: 0032-0633. DOI: 10.1016/j.pss.2005.03.005. [Online]. Available: https://www.sciencedirect.com/science/article/pii/S0032063305000486 (visited on 08/18/2023).

[46] D. Mostaza Prieto, B. P. Graziano, and P. C. E. Roberts, "Spacecraft drag modelling," *Progress in Aerospace Sciences*, vol. 64, pp. 56–65, Jan. 1, 2014, ISSN: 0376-0421. DOI: 10.1016/j.paerosci.2013.09.001. [Online]. Available: https://www.sciencedirect.com/science/article/pii/S0376042113000754 (visited on 08/18/2023).

[47] S. Livadiotti, N. H. Crisp, P. C. E. Roberts, *et al.*, "A review of gas-surface interaction models for orbital aerodynamics applications," *Progress in Aerospace Sciences*, vol. 119, p. 100 675, Nov. 1, 2020, ISSN: 0376-0421. DOI: 10.1016/j.paerosci.2020.100675. [Online]. Available: https://www.sciencedirect.com/science/article/pii/S0376042120300877 (visited on 08/18/2023).

[48] D. R. Jackson, S. Bruinsma, S. Negrin, *et al.*, "The space weather atmosphere models and indices (SWAMI) project: Overview and first results," *Journal of Space Weather and Space Climate*, vol. 10, p. 18, 2020, Publisher: EDP Sciences, ISSN: 2115-7251. DOI: 10.1051/swsc/2020019. [Online]. Available: https://www.swsc-journal.org/articles/swsc/abs/2020/01/swsc190071/swsc190071.html (visited on 08/18/2023).

[49] V. Starlinger, A. Behnke, J.-P. Baumann, *et al.*, "Increasing the Success of CAPE using Precursor Missions," Apr. 2017. [Online]. Available: https://www.researchgate.net/publication/316788037_Increasing_the_Success_of_CAPE_using_Precursor_Missions.

[50] A. Pagan, M. Fugmann, and G. Herdrich, "A System Approach towards a Miniaturized Pulsed Plasma Thruster for a CubeSat-Type Deorbit Module," Sep. 2014. [Online]. Available: https://www.researchgate.net/pu

blication/280084980_A_System_Approach_towards_a_Miniaturized_Pulsed_Plasma_Thruster_for_a_CubeSat-Type_Deorbit_Module.

[51] M. Ehresmann, A. Behnke, J.-P. Baumann, *et al.*, "CubeSat-sized Re-entry Capsule MIRKA2," Apr. 2015. [Online]. Available: https://www.researchgate.net/publication/305807017_CubeSat-sized_Re-entry_Capsule_MIRKA2.

[52] G. Herdrich, J.-P. Baumann, P. Geissler, *et al.*, "MIRKA2: SMALL RE-ENTRY DEMONSTRATOR FOR ADVANCED MINIATURIZED SENSORS," Oct. 2012. [Online]. Available: https://www.researchgate.net/publication/351786281_MIRKA2_SMALL_RE-ENTRY_DEMONSTRATOR_FOR_ADVANCED_MINIATURIZED_SENSORS.

[53] E. Kulu, *Nanosats Database*, en. [Online]. Available: https://www.nanosats.eu/index.html (visited on 12/19/2022).

[54] I. Akyol, "Design of Data Acquisition Subsystem of QARMAN Payloads and Validation in Plasma Facilities-Hardware," Ph.D. dissertation, Aug. 2013. DOI: 10.13140/2.1.1098.1125.

[55] M. Aksulu, "Design of Data Acquisition System of QARMAN Subsystems and Validation in Plasma Facilities – Software," Ph.D. dissertation, Sep. 2013.

[56] B. Smith, A. Cassell, C. Kruger, E. Venkatapathy, C. Kazemba, and K. Simonis, "Nano-ADEPT: An entry system for secondary payloads," in *2015 IEEE Aerospace Conference*, ISSN: 1095-323X, Mar. 2015, pp. 1–11. DOI: 10.1109/AERO.2015.7119095.

[57] A. Cassell, *ADEPT for Interplanetary Small Satellite Missions*, Library Catalog: NASA NTRS, Apr. 2019. [Online]. Available: https://ntrs.nasa.gov/search.jsp?R=20190004912.

[58] A. Cassell, B. Smith, P. Wercinski, *et al.*, "ADEPT, A Mechanically Deployable Re-Entry Vehicle System, Enabling Interplanetary CubeSat and Small Satellite Missions," in *Small Satellite Conference*, Aug. 2018. [Online]. Available: https://digitalcommons.usu.edu/smallsat/2018/all2018/265.

[59] B. Smith, B. Yount, C. Kruger, *et al.*, "Nano-ADEPT aeroloads wind tunnel test," in *2016 IEEE Aerospace Conference*, Mar. 2016, pp. 1–20. DOI: 10.1109/AERO.2016.7500719.

[60] A. Cassell, *ADEPT Sounding Rocket One (SR-1) Flight Test*, Library Catalog: NASA NTRS, Sep. 2019. [Online]. Available: https://ntrs.nasa.gov/search.jsp?R=20190031937.

[61] P. Wercinski, B. Smith, B. Yount, *et al.*, "ADEPT sounding rocket one (SR-1) flight experiment overview," in *2017 IEEE Aerospace Conference*, Mar. 2017, pp. 1–7. DOI: 10.1109/AERO.2017.7943889.

[62] Y. Watanabe, K. Suzuki, O. Imamura, and K. Yamada, "Attitude Estimation of Nano-satellite with Deployable Aeroshell during Orbital Decay," en, *TRANSACTIONS OF THE JAPAN SOCIETY FOR AERONAUTICAL AND SPACE SCIENCES, AEROSPACE TECHNOLOGY JAPAN*, vol. 14, no. ists30, Pf_1–Pf_5, 2016, ISSN: 1884-0485. DOI: 10.2322/tastj.14.Pf_1. [Online]. Available: https://www.jstage.jst.go.jp/article/tastj/14/ists30/14_Pf_1/_article.

[63] Y. Takahashi and K. Yamada, "Aerodynamic heating of inflatable aeroshell in orbital reentry," en, *Acta Astronautica*, vol. 152, pp. 437–448, Nov. 2018, ISSN: 0094-5765. DOI: 10.1016/j.actaastro.2018.08.003. [Online]. Available: http://www.sciencedirect.com/science/article/pii/S0094576518306891.

[64] T. Hashimoto, T. Yamada, M. Otsuki, *et al.*, "Nano Semihard Moon Lander: OMOTENASHI," *IEEE Aerospace and Electronic Systems Magazine*, vol. 34, no. 9, pp. 20–30, Sep. 2019, Conference Name: IEEE Aerospace and Electronic Systems Magazine, ISSN: 1557-959X. DOI: 10.1109/MAES.2019.2923311.

[65] Y. Takahashi, T. Koike, N. Oshima, and K. Yamada, "Aerothermodynamic analysis for deformed membrane of inflatable aeroshell in orbital reentry mission," en, *Aerospace Science and Technology*, vol. 92, pp. 858–868, Sep. 2019, ISSN: 1270-9638. DOI: 10.1016/j.ast.2019.06.047. [Online]. Available: http://www.sciencedirect.com/science/article/pii/S1270963819311137.

[66] Y. Zhao, H. Liu, Z. Liu, and C. Yan, "Numerical study of the cone angle effects on transition and convection heat transfer for hypersonic inflatable aerodynamic decelerator aeroshell," en, *International Communications in Heat and Mass Transfer*, vol. 110, pp. 104–406, Jan. 2020, ISSN: 0735-1933. DOI: 10.1016/j.icheatmasstransfer.2019.104406. [Online]. Available:

http://www.sciencedirect.com/science/article/pii/S0735193319302726.

[67] K. Matsumaru, M. Tanaka, O. Imamura, and K. Yamada, "Thermal-durability Evaluation of Inflatable Structure for a Deployable Aeroshell Using ICP Heater," en, *TRANSACTIONS OF THE JAPAN SOCIETY FOR AERONAUTICAL AND SPACE SCIENCES, AEROSPACE TECHNOLOGY JAPAN*, vol. 16, no. 6, pp. 520–527, 2018, ISSN: 1884-0485. DOI: 10.2322/tastj.16.520. [Online]. Available: https://www.jstage.jst.go.jp/article/tastj/16/6/16_520/_article.

[68] D. Guglielmo, S. Omar, R. Bevilacqua, *et al.*, "Drag Deorbit Device: A New Standard Reentry Actuator for CubeSats," *Journal of Spacecraft and Rockets*, vol. 56, no. 1, pp. 129–145, 2019, ISSN: 0022-4650. DOI: 10.2514/1.A34218. [Online]. Available: https://doi.org/10.2514/1.A34218.

[69] T. Martin, S. Omar, and R. Bevilacqua, "Controlled Spacecraft Re-Entry of a Drag De-Orbit Device (D3)," en, *UF Journal of Undergraduate Research*, vol. 21, no. 1, Dec. 2019, Number: 1, ISSN: 2638-0668. DOI: 10.32473/ufjur.v21i1.108233. [Online]. Available: https://journals.flvc.org/UFJUR/article/view/108233.

[70] S. Omar, D. Guglielmo, G. Mauro, T. Martin, and R. Bevilacqua, "CubeSat Mission to Demonstrate Aerodynamically Controlled Re-Entry using the Drag De-Orbit Device (D3)," *Small Satellite Conference*, Aug. 2018. [Online]. Available: https://digitalcommons.usu.edu/smallsat/2018/all2018/335.

[71] S. R. Omar and R. Bevilacqua, "Hardware and GNC solutions for controlled spacecraft re-entry using aerodynamic drag," en, *Acta Astronautica*, vol. 159, pp. 49–64, Jun. 2019, ISSN: 0094-5765. DOI: 10.1016/j.actaastro.2019.03.051. [Online]. Available: http://www.sciencedirect.com/science/article/pii/S0094576519300359.

[72] M. Murbach, R. Alena, and A. Luna, "The TechEdSat/PhoneSat Missions for Small Payload Quick Return," *Small Satellite Conference*, Aug. 2016. [Online]. Available: https://digitalcommons.usu.edu/smallsat/2016/S7Comm/6.

[73] F. Tavares, *TechEdSat-10 Deploys from the Space Station*, und, Text, Aug. 2020. [Online]. Available: http://www.nasa.gov/image-feature/ames/techedsat-10-deploys (visited on 12/19/2022).

[74] M. S. P. Murbach, *Modeling the Exo-Brake and the Development of Strategies for De-Orbit Drag Modulation*, Library Catalog: NASA NTRS, Jun. 2016. [Online]. Available: https://ntrs.nasa.gov/search.jsp?R=20160008903.

[75] M. S. P. Murbach, *Modulated Exo-Brake Flight Testing - Modeling and Test Results - Successes with Exo-Brake Development and Targeting for Future Sample Return Capability: TES-6,7,8 Flight Experiments*, Library Catalog: NASA NTRS, Jun. 2019. [Online]. Available: https://ntrs.nasa.gov/search.jsp?R=20190028931.

[76] M. N. Sweeting, "Modern Small Satellites-Changing the Economics of Space," *Proceedings of the IEEE*, vol. 106, no. 3, pp. 343–361, Mar. 2018, ISSN: 1558-2256. DOI: 10.1109/JPROC.2018.2806218.

[77] *Launch Services | Tyvak International*. [Online]. Available: https://www.tyvak.eu/launch-services/ (visited on 12/21/2022).

[78] M. Cho, T. Yamauchi, M. Sejera, Y. Ohtani, S. Kim, and H. Masui, "CubeSat Electrical Interface Standardization for Faster Delivery and More Mission Success," *Small Satellite Conference*, Aug. 2020. [Online]. Available: https://digitalcommons.usu.edu/smallsat/2020/all2020/3.

[79] D. Sadhukhan, A. Guzik, O. Benafan, *et al.*, "Advanced eLectrical Bus (ALBus) CubeSat: From Build to Flight," *Small Satellite Conference*, Aug. 2020. [Online]. Available: https://digitalcommons.usu.edu/smallsat/2020/all2020/9.

[80] K. Rankin, I. McNeil, I. Rankin, and S. Stochaj, "How Not to Build a CubeSat – Lessons Learned from Developing and Launching NMSU's First CubeSat," *Small Satellite Conference*, Aug. 2019. [Online]. Available: https://digitalcommons.usu.edu/smallsat/2019/all2019/54.

[81] L. Sato, L. Costa, J. Fulindi, *et al.*, "The ITASAT – The Lessons Learned from the Mission Concept to the Operation," *Small Satellite Conference*, Aug. 2019. [Online]. Available: https://digitalcommons.usu.edu/smallsat/2019/all2019/51.

[82] Y.-C. Chiu, L. C. Chang, C.-K. Chao, *et al.*, "Lessons Learned from IDEASSat: Design, Testing, on Orbit Operations, and Anomaly Analysis of a First University CubeSat Intended for Ionospheric Science," en, *Aerospace*, vol. 9, no. 2, p. 110, Feb. 2022, ISSN: 2226-4310. DOI: 10.3390/aerospace9020110. [Online]. Available: https://www.mdpi.com/2226-4310/9/2/110 (visited on 12/21/2022).

[83] S. Wu, W. Chen, and C. Chao, "The STU-2 CubeSat Mission and In-Orbit Test Results," *Small Satellite Conference*, Aug. 2016. [Online]. Available: https://digitalcommons.usu.edu/smallsat/2016/TS3YearInReview/8.

[84] A. Greenberg, D. Lay, G. Lebrasseur, *et al.*, "OreSat: A Student Team-Based Approach to an Inexpensive, Open, and Modular (1-3U) CubeSat Bus," *Small Satellite Conference*, Aug. 2021. [Online]. Available: https://digitalcommons.usu.edu/smallsat/2021/all2021/236.

[85] G. Li, L. Spence, M. Miller, *et al.*, "Lessons Learned from the Development and Flight of the First Miniature Tethered Electrodynamics Experiment (MiTEE-1)," *Small Satellite Conference*, Aug. 2021. [Online]. Available: https://digitalcommons.usu.edu/smallsat/2021/all2021/249.

[86] J. Fuchs, M. Halvorson, and V. Lopez, "An Overview of the Alabama Burst Energetics eXplorer (ABEX) Mission," *Small Satellite Conference*, Aug. 2021. [Online]. Available: https://digitalcommons.usu.edu/smallsat/2021/all2021/239.

[87] P. A. Bland, P. Spurný, A. R. Bevan, *et al.*, "The Australian Desert Fireball Network: A new era for planetary science," *Australian Journal of Earth Sciences*, vol. 59, no. 2, pp. 177–187, Mar. 2012, ISSN: 0812-0099. DOI: 10.1080/08120099.2011.595428. [Online]. Available: https://doi.org/10.1080/08120099.2011.595428.

[88] *JEM Payload Accomodation Handbook - Vol. 8 - Small Satellite Deployment Interface Control Document - Rev. D*, Jul. 2020. [Online]. Available: https://iss.jaxa.jp/kibouser/library/item/jx-espc_8d_en.pdf (visited on 12/21/2022).

[89] A. Sandberg and T. Smith, "Streamlining CubeSat Solar Panel Fabrication Processes," *Small Satellite Conference*, Aug. 2016. [Online]. Available: https://digitalcommons.usu.edu/smallsat/2016/TS8StudentComp/2.

[90] A. Dahir, A. Sandberg, and J. Mason, "Advancement, Testing and Validation of an Innovative SmallSat Solar Panel Fabrication Process," *Small Satellite Conference*, Aug. 2017. [Online]. Available: https://digitalcommons.usu.edu/smallsat/2017/all2017/27.

[91] V. Knap, L. K. Vestergaard, and D.-I. Stroe, "A Review of Battery Technology in CubeSats and Small Satellite Solutions," en, *Energies*, vol. 13, no. 16, p. 4097, Jan. 2020, ISSN: 1996-1073. DOI: 10.3390/en13164097. [Online]. Available: https://www.mdpi.com/1996-1073/13/16/4097.

[92] F. C. Krause, J. A. Loveland, M. C. Smart, E. J. Brandon, and R. V. Bugga, "Implementation of commercial Li-ion cells on the MarCO deep space CubeSats," en, *Journal of Power Sources*, vol. 449, p. 227 544, Feb. 2020, ISSN: 0378-7753. DOI: 10.1016/j.jpowsour.2019.227544. [Online]. Available: https://www.sciencedirect.com/science/article/pii/S037877531931537X (visited on 12/21/2022).

[93] A. Edpuganti, V. Khadkikar, M. S. E. Moursi, H. Zeineldin, N. Al-Sayari, and K. Al Hosani, "A Comprehensive Review on CubeSat Electrical Power System Architectures," *IEEE Transactions on Power Electronics*, vol. 37, no. 3, pp. 3161–3177, Mar. 2022, ISSN: 1941-0107. DOI: 10.1109/TPEL.2021.3110002.

[94] R. M. Sharma, R. Kawari, S. Bhandari, S. Panta, R. C. Prajapati, and N. B. Adhikari, "Simulation of CubeSat Detumbling Using B-Dot Controller," en, in *Proceedings of International Conference on Sustainable Expert Systems*, S. Shakya, V. E. Balas, W. Haoxiang, and Z. Baig, Eds., ser. Lecture Notes in Networks and Systems, Singapore: Springer, 2021, pp. 541–553, ISBN: 978-981-334-355-9. DOI: 10.1007/978-981-33-4355-9_40.

[95] M. D'Alessio, C. Poivey, D. Walter, *et al.*, "NAND flash memory in-flight data from PROBA-II spacecraft," in *2013 14th European Conference on Radiation and Its Effects on Components and Systems (RADECS)*, Sep. 2013, pp. 1–6. DOI: 10.1109/RADECS.2013.6937432.

[96] *PCB Design Software & Tools | Altium*, en. [Online]. Available: https://www.altium.com/ (visited on 12/22/2022).

[97] *Small - Affordable - Expandable.* [Online]. Available: https://openmv.io/ (visited on 12/23/2022).

[98] D. J. White, I. Giannelos, A. Zissimatos, E. Kosmas, and D. Papadeas, "SatNOGS: Satellite Networked Open Ground Station," en, Oct. 2015. [Online]. Available: https://scholar.valpo.edu/cgi/viewcontent.cgi?article=1039&context=engineering_fac_pub.

[99] M. Swartwout, "Reliving 24 Years in the next 12 Minutes: A Statistical and Personal History of University-Class Satellites," *Small Satellite Conference*, Aug. 2018. [Online]. Available: https://digitalcommons.usu.edu/smallsat/2018/all2018/465.

[100] L. Berthoud, M. Swartwout, J. Cutler, D. Klumpar, J. Larsen, and J. Nielsen, "University CubeSat Project Management for Success," *Small Satellite Conference*, Aug. 2019. [Online]. Available: https://digitalcommons.usu.edu/smallsat/2019/all2019/63.

[101] M. R. Mughal, J. Praks, R. Vainio, *et al.*, "Aalto-1, multi-payload CubeSat: In-orbit results and lessons learned," en, *Acta Astronautica*, vol. 187, pp. 557–568, Oct. 2021, ISSN: 0094-5765. DOI: 10.1016/j.actaastro.2020.11.044. [Online]. Available: https://www.sciencedirect.com/science/article/pii/S0094576520307190.

[102] P. Kovář, P. Puričer, and K. Kovářová, "Study of the Two-Line Element Accuracy by 1U CubeSat with a GPS Receiver," en, *Sensors*, vol. 22, no. 8, p. 2902, Jan. 2022, ISSN: 1424-8220. DOI: 10.3390/s22082902. [Online]. Available: https://www.mdpi.com/1424-8220/22/8/2902.

[103] K. Riesing, "Orbit Determination from Two Line Element Sets of ISS-Deployed CubeSats," *Small Satellite Conference*, Aug. 2015. [Online]. Available: https://digitalcommons.usu.edu/smallsat/2015/all2015/58.

[104] G. D. Krebs, *Gunter's Space Page - Information on spaceflight, launch vehicles and satellites*. [Online]. Available: https://space.skyrocket.de/ (visited on 01/10/2023).

[105] *Sweedish space corporation - satellite Ground Station Services*, en-US. [Online]. Available: https://sscspace.com/services/satellite-ground-stations/ (visited on 01/12/2023).

[106] *Ksat - ground Network Services*, en. [Online]. Available: https://www.ksat.no/ground-network-services/ (visited on 01/12/2023).

[107] D. White, C. Shields, P. Papadeas, *et al.*, "Overview of the Satellite Networked Open Ground Stations (SatNOGS) Project," *Small Satellite Conference*, Aug. 2018. [Online]. Available: https://digitalcommons.usu.edu/smallsat/2018/all2018/313.

[108] K. Croissant, D. White, X. Álvarez, *et al.*, "An Updated Overview of the Satellite Networked Open Ground Stations (SatNOGS) Project," *Small Satellite Conference*, Aug. 2022. [Online]. Available: https://digitalcommons.usu.edu/smallsat/2022/all2022/172.

[109] J. Bordalo Monteiro, J. Santos, P. Antunes, A. Guerman, and F. Jorge, "A review of small satellite constellations for IoT connectivity," Sep. 2022. [Online]. Available: https://www.researchgate.net/publication/364213241_A_review_of_small_satellite_constellations_for_IoT_connectivity.

[110] *Iridium 9603 Module | Iridium Satellite Communications*. [Online]. Available: https://www.iridium.com/products/iridium-9603/ (visited on 01/10/2023).

[111] J. Claybrook, "Feasibility Analysis on the Utilization of the Iridium Satellite Communications Network for Resident Space Objects in Low Earth Orbit," *Theses and Dissertations*, Mar. 2013. [Online]. Available: https://scholar.afit.edu/etd/819.

[112] V. J. Riot, L. M. Simms, and D. Carter, "Lessons Learned Using Iridium to Communicate with a CubeSat in Low Earth Orbit," English, *Journal of Small Satellites*, vol. 10, no. 1, Feb. 2021, ISSN: 2327-4123. [Online]. Available: https://www.osti.gov/pages/biblio/1770026.

[113] R. Shimmin, R. Alena, C. Priscal, *et al.*, "The successful PhoneSat wifi experiment on the Soarex-8 flight," in *2016 IEEE Aerospace Conference*, Mar. 2016, pp. 1–9. DOI: 10.1109/AERO.2016.7500826.

[114] K. Alexandrou, "Ionizing Radiation Effects on Graphene Based Field Effects Transistors," en, Ph.D. dissertation, Columbia University, 2016. DOI: 10.7916/D86D5T53. [Online]. Available: https://doi.org/10.7916/D86D5T53.

[115] N. Enoki, Y. Takahashi, N. Oshima, K. Yamada, and K. Suzuki, "Aerodynamics of inflatable nano-satellite "EGG" in low earth orbit and reentry duration," en, *AIP Conference Proceedings*, vol. 2132, no. 1, p. 100 002, Aug. 2019, ISSN: 0094-243X. DOI: 10.1063/1.5119597. [Online]. Available: https://aip.scitation.org/doi/abs/10.1063/1.5119597.

[116] Y. Prevereaud, F. Sourgen, D. Mimoun, A. Gaboriaud, J.-L. Vérant, and J.-M. Moschetta, "Predicting the Atmospheric Re-entry of Space Debris Through the QB50 EntrySat Mission," Apr. 2013. [Online]. Available: https://www.researchgate.net/publication/265139721_Predicting_the_Atmospheric_Re-entry_of_Space_Debris_Through_the_QB50_EntrySat_Mission.

[117] M. Murbach, R. Ntone-Johansen, A. Salas, *et al.*, *TECHEDSAT-7 and 10: The Little Spacecraft That Could*, NTRS Author Affiliations: Ames Research Center, Millennium Engineering and Integration (United States), Wyle (United States) NTRS Meeting Information: Interplanetary Small Satellite Conference; 2021-05-03 to 2021-05-04; undefined NTRS Document ID: 20210014950 NTRS Research Center: Ames Research Center (ARC), 2021. [Online]. Available: https://ntrs.nasa.gov/citations/20210014950.

[118] *CACTUS-1: Mission Complete!* en. [Online]. Available: https://www.captechu.edu/news-events/cactus-1-mission-complete (visited on 01/10/2023).

[119] G. Morelli, G. Parissenti, R. Navoni, *et al.*, "FLEXIBLE EXPERIMENTAL EMBEDDED SATELLITE," en, 2019. [Online]. Available: https://icubesat.org/papers/2019-2/2019-b-1-3-fees-flexible-experimental-embedded-satellite/.

[120] *Hatchling Veery "Clay" Mission Detail*, en. [Online]. Available: https://careweather.com/mission/veery-rl1-1615347564369x827669778420672500 (visited on 01/10/2023).

[121] T. Sakamoto, *Get clues about sudden celestial gamma-ray bursts with the micro-miniature "ARICA"!* ja, 2022. [Online]. Available: https://ademist-cf.com/projects/234/progresses?lang=ja (visited on 01/10/2023).

[122] M. Murbach, A. Salas, M. Lowry, *et al.*, *TechEdSat-13: The First Flight of a Neuromorphic Processor*, Apr. 2022. [Online]. Available: https://ntrs.nasa.gov/citations/20220005780.

[123] H. Voss, J. Dailey, M. Orvis, and M. Voss, "Thin CubeSats and Compact Sensors for Constellations in VLEO to Deep Space," *Small Satellite Conference*, Aug. 2022. [Online]. Available: https://digitalcommons.usu.edu/smallsat/2022/all2022/8.

[124] *STX3 | Globalstar AP*, en-ap. [Online]. Available: https://www.globalstar.com/en-ap/products/iot/stx3 (visited on 01/10/2023).

[125] M. O'Connell, *STX3 Declanation of Conformity*, English, 2017. [Online]. Available: https://www.globalstar.com/Globalstar/media/Globalstar/Downloads/Regulatory/Declaration_of_Conformity_STX3.pdf (visited on 01/10/2023).

[126] H. Voss, J. Dailey, M. Orvis, A. White, and S. Brandle, "Globalstar Link: From Reentry Altitude and Beyond," *Small Satellite Conference*, Aug. 2016. [Online]. Available: https://digitalcommons.usu.edu/smallsat/2016/S7Comm/1.

[127] M. Ovchinnikov, D. Ivanov, O. Pansyrnyi, *et al.*, "Flight Results of the Mission of TNS-0 #2 Nanosatellite Connected via Global Communication System," Oct. 2018. [Online]. Available: https://www.researchgate.net/publication/328102767_Flight_Results_of_the_Mission_of_TNS-0_2_Nanosatellite_Connected_via_Global_Communication_System.

[128] H. Voss, J. Dailey, J. Crowley, B. Bennett, and A. White, "TSAT Globalstar ELaNa-5 Extremely Low-Earth Orbit (ELEO) Satellite," *Small Satellite Conference*, Aug. 2014. [Online]. Available: https://digitalcommons.usu.edu/smallsat/2014/Workshop/3.

[129] C. Nogales, B. Grim, M. Kamstra, *et al.*, "MakerSat-0: 3D-Printed Polymer Degradation First Data from Orbit," *Small Satellite Conference*, Aug. 2018. [Online]. Available: https://digitalcommons.usu.edu/smallsat/2018/all2018/434.

[130] *HSAT-1 Experiment Description Document for FCC Application*, English, Aug. 2016. [Online]. Available: https://apps.fcc.gov/els/GetAtt.html?id=185034&x=..

[131] D. Werner, *Harris says first cubesat performing well in orbit*, en-US, Dec. 2018. [Online]. Available: https://spacenews.com/harris-hsat/ (visited on 01/10/2023).

[132] G. Kissel, R. Loehrlein, N. Kalsch, W. Helms, Z. Snyder, and S. Kaphle, "UNITE CubeSat: From Inception to Early Orbital Operations," *Small Satellite Conference*, Aug. 2019. [Online]. Available: https://digitalcommons.usu.edu/smallsat/2019/all2019/50.

[133] M. Goggin, S. Tamrazian, R. Carlson, A. Tidwell, and D. Parkos, "CubeSat Sensor Platform for Reentry Aerothermodynamics," *Small Satellite Conference*, Aug. 2017. [Online]. Available: https://digitalcommons.usu.edu/smallsat/2017/all2017/132.

[134] R. Twiggs, A. Zucherman, E. Bujold, *et al.*, "The ThinSat Program: Flight Opportunities for Education, Research and Industry," *Small Satellite Conference*, Aug. 2018. [Online]. Available: https://digitalcommons.usu.edu/smallsat/2018/all2018/475.

[135] H. Voss, J. Dailey, M. Orvis, *et al.*, "Architecture & Manufacture for 1/7U to 27U 60 ThinSat Constellations: Flight Results," *Small Satellite Conference*, Aug. 2019. [Online]. Available: https://digitalcommons.usu.edu/smallsat/2019/all2019/298.

[136] A. Martinez and C. Munoz, "AztechSat-1, a First Collaborative CubeSat Between NASA and Mexico," Brasilia, Dec. 2014. [Online]. Available: https://ntrs.nasa.gov/citations/20190001961 (visited on 01/10/2023).

[137] B. Campbell, C. Nogales, B. Grim, M. Kamstra, J. Griffin, and S. Parke, "On-Orbit Polymer Degradation Results from MakerSat-1: First Satellite Designed to be Additively Manufactured in Space," *Small Satellite Conference*, Aug. 2020. [Online]. Available: https://digitalcommons.usu.edu/smallsat/2020/all2020/45.

[138] T. Gies, T. Rodriquez, G. Holt, *et al.*, "Very Low Frequency Propagation Mapper (VPM) Experience and Results from the Systems Engineering Cycle of a Small Satellite," *Small Satellite Conference*, Aug. 2020. [Online]. Available: https://digitalcommons.usu.edu/smallsat/2020/all2020/114.

[139] M. Nunes, L. French, P. Englert, *et al.*, "NEUTRON-1 Mission: Low Earth Orbit Neutron Flux Detection and COSMOS Mission Operations Technology Demonstration," *Small Satellite Conference*, Aug. 2019. [Online]. Available: https://digitalcommons.usu.edu/smallsat/2019/all2019/124.

[140] J. Hanson, "PTD Management and Governance," en, *CubeSat Developers Workshop 2019*, Apr. 2019. [Online]. Available: http://mstl.atl.calpoly.edu/~workshop/archive/2019/Spring/Day%201/Session%202/JohnHanson.pdf.

[141] M. B. Orvis, J. F. Dailey, H. D. Voss, and J. N. Fritsch, "Flight Results Including the ThinSat-2 Constellation, TROOP Payload Host, and Miniaturized GPS Integrated into the EyeStar-S3," en, 2021. [Online]. Available: http://mstl.atl.calpoly.edu/~workshop/archive/2021/presentations/Day%203/Subsytems%20Part%202/Matthew%20Orvis.pdf.

[142] S. T. Goh, L. Lim, V. Bui, *et al.*, "VELOX-II: Summary of One Year in Operation," Jun. 2017. [Online]. Available: https://www.researchgate.net/publication/317589990_VELOX-II_Summary_of_One_Year_in_Operation.

[143] *OG2 AND OGi MODEMS*. [Online]. Available: https://www.orbcomm.com/PDF/datasheet/OG2-OG-ISAT-Satellite-Modems.pdf (visited on 01/10/2023).

[144] D. F. Bruhn, "TechEdSat – CubeSat Technology demonstration mission featuring Plug- and-play and radiation hardened electronics," en, [Online]. Available: http://mstl.atl.calpoly.edu/~workshop/archive/2012/Spring/43-Bruhn-TechEdSat.pdf.

[145] V. Braun, Q. Funke, S. Lemmens, and S. Sanvido, "DRAMA 3.0 - Upgrade of ESA's debris risk assessment and mitigation analysis tool suite," en, *Journal of Space Safety Engineering*, Space Debris: The State of Art, vol. 7, no. 3, pp. 206–212, Sep. 2020, ISSN: 2468-8967. DOI: 10.1016/j.jsse.2020.07.020. [Online]. Available: https://www.sciencedirect.com/science/article/pii/S2468896720300847 (visited on 01/10/2023).

[146] T. Kelso, *CelesTrak*. [Online]. Available: https://celestrak.org/ (visited on 01/10/2023).

[147] *Cartopy: A cartographic python library with Matplotlib support for visualisation*. [Online]. Available: https://scitools.org.uk/cartopy/docs/latest/ (visited on 01/10/2023).

[148] B. Rhodes, *Skyfield: Elegant astronomy for Python*. [Online]. Available: http://github.com/brandon-rhodes/python-skyfield/ (visited on 01/10/2023).

[149] M. Fairclough and R. Dutch, *Mineralisation and mineral potential of the Woomera Prohibited Area, central Gawler Province, South Australia. Davies, M., Fairclough, M., Dutch, R., Katona, L., South, R. and McGeough, M.: 2008.South Australia. Department of Primary Industries and Resources. Report Book 2008/18*. Sep. 2008.

[150] *Ansys STK | Digital Mission Engineering Software*. [Online]. Available: https://www.ansys.com/products/missions/ansys-stk (visited on 01/10/2023).

[151] S. Yan, L. Chen, A. Yob, *et al.*, "Multifunctional Metal Matrix Composites by Friction Stir Additive Manufacturing," en, *Journal of Materials Engineering and Performance*, vol. 31, no. 8, pp. 6183–6195, Aug. 2022, ISSN: 1544-1024. DOI: 10.1007/s11665-022-07114-7. [Online]. Available: https://doi.org/10.1007/s11665-022-07114-7.

[152] K. Petrovay, "Solar cycle prediction," en, *Living Reviews in Solar Physics*, vol. 17, no. 1, p. 2, Mar. 2020, ISSN: 1614-4961. DOI: 10.1007/s41116-020-0022-z. [Online]. Available: https://doi.org/10.1007/s41116-020-0022-z.

[153] B. Frieske and S. Stieler, "The "Semiconductor Crisis" as a Result of the COVID-19 Pandemic and Impacts on the Automotive Industry and Its Supply Chains," en, *World Electric Vehicle Journal*, vol. 13, no. 10, p. 189, Oct. 2022, ISSN: 2032-6653. DOI: 10.3390/wevj13100189. [Online]. Available: https://www.mdpi.com/2032-6653/13/10/189.

[154] *Planet Releases OpenLST, an Open Radio Solution*. [Online]. Available: https://www.planet.com/pulse/planet-openlst-radio-solution-for-cubesats/ (visited on 01/11/2023).

[155] *NASA Systems Engineering Handbook Revision 2*, en, Jun. 2017. [Online]. Available: http://www.nasa.gov/connect/ebooks/nasa-systems-engineering-handbook (visited on 01/24/2023).

[156] *NPR 7123.1C - main*. [Online]. Available: https://nodis3.gsfc.nasa.gov/displayDir.cfm?t=NPR&c=7123&s=1B (visited on 01/11/2023).

[157] S. Song, H. Kim, and Y.-K. Chang, "Design and Implementation of 3U CubeSat Platform Architecture," en, *International Journal of Aerospace Engineering*, vol. 2018, e2079219, Dec. 2018, ISSN: 1687-5966. DOI: 10.1155/2018/2079219. [Online]. Available: https://www.hindawi.com/journals/ijae/2018/2079219/.

[158] S. Busch, P. Bangert, S. Dombrovski, and K. Schilling, "UWE-3, in-orbit performance and lessons learned of a modular and flexible satellite bus for future pico-satellite formations," en, *Acta Astronautica*, vol. 117, pp. 73–89, Dec. 2015, ISSN: 0094-5765. DOI: 10.1016/j.actaastro.2015.08.002. [Online]. Available: https://www.sciencedirect.com/science/article/pii/S0094576515003185.

[159] M. Sejera, T. Yamauchi, N. C. Orger, Y. Otani, and M. Cho, "Scalable and Configurable Electrical Interface Board for Bus System Development of Different CubeSat Platforms," en, *Applied Sciences*, vol. 12, no. 18, p. 8964, Jan. 2022, ISSN: 2076-3417. DOI: 10.3390/app12188964. [Online]. Available: https://www.mdpi.com/2076-3417/12/18/8964.

[160] M. Samsuzzaman, M. T. Islam, S. Kibria, and M. Cho, "BIRDS-1 CubeSat Constellation Using Compact UHF Patch Antenna," *IEEE Access*, vol. 6, pp. 54 282–54 294, 2018, ISSN: 2169-3536. DOI: 10.1109/ACCESS.2018.2871209.

[161] M. H. Azami, B.-2. P. M. BIRDS Partners, G. Maeda, *et al.*, "BIRDS-2: A Constellation of Joint Global Multi-Nation 1U CubeSats," en, *Journal of Physics: Conference Series*, vol. 1152, no. 1, p. 012 008, Jan. 2019, ISSN: 1742-6596. DOI: 10.1088/1742-6596/1152/1/012008. [Online]. Available: https://dx.doi.org/10.1088/1742-6596/1152/1/012008.

[162] S. B. M. Zaki, M. H. Azami, B.-2. P. Members, *et al.*, "Design, Analysis and Testing of Monopole Antenna Deployment Mechanism for BIRDS-2 CubeSat Applications," en, *Journal of Physics: Conference Series*, vol. 1152, no. 1, p. 012 007, Jan. 2019, ISSN: 1742-6596. DOI: 10.1088/1742-6596/1152/1/012007. [Online]. Available: https://dx.doi.org/10.1088/1742-6596/1152/1/012007.

[163] S. Kim, T. Yamauchi, H. Masui, and M. Cho, "BIRDS BUS: A Standard CubeSat BUS for an Annual Educational Satellite Project," en, *Journal of Small Satellites*, vol. 10, no. 2, pp. 1015–1034, Jul. 2021. [Online]. Available: https://jossonline.com/wp-content/uploads/2021/07/Kim-first-pg.pdf.

[164] A. Cespedes, I. Bautista, G. Maeda, *et al.*, "An Overview of the BIRDS-4 Satellite Project and the First Satellite of Paraguay," *Small Satellite Conference*, Aug. 2021. [Online]. Available: https://digitalcommons.usu.edu/smallsat/2021/all2021/245.